



# **Antibody Conjugates via Disulfide Bridging:**

*Towards therapeutic and  
diagnostic applications*

**Elizabeth Ann Hull**

A thesis submitted to University College London in accordance  
with the requirements of the degree of Doctor of Philosophy

Supervisor: Dr James R Baker

December 2014

---

I, Elizabeth Ann Hull confirm that the work presented in this thesis is my own. Where information has been derived from other sources, I confirm that this has been indicated in the thesis.

.....

---

## Abstract

Antibodies play a prominent role in chemical and biological research and the largest application of chemical bioconjugation reagents is in the production of antibody conjugates. These conjugates provide a means of highly sensitive detection, for example in enzyme-linked immunosorbent assay (ELISA) systems. In therapeutics, such conjugates have enabled the development of bispecifics and antibody-enzyme directed prodrug therapy (ADEPT).

Long-established chemical modification techniques for the conjugation of antibodies yield highly heterogeneous products. This heterogeneity is far from optimal and for therapeutic use antibody conjugates must be of a defined composition. Recently the site-specific introduction of chemical linkers has been reported through unnatural amino acid insertion. In this approach however, each protein must undergo successful mutation and expression prior to conjugation. To avoid this, an ideal site-directed conjugation technique would use residues natural to the protein.

A new class of chemical bioconjugation reagents, the 3,4-substituted maleimides, allow the selective modification and bridging of naturally occurring protein disulfide bonds. In this thesis, the generation of homogeneous antibody-protein conjugates using 3,4-substituted maleimide based cross-linkers is investigated, with a focus on producing conjugates for ADEPT and bispecific therapeutics. A range of direct and indirect chemical cross-linking strategies via disulfide bridging are explored and the consequences of each approach examined.

Ultimately, a new chemical platform to generate site-specific, homogeneous, antibody-antibody conjugates by targeting and bridging disulfide bonds was developed. A bispecific antibody construct was produced in good yield using a readily synthesised *bis*-dibromomaleimide cross-linker. Binding activity of antibodies was maintained, and *in vitro* binding of target antigens was observed. This technology is demonstrated through linking scFv and Fab antibody fragments, showing its potential for the construction of a diverse range of bispecifics.

Finally, the ability of 3,4-substituted maleimide based reagents to functionalise antibodies for diagnostic applications is investigated. A strategy for the modification of a scFv-Fc construct with commercially available fluorophores is achieved and a synthetic route towards reagents suitable for immuno-PET applications determined.

---

*For my parents,  
Martin & Karen Hull*

*In loving memory of Arthur George Derek Godfrey  
1930 - 2014*

---

## Acknowledgements

I would like to start by thanking my supervisor, Dr James “Jamie” Baker. It has been a great pleasure to be part of his group for the past three (and a bit!) years. I feel very lucky to have had a supervisor who is so enthusiastic, encouraging and supportive, as well as a much needed calming influence at times! I would also like to thank my second supervisor, Professor Kerry Chester, for her constant encouragement and confidence boosting! I am grateful to Jamie and Kerry for the freedom they have given me over my PhD research and for the fantastic opportunity to learn a huge range of research skills.

Thanks to Dr Abil Aliev for providing me with great guidance and support in everything NMR during my PhD and to Dr Lisa Harris, Dr Kersti Karu and Eifion Robinson for their excellent mass spectrometry advice and assistance.

I would also like to acknowledge those who have provided additional supervision and support, namely my thesis chair Professor Elizabeth Shephard, Dr Mark Smith and Professor Stephen Caddick.

I would particularly like to thank past and present members of the Baker group; Sally Fletcher, Rosemary Huckvale, Dr Favaad Iqbal, Dr Cristina Marculescu, Dr João Nunes, Daniel Richards, Dr Andrew Roupamy and Dr Felix Schumacher. More recently, to Nafsika Forte and Dr Florian Kampmeier. Particular thanks to Felix, who patiently taught me the art of protein modification in those early days! I would like to thank many KLB 230 and 237 lab members; I have made many lasting friendships here and laughed a lot. Particular thanks to Dr Rhian Turner, Dr Vincent Gray, Samantha Gibson and Antoine Maruani. At the Cancer Institute I would like to thank the Chester group, who have dealt with my coming and going over the last three years! Particular thanks to Maria Livanos and Dr Enrique Miranda Rota, for their friendship and assistance to the “resident chemist”!

I would like to say a special thanks to Sally Fletcher and Joanna Hemming. After meeting in the first week of our PhD programmes four years ago, we made a life-long friendship. Your support and presence throughout the PhD has been invaluable.

---

Finally, I would like to thank my family. My sister, Katherine, is endlessly supportive of my research career and always willing to provide scientific advice and assistance, and happily proof-read this thesis! My incredibly supportive and loving husband Anthony, who has successfully dealt with the emotional rollercoaster that is a PhD! His undoubting belief in my capabilities has given me the confidence to succeed. Most of all, I would like to thank my parents, to whom this thesis is dedicated. They have worked tirelessly to ensure my sister and I received a good education and a life full of opportunities. Without their unyielding support we would not be where we are today.

---

## Contents

<b>Abstract.....</b>	<b>3</b>
<b>Acknowledgements.....</b>	<b>5</b>
<b>Table of contents.....</b>	<b>7</b>
<b>Abbreviations.....</b>	<b>10</b>
<b>1 Introduction.....</b>	<b>13</b>
<b>1.1 Antibodies.....</b>	<b>13</b>
<b>1.2 Antibody Structure.....</b>	<b>13</b>
<b>1.3 Engineering Therapeutic Antibodies.....</b>	<b>15</b>
<b>1.4 Antibody fragments.....</b>	<b>16</b>
1.4.1 scFv.....	17
1.4.2 Extending fragment half-life.....	18
<b>1.5 Antibody conjugates for targeted therapeutics.....</b>	<b>19</b>
1.5.1 Direct targeting.....	20
1.5.1.1 Radio-immunoconjugates.....	20
1.5.1.2 Antibody-drug conjugates.....	20
1.5.1.3 Immunotoxins.....	21
1.5.2 Indirect targeting.....	21
1.5.2.1 ADEPT.....	22
<b>1.6 Bispecific antibody therapeutics.....</b>	<b>24</b>
<b>1.7 Antibody conjugates for diagnostics.....</b>	<b>27</b>
1.7.1 Immunoassays.....	27
1.7.2 Immunohistochemistry.....	28
1.7.3 Flow cytometry.....	29
1.7.4 Immuno-PET & Immuno-SPECT.....	30
<b>1.8 Chemical modification of antibodies.....</b>	<b>31</b>
1.8.1 Heterobifunctional cross-linkers.....	31
1.8.2 Site-directed conjugation.....	36
1.8.2.1 Reduction of interchain disulfides.....	36
1.8.2.2 Oxidation of carbohydrate chains.....	38
1.8.2.3 Cysteine introduction by mutagenesis.....	38
1.8.2.4 Bioorthogonal reagents.....	39
1.8.3 Bridging of disulfide bonds: a new class of reagents.....	46
<b>1.9 Project aims.....</b>	<b>57</b>
<b>2 Results and Discussion.....</b>	<b>61</b>
<b>2.1 Synthesis and application of a disulfide to lysine linker.....</b>	<b>61</b>
2.1.1 Synthesis of dibromomaleimide linker.....	61
2.1.2 Synthesis of dithiomaleimide linker.....	63
2.1.3 Small molecule selectivity investigation.....	66
2.1.4 Selectivity investigation using Carboxypeptidase G2.....	69
2.1.5 Conjugation of linker to Carboxypeptidase G2.....	71
2.1.6 Conjugation of modified CPG2 to anti-CEA ds-scFv.....	74
2.1.6.1 Preliminary conjugation reactions.....	74

2.1.6.2	Conjugation following protocol development .....	77
<b>2.2</b>	<b>Substituted maleimide reagents with a bioorthogonal handle.....</b>	<b>85</b>
2.2.1	Synthesis of an azide functionalised disulfide bridging linker .....	85
2.2.2	Synthesis of a strained alkyne functionalised disulfide bridging linker .....	87
2.2.3	Synthesis of a linear alkyne functionalised disulfide bridging linker .....	92
2.2.4	Functionalisation of an anti-CEA ds-scFv fragment.....	93
2.2.4.1	Disulfide bridging with an azide functionalised linker.....	94
2.2.4.2	Disulfide bridging with a strained alkyne functionalised linker.....	96
2.2.4.3	Disulfide bridging with a linear alkyne functionalised linker .....	100
2.2.5	Functionalisation of Herceptin Fab.....	101
2.2.5.1	Disulfide bridging with an azide functionalised linker.....	101
2.2.5.2	Disulfide bridging with a strained alkyne functionalised linker.....	103
2.2.5.3	Disulfide bridging with a linear alkyne functionalised linker .....	104
2.2.6	Copper-free conjugation towards homogeneous bispecifics.....	105
2.2.7	Copper-catalysed conjugation towards homogeneous bispecifics.....	115
<b>2.3</b>	<b>Synthesis and application of a disulfide to disulfide linker.....</b>	<b>123</b>
2.3.1	Synthesis of homobifunctional linkers.....	123
2.3.2	Generation of scFv homodimer.....	124
2.3.3	Generation of a homogeneous bispecific: scFv-Fab heterodimer.....	129
2.3.4	Generation of Fab homodimer .....	130
2.3.5	Analysis of conjugates by ELISA .....	135
2.3.6	Analysis of conjugates by FACS .....	136
<b>2.4</b>	<b>Disulfide bridging for diagnostic applications .....</b>	<b>139</b>
2.4.1	Functionalisation of a scFv-Fc antibody construct .....	139
2.4.2	Disulfide bridging for Immuno-PET applications .....	143
<b>3</b>	<b>Summary.....</b>	<b>148</b>
<b>3.1</b>	<b>Future outlook.....</b>	<b>152</b>
<b>4</b>	<b>Experimental.....</b>	<b>154</b>
<b>4.1</b>	<b>General Experimental Procedure.....</b>	<b>154</b>
<b>4.2</b>	<b>Proteins .....</b>	<b>155</b>
<b>4.3</b>	<b>Abbreviations .....</b>	<b>155</b>
<b>4.4</b>	<b>Synthesis .....</b>	<b>156</b>
4.4.1	Selectivity investigation using 1:1 of Linker 13 : Amine .....	160
4.4.2	Selectivity investigation using 3:1 of Linker 13 : Amine .....	161
4.4.3	Selectivity investigation using 3:1 of SMCC : Amine.....	162
4.4.4	Selectivity investigation using 3:1 of Linker 19 : Amine .....	163
<b>4.5</b>	<b>Application of disulfide to lysine linker .....</b>	<b>178</b>
4.5.1	<i>In situ</i> bridging of anti-CEA ds-scFv .....	178
4.5.2	Incubation of CPG2 with dibromomaleimide or dithiophenolmaleimide.....	178
4.5.3	Conjugation of dithiophenolmaleimide-NHS ester linker to CPG2 .....	178
4.5.4	General method for the conjugation of modified CPG2 to anti-CEA ds-scFv via the stepwise protocol .....	178
4.5.5	General method for the conjugation of modified CPG2 to anti-CEA ds-scFv via the <i>in situ</i> portionwise protocol .....	179
4.5.6	Bradford assay for determining concentration of modified CPG2 .....	179
4.5.7	General method for the conjugation of modified CPG2 to anti-CEA ds-scFv via the <i>in situ</i> protocol using selenocystamine dihydrochloride and TCEP.....	179

4.5.8	Western blot for ds-scFv and CPG2 .....	179
<b>4.6</b>	<b>Application of substituted maleimide reagents with a bioorthogonal handle</b>	<b>180</b>
4.6.1	General method for anti-CEA ds-scFv bridging with dithiophenolmaleimide linkers via the <i>in situ</i> protocol .....	180
4.6.2	General method for anti-CEA ds-scFv bridging with dibromomaleimide linkers via the sequential protocol .....	180
4.6.3	Trastuzumab (Herceptin) Fab Fragment Preparation.....	180
4.6.4	General method for Herceptin Fab bridging with dibromo- and dithiophenol-maleimide linkers via the sequential protocol .....	181
4.6.5	General method for Herceptin Fab bridging with dithiophenolmaleimide linkers via the <i>in situ</i> protocol .....	181
4.6.6	General method for SPAAC conjugation between azide or strained alkyne modified scFv or Fab and other functional molecule.....	181
4.6.7	General method for generation of scFv or Fab homodimer via SPAAC ..	182
4.6.8	Stock solutions for CuAAC conjugation <sup>188</sup> .....	182
4.6.9	Final concentrations for CuAAC conjugation <sup>188</sup> .....	182
4.6.10	General procedure for 10 µl CuAAC conjugation between azide or linear alkyne functionalised antibody fragment and other functional molecule .....	182
4.6.11	General procedure to generate Fab homodimer via CuAAC.....	183
<b>4.7</b>	<b>Application of disulfide to disulfide linkers.....</b>	<b>183</b>
4.7.1	Disulfide bridging of scFv with linker BDBM(PEG) <sub>2</sub> to generate scFv-scFv homodimer.....	183
4.7.2	Disulfide bridging of scFv with linker BDBM(PEG) <sub>19</sub> to generate scFv-scFv homodimer .....	183
4.7.3	Disulfide bridging of scFv with linker BDBM(PEG) <sub>19</sub> to generate a scFv-scFv heterodimer .....	183
4.7.4	Disulfide bridging of scFv and Fab with linker BDBM(PEG) <sub>19</sub> to generate scFv-Fab heterodimer .....	184
4.7.5	Disulfide bridging of Fab with linker BDBM(PEG) <sub>19</sub> to generate Fab-Fab homodimer.....	185
4.7.6	Protocol for CEA ELISA .....	185
4.7.7	Protocol for HER2 ELISA .....	185
4.7.8	Protocol for Sandwich ELISA .....	186
4.7.9	Cell Lines .....	186
4.7.10	Flow cytometry analysis .....	187
4.7.10.1	FACS controls .....	188
<b>4.8</b>	<b>Modification of scFv-Fc.....</b>	<b>190</b>
4.8.1	scFv-Fc reduction study .....	190
4.8.2	scFv-Fc bridging study.....	190
4.8.3	scFv-Fc modification with <i>N</i> -alkyne dibromomaleimide .....	190
4.8.4	CuAAC between alkyne functionalised scFv-Fc and azide Atto-565 .....	191
<b>4.9</b>	<b>Modification of anti-PSMA ds-scFv with dithiophenolmaleimide-DFO ..</b>	<b>191</b>
<b>5</b>	<b>References.....</b>	<b>192</b>
<b>6</b>	<b>Appendix .....</b>	<b>211</b>

---

## Abbreviations

μl	microliter
μM	micromolar
Å	angstrom
AcOH	acetic acid
ADC	antibody-drug conjugate
ADCC	antibody-dependent cellular cytotoxicity
ADEPT	antibody-directed enzyme prodrug therapy
AU	arbitrary units
BCN	bicyclononyne
BiTE	bispecific T-cell engager
Boc	<i>tert</i> -butyloxycarbonyl
CDC	complement-dependent cytotoxicity
CDRs	complementarity-determining regions
CEA	carcinoembryonic antigen
CI	chemical ionisation
CPG2	carboxypeptidase G2
CuAAC	copper-catalysed azide-alkyne [3+2] cycloaddition
d	day
Da	dalton
DCM	dichloromethane
DCC	<i>N,N'</i> -Dicyclohexylcarbodiimide
DMF	dimethylformamide
DMSO	dimethyl sulfoxide
DNA	deoxyribonucleic acid
ds-scFv	disulfide-stabilised single-chain variable fragment
DTT	dithiothreitol
EDTA	ethylenediaminetetraacetic acid
EI	electron ionisation
ELISA	enzyme-linked immunosorbent assay
equiv	equivalent(s)
ES	electrospray
Et <sub>2</sub> O	ether
Fab	fragment antigen-binding

---

FACS	fluorescence activated cell-sorting
Fc	fragment crystallisable region
FDA	food and drug administration
FPLC	fast protein liquid chromatography
FRET	Förster resonance energy transfer
Fv	variable fragment
g	gram
h	hour
HER2	human epidermal growth factor receptor 2
HOBt	hydroxybenzotriazole
HPLC	high-performance liquid chromatography
HRP	horseradish peroxidase
Ig	immunoglobulin
IHC	immunohistochemistry
IMAC	immobilised metal ion affinity chromatography
IR	infrared spectroscopy
kDa	kilodalton
L	litre
LCMS	liquid chromatography mass spectrometry
LLS	longest linear sequence
M	molar concentration
m/z	mass-to-charge ratio
mAb	monoclonal antibody
MALDI	matrix-assisted laser desorption/ionisation
MHC	major histocompatibility complex
mg	milligram
min	minute
ml	millilitre
mM	millimolar
mmol	millimole
MS	mass spectrometry
MW	molecular weight
MWCO	molecular weight cut-off
NHS	<i>N</i> -hydroxysuccinimide
nM	nanomolar

---

NMM	<i>N</i> -methylnmorpholine
NMR	nuclear magnetic resonance
PBS	phosphate buffered saline
PEG	polyethylene glycol
PET	positron emission tomography
ppm	parts per million
PSMA	prostate-specific membrane antigen
RNA	ribonucleic acid
RT	room temperature
s	second
scFv	single-chain variable fragment
SDS	sodium dodecyl sulfate
SDS-PAGE	sodium dodecyl sulfate – polyacrylamide gel electrophoresis
SEC	size exclusion chromatography
SMCC	succinimidyl 4-( <i>N</i> -maleimidomethyl)cyclohexane-1-carboxylate
SPECT	single photon emission computed tomography
SST	somatostatin
TCEP	<i>tris</i> (2-carboxyethyl)phosphine
TFA	trifluoroacetic acid
THF	tetrahydrofuran
TLC	thin layer chromatography
UAA	unnatural amino acid
UCL	University College London
UV	ultraviolet

---

# 1 Introduction

## 1.1 Antibodies

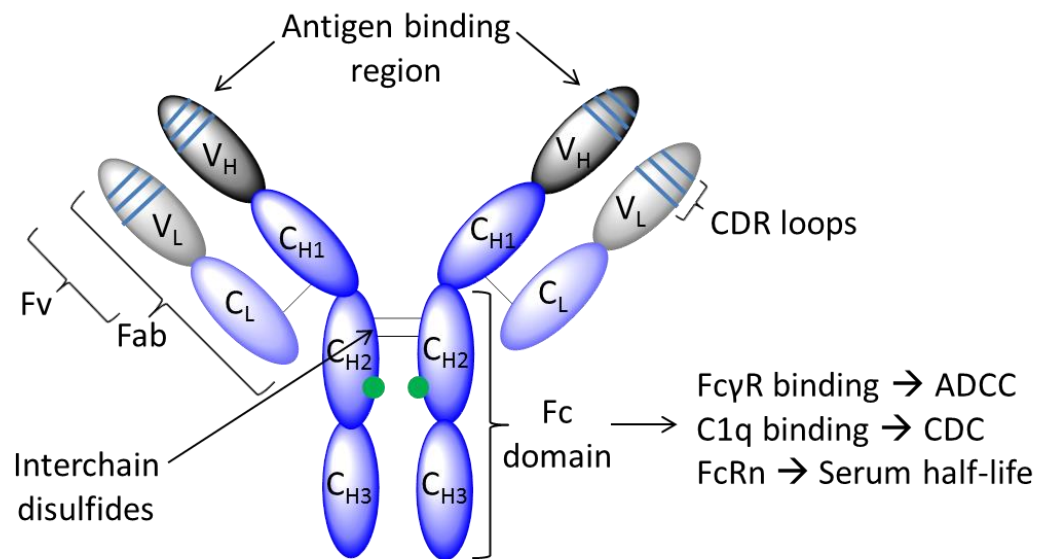
Antibodies are an integral part of the body's defence system, identifying and attacking foreign substances such as bacteria and viruses. Identification is achieved through antibody recognition of a specific, unique structure on the surface of the foreign substance, termed an antigen. In order to successfully defend, numerous antibodies with different specificities are required. This diverse range of antibodies is generated through the variation of a relatively limited set of antibody genes in the B-cells of our lymphatic system. The variability and high targeting specificity of antibodies has given them a prominent role in chemical and biological research. Subsequently, this has led to the development of numerous antibody-based research techniques, for example, immunoassays, immunohistochemistry and flow cytometry.

In recent years, there has been an increasing interest in the use of monoclonal antibodies (mAbs) and antibody fragments as therapeutic entities. The first antibody to be used as a therapeutic in humans was Muromonab, which was approved in 1986 for use in acute transplant rejection. Since then, antibody therapeutic development has continued, with more than 30 antibodies approved for clinical use and over 150 in clinical development (1,2). Monoclonal antibodies represent the highest-earning category of all biological drugs and have been applied to a variety of diseases including immunological disorders and viral infections (3,4). Oncology though is the major focus of this growing class of therapeutics owing to the identification of numerous antigens over-expressed in cancer cells.

## 1.2 Antibody Structure

Antibodies (or immunoglobulins, Ig) are macromolecular glycoproteins, with each monomer consisting of four polypeptide chains; two identical heavy chains and two identical light chains (*Figure 1.1*). The amino terminal ends of these chains are responsible for antigen binding, and as such these show great variation in amino acid composition. These are referred to as the variable regions, distinguishing them from the more conserved constant regions. Each heavy chain is composed of one variable ( $V_H$ ) and three constant domains ( $C_{H1}$ ,  $C_{H2}$ ,  $C_{H3}$ ), whereas each light chain contains only a single variable ( $V_L$ ) and constant ( $C_L$ ) domain. The heavy and light chains are held

together by both non-covalent interactions and a series of covalent interchain disulfide bonds. Together these chains form a bilateral symmetric structure.



### Immunoglobulin, 150 kDa

**Figure 1.1** Human IgG antibody; it is composed of light (L) and heavy (H) polypeptide chains, and within these chains there are variable (V) and constant (C) domains. The heavy (H) and light (L) chains are linked through disulfide bonds. Green spheres indicate glycosylation sites of the C<sub>H2</sub> domain.

Antibodies can be divided into two distinct functional entities: the fragment of antigen binding (Fab) and the constant fragment (Fc, for “fragment crystallisable”) (Figure 1.1). The Fab contains the regions V<sub>L</sub> and V<sub>H</sub>, together forming the variable fragment (Fv). In each Ig monomer there are two antigen-binding sites embedded within the Fv region, generated by three hypervariable complementarity-determining regions (CDRs) in each of the V<sub>L</sub> and V<sub>H</sub> chains. It is the CDRs that confer antigen specificity. Between the C<sub>H1</sub> and C<sub>H2</sub> domains exists an exposed proline-rich hinge region, which confers some flexibility to this large glycoprotein structure. Together with interchain disulfides, this region links the two Fab fragments to the Fc fragment. The immunological effector function-mediating region is located in the Fc fragment, and this is capable of prompting targeted cell killing via antibody-dependent cellular cytotoxicity (ADCC) and complement-dependent cytotoxicity (CDC). The Fc region is also responsible for regulating antibody serum half-life through interaction with the neonatal Fc receptor (FcRn) of the reticuloendothelial system.

---

Five classes of antibodies have been identified in vertebrates based on the sequence of their heavy chain constant regions: IgM, IgD, IgG, IgE and IgA. These antibody classes differ in valency depending on the number of antibody monomers that link to form the complete protein. For example, human IgM antibodies consist of five monomers, thus giving this class a valency of 10, since each monomer is bivalent. In contrast, IgG antibodies exist as the monomer and this bivalent species constitutes the predominant Ig class in human serum. For this reason, combined with their high targeting specificity, IgG antibodies are the most frequently used class in research tools, and for therapeutic and diagnostic applications. Within the IgG class, there are four subclasses: IgG1, IgG2, IgG3, and IgG4. These are defined by the structural differences in their Fc domains, and their consequent altered ability to initiate immune effector functions. The IgG1 class are the most abundant in human serum and are highly active in initiating ADCC and CDC mechanisms. Consequently, IgG1 is the main class of monoclonal antibodies in therapeutic and diagnostic use.

### ***1.3 Engineering Therapeutic Antibodies***

The modern era of antibody therapeutics was truly launched by the invention of hybridoma technology in 1975 (5). Through the fusion of B-cells with myeloma cells from the same species, an immortalised cell line can be prepared. Such hybridoma cell lines can be frozen for long periods of time, and simply cultured when required to produce the desired specific monoclonal antibody. Although this facilitated the generation of mouse monoclonal antibodies on a large scale, early clinical success using murine antibodies was limited. Key issues included high immunogenicity, short serum half-life, and poor ability to induce an immune effector response. Over the past two decades considerable developments in antibody technologies have led to the dawn of antibody chimerisation and subsequently, complete humanisation (*Figure 1.2*). Chimerisation attempts to overcome many of the problems associated with murine antibodies by replacing the constant regions with those from a human antibody (6). The first FDA approved chimeric antibody was Rituximab in 1997 for the treatment of B-cell non-Hodgkin's lymphoma. Humanised antibodies go a step further; apart from the murine CDRs, the sequence of the antibody is identical to the human variant (7).

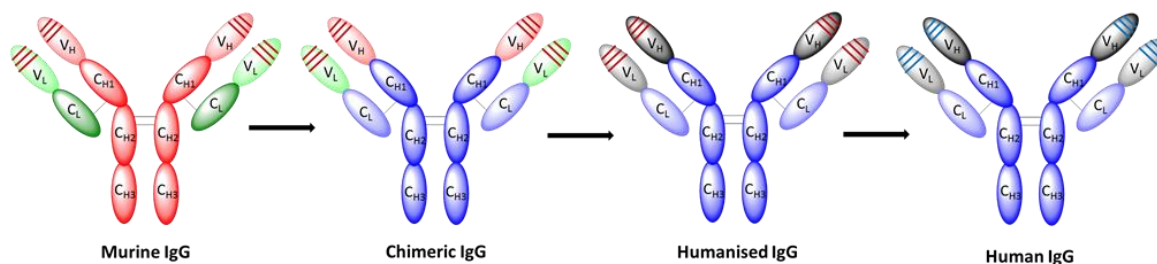


**Figure 1.2** The development of monoclonal antibodies from murine to human IgG.

Attempts to generate human monoclonal antibodies using hybridoma technology have been hampered by the lack of a suitable human myeloma cell line. In recent years, significant progress has been made on new technologies to produce human antibodies directly from human germline sequences. These technologies can be broadly classified into two methods; acquisition of antigen-specific B cells via phage display (8,9) and *in vivo* production from transgenic mice (10-12). These recombinant approaches have also enabled improvement of antibody features for better tumour targeting e.g. affinity, avidity and specificity.

To date, 36 monoclonal antibodies have been approved for therapeutic use in the EU and USA. Although full antibodies have made an impact as cancer therapeutics, their effectiveness is often limited and most must be used in combination with other treatments (13). The large size of these proteins results in poor tumour penetration (14) and long *in vivo* half-lives, which can in turn result in toxicity due to the inappropriate activation of Fc receptor expressing cells. However, inadequate cell-killing activity is the main reason for the failure of monoclonal antibodies in clinical trials (15).

### 1.4 Antibody fragments

The segmental structure of antibodies allows their cleavage into fragments with distinct properties. Originally, this was achieved using proteolytic digestion; the hinge region is particularly susceptible to proteases, and two principal digested forms of IgG antibodies are useful for preparing immunological reagents (*Figure 1.3*). Digestion with pepsin removes the Fc domain, degrading it into many smaller fragments, leaving a large F(ab')<sub>2</sub> fragment held together by the disulfide bonds in the hinge region (16). This retains the bivalent antigen-binding properties of the parent IgG antibody, but without the Fc effector region. Alternatively, digestion with papain releases two identical monovalent antigen-binding Fab fragments, each containing the V<sub>H</sub>-C<sub>H1</sub> and V<sub>L</sub>-C<sub>L</sub> segments linked by a disulfide bond, and one larger Fc fragment containing the remaining heavy chains (17). Through removal of the Fc domain, the Fab and F(ab')<sub>2</sub>

---

fragments confer many advantages over full antibodies. The reduced size of these fragments improves their diffusion through solid tumour mass (14), decreases their *in vivo* half-life, a key advantage in imaging applications, and negates off-target toxic effects caused by the Fc region. Advances in recombinant DNA technology and antibody engineering have since enabled the generation of antibody fragments without the requirement for proteolytic digestion (18,19). Many recombinant antibody fragments can now be readily expressed in microbial systems on a large and cost-effective scale (20).

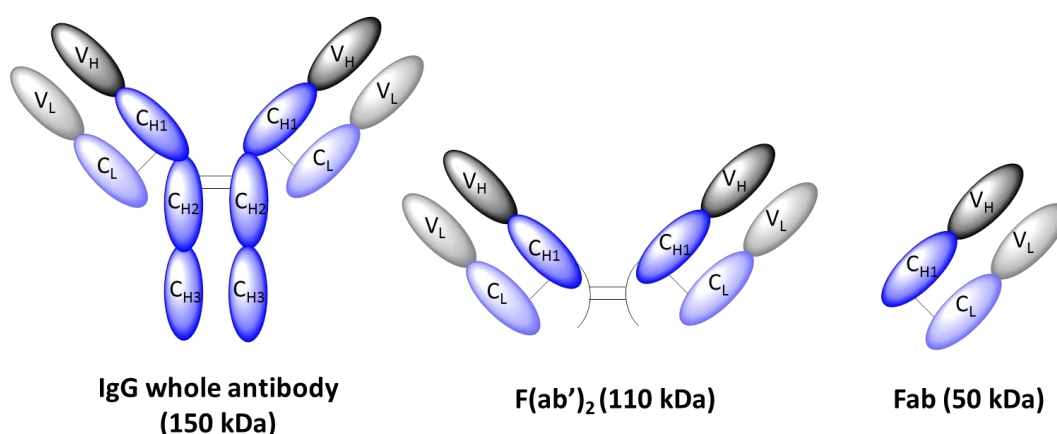


**Figure 1.3** F(ab')<sub>2</sub> and Fab fragments obtained by digestion with pepsin and papain respectively.

#### 1.4.1 scFv

The variable fragment (Fv) consists only of the variable domains of the heavy and light chains (V<sub>H</sub> and V<sub>L</sub>), and as such is the smallest antibody fragment (~25 kDa) that retains full specificity and antigen binding activity (*Figure 1.4*). The Fv is only associated through non-covalent interactions between the V<sub>H</sub> and V<sub>L</sub> domains, and is too unstable for clinical and research applications (21). A common practice to overcome this instability is to incorporate a short peptide linker between the two domains, yielding a single-chain Fv (scFv) (*Figure 1.4*) (22,23). Generally a 15 residue (Gly<sub>4</sub>Ser)<sub>3</sub> linker is used which provides flexibility, hydrophilicity and protease resistance. An alternative stabilisation strategy is the incorporation of a single interchain disulfide bond between the V<sub>H</sub> and V<sub>L</sub> domains, giving a disulfide-stabilised Fv (dsFv) (*Figure 1.4*) (24-26). Many groups have now combined these two stabilisation strategies, generating a disulfide-stabilised single-chain Fv (ds-scFv) (*Figure 1.4*) (27-29). Uniting the two

---

approaches creates fragments that are readily expressed in high yields in microbial systems, possess good thermal stability, and are less prone to aggregation.

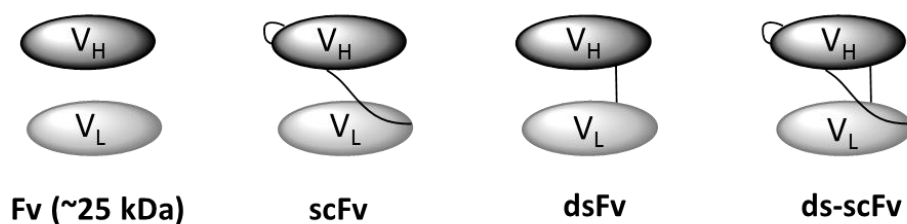


**Figure 1.4** The smallest antibody fragment that retains full specificity and binding activity, the Fv, and the three common stabilised variants, scFv, dsFv, and ds-scFv.

A significant advantage offered by these fragments is their small size; studies have demonstrated that tumour penetration is inversely proportional to the size of the antibody (30). In comparison to full IgG antibody molecules, scFvs penetrate and distribute homogeneously in tumours much more efficiently, a key advantage in both imaging and therapeutic applications (31-33). Antibody fragments below 65 kDa, such as Fabs and scFvs, undergo rapid, first-pass renal clearance (34), and so have much reduced *in vivo* half-lives compared to full antibodies. This can be advantageous for imaging applications as this limits non-specific binding and thus achieves better contrast (15). Furthermore, the monovalent nature of these fragments leads to lower retention times on the antigen compared to full antibodies (15,35). Although these features of scFvs are beneficial in terms of toxicity, they can also prove a disadvantage therapeutically, since the concentration of antibody at the tumour is low.

#### 1.4.2 Extending fragment half-life

In order to tailor the *in vivo* half-lives and retention times of Fabs and scFvs, several strategies have been investigated including fusion with albumin (36,37), fusion with toxins (38) and affinity maturation (39). One of the most widely used techniques is PEGylation (40,41). Attaching an ethylene glycol polymer of the appropriate size via chemical modification has been shown to significantly reduce renal clearance of biologicals and increase protection against proteolytic degradation, as well as providing the additional benefit of reduced immunogenicity (42). This effect has been attributed to the interaction of PEG with water; each monomer of ethylene glycol binds to two water molecules, and so the hydrodynamic radii of PEG is 5- to 10-fold greater than would be

---

predicted by its nominal molecular weight (43). Thus the effective molecular size of the PEG conjugate is significantly increased.

The half-lives of scFv and Fab antibody fragments can also be improved by increasing their valency. Through increasing the number of antigen binding sites both the size and also avidity of the antibody is increased, generating a construct with superior binding activity to the monomeric fragment. scFv fragments can be encouraged to undergo spontaneous multimerisation through shortening of the peptide linker (< 12 residues) (44). Alternatively, bivalent scFvs or Fabs can be generated by genetic engineering approaches. For example, so termed ‘diabodies’ can be readily constructed in reasonable yields through the complementary pairing of the variable domains of one scFv with another, forming a non-covalently associated dimer (45). Fragment dimers can also be produced by genetic fusion and through the introduction of disulfides (46-48). Chemical conjugation approaches have also been attempted, though reported strategies generally result in heterogeneous multimers (49).

### ***1.5 Antibody conjugates for targeted therapeutics***

For many diseases, antibodies act as a therapeutic by blocking the function of their target molecule. In the case of cancer therapy, the antibodies must specifically recognise tumour cells and elicit cell death. Therapeutic antibodies have been suggested to prompt tumour cell elimination through several mechanisms including immune system recruitment and apoptosis. Although there has been some success using unmodified mAbs, many biological barriers must be overcome for significant accumulation in the target tissue, and even at this stage therapeutic efficacy is reliant upon the extent of antibody-induced cell death. It is the case that many antibodies simply do not have the cytotoxic potential to entirely destroy malignant cells. As a consequence, antibodies and antibody fragments are increasingly being developed as targeting agents for administering cytotoxic substances or delivering potent effectors to selectively destroy cancerous cells. The antibody therefore becomes responsible for recognition and binding, whilst the linked toxic component causes cellular alterations leading to cell death. The payload can be delivered by the antibody through two methods: direct or indirect targeting.

---

### **1.5.1 Direct targeting**

The direct targeting or “Magic-Bullet” approach is the delivery of a cytotoxic compound such as a radioisotope or drug to only cells expressing the target antigen (50). This therapeutic strategy has great potential to drastically reduce the side-effects observed with standard chemo- or radiotherapy by concentrating the chemotherapeutic agent at the location of the tumour. Delivery of the cytotoxic element of immunoconjugates is achieved by endocytosis. Once bound to their target antigen on the cell surface, endocytosis can take place and the cytotoxic compound is released, inducing cell death (51).

#### **1.5.1.1 Radio-immunoconjugates**

Two radio-immunoconjugates have been approved for cancer treatment, <sup>90</sup>Y-Ibritumomab and <sup>131</sup>I-Tositumomab. These conjugates deliver lethal doses of radiation to the target tumour cells, resulting mainly in heavy DNA damage. Despite this, the level of radiation delivered is often insufficient to completely destroy solid tumours (52,53).

#### **1.5.1.2 Antibody-drug conjugates**

Over the last decade, antibody-drug conjugates (ADCs) have shown considerable promise as cancer therapeutics. Two ADCs have been approved in recent years; T-DM1 (Kadcyla) from Genentech for the treatment of HER2-positive breast cancer and Brentuximab vedotin (Adcetris) from Seattle Genetics, for the treatment of relapsed Hodgkin and systemic anaplastic large cell lymphomas (54-56). In fact, ADCs are now the main interest of immunoconjugate research since radioactive treatments are difficult to handle and immunotoxins are generally immunogenic (57) (see *Section 1.5.1.3*). For an ADC to be successful in the clinic, both the drug and the antibody must be validated. The cytotoxic drug must be extremely potent, as delivery levels are low (58). Furthermore, the antibody must be highly specific for its target antigen, which in turn must only be expressed on cancerous cells. The linker used to attach the drug to the antibody must also be chosen carefully, as it is required to be stable in blood and subsequently release the cytotoxic cargo once inside the cell. In the ADC field there is currently extensive investigation into the chemical conjugation approach used to attach the drug to the antibody. Despite small molecule drug therapies requiring extensive investigation to ensure the synthesis of chemically defined products, the chemical conjugation strategies used to produce ADCs to date have generally been nonspecific

---

with little stoichiometric control. Thus ADCs are commonly produced as heterogeneous mixtures, with each conjugate possessing different pharmacokinetic, stability, affinity and safety profiles. An efficient chemical modification strategy to produce ADCs is key to future therapeutic success.

### **1.5.1.3 Immunotoxins**

Immunotoxins are conjugates or fusion proteins of antibodies and protein toxins. A variety of toxins have been investigated for their use in the treatment of cancer with the plant-derived toxins ricin, abrin and modeccin, as well as the bacterial derived diphtheria toxin, being the most popular. The ability of most toxins to cause cell death derives from their enzymatic inhibition of protein synthesis. In order for the immunotoxin to elicit its cytotoxic effect, it must first bind and be internalised by the target cell. The enzymatic portion of the toxin must then undergo translocation to the cytosol. To date, only one immunotoxin, denileukin diftitox (Ontak), a fusion protein of truncated diphtheria toxin and interleukin 2, has been FDA approved, though several fusion proteins are currently in clinical trials (59). A major challenge in immunotoxin application is immunogenicity; neutralising antibodies are developed by most patients against the non-human toxin, limiting the number of treatment cycles.

### **1.5.2 Indirect targeting**

Therapeutic systems with a two-step approach have been designed whereby the antibody is conjugated to an intermediate agent, which when combined with another non-toxic agent, can elicit cytotoxicity. One approach to generating indirect targeting therapeutics is to tag an antibody with a biotin label, and then a secondary avidin-toxin conjugate can be administered once the antibody is bound to the target cell. This strategy is used by pre-targeted radioimmunotherapy (RIT); a biotin-labelled radionuclide is administered which possesses high affinity for a pre-targeted antibody fused to streptavidin (60).

The most investigated method of indirect targeting is antibody-directed enzyme prodrug therapy (ADEPT), an approach first described in the late 1980s (61-63). The development of antibody-enzyme conjugates for use in this therapeutic system is one of the areas under investigation in this thesis.

---

### 1.5.2.1 ADEPT

ADEPT was designed with the principal aim to restrict cytotoxic action to the site of the tumour. It is a two-step therapeutic; first an antibody or antibody fragment directed to tumour associated antigen carries the conjugated enzyme to the tumour sites, and once the conjugate is cleared from the blood, a non-toxic prodrug can be administered which is converted by the enzyme at the site of cancer, to a potent, cytotoxic drug (*Figure 1.5*). Since one enzyme can act on many prodrug molecules, a high concentration of the toxic drug will be produced at the site of the tumour. In addition, the small drug molecules can diffuse to surrounding cells, destroying antigen negative cells and tumour supportive stromal elements, referred to as a local bystander effect.

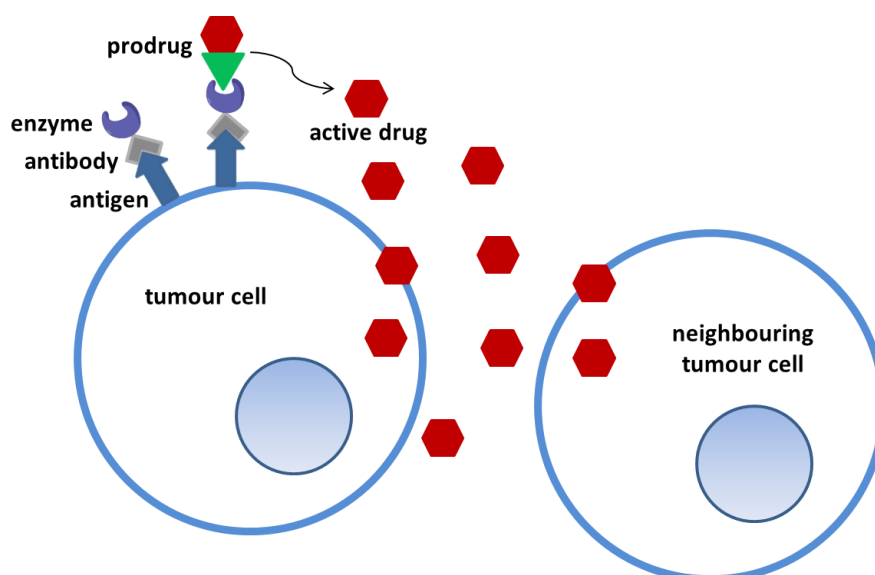


**Figure 1.5** Antibody-directed enzyme prodrug therapy (ADEPT); a two-stage therapeutic. **Stage 1:** The antibody-enzyme conjugate is allowed to localise in tumour tissue. **Stage 2:** Once cleared from the blood, a non-toxic prodrug can be administered, which is converted to a potent, cytotoxic drug by the targeted enzyme. The active drug diffuses through the tumour cells, causing localised cytotoxicity. Since one enzyme can act on many prodrug molecules, a high concentration of the toxic drug will be produced at the site of the tumour.

ADEPT has many advantages over standard chemotherapy. Firstly, the highly toxic drug is delivered selectively and specifically at the site of the tumour. Secondly, through the use of a non-toxic prodrug, higher doses can be administered as the toxic effects will only be released at the site of cancer. Indeed, since ADEPT produces the cytotoxic drug at the tumour, it allows for the possibility of using drugs which would be deemed too

---

toxic to use as standard chemotherapeutics. Furthermore, as one enzyme can act on many prodrug molecules, ADEPT overcomes problems such as antigen heterogeneity, since the toxic drug molecules produced can diffuse to surrounding cells (local bystander effect). Conversely, antibody-drug conjugates require homogeneous expression of the target antigen across the entire tumour cell population, as this approach relies on internalisation to release the cytotoxic drug.

Many of the enzymes used for ADEPT are of bacterial origin and do not have a human equivalent. Although these non-human enzymes have an immunogenic effect, human enzymes are unsuitable for this system as endogenous conversion of prodrug would occur, resulting in off-target toxicity. ADEPT therapy can therefore only be administered before the patient experiences an immune response. The only enzyme to have been clinically assessed in the ADEPT system is the bacterial enzyme carboxypeptidase G2 (CPG2). CPG2 is a dimeric zinc-dependent exopeptidase; it hydrolyses the C-terminal glutamate moiety from folates, and has been used in ADEPT to facilitate the cleavage of nitrogen mustard L-glutamate prodrugs (64,65).

Antibody and antibody fragment chemical conjugates to CPG2 have been constructed, however these conjugates are highly heterogeneous and result in a significant loss of both antibody and enzyme activity (62,66-72). Production of a conjugate of CPG2 linked to the F(ab')<sub>2</sub> fragment of an anti-carcinoembryonic antigen monoclonal antibody (A5B7) has undergone extensive optimisation (73). This conjugation procedure used the currently available reagents *N*-succinimidyl *S*-acetylthioacetate (SATA) and succinimidyl 4-(*p*-maleimidophenyl)butyrate (SMPB) for lysine to lysine coupling (see *Section 1.8.1*). After optimisation, Melton *et al.* typically achieved yields of 30% in the crude reaction mixture, obtaining only 15% or less of 1:1 antibody-enzyme conjugate linked heterogeneously after purification (74).

Developments in molecular biology have enabled antibody-enzyme recombinant fusion proteins to be generated for use in ADEPT (75-78). An anti-CEA scFv fusion to CPG2, called MFECF, has been successfully expressed as a stable homodimer in *E. coli* with maintained specificity and functional affinity (79). Although this is currently the most efficient approach to producing homogeneous antibody-enzyme conjugates, it is not without its issues. In fusion, antibodies and enzymes are linked by the direct expression of polypeptide chains between their N and C termini. This strategy is not suitable for all

---

proteins as many require unmodified termini for optimal activity (80-82). Furthermore, this fusion can complicate the folding and processing of proteins, resulting in expression difficulties (83). Certainly in the case of MFECP, several problems have been encountered. In *E. coli* the yields of fusion protein are variable and often insufficient for use in clinical studies (75). Expression was also achieved in yeast, however glycosylation of the MFECP construct resulted in rapid plasma clearance (76,77,84).

## **1.6 Bispecific antibody therapeutics**

The limited ability of monoclonal antibodies to induce significant anti-tumour activity has also led to the development of bispecifics; fundamentally these are antibodies that can bind two different antigens. Presently, the concept of administering one antibody therapeutic to bind at least two molecular targets is one of the most exciting and highly investigated areas of cancer treatment. In recent years, several clinical successes of bispecific antibody therapeutics have been reported, with the first bispecific Catumaxomab (Removab), being approved for the treatment of malignant ascites in 2009 (85). This biotherapeutic operates by guiding T-cells to epithelial cell adhesion molecule (EpCAM)-expressing tumour cells. Currently, bispecific therapeutics are also being developed to facilitate simultaneous inhibition of two cell surface receptors, or blocking of two ligands, cross-linking of two receptors, and T-cell recruitment to target tumour cells (86). Chemical construction of this therapeutic system is one of the main areas under investigation in this thesis.

Bispecific antibodies can be produced by three main approaches: (i) chemical conjugation; (ii) fusion of two different hybridoma cell lines; (iii) recombinant DNA technology (87). The majority of reported chemical conjugation methods for bispecific production rely on modification of lysine residues, which leads to highly heterogeneous products (88,89). Recently the site-specific introduction of chemical linkers has been reported through unnatural amino acid insertion (90,91). Using this approach, Schultz *et al.* described the synthesis of a homogeneous anti-HER2/anti-CD3 bispecific in good yield (91). This technology and the use of lysine modification reagents will be discussed in detail in *Section 1.8*. The earliest approach used to generate bispecifics was the hybrid hybridoma or quadroma approach (92). Through somatic fusion of two hybridoma cell lines, the formed quadroma cell line produces the two antibodies of different specificities, as well as a bispecific antibody with two distinct binding arms

---

(94). However, the bispecific is produced in very low yields, and extensive and difficult purification techniques are required to separate the desired antibody.

The development of recombinant DNA technology has allowed for many of the shortcomings associated with chemical conjugation and quadroma bispecific production to be overcome. The flexibility of this approach has enabled a variety of bispecific antibody formats to be produced, from whole IgG like molecules for example Triomabs, to small recombinant formats, such as BiTEs (Bispecific T cell Engager) (*Figure 1.6*). These smaller bispecifics can be readily expressed at high levels in bacteria and their small size increases their ability to penetrate tumours. As discussed earlier, their size also results in a reduced serum half-life. Although sometimes an advantage, this can be a major drawback to therapeutic success, particularly if continuing high levels of therapeutic are required.

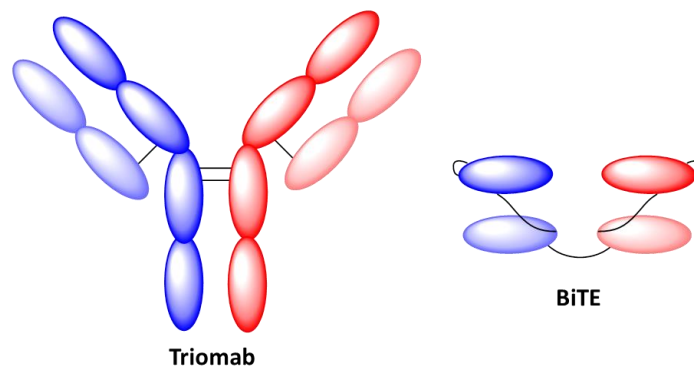


**Figure 1.6** Examples of bispecific antibody formats for the recruitment of effector cells. Triomabs are based on rat IgG structure; one arm is specific for a tumour-associated antigen (blue) and the other for CD3 (red), a surface antigen expressed by cytotoxic T-cells. The Fc fragment can activate the innate immune system, recruiting accessory cells. There are also several recombinant human bispecific formats, perhaps the most popular of which is the BiTE format. This is based on two scFv fragments joined by a peptide linker, one for tumour cell-binding (blue) and the other for binding effectors (red), such as T cells or NK cells.

One of the most exciting bispecific formats currently in clinical development is the Bispecific T cell Engager or BiTE. These constructs are commonly a fusion of two scFv fragments (~55 kDa total); one fragment with high specificity for the cancerous cell linked to another which engages T cells via binding to CD3, an invariant signalling

component of the T cell receptor (TCR) complex (90) (*Figure 1.7*). Through engaging a polyclonal population of T cells, lysis of the tumour cell is made independent of T cell receptor specificity and MHC (major histocompatibility complex) presentation (95). This polyclonal T cell engaging approach thus bypasses the immune escape mechanisms observed in many tumour cell populations.

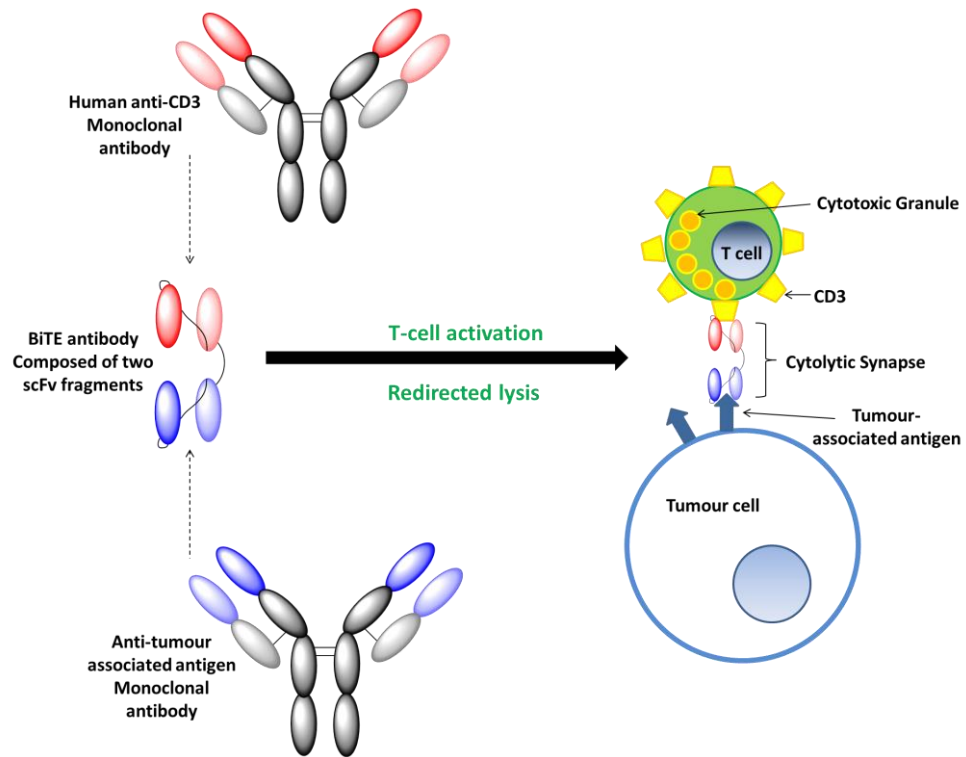


**Figure 1.7** Construction, design and mode of action of BiTEs.

Blinatumomab (anti-CD19/anti-CD3) is the most advanced BiTE in clinical trials to date (95). This construct has demonstrated clinical activity in acute lymphoblastic leukaemia (ALL) and non-Hodgkin's lymphoma patients. However, its approval as a therapeutic has been limited by its short serum half-life, since patients require dose escalation and long-term exposure. Improving the half-life of homogeneous BiTEs is the next step in achieving a truly efficacious therapeutic.

---

## 1.7 Antibody conjugates for diagnostics

### 1.7.1 Immunoassays

Antibodies are extensively used in diagnostics, with the immunoassay being the most commonly used analytical assay. Immunoassays facilitate the identification of the presence or concentration of a substance, the ‘analyte’, within a complex mixture. The chemical conjugation of antibodies to radioisotopes, dyes and enzymes enabled such technology to rapidly expand, particularly in biomedical research. One of the most commonly employed immunoassays is the two antibody “sandwich” ELISA (*Figure 1.8*). This is used in diagnostics to determine antigen concentration in unknown samples, for example the blood plasma. This assay is quantified by using a secondary antibody conjugated to an enzyme e.g. horseradish peroxidase (HRP), through the use of a colorimetric substrate. This antibody-enzyme conjugate is generally produced using a cross-linker between two lysine residues, and is a heterogeneous mixture ranging from free antibody to that with several enzymes attached.

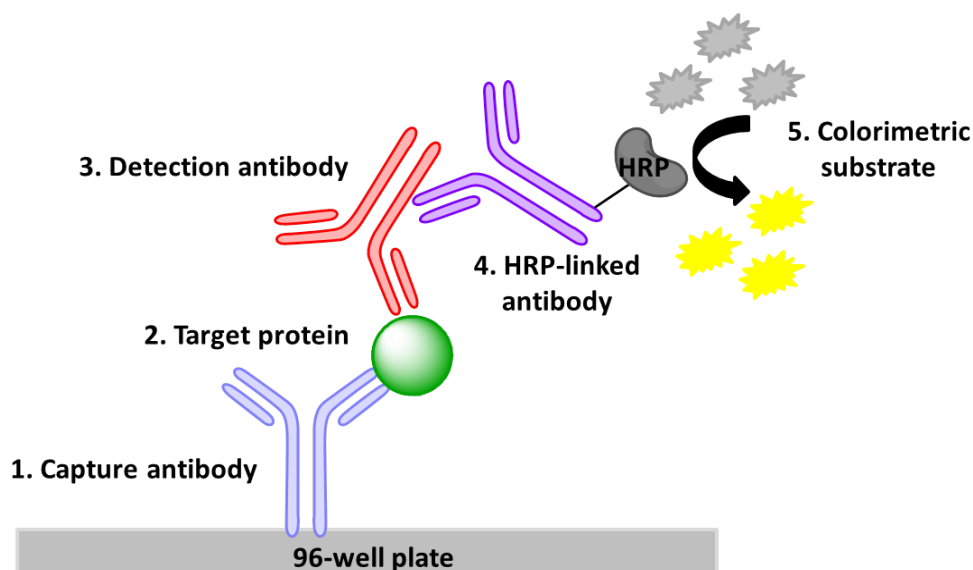


**Figure 1.8** Sandwich ELISA; termed such as the antigen is bound between two antibodies. **1.** A known quantity of capture antibody is bound to a 96-well plate. **2.** After a blocking step, the antigen containing sample is added. **3.** After washing, the detection antibody binds to the antigen. **4.** After a second washing step, an enzyme-linked secondary antibody specific for the detection antibody’s Fc region is added. Horse radish peroxidase (HRP) is generally the enzyme of choice. **5.** After washing, a chemical is added which is converted by the enzyme to a colour signal. The absorbance of this colorimetric substrate is used to determine presence and quantity of antigen.

## 1.7.2 Immunohistochemistry

Immunohistochemistry (IHC) is widely used for the diagnosis of solid tumours. It can be used to determine the stage and grade of a tumour, whether it is benign or malignant, and to identify the origin of a metastasis in order to define the location of the primary tumour. IHC, similarly to an ELISA, uses a detection antibody that is conjugated to an enzyme such as HRP or a fluorophore. However, in this case the sample used is a tissue section, a biopsy from a patient. The simplicity of this technique means that it is readily available in most pathology laboratories, low-cost and yields rapid results. An example of IHC is the HercepTest; this determines HER2 expression levels in breast cancer to evaluate if treatment with the anti-HER2 monoclonal therapeutic Trastuzumab will be beneficial (*Figure 1.9*). The HercepTest is an early example of the newly evolving field of theranostics, which is the merging of the therapeutic ('thera') and diagnostic ('nostic') potential of a compound. Through using a therapeutic e.g. Trastuzumab in a diagnostic test prior to treatment, the ability of a compound to exert a therapeutic effect can be ascertained. This field provides a step towards developing more personalised medicine, and will also enable more precise prediction and monitoring of tumours in the clinic.

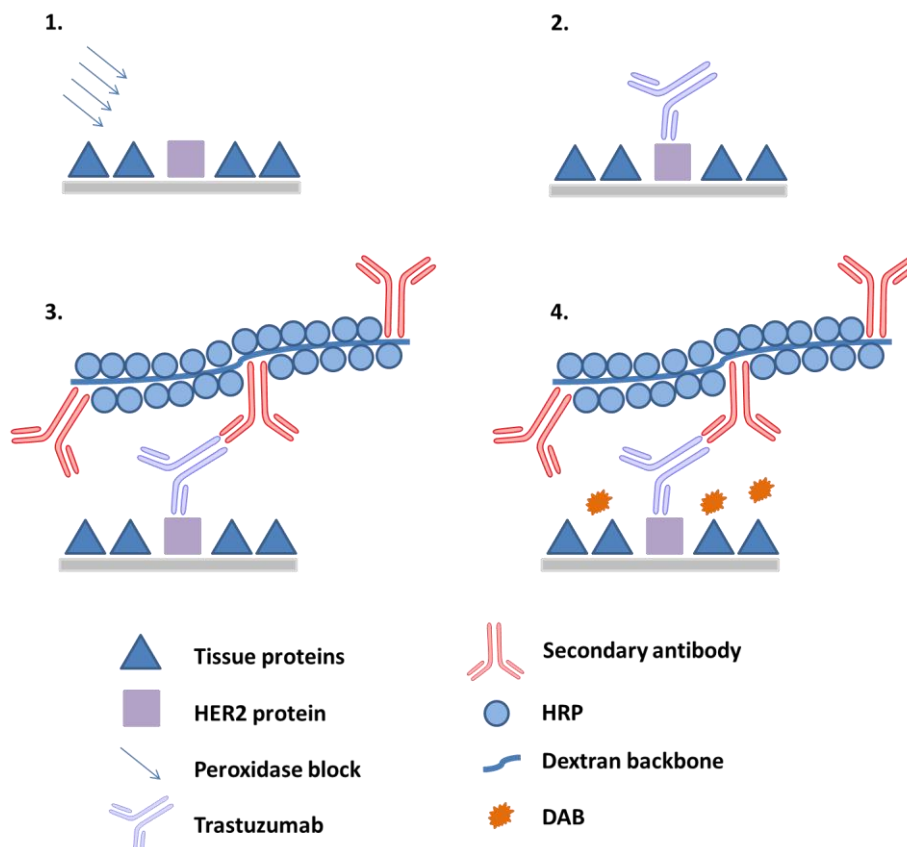


**Figure 1.9** HercepTest. **1.** Application of peroxidase block to tissue sample, preventing any endogenous peroxidase activity. **2.** Application of Trastuzumab. **3.** Application of

---

secondary antibody-HRP labelled polymer. Use of a polymer gives much higher assay sensitivity, as there are more enzyme labels per secondary antibody. **4.** Application of 3,3'-Diaminobenzidine (DAB). This chromogen is widely used for immunohistochemical staining; in the presence of HRP, DAB produces a brown precipitate which is insoluble in alcohol and xylene.

### **1.7.3 Flow cytometry**

Another crucial antibody-dependent diagnostic technology is flow cytometry, routinely used for diagnosis of haematological malignancies. This diagnostic technique provides not only immunophenotypic data, but also information on the morphology of cells (96,97). In fact, the high sensitivity of flow cytometry means that it can be used to detect minimal levels of remaining cancerous cells, with an analytical sensitivity of approximately one neoplastic cell to every  $10^4$  normal cells (98). Most commonly, this technique measures the fluorescence intensity of a fluorophore-conjugated antibody (*Figure 1.10*). This conjugation may be on the diagnostic, primary antibody (direct staining), or on a secondary antibody with high specificity for the primary (indirect staining). An alternative indirect approach is facilitated by avidin-biotin; the diagnostic antibody is chemically conjugated to avidin and in a subsequent incubation step a biotin labelled fluorophore added. The choice of conjugated fluorophore is imperative for precise results; antigens that are highly expressed may be resolved from background signal with almost any fluorophore, however low antigen expression requires a much higher signal to background ratio that can only be provided by the most intense fluorophores e.g. PE (R-phycoerythrin).

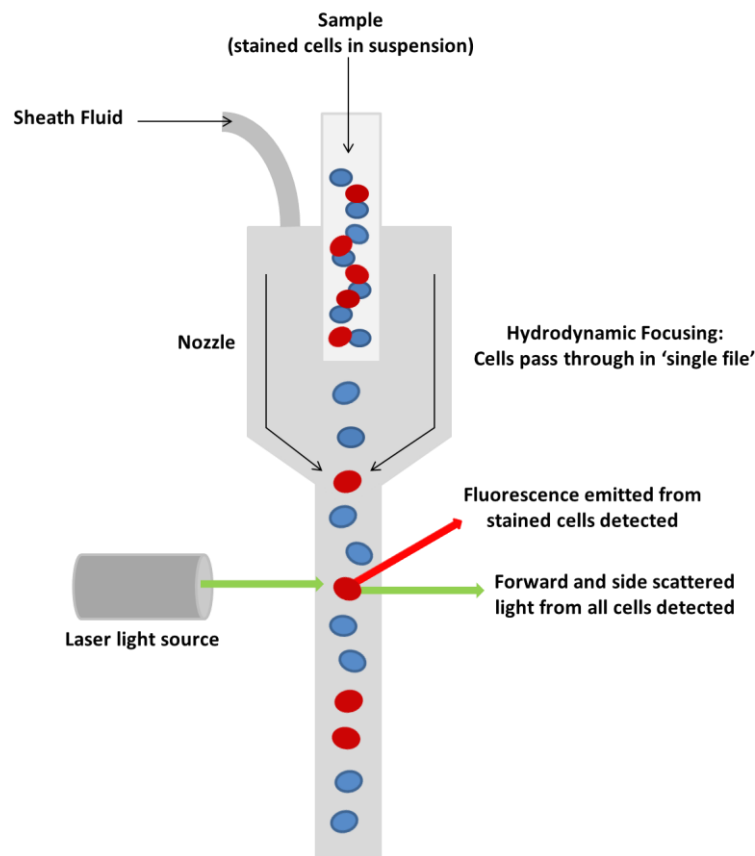


**Figure 1.10** Illustration of the fluidics system of a flow cytometer.

#### 1.7.4 Immuno-PET & Immuno-SPECT

Antigen expression levels can also be determined *in vivo* using molecular imaging technology. For both haematological and solid tumours, immuno-positron emission tomography (PET) and immuno-single photon emission computed tomography (SPECT) can be used. Both techniques use a radioimmunoconjugate, specifically an antibody conjugated to a positron or  $\gamma$ -emitter, which is injected intravenously. Using a PET or SPECT scanner, the distribution of the conjugated antibody can be visualised. This non-invasive diagnostic technique thus provides target visualisation throughout the whole body.

Immunoassays, immunohistochemistry, flow cytometry and molecular imaging, all rely on chemically conjugated antibodies. Improved antibody conjugation strategies would result in improved specificity and sensitivity, and thus improved diagnosis. The chemical modification of antibodies for diagnostics is an area of investigation in this thesis.

---

## 1.8 Chemical modification of antibodies

The chemical modification of antibodies, and particularly antibody fragments, has a crucial role to play in the development of the next generation of immunotherapeutics and diagnostic tools. Through attachment of groups such as polyethylene glycol (PEG), the *in vivo* lifetimes can be altered, stability of antibodies improved, and immunogenicity reduced (40,41). New functions can also be conferred on antibodies and antibody fragments through attachment of radiolabels and fluorophores. For antibody-drug conjugates (ADCs), bispecifics and antibody-directed enzyme prodrug therapy (ADEPT), efficient chemical modification of the antibody is key to therapeutic success.

There are several long-established techniques for the chemical modification of antibodies, particularly for the production of antibody-enzyme conjugates. Many of the methods were developed to produce conjugates for immunoassays such as ELISAs. These focus on achieving high yields of conjugate with retention of biological activity. However, more precise techniques are required for the generation of therapeutic antibody conjugates. Investigations into the chemical modification of antibodies have revealed that the strategy used can dramatically affect its behaviour *in vivo*. It is essential that conjugates maintain the antigen binding character of the antibody, and in the case of ADEPT for example, not block the activity of the linked enzyme. In addition, site-specific couplings are required in order to control the number of toxophores e.g. drug or radiolabel per antibody, as this is key to the pharmacokinetic properties of the immunoconjugate. Site-specificity of conjugation is even more necessary when using antibody fragments, since it is increasingly likely that amino acid side chains will be involved in antigen-binding. In the case of bispecific therapeutics and ADEPT constructs, site-specificity is necessary to avoid large aggregates which would be taken up by the reticuloendothelial system, to achieve maximum penetration of the target tumour, and prevent blocking of antigen-binding sites by the other conjugated protein.

### 1.8.1 Heterobifunctional cross-linkers

Methods for the chemical modification of proteins have largely targeted the side chains of naturally occurring amino acid residues. Development of modification reagents for many of the hydrophilic amino acids has been attempted; these include lysine, cysteine,

histidine, tyrosine, aspartic acid, arginine, tryptophan, serine, threonine and glutamate residues (99,100). However, the majority of bioconjugation research, and certainly for antibody modification, has focused on the nucleophilic functional groups of two amino acids, lysine and cysteine (*Figure 1.11*) (101).

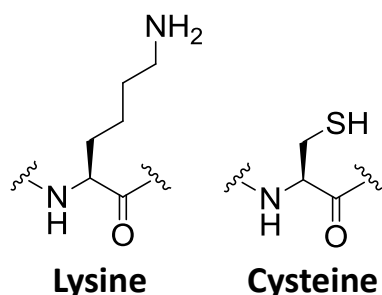


**Figure 1.11** Many bioconjugation reagents have been developed which target the amino acids lysine and cysteine, owing to the nucleophilic primary amine of lysine residues and the primary thiol of cysteine residues.

The most widely used reagents for chemical conjugation are heterobifunctional, which react with the amino group of a lysine residue on one protein and the thiol group on a second. Commonly such linkers possess an amine reactive *N*-hydroxysuccinimide (NHS) ester, together with a maleimide or activated sulfhydryl for thiol modification. The basic structures of the two linkages formed between the antibody and conjugated protein or other functional molecule are shown in *Figure 1.12*. The key difference between the two linker types is the formation of a thioether or disulfide bond, depending on whether the reactive thiol group is a maleimide or an activated sulfhydryl respectively.

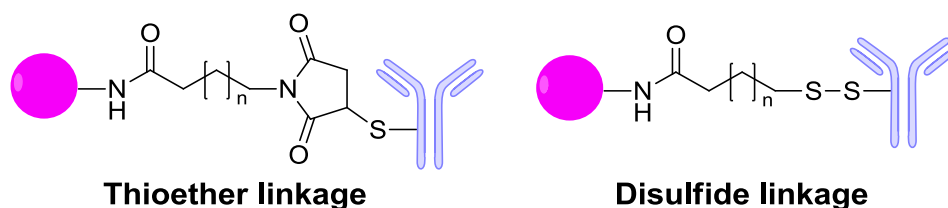


**Figure 1.12** Two main types of linkages formed between antibody (blue) and conjugate (pink) e.g. enzyme, drug, radiolabel.

Heterobifunctional reagents forming thioether linkages are by far the most popular commercial reagents currently available. They are preferable to disulfide linkers largely because of their stability, as the thioether linkage is maintained under a wide variety of conditions where the disulfide would be reduced. For example, disulfide linkages are

extremely unstable in blood plasma, a feature which would be highly undesirable for the production of most therapeutic and diagnostic conjugates. The most popular of the thioether heterobifunctional reagents are succinimidyl-4-(*N*-maleimidomethyl)cyclohexane-1-carboxylate (SMCC), *m*-maleimidobenzoyl-*N*-hydroxysuccinimide ester (MBS) and *N*-( $\gamma$ -maleimidobutyryloxy)succinimide ester (GMBS), the structures of which are shown in *Figure 1.13*. The linker SMCC is the most widely used as it is less susceptible to maleimide hydrolysis (74). The aromatic ring adjacent to the maleimide of MBS causes this linker to be highly labile to ring opening in an aqueous medium. In contrast, the maleimide of SMCC is adjacent to a bulky cyclohexane ring with no aromatic character.

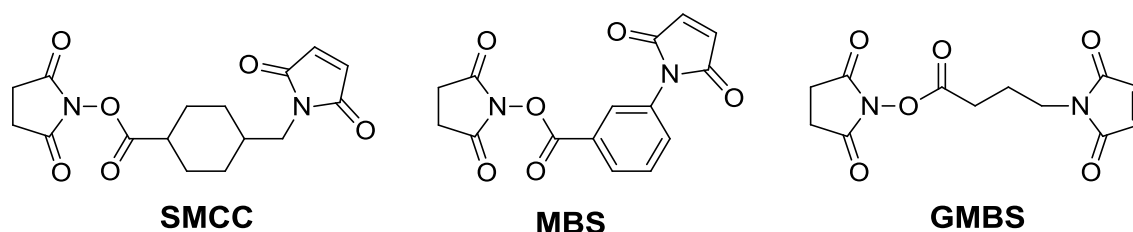
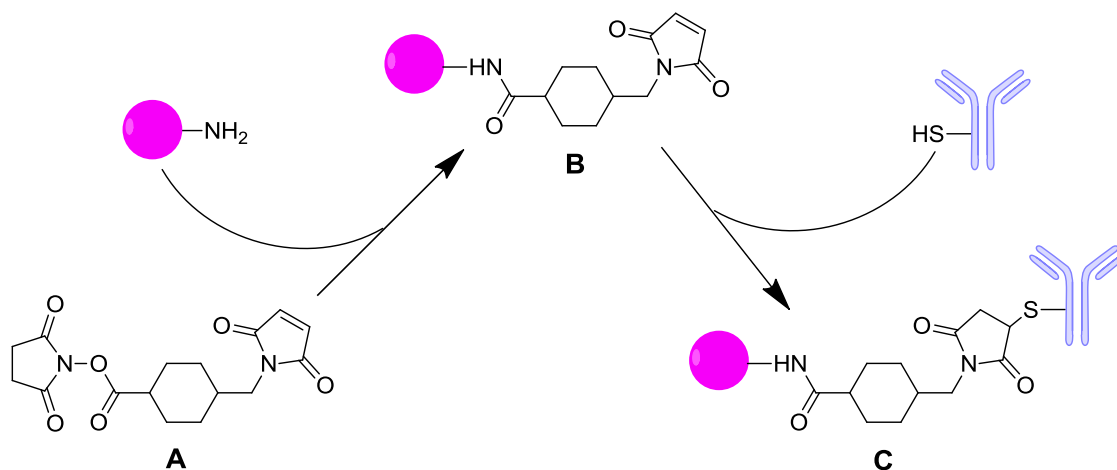
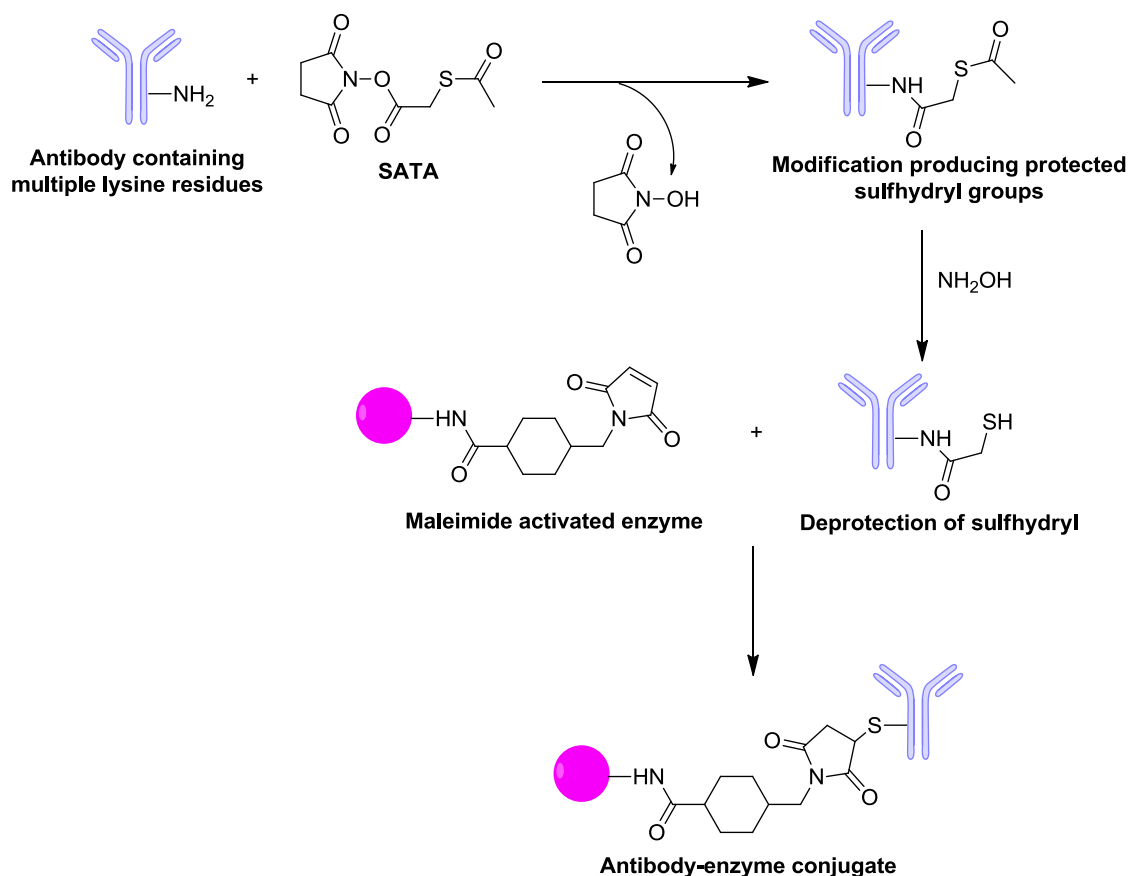


**Figure 1.13** Common heterobifunctional linkers.

In the case of all these linkers, the NHS ester moiety is generally first reacted with the amino group of a lysine residue of a protein or other functional molecule at a slightly alkaline pH (normally pH 7.5). Thus an amide bond is generated and the protein or other functional molecule is joined to active maleimide groups. Following purification the maleimide activated protein or functional molecule can be reacted with the thiol groups of an antibody. This process is shown in *Scheme 1.1*. The free sulfhydryl groups on the antibody may be endogenous or chemically introduced. Endogenous thiols are commonly obtained through incubation of the antibody with a reducing agent, cleaving the interchain disulfide bonds in the hinge and switch regions to reveal the requisite sulfhydryls. Chemical introduction is achieved using thiolation reagents such as *N*-succinimidyl-*S*-acetylthioacetate (SATA) to modify the intact antibody, again utilising the reaction of lysine residues with an NHS ester (*Scheme 1.2*).



**Scheme 1.1** Use of heterobifunctional reagent SMCC (**A**) to generate an antibody conjugate (**C**). SMCC (**A**) is first reacted with the lysine residues of e.g. an enzyme, or the amine group of another functional molecule, e.g. a drug (pink). This generates **B**, an enzyme or drug with an active maleimide group attached. Subsequent addition of an antibody or antibody fragment with a free thiol group yields the antibody conjugate **C**. Addition of one SMCC molecule is shown here for simplicity; in reality multiple SMCC molecules react with multiple amine groups, and subsequently react with multiple thiols.



**Scheme 1.2** Chemical introduction of thiols to produce e.g. an antibody-enzyme conjugate. Available lysine residues on an antibody may be modified with the NHS ester of SATA reagent to produce protected sulfhydryls. Following deprotection with hydroxylamine at alkaline pH, conjugation to a maleimide protected enzyme can proceed.

A fundamental issue with current available methods for the chemical modification of antibodies, particularly in the production of antibody-protein conjugates, is the dependence upon lysine residues. Amine groups are plentiful in most proteins; in fact there are an average of 100 lysine residues per antibody and their distribution within the three-dimensional structure is nearly uniform throughout the surface topology of the Fab and Fc regions. As such, conjugation techniques using lysine residues will randomly cross-link to virtually all areas of the antibody molecule, resulting in a highly heterogeneous mixture of products. One such example is the conjugation of antibody huN901, which contains 86 lysine residues, with a drug molecule. Characterisation by mass spectrometry and peptide mapping revealed a two-fold heterogeneity in the conjugate; first, antibody conjugates were formed with between 1 and 6 drug molecules attached and second, antibodies with the same drug loading were conjugated by

---

different lysine residues (102). In fact, 40 different lysine residues were involved in these conjugates. Hence there are potentially  $10^6$  antibody-drug conjugates present (103). In addition, within these heterogeneous mixtures there is random orientation of the antibody within the modified structure and so the surface of another attached protein or molecule may block antigen binding sites. This produces a conjugate with decreased antigen binding activity compared to the unmodified antibody (102-105). This is also the case for conjugated enzymes, as the modification may occur at residues essential for protein function. Furthermore the use of heterogeneous mixtures in therapeutics is far from optimal, as each component of the mixture will have a different pharmacological profile (103,106). Certainly for the production of ADCs by lysine modification a complete lack of stoichiometric control is observed, which leads to typical distributions of zero to eight drug molecules per antibody (107). Thus such conjugates often have a narrow therapeutic window (108) as well as over modification of a charged residue such as lysine resulting in decreased solubility and faster blood clearance rates (109,110). As a result regulatory approval is increasingly requiring homogeneity in biologicals.

## **1.8.2 Site-directed conjugation**

Bioconjugation to antibodies is generally more successful at maintaining biological activity if the functional groups used are present in low quantities and at particular sites on the molecule. A “site-directed conjugation” approach joins cross-linking reagents with residues that are present only at discrete positions on the antibody surface, distant from antigen binding sites. Such approaches use existing knowledge of antibody structure to determine where a chemical entity can be attached to the immunoglobulin without interfering with its binding potential. The conjugated products of these strategies are therefore generally more successful in maintaining antibody activity.

### **1.8.2.1 Reduction of interchain disulfides**

Unlike lysine residues, there are no free cysteine residues in antibodies, the side chain of which is commonly used in protein modification owing to its nucleophilic sulfhydryl. Antibodies do however contain disulfide bonds in the hinge region between the heavy-heavy chains and between the heavy-light chains in the Fab fragment (switch region). These interchain disulfides are distant to the antigen binding sites and so conjugation of proteins or molecules at the generated cysteine residues generally avoids the blocking of antigen binding regions, thus maintaining antibody activity.

---

A common strategy for antibody interchain disulfide bond reduction is to use the reductant 2-mercaptoethylamine (2-MEA). This relatively mild reducing agent has been used for many years for the reportedly selective cleavage of the interchain disulfides in the hinge region. Current improved analytical techniques have shown however that 2-MEA is not fully selective for the hinge region disulfides, though it is still sold commercially by some companies as a selective reducing agent. Sun *et al.* revealed that treatment with 2-MEA produces a nearly 1:1 mixture of antibody where the heavy-light chains have been reduced and that where only the hinge region heavy-heavy chains have undergone reduction (111).

Different reducing agents do demonstrate some preference for particular interchain disulfides, however this is not simple to control and appears to depend on a number of variables including concentration of protein and temperature (111). Despite this, the interchain disulfide reduction strategy holds significant advantages over lysine modification; it is a step towards control of conjugation location and so the production of homogenous conjugates (*Figure 1.14*). One of the two clinically approved ADCs currently on the market, Brentuximab vedotin, is obtained through a partial reduction approach (112). Despite this approach being site-specific compared to lysine modification, a heterogeneous ADC still results, containing between 0 and 8 drugs per antibody with a species holding 4 drugs being the predominant species. In addition, disulfide bonds play an important role in both the activity and stability of antibodies (103,113). Intact disulfides are necessary to stabilise antibodies when exposed to heat or chaotropic substances, and so their absence can lead to significant aggregation during storage (114,115). Furthermore, it has been demonstrated by both reduction and mutation approaches that the hinge region disulfides are essential for Fc mediated effector functions, including ADCC and CDC (116-120). Therefore the ideal solution would be to use reagents that modify these native disulfide bonds whilst retaining a bridge between the two cysteine residues, maintaining this key stabilising feature (see *Section 1.8.3*).

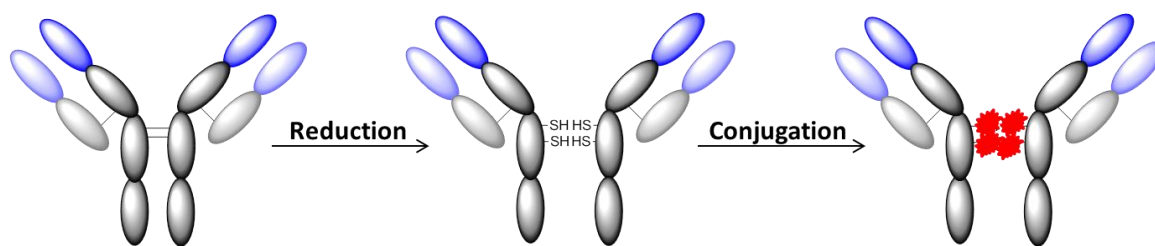


**Figure 1.14** Drug conjugation to cysteine residues by partial reduction of interchain disulfides. A partial reduction approach yields less heterogeneity as the drugs are attached at defined sites. However, an average drug loading of 4 is still obtained due to the presence of small amounts of ADC with 0, 2, 6 and 8 drugs attached.

### 1.8.2.2 Oxidation of carbohydrate chains

Antibodies are often glycosylated on the  $C_{H2}$  domains of the Fc fragment. Another popular site-directed conjugation approach involves the oxidation of these polysaccharides with sodium periodate to generate free aldehydes. These aldehyde groups can then be reacted with hydrazide-containing cross-linking reagents, or molecules directly connected to the hydrazide group e.g. biotin-hydrazide. This method is generally very successful at maintaining the antigen binding activity of the antibody, since the site of conjugation is far removed from the variable fragments. However, a clear limitation of this strategy is the requirement for antibodies to be glycosylated. Although polyclonal antibodies obtained from antisera are normally glycosylated, monoclonals obtained using hybridoma technology are often not post-translationally modified (121). Antibodies and antibody fragments produced in bacteria are also free of carbohydrate.

### 1.8.2.3 Cysteine introduction by mutagenesis

As mentioned in *Section 1.8.2.1*, in contrast to lysine residues, there are no free cysteines in antibodies. Hence, the introduction of a cysteine by mutagenesis can be used to provide a single point of attachment in this “site-directed conjugation” approach (103,106,122-124). In 2008, Genentech achieved a site-specific ADC through introducing cysteine substitutions at designated positions on an antibody, termed a ‘Thiomab’ (*Figure 1.15*) (103). These engineered cysteine sites were chosen to produce reactive thiol groups without affecting the folding or assembly of the antibody, nor the antigen binding ability. This ADC was restricted to two drug molecules per antibody and was shown to possess similar activity to randomly labelled ADCs which can hold up to eight drug molecules. Furthermore, it was demonstrated to have a greater

therapeutic index and improved pharmacokinetic properties in rodents. The results of this study further demonstrate that site selective chemical conjugation and stoichiometric control are key to the future of ADC therapeutic success. However, this approach is not without limitations, as cysteine mutagenesis commonly leads to reduced expression yields and undesirable properties such as susceptibility to dimerisation, mixed disulfide formation or disulfide scrambling (103,122,125-127).

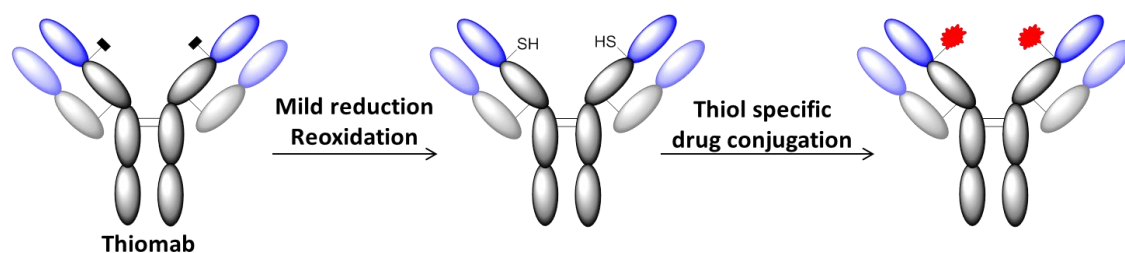


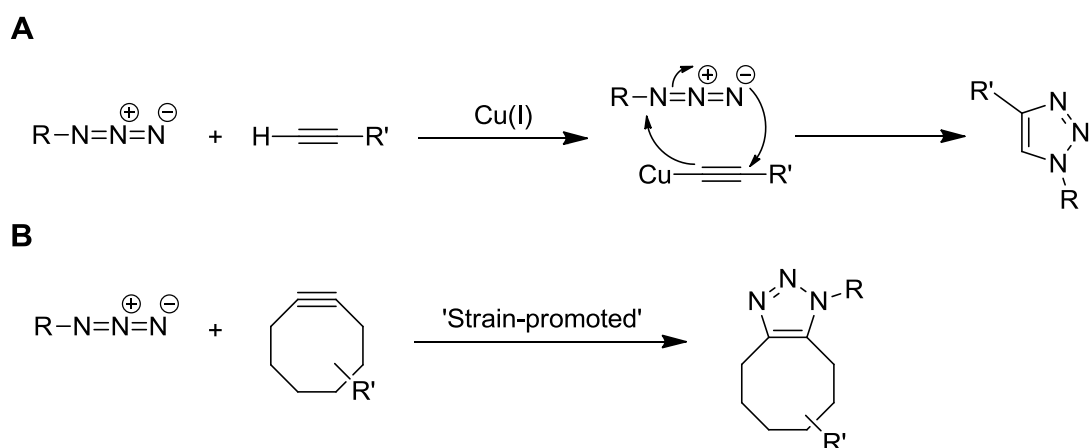
**Figure 1.15** Generation of a site-specific ADC using a Thiomab; a mAb carrying an A114C mutation in the heavy chain. The introduced cysteines are capped by either cysteine or glutathione. Mild reduction followed by reoxidation produces two free thiols without disturbing the correct formation of the interchain disulfide bonds. These thiols can then be used to generate a homogeneous ADC (uniform drug loading of 2 per mAb).

#### 1.8.2.4 Bioorthogonal reagents

In recent years, several chemical reactions have been developed that are orthogonal to the functional groups present in proteins. Through incorporating a bioorthogonal functional group into an antibody, unprecedented conjugation selectivity to other functional molecules containing a specific reaction partner has been achieved. The leading reaction in this field of bioorthogonal chemistry is the azide-alkyne [3+2] cycloaddition, often referred to as a ‘click’ reaction.

The motivation behind click chemistry was to produce a reaction that would ensue rapidly under ambient conditions to achieve a single product in high yield (128). In order for such a reaction to occur, a high thermodynamic driving force is required that is orthogonal to any other functional groups present. For this reason, the azide group is perhaps the most popular bioorthogonal click reagent; it is highly reactive but in a selective manner, in addition to being inert in the biological environment. Selective [3+2] cycloaddition between an azide and an acyclic alkyne was first described by Huisgen (129); however this required large amounts of heat in order to form the

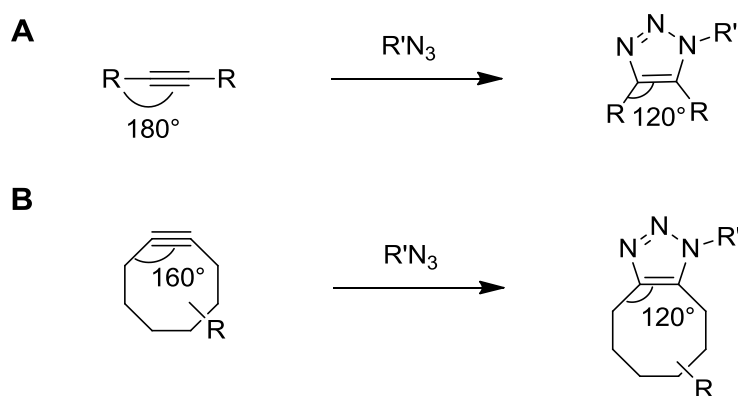
corresponding triazole. The click chemistry vision was realised in 2002 when Sharpless *et al.* and Meldal *et al.* simultaneously reported a dramatic acceleration in the rate of reaction through the use of copper(I) catalysts (130,131) (*Scheme 1.3A*). In addition, the copper-catalysed cycloaddition shows greater reaction scope, tolerates aqueous conditions and a range of pH, and has improved chemo- and regioselectivity (132). This highly selective and rapid cycloaddition was hampered in its use however by the requirement for copper; protein damage was observed at the high metal concentration necessary for efficient labelling (133). Other metal-free bioorthogonal reactions were developed, including the Staudinger ligation which consists of the covalent ligation of phosphines to azides. Unfortunately these reactions are slow and the oxygen sensitivity of phosphines limits their use in biological applications. Then in 2004, a new generation of click chemistry was born, when Bertozzi *et al.* introduced strain-promoted azide-alkyne cycloaddition (SPAAC) (134) (*Scheme 1.3B*).



**Scheme 1.3** Click reactions (A) Copper-catalysed azide-alkyne cycloaddition (CuAAC); (B) Strain-promoted azide-alkyne cycloaddition (SPAAC).

The incorporation of an alkyne into a strained cyclooctyne ring system dramatically increases its intrinsic reactivity; the bond angles of sp-hybridised carbons in cyclooctynes are  $\sim 160^\circ$  and so less distortion energy is required to move towards the transition state of the cycloaddition reaction (*Scheme 1.4*). In fact, the significant deformation of the acetylene bond angle accounts for approximately 18 kcal/mol of ring strain (135). Thus resulting reactions with azides can occur at rates comparable to the copper-catalysed click. A number of strained cyclooctynes have successfully been applied as bioorthogonal reagents, including DIFO, DIBO, DIBAC and BARAC (136-138) (*Figure 1.16*). The application of strained cyclooctynes has been slightly mired by

their lengthy and difficult synthesis and consequent lack of commercial availability. Although the dibenzocyclooctynes are somewhat simpler to synthesise, these suffer from increased lipophilicity and consequently non-specific binding to proteins. More readily available strained cyclooctynes are being developed, with bicyclo[6.1.0]nonyne (BCN) being particularly successful (139) (*Figure 1.16*). Such bicyclononyne derivatives are  $C_s$  symmetrical and exhibit excellent kinetics in SPAAC reactions, and can be obtained through the cyclopropanation of the low-cost 1,5-cyclooctadiene. A major advantage of the  $C_s$  symmetry of BCN, particularly in comparison to other popular cyclooctynes such as DIFO, is the formation of a single regioisomer upon cycloaddition. This is crucial for future therapeutic applications of this conjugation chemistry, including ADEPT and ADCs, where the formation of homogeneous products is desired.



**Scheme 1.4** Click reactions (A) A comparison between the bond angles of linear alkynes and triazoles; (B) A comparison between the bond angles of strained cyclooctynes and its corresponding triazole product.

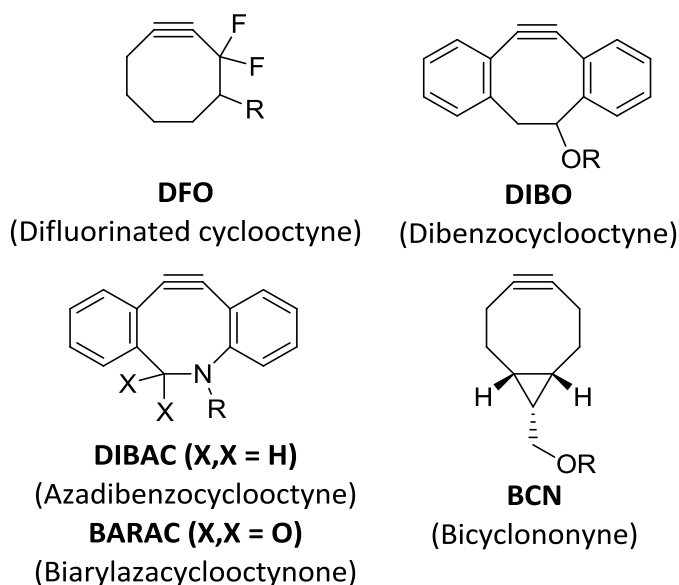
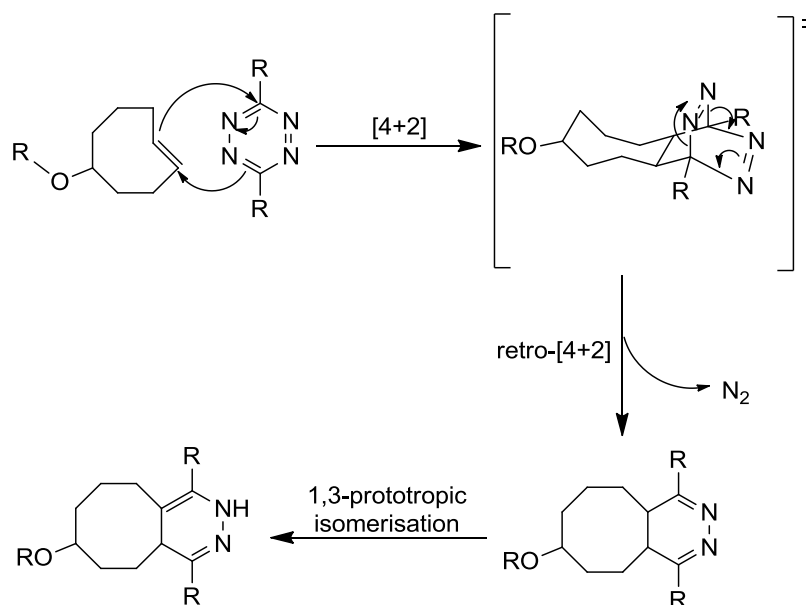


**Figure 1.16** Structures of commonly employed cyclooctynes.

Another bioorthogonal reaction that occurs with high reaction rates and in good yield without requiring metal catalysis is the strain-promoted inverse-electron-demand Diels-Alder cycloaddition (SPIEDAC). Tetrazines are exceptional dienes, reacting irreversibly with a diverse range of strained alkenes and alkynes in this retro-[4+2] cycloaddition to yield  $N_2$  as the only byproduct (*Scheme 1.5*). The most reactive dienophile is *trans*-cyclooctene and a variety of these reagents are currently being used in bioorthogonal reactions. This click variant carries some practical advantages over the SPAAC reaction. The *trans*-cyclooctene starting materials are easily accessible from commercially available *cis*-cyclooctenes, and unsymmetrical tetrazine can be synthesised on a large scale from hydrazine with commercially available cyanopyridines. In addition, several functionalisable handles can be incorporated into the tetrazines. The compatibility of SPIEDAC with strained cyclooctynes has recently been demonstrated using BCN, in which the alkyne demonstrated a comparable rate of reaction to a range of strained cyclooctenes (140). In fact, current literature suggests that BCN reagents are proving to be the key tool in bioorthogonal click chemistry (91,140). Many fluorescent and fluorogenic dyes are commercially available or readily synthesised as the azide or tetrazine derivative, hence using a cyclooctyne reagent that can react with both would be a powerful tool for many biological applications.



**Scheme 1.5** Inverse-electron demand Diels-alder reaction of strained *trans*-cyclooctene.

---

#### 1.8.2.4.1 Introduction of unnatural amino acids

For bioorthogonal click reactions such as SPAAC and SPIEDAC to be used in the production of homogeneous protein conjugates, individual functionalities must first be introduced to the proteins site-specifically. One approach is to introduce an unnatural amino acid (UAA) into the protein(s) to be conjugated, thus providing a means of site-specific protein functionalisation. Schultz *et al.* recently produced a homogeneous anti-HER2/anti-CD3 Fab bispecific using this approach (91). Using an evolved tRNA/aminoacyl-tRNA synthetase pair in response to an amber nonsense codon, *p*-acetylphenylalanine residues were introduced into each Fab site-specifically. These site-specific residues could then be reacted with alkoxyamine linkers containing azide or cyclooctyne moieties. The subsequent click reaction of these two Fab fragments produced bispecifics with excellent activity *in vitro*, with no loss of antibody binding activity or stability. Thus this combined approach has successfully produced a chemically linked, site-specific, homogeneous antibody conjugate in good yield.

Developments in mutation technology in the last decade have made it possible to incorporate almost any functionality into a protein through site-specific genetic encoding of unnatural amino acids. This can be achieved by codon reassignment (141,142) or suppression of the amber stop codon (143,144). Thus it was envisaged that copper-free click chemistry could be used to generate protein conjugates using artificial amino acids containing cyclooctyne and azide functionalities. Installing azide groups has proved problematic, since they can be reduced during the lengthy *in vivo* expression and purification steps (145). However, Schultz *et al.* recently successfully installed a variety of cyclooctene and a cyclooctyne containing UAAs into *E. coli* and mammalian cells through suppression of the amber stop codon (91,140). The bioorthogonal reaction of these with azide and tetrazine labelled fluorescent and fluorogenic dyes was subsequently demonstrated. This technique has great potential, particularly in cellular imaging, as it will facilitate site-specific labelling of proteins with small photostable fluorophores in mammalian cells, negating the need for large fluorescent proteins with less favourable photophysical properties.

#### 1.8.2.4.2 Enzymatic labelling of antibodies

In recent years, chemo-enzymatic methods for the site-specific modification of antibodies have become an increasingly active and developed area of research (146).

---

One such popular tool for site-specific modification is ‘sortagging’, which refers to the use of the enzyme sortase for protein labelling. Harrenga *et al.* successfully demonstrated the conjugation of a single fluorophore to a Fab fragment using Sortase A (SrtA) (147). This recognises the pentapeptide sequence LPXTG, which was incorporated at the C-terminus of the Fab fragment light chain. Upon recognition, SrtA cleaves the bond between the threonine and glycine residues generating a thioester between a cysteine of SrtA and the Fab fragment. This thioester subsequently underwent aminolysis with the addition of a fluorescent oligoglycine probe in good yield. A key limitation of sortagging is its reversibility; the glycine residue released by enzyme cleavage can act as nucleophile, reforming the original protein species. To overcome this, Turnbull *et al.* generated a depsipeptide where an ester replaces the amide bond between the threonine and glycine of the pentapeptide recognition sequence (148). It was envisaged that the hydroxyacetyl byproduct would not be a substrate for the reverse reaction, rendering it irreversible. Indeed this strategy vastly improved reaction efficiency, enabling 100% conversion to the desired product using just a 1:1 ratio of the two peptide starting materials. Thus the sortagging approach can now be used without the requirement for excess amounts of protein or peptide for sufficient labelling. The key advantage of this approach is that no limitations have been observed in the size of the modification that maybe introduced, avoiding the requirement for a two-step chemo-enzymatic strategy (101). However, it is limited to N-terminal modifications, which is not ideal for every antibody or antibody fragment.

A number of two-step chemo-enzymatic approaches have recently successfully generated homogeneous antibody-protein or antibody-small molecule conjugates in good yield. For example, Bertozzi *et al.* achieved homogeneous chemical conjugation of whole human IgG to human growth hormone (hGH) and maltose-binding protein (MBP) using formylglycine generating enzyme (FGE) in combination with copper-free click chemistry (90). This was achieved through introducing the five-residue sequence (CXPXR) recognised by FGE at specific sites in the antibody. During protein expression in *E. coli* or mammalian cells, FGE subsequently oxidises the cysteine in this sequence to the aldehyde residue formylglycine (fGly). This site-specific aldehyde tag can then be functionalised with a bioorthogonal reagent for further conjugation. Using this strategy, Bertozzi *et al.* successfully site-specifically conjugated human IgG functionalised with two strained alkynes to either hGH or MBP containing a single azide group (90).

---

Another family of enzymes, the transglutaminases, have recently been applied to generate homogeneous antibody-small molecule conjugates. In one such example, Schibli *et al.* used microbial transglutaminase (MTGase), which forms isopeptidic bonds between glutamine and primary amines, to obtain homogeneous antibody-drug conjugates (*Figure 1.17*) (149). MTGase has previously been shown to selectively recognise the Gln295 residue in the heavy chain of deglycosylated IgG molecules (150). Modification of Trastuzumab using MTGase and a small azido-PEG-amine linker generated antibody with two sites for selective attachment in quantitative yield. Subsequent addition of only 2.5 equivalents of strained alkyne functionalised drug gave the desired homogeneous antibody-drug conjugate. Thus this chemo-enzymatic approach generated an ADC with an exact DAR of 2 using minimal amounts of toxic drug, a crucial advantage when producing ADCs on a large scale. This combined approach can be transferred to any IgG1 molecule and will surely be a powerful tool in the development of the next generation ADCs.

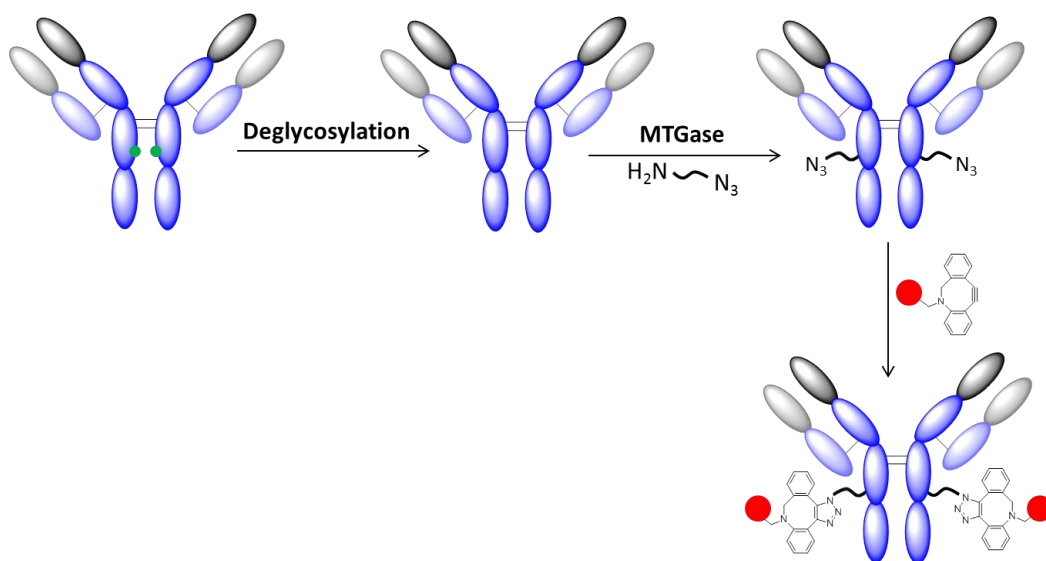


**Figure 1.17** Generation of a site-specific ADC using microbial transglutaminase (MTGase). Following deglycosylation, the antibody can be site-specifically modified at Gln295 by MTGase to incorporate two azide functionalities. Strained alkyne functionalised drug molecule (red circle) can then be directly attached to achieve a well-defined ADC with a DAR of 2.

The use of bioorthogonal reagents in combination with unnatural amino acids and enzymatic labelling has provided an excellent route to homogeneous, site-specific

---

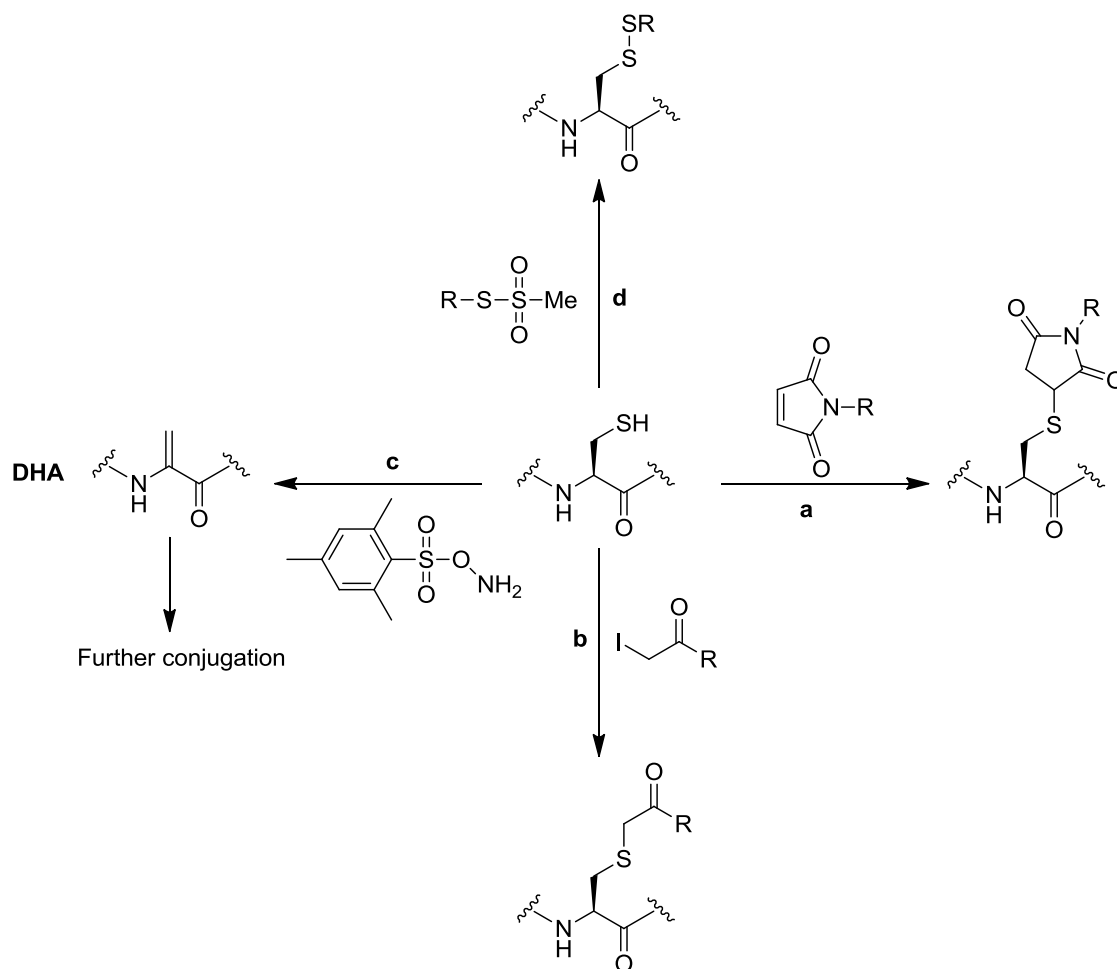
antibody conjugates. Whilst this technology is elegant, it is not without limitations. The kinetics of many bioorthogonal reactions are still comparatively slow (151,152), thus requiring high reagent concentrations (153) and often resulting in non-quantitative conversion (154,155). In addition, the introduction of unnatural amino acids or sequences for enzymatic labelling is not easily transferred; each antibody to be conjugated must undergo prior investigation to determine appropriate mutation sites, the site of introduction may be restricted e.g. to the N- or C-terminus, and in the case of unnatural amino acids substitution is often incomplete and expression yields are generally low due to the cellular toxicity of artificial amino acids at the high concentrations necessary (156,157). To avoid these difficulties, an ideal site-directed conjugation technique would use residues natural to the protein that are revealed for modification only under defined conditions.

### **1.8.3 Bridging of disulfide bonds: a new class of reagents**

Currently, insertion of unnatural amino acids and enzymatic labelling for the site-specific introduction of bioorthogonal click chemistry reagents has proved the most successful strategy for producing homogenous antibody conjugates in high yield. It would be ideal if site-directed conjugation could be simplified and use residues natural to the protein. As previously discussed, cysteine residues have a low natural abundance in proteins, constituting only 0.2% of naturally occurring amino acids (158), and are often found tied up in disulfide bonds (159). In the case of antibodies and antibody fragments there are no free cysteine residues, and site-directed conjugation has been attempted via interchain disulfide bond reduction and subsequent conjugation of the free cysteines (see *Section 1.8.2.1*). However disulfide bonds in antibodies, and in the majority of proteins, play an essential role in both their activity and stability (103,113,115). Therefore the ideal solution would be to use reagents that bridge native disulfide bonds, maintaining this key stabilising feature.

Chemical modification reagents targeting individual cysteine residues are well-established and regularly used to generate bioconjugates. Popular cysteine modification reagents include  $\alpha$ -halocarbonyls, Michael acceptors such as the maleimide, and activated disulfides (*Scheme 1.6*). In addition, dehydroalanine (DHA) can be formed by the activation and subsequent elimination of a cysteine

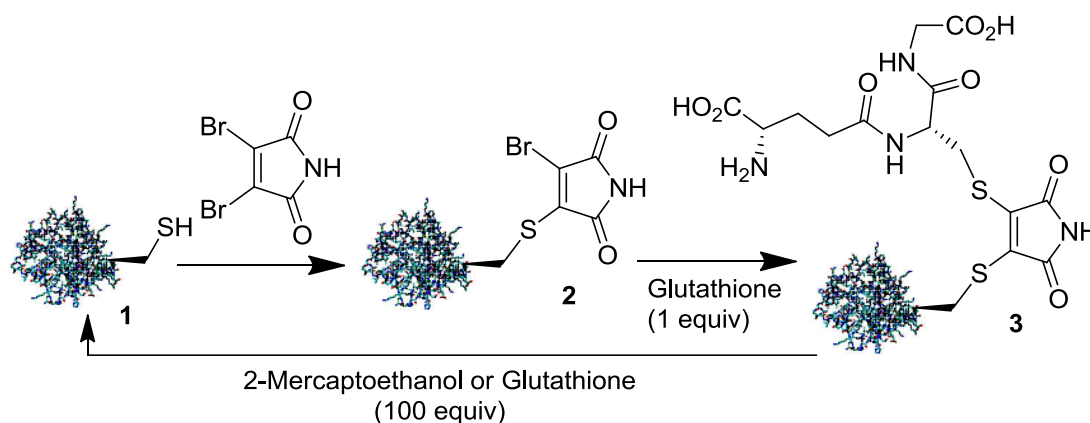
residue, providing a unique site for further modification (160) (Scheme 1.6c).



**Scheme 1.6** Reagents widely used for the modification of cysteine a) maleimides; b)  $\alpha$ -halocarbonyls; c) formation of dehydroalanine (DHA); d) disulfides.

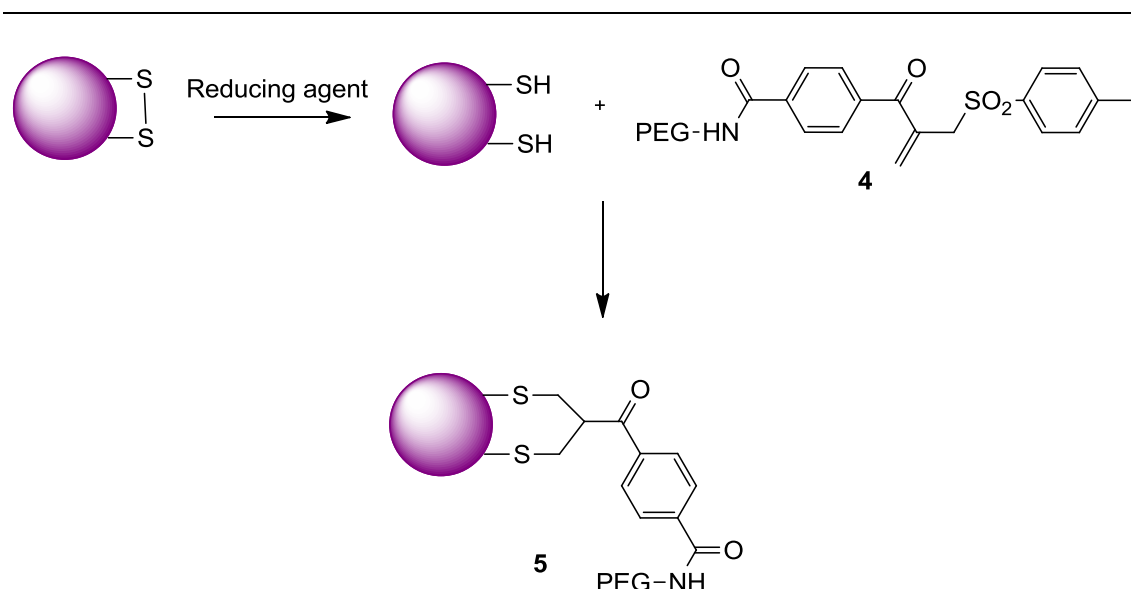
Maleimides are perhaps the most widely employed reagents for cysteine modification (161), undergoing rapid and highly selective reactions with thiols over a wide pH range (161-64). However traditional maleimides suffer from limitations. They are generally considered to react irreversibly, preventing cleavage to regenerate the unmodified protein. Making this reaction reversible would be highly advantageous as it would allow for the temporary modification of proteins, which may be desirable for *in vitro* or *in vivo* applications. Recent literature has observed that maleimides conjugated to small molecule thiols can undergo retro and exchange reactions in the presence of free thiol at physiological pH and temperature (165). However, this is very slow and not a convenient protocol for reversibility. Maleimides are further limited by possessing only two points of attachment for bioconjugation. Hence only two entities of interest can be linked to each other via the maleimide, and it is not able to effectively bridge a disulfide bond. In the Baker

and Caddick groups we have recently reported a new class of maleimides, of which the bromomaleimides are the parent members, that provide new opportunities for protein modification at cysteine residues. These new reagents enable rapid, selective, and reversible modification of cysteine, and efficient and facile construction of triconjugates. The application of both mono- and dibromomaleimides has been demonstrated through single amino acid and protein studies (166-171). It is the incorporation of leaving groups such as bromine across the maleimide double bond that allows an addition-elimination sequence to take place on reaction with cysteine. For example, as shown in *Scheme 1.7*, the addition of dibromomaleimide to the L111C mutant of the Grb2 protein **1** formed the monobromide **2** exclusively. Bioconjugate **2** could then undergo a further thiol addition with glutathione to afford dithiomaleimide bioconjugate **3**. Both of these steps are near quantitative and reversible, as they can be cleaved using a large excess of a thiol including 2-mercaptoethanol or glutathione.



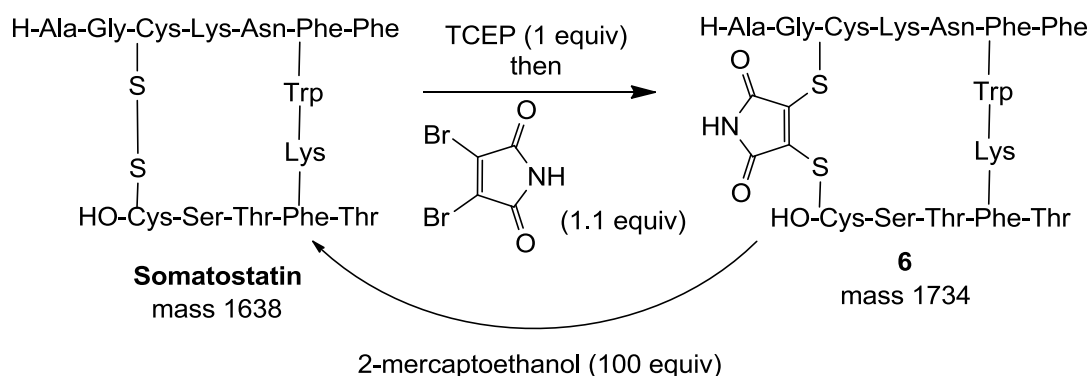
**Scheme 1.7** Reversible modification of the Grb2 SH2 Domain (L111C) with Dibromomaleimide (167).

In 2006, Brocchini *et al.* reported an enone-sulfonyl reagent **4** that provided the first example of a reagent that mimicked the role of a disulfide bond, installing a 3-carbon bridge between the two cysteine residues (172-174) (*Scheme 1.8*). It was envisaged that dibromomaleimides could also serve as disulfide bridging reagents and provide significant advantages. These include rapid reaction rate, no introduction of a chiral centre, installation of a rigid two-carbon bridge minimising disulfide bond disturbance, and reversibility of disulfide bridging.



**Scheme 1.8** Modification of protein (purple) disulfide bond using a PEG-monosulfone reagent. The disulfide bond must be reduced before conjugation.

The disulfide bridging ability of this new class of maleimides was initially investigated using the cyclic peptide hormone somatostatin as a model system (167). This is a 14-amino acid peptide containing a single disulfide bond. Treatment of somatostatin with 1 equivalent of the reducing agent TCEP (tris(2-carboxyethyl)phosphine) followed by just 1.1 equivalents of dibromomaleimide, yielded fully bridged somatostatin **6** (Scheme 1.9). Furthermore, incubation of the fully bridged peptide with 2-mercaptoethanol for 1h at rt gave complete reversion to reduced somatostatin. Thus, dibromomaleimides were successfully demonstrated to be the second class of reagents suitable for disulfide bridging, and the first to facilitate reversibility.



**Scheme 1.9** Reversible modification of the disulfide bond of somatostatin by dibromomaleimide (167).

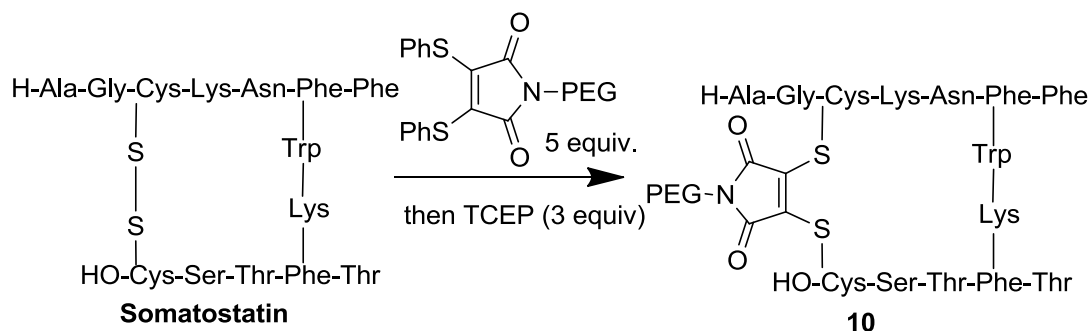
---

Both the stepwise bridging protocol initially developed using dibromomaleimides and the related procedure described by Brocchini and co-workers (166-175) suffer a potential limitation. These methods require cleavage of the disulfide bond with reducing agents releasing two free cysteines to which the bridging reagent can then be added. It is possible that in the time between disulfide cleavage and completion of the bridging reaction structurally sensitive proteins may begin to unfold. Moreover, even in the case that disulfide bond opening does not cause any immediate problems, the presence of free thiols in a structure can lead to aggregation and disulfide scrambling (176). Thus the ideal bridging protocol would require a bridging reagent that can be used in tandem with a reducing agent, in order for disulfide bridging to occur immediately on thiol release. To this end, an *in situ* protocol was developed using a selection of new 3,4-substituted maleimide reagents (168).

Development of an efficient *in situ* bridging protocol required substituted maleimides that would tolerate the presence of the reducing agent TCEP. Test reactions suggested that halomaleimide reagents, for example dibromomaleimide and diodomaleimide, show greater cross-reactivity with TCEP than thiomaleimides (168). In light of this, several dithiomaleimide reagents have been synthesised, and dibromomaleimide **8** and dithiophenolmaleimide **9** were used for comparison in the *in situ* trial studies (*Scheme 1.10*) (168). In each case, 5 equivalents of 3,4-substituted maleimide were added to somatostatin, followed by varying quantities of TCEP. For dibromomaleimide, up to 60% bridged somatostatin was observed. Full conversion was prevented by the formation of TCEP-dibromomaleimide adducts, as observed by mass spectrometry. Dithiophenolmaleimide and TCEP however, gave fully bridged somatostatin within 20 minutes. Therefore, through the creation of a compatible bridging reagent, the *in situ* protocol was realised. Dithiophenolmaleimide is thus the first reagent to facilitate efficient *in situ* bridging of disulfide bonds.

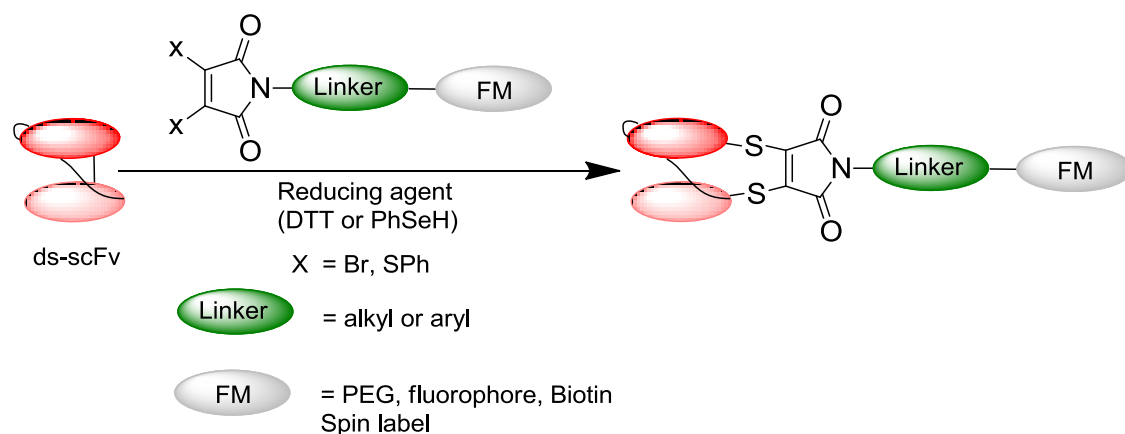


substituted maleimide bridged conjugates of somatostatin maintained activity. Furthermore, a fluorescein-maleimide was also used to bridge the disulfide of somatostatin and this too demonstrated sustained activity. This early evidence suggests that the 3,4-substituted maleimides are a new class of disulfide bridging reagents, successfully avoiding the negative effects previously associated with disulfide bond modification.



**Scheme 1.11** *In situ* modification of the disulfide bond of somatostatin with *N*-PEG dithiophenolmaleimide (168).

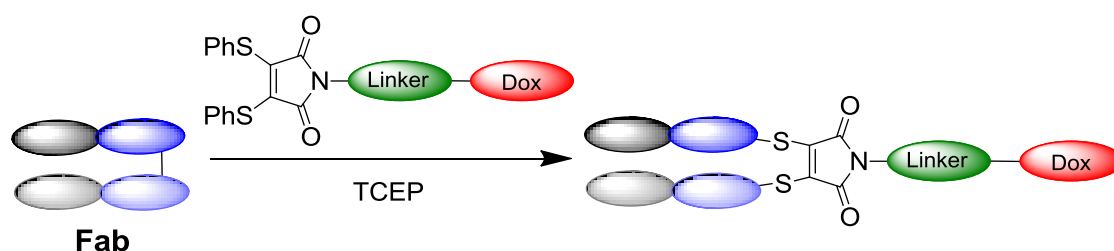
This *in situ* approach has recently been applied to more complex protein systems, for example the artificial disulfide bond of an anti-carcinoembryonic antigen (CEA) scFv antibody fragment (ds-scFv) (170). The scFv disulfide has been bridged selectively and quantitatively with a range of labelled 3,4-substituted maleimides, including fluorescein, biotin, a 5 kDa PEG chain and even a spin label (170) (*Scheme 1.12*). These conjugates have been demonstrated to maintain full binding activity by ELISA and Biacore assays, as well as functionality of the modifications. Having demonstrated that this bridging technology is reversible in the presence of excess thiol, the stability of bridged scFv in human plasma was next investigated.



**Scheme 1.12** The *in situ* bridging of the disulfide bond of an anti-CEA ds-scFv.

Human plasma typically contains around 18  $\mu\text{M}$  of free thiol. The modified scFv was incubated in plasma for 7 days at physiological temperature. Gratifyingly, the antibody fragment could be isolated in constant amounts and LCMS spectra of the samples revealed no loss of the maleimide bridge over time (170). In addition, the modified fragment retains 80% of its binding activity after 7 days incubation. The bridged scFv was also incubated in buffer containing the concentration of glutathione or other reducing agent found in the cytoplasm (7 mM). This resulted in a loss of the maleimide bridge over time (for glutathione 40% loss over 50 h), providing early evidence of a possible intracellular cargo-release mechanism for antibodies modified with the maleimide bridging technology under *in vivo* conditions.

Recently, the Baker and Caddick groups have also reported the modification of the Fab fragment of Trastuzumab with a single molecule of the drug doxorubicin (171). Generation of a homogeneous antibody-drug conjugate was achieved through linking doxorubicin to a dithiomaleimide. In the presence of TCEP, the single interchain disulfide bond of the Fab fragment was bridged quantitatively (*Scheme 1.13*). The bridged conjugate displayed comparable antigen binding to unmodified Fab by ELISA.

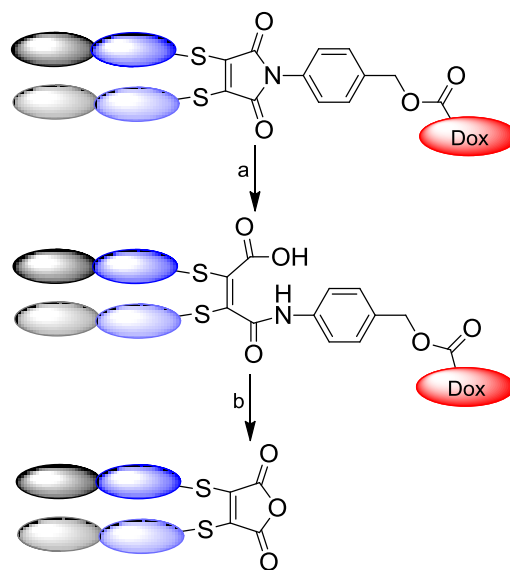


**Scheme 1.13** The modification of anti-HER2 Fab with an *N*-arylthiophenolmaleimide-PABC-doxorubicin linker to yield a homogeneous antibody-drug conjugate.

The linker chemistry of the ADC generated in *Scheme 1.13* was carefully designed. Previous research has demonstrated that the hydrolysis of *N*-aryl functionalised substituted maleimides can be judiciously controlled by pH, with the maleamic acid derivative being readily generated at pH 7.4 (169). At acidic pH, maleamic acids are labile. Thus this provides a direct route to controlled cargo release of the amine linked through the amide functionality. An antibody fragment functionalised with *N*-aryl substituted maleimide would therefore maintain its cargo at physiological pH and temperature, whilst readily cleaving at lysosomal pH to release the drug (*Scheme 1.14*). To achieve this, the linker used for the anti-HER2 Fab-doxorubicin conjugate contained

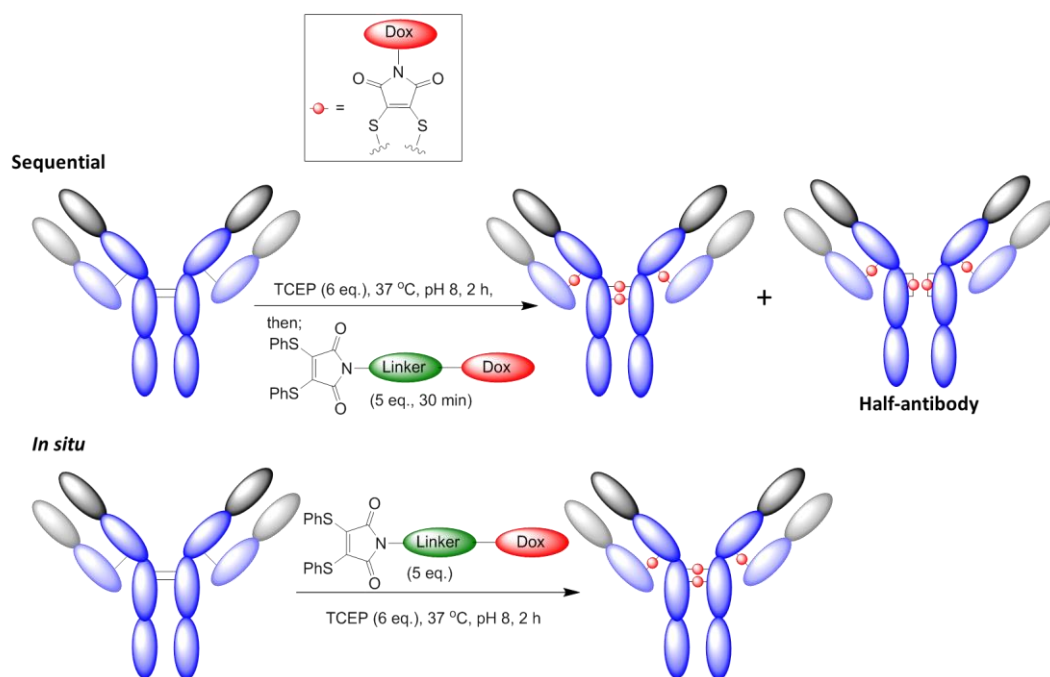
---

*N*-aryl maleimide linked to doxorubicin via the known self-immolative *p*-aminobenzyloxycarbonyl (PABC) spacer (179).



**Scheme 1.14** Cleavage of Fab ADC. (a) pH 7.4, 20 h; (b) pH 4.5, 72 h.

Following the successful modification of ds-scFv and Fab antibody fragments without loss in biological activity, the next generation maleimides were recently applied to full antibodies. Two ADCs, Kadcylya and Adcetris, have been approved for use in the clinic. Many more ADCs have failed in the development stages, often due to detrimental effects of the employed conjugation chemistry. It was envisaged that disulfide bridging using substituted maleimides would overcome many of these issues, providing site-specific modification to deliver a homogeneous ADC whilst maintaining the stabilising effect of interchain disulfide bonds. Both sequential and *in situ* conjugation strategies were applied to the monoclonal IgG1 antibody Trastuzumab (*Scheme 1.15*) (180).

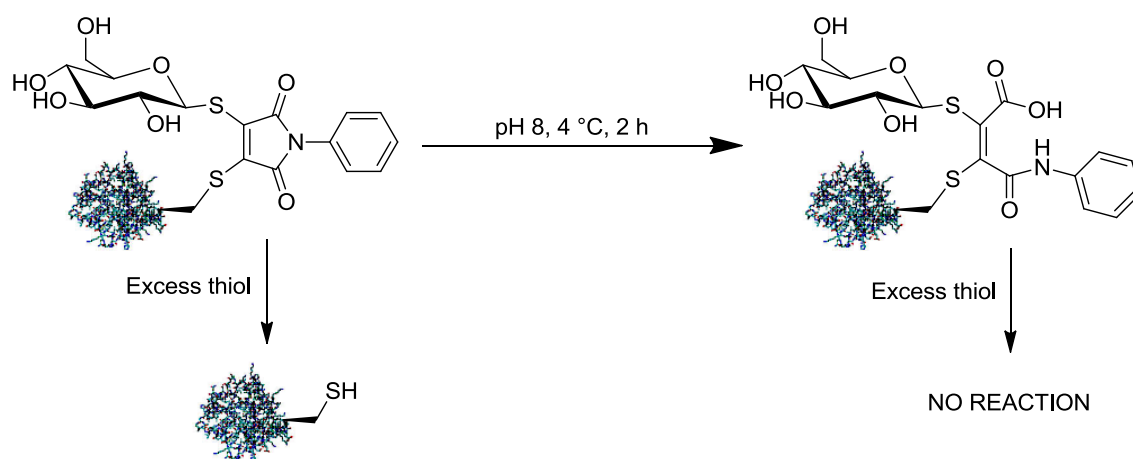


**Scheme 1.15** Construction of ADCs using substituted maleimides via sequential and *in situ* approaches. The sequential bridging protocol yielded a mixture of correctly bridged ADC and incorrectly bridged half-antibody due to the formation of intrachain bridges. The *in situ* bridging protocol avoided the formation of half-antibody, yielding a homogeneous ADC with a drug loading of 4.

As can be seen in *Scheme 1.15*, the sequential bridging protocol yielded a mixture of ADC products; one in which the disulfide bridging connectivity is correctly maintained, and a second half-antibody product. This half-antibody species is produced as a result of intrachain bridges forming between cysteines on the same heavy chain in the hinge region. Misbridging is perhaps not surprising considering these cysteine residues are separated only by two amino acids. Hence, through complete reduction and subsequent rebridging some of the cysteines have formed intrachain bonds. This disulfide bond shuffling however is largely avoided using the developed *in situ* protocol, facilitating immediate rebridging of reduced disulfides. Indeed, using TCEP or benzeneselenol as the reducing agent, the *in situ* protocol produced a highly homogeneous ADC with a drug loading of 4 in good yield with maintained binding activity to HER2.

In summary, substituted maleimides are a new class of bridging reagent which offer many advantages over previous cysteine and disulfide modification strategies. These include rapid and quantitative conversion to the modified product, no introduction of chiral centres, which avoids formation of diastereomers, installation of a two-carbon

bridge providing minimum disturbance to the disulfide bond, and use of an *in situ* bridging protocol avoiding aggregation and disulfide scrambling products. In addition, the modification may be reversible or irreversible, as research within the group has demonstrated control of maleimide hydrolysis (*Scheme 1.16*) (169). Successful bridging, conjugation and maintained activity of both the protein and the functionality have been demonstrated for a small peptide, ds-scFv, Fab and a full antibody. These studies suggest substituted maleimides could be utilised for a wide range of therapeutic and diagnostic applications in the site-selective modification of antibodies.



**Scheme 1.16** Reversible and irreversible protein modification using *N*-aryl substituted maleimides.

---

## 1.9 Project aims

Research has demonstrated that 3,4-substituted maleimides offer a powerful approach to the selective, rapid, quantitative and reversible modification of peptide and protein disulfide bonds (166-171,180). Furthermore, in recent work it has been shown that next generation maleimides can be used for the extremely efficient re-bridging of disulfide bonds in Fab and disulfide-stabilised scFv antibody fragments, to produce fully active, homogeneous protein conjugates (170,171). The principal aim of this project is to design and synthesise a range of optimised 3,4-substituted maleimide reagents to enable the efficient bioconjugation of antibodies, with a focus on applying this technology to the construction of antibody-enzyme conjugates for ADEPT and antibody-antibody conjugates for bispecifics.

### *Synthesis of reagents for ADEPT*

A concept first described in the late 1980s, antibody-directed enzyme prodrug therapy (ADEPT) was developed with the aim of generating cytotoxic agents *in vivo* specifically at cancerous tissue (see *Section 1.5.2.1*). For ADEPT to be a viable and effective cancer therapy the antibody-enzyme conjugates must maintain both antibody and enzyme activity. Current chemical conjugation techniques based on natural amino acid modification produce highly heterogeneous conjugates with a loss of bioactivity. Developments in molecular biology have enabled a range of antibody-enzyme recombinant fusion proteins to be generated in recent years. This is currently the most efficient approach to producing active and homogenous antibody-enzyme conjugates. However, chemical conjugation still plays an important role as cross-linking proteins is a more practical, rapid, versatile and economic route.

In this project, a range of 3,4-substituted maleimide based linkers will be produced to achieve more defined antibody-enzyme conjugates. A variety of human and non-human enzymes have undergone pre-clinical investigation for ADEPT and one of the earliest examples, and the only to be clinically assessed, is the bacterial enzyme carboxypeptidase G2 (CPG2). In this project an anti-CEA disulfide-stabilised scFv (ds-scFv) fragment will first be used as a model system for the proof-of-concept experiments. The zinc metalloenzyme CPG2 will act as the enzyme conjugate. CPG2 does not contain any free cysteine residues or native disulfide bonds; initial research therefore will focus on developing reagents to link the disulfide bond of the anti-

CEA scFv fragment and a native lysine residue on CPG2 (*Figure 1.18*). Hence this already provides a significant improvement on existing chemical conjugation techniques, as site-specific modification will be achieved at the antibody.

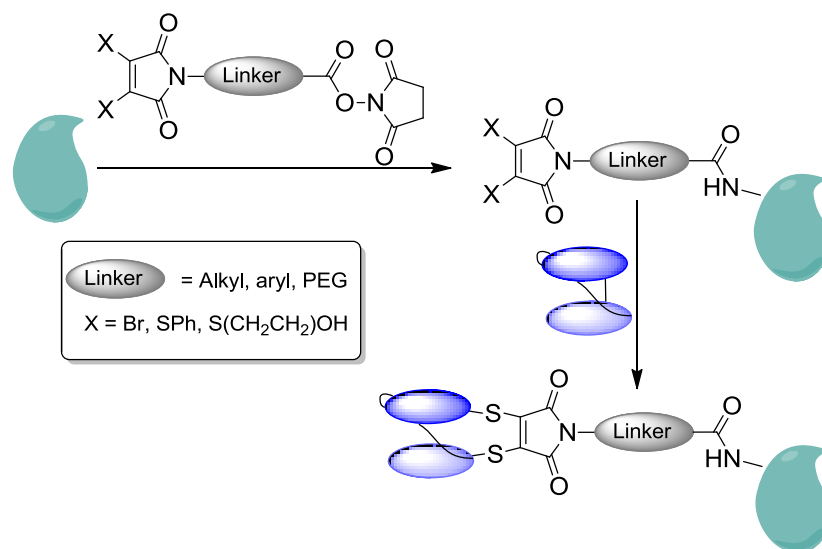


**Figure 1.18** Basic linker design for disulfide to lysine conjugation. The enzyme will first be functionalised through lysine conjugation via NHS ester chemistry. The antibody fragment disulfide bond can then be bridged with a substituted maleimide. Note: this is a simplified representation and some product heterogeneity will result due to lysine conjugation at the enzyme.

### *Synthesis of reagents for bispecifics*

The limited ability of conventional monoclonal antibody therapies to induce significant anti-tumour activity has led to the development of bispecifics; antibodies that can simultaneously bind two different antigens (see *Section 1.6*). Recombinant technologies have produced a diverse range of bispecific antibodies, generating 45 formats in the last two decades (87). Despite this variety of topologies, the approach is not suited to every protein combination. The fusion of proteins via their N or C termini can result in a reduction or loss of bioactivity and variable expression yields can be observed due to complications in folding and processing (80-83). An alternative and potentially more versatile approach to generating bispecific therapeutics is chemical conjugation.

Antibody fragments including Fabs and scFvs are commonly used in a range of bispecific topologies. It is envisaged that the single interchain disulfide bond of such fragments could facilitate the generation of homogeneous bispecific constructs via next generation maleimide based cross-linking reagents. In this project, a range of disulfide

to disulfide based cross-linking reagents will be designed, synthesised and tested (*Figure 1.19*). Direct and indirect conjugation strategies will be investigated; direct involves the chemical modification of a single antibody fragment and subsequent conjugation to the second, unmodified fragment, in contrast, indirect conjugation comprises of the functionalisation of both fragments with a reactive moiety prior to conjugation. It is anticipated that successful linkers can be readily translated to any disulfide or single cysteine containing protein, enabling the generation of a wide range of homogeneous antibody-protein conjugates.

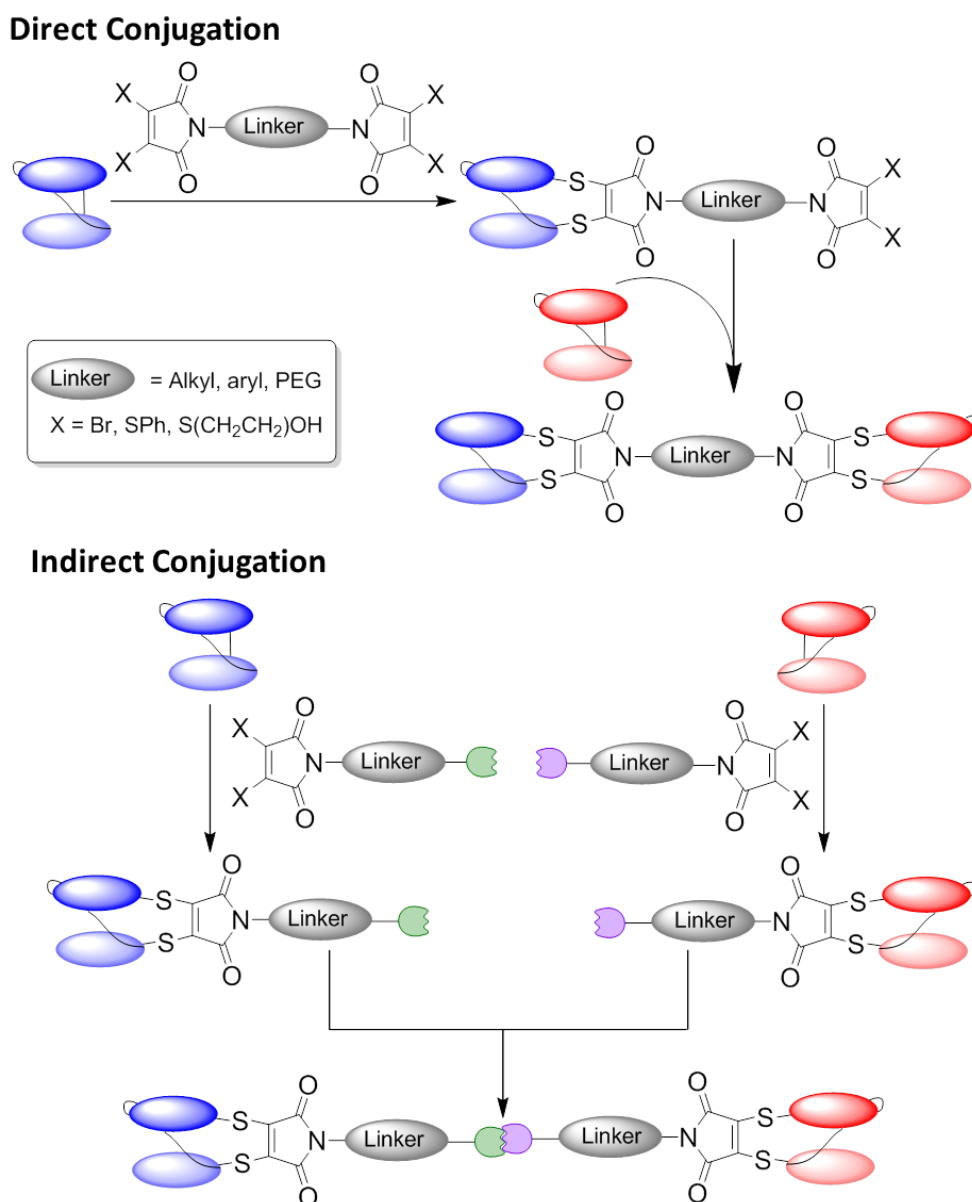


**Figure 1.19** Basic linker designs for disulfide to disulfide conjugation via direct and indirect conjugation strategies. Using ds-scFv here as an example, direct conjugation involves the modification of a single scFv fragment and subsequently linking to a second, unmodified fragment. Indirect conjugation comprises of the functionalisation of

---

each antibody fragment with a reactive moiety which can participate in a chemoselective reaction when the two modified fragments are incubated together.

This thesis also investigates, with collaborators, the use of 3,4-substituted maleimide reagents for FRET and immuno-PET applications.

---

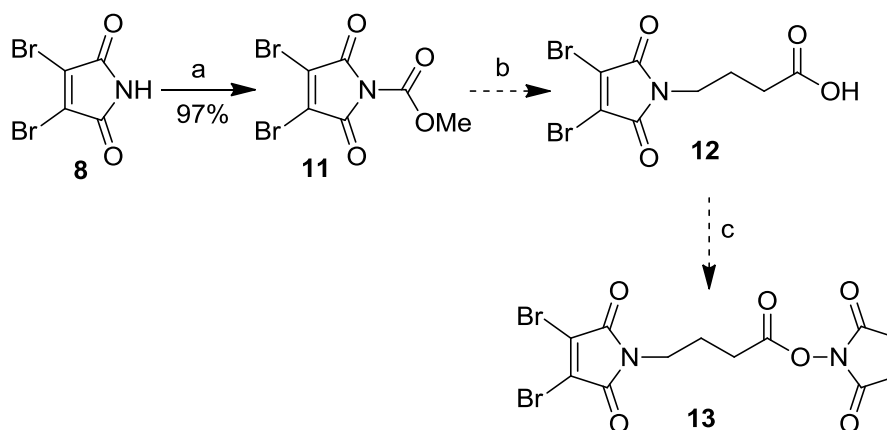
## 2 Results and Discussion

### 2.1 Synthesis and application of a disulfide to lysine linker

Investigations initially centred on the synthesis of an efficient disulfide to lysine linker, using an anti-CEA ds-scFv and CPG2 as the model system for conjugation. The design of this linker was based on widely used, currently available commercial linkers such as SMCC and GMBS (see Section 1.8.1).

#### 2.1.1 Synthesis of dibromomaleimide linker

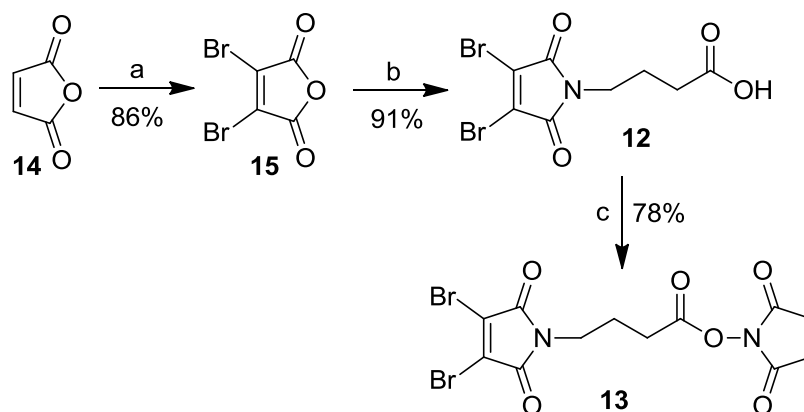
A dibromomaleimide analogue of the desired disulfide to lysine linker was considered the first synthetic target. The initial synthetic approach towards this linker **13** is outlined in Scheme 2.1. This strategy uses a method recently developed in the group towards the synthesis of *N*-substituted maleimides through an *N*-(methoxycarbonyl) derivative of dibromomaleimide **11**. The introduction of a carbonyl group on the maleimide nitrogen effectively activates the maleimide to amine attack through creation of a better leaving group, facilitating *N*-substitution under mild conditions (181).



**Scheme 2.1** Reagents and conditions: (a) MeOCOC<sub>1</sub>, NMM, THF; (b) H<sub>2</sub>N(CH<sub>2</sub>)<sub>3</sub>COOH, DCM; (c) NHS, DCC, EtOAc.

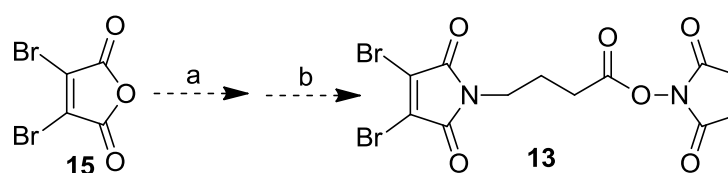
The *N*-(methoxycarbonyl)-3,4-dibromomaleimide **11** was readily generated from **8** in 97% yield. The most efficient conditions established for the production of *N*-substituted dibromomaleimides from the activated ester **11** simply involve the addition of the desired amine in dichloromethane (181). However, these conditions proved unsuitable as the amine in this case is  $\gamma$ -aminobutyric acid, which exists as a zwitterion and as such will not dissolve in dichloromethane. Alternative solvents were used, including DMF

and acetic acid with gentle heating. Nevertheless, the reaction did not proceed. It is likely that due to the zwitterionic nature of  $\gamma$ -aminobutyric acid, there is insufficient uncharged amine present to promote ring opening of **11**. This approach was further attempted in acetic acid at reflux, resulting in a mixture of products of which none were the desired compound **12**. In parallel to this route, an alternative synthetic strategy shown in *Scheme 2.2* was attempted.



**Scheme 2.2** *Reagents and conditions:* (a)  $\text{AlCl}_3$ ,  $\text{Br}_2$ ,  $160^\circ\text{C}$ , 20 h; (b)  $\text{H}_2\text{N}(\text{CH}_2)_3\text{COOH}$ ,  $\text{AcOH}$ , reflux, 4 h; (c) NHS, DCC,  $\text{EtOAc}$ ,  $0^\circ\text{C}$  to rt, overnight.

An alternative approach to synthesising *N*-substituted maleimides requires harsh conditions, refluxing maleic anhydride with the desired amine in acetic acid for several hours (169). This synthetic strategy was applied towards linker **13**. This approach first necessitates the generation of dibromomaleic anhydride **15**, and this was achieved using the method of Dubernet from maleic anhydride **14** in 86% yield (182). The disubstituted maleic anhydride **15** was then heated at reflux with  $\gamma$ -aminobutyric acid in acetic acid for 4 h, yielding 91% of the desired compound **12**. Coupling of the *N*-substituted maleimide **12** with *N*-hydroxysuccinimide (NHS) was subsequently achieved using DCC, furnishing the proposed disulfide to lysine linker **13** (78% yield). Song *et al.* have reported a one-pot preparation of maleimido-carboxylic NHS-esters (183). This one-pot approach shown in *Scheme 2.3* was applied to dibromomaleic anhydride **15**, however the desired linker **13** was not formed.

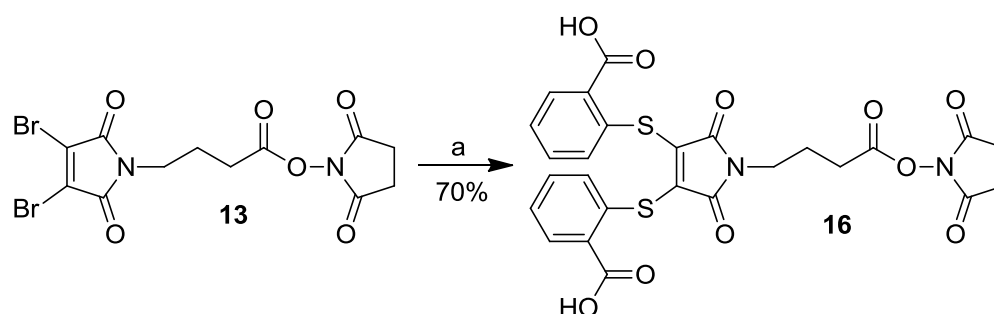


**Scheme 2.3** *Reagents and conditions:* (a)  $\text{H}_2\text{N}(\text{CH}_2)_3\text{COOH}$ , DMF, rt; (b) NHS, DCC,  $0^\circ\text{C}$  to rt (183).

### 2.1.2 Synthesis of dithiomaleimide linker

Following the successful synthesis of the dibromomaleimide disulfide to lysine linker **13**, it was considered that generation of a dithiomaleimide analogue should be attempted. The dithiomaleimides hold several advantages over the dihalomaleimides, for example lower cross-reactivity with the reducing agent TCEP. For a reagent to be suitable for *in situ* disulfide bridging tolerance to the presence of reducing agent is crucial. In addition, in combination with selenol, dithiomaleimides have been demonstrated to efficiently reduce and bridge a disulfide bond. Bridging ability with a wide range of reducing agents is highly desirable as different protein disulfides necessitate different reagents for successful reduction. Furthermore, the first reagent to be reported as suitable for *in situ* disulfide bridging is a dithiomaleimide (168).

Initially the dithiosalicylic acid maleimide **16** was the choice thiol analogue of the disulfide to lysine linker (*Scheme 2.4*). At the time of synthesis, initial investigations into using thiosalicylic acids as maleimide leaving groups had begun. Through the presence of carboxylic acids, it was proposed that the thiosalicylic acid maleimide reagents would have increased solubility in the aqueous conditions required for protein modification (184).



**Scheme 2.4** Reagents and conditions: (a) HSP<sub>2</sub>CO<sub>2</sub>H, KOAc, MeCN.

Synthesis of **16** initially proved troublesome; early attempts included the reaction of **13** with thiosalicylic acid in methanol with an excess of base. This resulted in methanol attack at the NHS ester end of the linker. Several solvents were then investigated for use in this reaction and acetonitrile was established as the best choice, since it readily dissolved both starting materials and no attack on the NHS ester occurred in the presence of base. Following purification by column chromatography, linker **16** was achieved in 70% yield.

Unfortunately, attempts to scale up the synthesis outlined in *Scheme 2.4* proved difficult due to challenging and lengthy purifications leading to hydrolysis of the NHS ester over time. In parallel to the synthetic work, bridging of a disulfide stabilised analogue of the anti-CEA scFv fragment MFE-23, was attempted using both dithiophenol and dithiosalicylic acid maleimide (*Figure 2.1*).

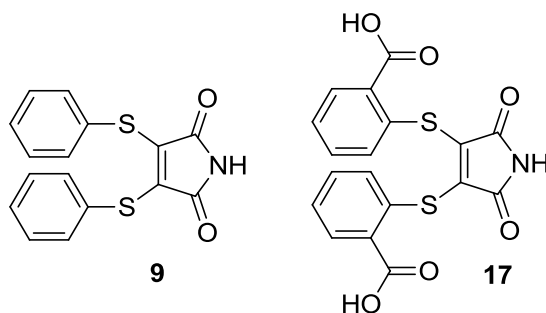


**Figure 2.1** Dithiophenol **9** and dithiosalicylic acid **17** maleimide.

An *in situ* protocol for the bridging of the anti-CEA ds-scFv with dithiophenol maleimide has been established in our group (170). This work was repeated and also applied using dithiosalicylic acid, and monitored by LCMS. The results of bridging with dithiophenol maleimide can be seen in *Figure 2.2*, which shows a deconvoluted LCMS spectrum of unmodified ds-scFv (*Figure 2.2A*) and after bridging with dithiophenolmaleimide (*Figure 2.2B*). Attempts at bridging the disulfide bond of the scFv with dithiosalicylic acid maleimide were also monitored by LCMS; however deconvolution of the mass spectra either failed or resulted in unusual masses, for example lower than the original mass of the antibody fragment. *Figure 2.3* shows the original mass spectra obtained for anti-CEA ds-scFv modified with dithiophenol maleimide (*Figure 2.3A*) and dithiosalicylic acid maleimide (*Figure 2.3B*). The quality of the mass spectrum obtained after dithiosalicylic acid maleimide modification is very poor; there is a lack of clarity of the ‘charge envelope’ expected due to the presence of multiply charged species, which normally form a Gaussian-type distribution. Research within the group found that when the same dithiosalicylic acid maleimide **17** was used on a peptide, one of the thiosalicylic acid groups was not released on disulfide bridging (184).

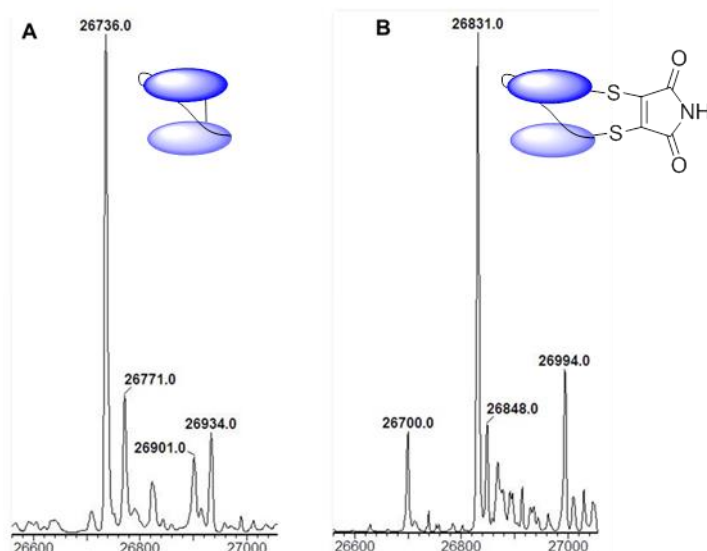


**Figure 2.2** Deconvoluted LCMS spectra (A) unmodified anti-CEA ds-scFv (26,736 Da); (B) ds-scFv modified with dithiophenolmaleimide (expected 26,831, observed 26,831).

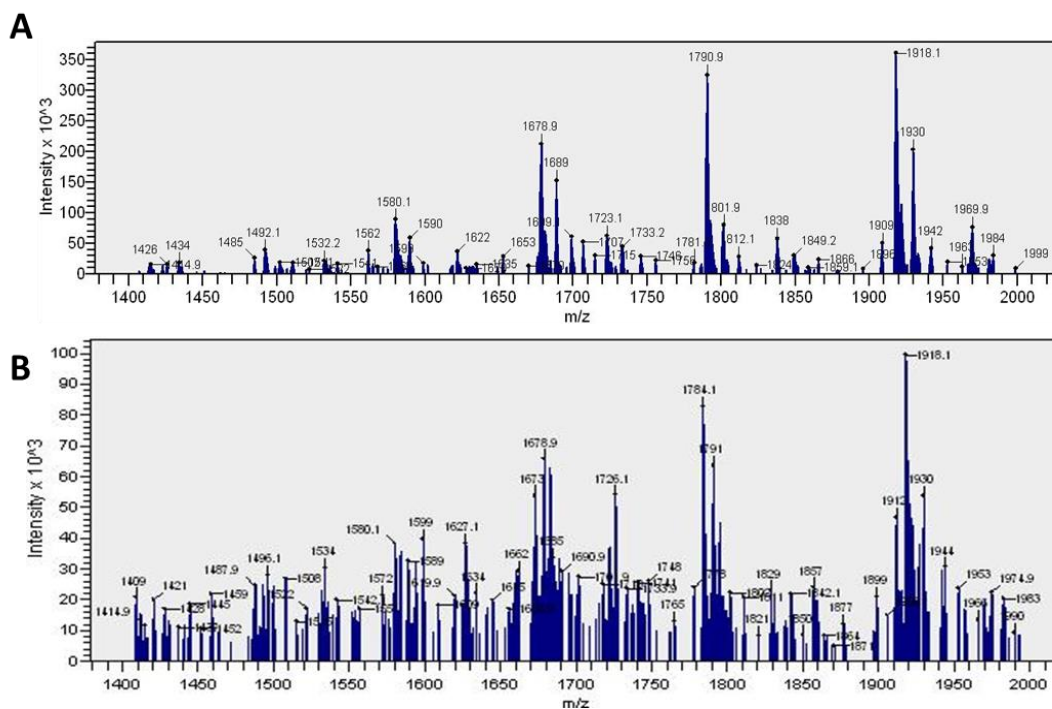
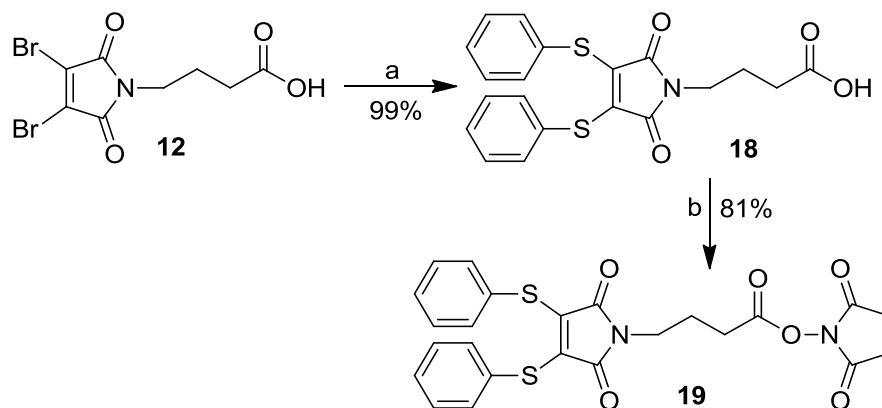


**Figure 2.3** Original LCMS spectra of (A) anti-CEA ds-scFv modification with dithiophenolmaleimide **9**; (B) anti-CEA ds-scFv modification with dithiosalicylic acid maleimide **17**.

The combination of an efficient synthesis of the dithiosalicylic acid maleimide linker **16** proving difficult, and the presence of charged groups apparently causing poor quality LCMS data, led focus away from this linker design to one using simply thiophenol as

the dithio analogue of the disulfide to lysine linker. A synthetic route to the dithiophenol linker **19** is outlined in *Scheme 2.5*.



**Scheme 2.5** *Reagents and conditions:* (a) PhSH, NaHCO<sub>3</sub>, MeOH; (b) NHS, DCC, EtOAc, 0°C to rt, overnight.

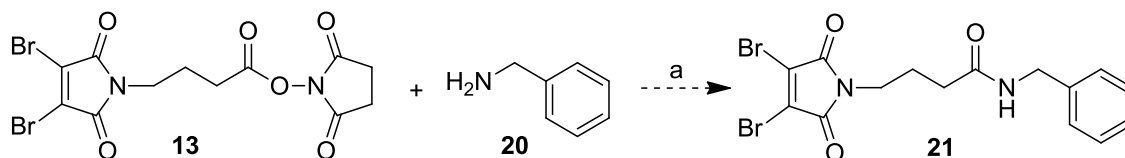
The first two steps of this synthetic strategy are analogous to those in the synthesis of the dibromomaleimide disulfide to lysine linker **13** (*Scheme 2.2*). The *N*-substituted maleimide **12** was then converted from dibromo to dithiophenol in methanol with an excess of base to give **18** in an excellent 99% yield. The dithiophenol derivative **18** was then coupled to *N*-hydroxysuccinimide (NHS) using DCC overnight, to furnish the dithiomaleimide analogue of the disulfide to lysine linker **19** in 81% yield.

### 2.1.3 Small molecule selectivity investigation

In order for the linkers **13** and **19** to be effective in producing more defined antibody-enzyme conjugates, these chemical cross-linkers must be selective for particular residues on a protein. The two linkers synthesised here are designed to possess an amine reactive NHS ester moiety for reaction with lysine residues, and a thiol reactive 3,4-substituted maleimide, for rapid disulfide bridging. In our model protein system, conjugation of an antibody fragment to the enzyme carboxypeptidase G2 (CPG2) will be attempted. This enzyme contains no cysteine residues or disulfide bonds and so will be conjugated to the linker first, with the view of free lysine residues reacting selectively with the NHS ester to form a stable amide bond. Before moving on to this system, it was decided that the selectivity of the commercially available cross-linking reagent SMCC and the synthesised linkers should be investigated.

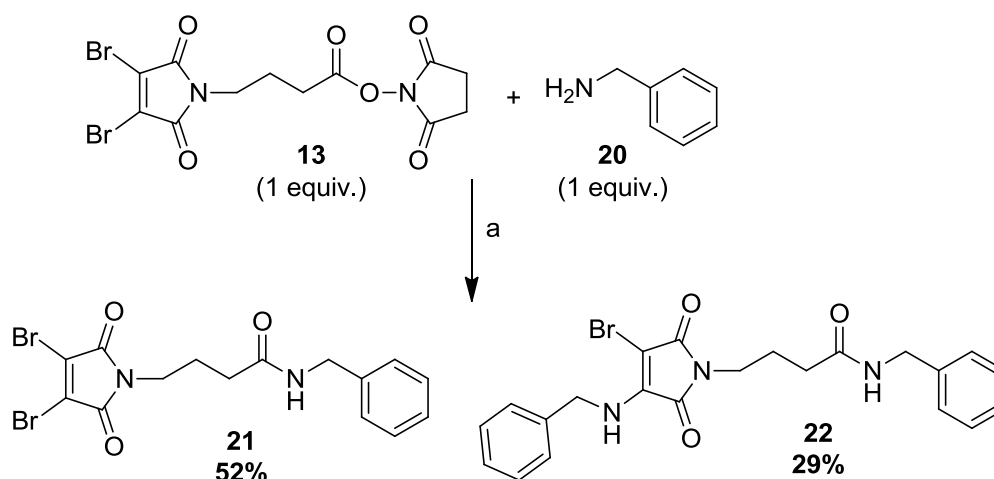
These initial selectivity investigations were carried out in an organic solvent system for ease of solubility and also with a view of determining the potential limits of synthetic

routes where amines may be reacted with compounds containing a 3,4-substituted maleimide. The first selectivity study is outlined in *Scheme 2.6*, where it was proposed that on reaction of benzylamine **20** with linker **13**, compound **21** will result.



**Scheme 2.6** Reagents and conditions: (a)  $\text{CH}_2\text{Cl}_2$ .

This reaction was first attempted using a 1:1 mixture of linker **13** and amine **20**. The reaction was monitored by TLC every 15 minutes until after two hours the reaction was stopped, as no further changes were observed. The results are shown in *Scheme 2.7*.



**Scheme 2.7** Results of selectivity investigation. Reagents and conditions: (a)  $\text{CH}_2\text{Cl}_2$ .

Three spots could be observed by TLC, of which one was the proposed product **21** as revealed by subsequent  $^1\text{H}$  and  $^{13}\text{C}$  NMR, obtained in a 52% yield (*Scheme 2.7*). In addition, the diaddition product **22** was isolated in a 29% yield. The third spot was due to the presence of hydrolysed linker **12** (19%) (*Figure 2.4*). The two reaction products **21** and **22** were thus obtained in a 1.8:1 yield respectively.

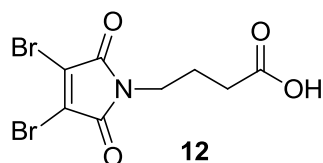
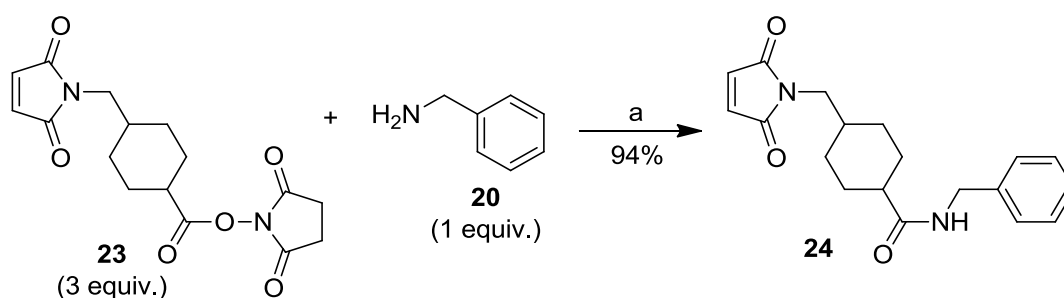


**Figure 2.4** Result of NHS ester linker hydrolysis.

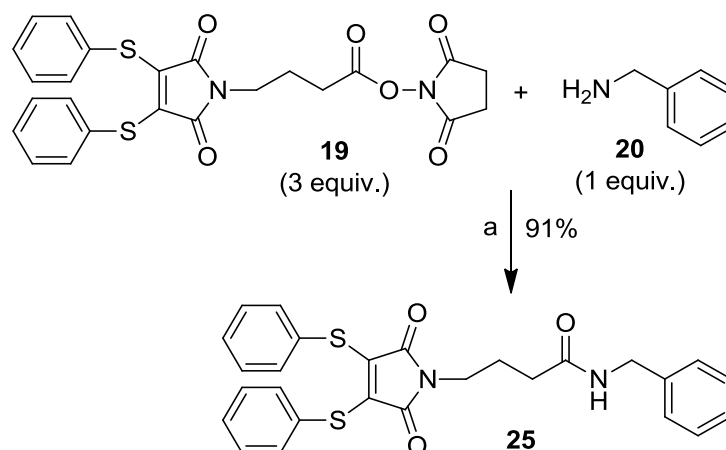
In order to rule out the possibility that the diaddition product was formed as a consequence of the loss of the amine reactive NHS ester through hydrolysis, this reaction was repeated using a 3:1 mixture of linker **13** to benzylamine **20**. Indeed this reaction also yielded the diaddition product, however the ratio of the proposed product **21** to diaddition product **22** increased to 2.5:1.

Once more using a 3:1 mixture of linker to amine, the commercially available linker SMCC **23** was reacted with benzylamine under the same conditions (*Scheme 2.8*). In this case the proposed product **24** was formed exclusively, although NHS hydrolysis of this linker was also observed.



**Scheme 2.8** Reagents and conditions: (a)  $\text{CH}_2\text{Cl}_2$ .

These simple selectivity investigations suggest that the presence of bromine on the maleimide double-bond has altered its reactivity to amines. Moreover, in the presence of excess linker the diaddition product **22** was still formed, demonstrating that the conjugate addition is indeed competitive with reaction at the NHS ester. In order to determine if a thiomaleimide achieves selectivity, the same investigation was carried out using 3 equivalents of thiophenol linker **19** to 1 equivalent of benzylamine **20** (*Scheme 2.9*). A single product was observed by TLC after stirring for several hours. Even on the addition of another equivalent of amine, still only one product could be seen. Although another faint spot could be observed by TLC, this corresponded to compound **18**, as hydrolysis of the NHS ester **19** had begun to occur. Following purification,  $^1\text{H}$  NMR revealed the product to be the proposed monoaddition compound **25**.



**Scheme 2.9** Reagents and conditions: (a) CH<sub>2</sub>Cl<sub>2</sub>.

The results of this selectivity investigation in organic solvent suggest that there is competition between the dibromomaleimide and NHS ester for amine addition. Although these results reveal the limits of synthetic routes where amines may be reacted with compounds containing a 3,4-substituted maleimide, they are not necessarily true for real protein systems. This is demonstrated in the following *Section 2.1.4*.

#### 2.1.4 Selectivity investigation using Carboxypeptidase G2

The results of the small molecule selectivity investigation suggest that the dithiophenol disulfide to lysine linker **19** would be suitable for the production of antibody-enzyme conjugates, as only the NHS ester moiety reacts with amines, leaving the substituted maleimide free for conjugation via disulfide bridging. In contrast, the dibromo linker **13** showed a lack of selectivity. In order to determine if these results are true for a real protein system, the enzyme carboxypeptidase G2 (CPG2) was incubated with 20 and 50 equivalents of both dibromomaleimide and dithiophenol maleimide for 1 hour. CPG2 contains no free thiols or disulfides, so any conjugation to these maleimides would be attributed to lysine residues.

Liquid chromatography mass spectrometry (LCMS) was used to monitor the reaction, if any, of CPG2 with the excess of either dibromo- or dithiophenolmaleimide. CPG2 was first analysed by LCMS in PBS buffer (pH 7.2) and the original and deconvoluted spectra are shown in *Figure 2.5*. The spectrum of CPG2 shows a main peak at 42,403 Da (*Figure 2.5B*). CPG2 naturally exists as a homodimer, held together at the dimer interface by hydrophobic interactions and hydrogen bonds. Using LCMS only the mass of the monomer is seen, as the non-covalent dimer forming interactions are disturbed

during the electrospray ionisation process. There is another prominent peak at 44,621 Da in the deconvoluted spectrum. SDS-PAGE analysis of CPG2 shows one distinct band (*Figure 2.6*), the original mass spectrum shows a typical Gaussian distribution (*Figure 2.14A*), and peptide mapping and analytical FPLC all indicate only CPG2 is present (data not shown). The peak may be an artefact of the deconvolution software, or in fact a small trace of a differently synthesised form of CPG2, as it is produced in bacteria and purified only through use of an IMAC column. For analytical purposes, the main peak at 42,403 Da was used.

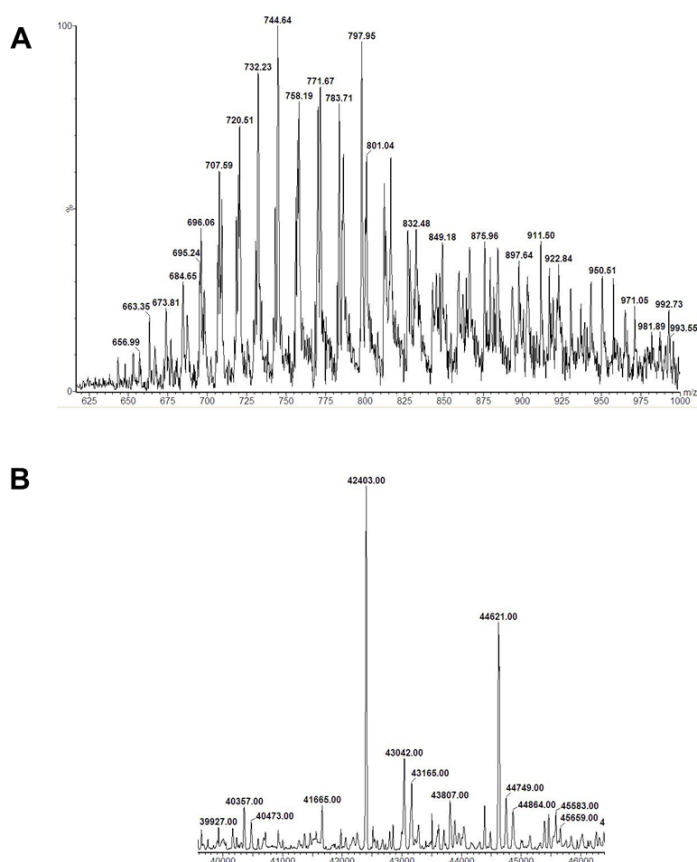


**Figure 2.5** LCMS analysis of CPG2 in PBS buffer. **(A)** Original mass spectrum; **(B)** Deconvoluted spectrum.

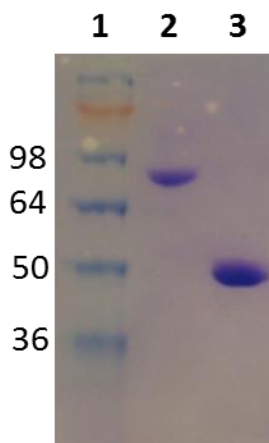


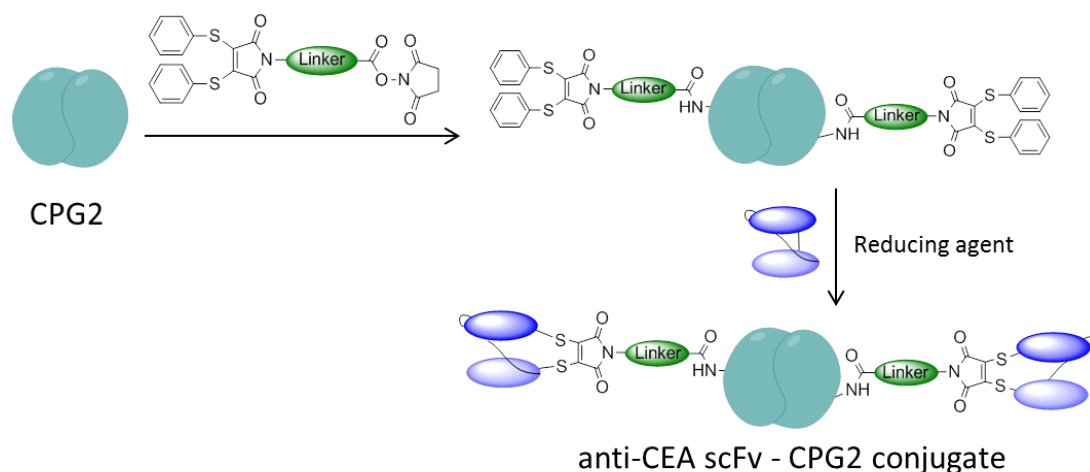
**Figure 2.6** SDS-PAGE analysis of CPG2. **Lane 1** contains protein ladder in kDa (SeeBlue® Plus2, Invitrogen). **Lane 2** contains MFECP fusion protein as control (~72 kDa). **Lane 3** contains CPG2 monomer.

Following incubation of CPG2 for 1 hour with 20 and 50 equivalents of dibromo- and dithiophenolmaleimide, no changes were observed in the LCMS spectrum. This indicates that in a real protein system, bromo-substituted maleimides do not react with amines. There are two significant differences between the small molecule and protein selectivity investigations. Firstly, the incubation of CPG2 with substituted maleimide took place at pH 7.2, a pH typically employed for protein modification. At this pH the lysine residues will be protonated and therefore have significantly attenuated nucleophilicity. Secondly, on the small molecule scale there is a much higher concentration of amine to substituted maleimide compared to the protein system. In all, these results indicate that both versions **13** and **19** of the disulfide to lysine linker are suitable as conjugation reagents at pH 7.2 for the production of more defined antibody-enzyme conjugates.

### 2.1.5 Conjugation of linker to Carboxypeptidase G2

The initial goal of this project was to produce a conjugate of the bacterial enzyme CPG2 to two anti-CEA disulfide-stabilised scFv antibody fragments (ds-scFv) using the designed disulfide to lysine linkers. This antibody-enzyme ratio corresponds to that found in the fusion protein MFECP, an ADEPT construct that has reached clinical trials (78). CPG2 contains no free cysteine residues or native disulfide bonds, so the first step would involve the reaction of CPG2 lysine residues with the NHS ester moiety of the linker. Thus, the enzyme would be functionalised with substituted maleimides, available for disulfide bond conjugation to the ds-scFv fragments. Owing to the success of

thiophenol maleimides in the *in situ* protocol, and their significantly lower cross-reactivity with reducing agents, the dithiophenolmaleimide-NHS ester linker **19** was used in this conjugation. A visualisation of the desired route to production of this antibody-enzyme conjugate using linker **19** is shown in *Scheme 2.10*.



**Scheme 2.10** Generation of antibody-enzyme conjugate using disulfide to lysine linker **19**. The first step involves the attachment of linker **19** to CPG2 via its lysine residues, producing CPG2 functionalised with two dithiophenolmaleimide molecules. This construct can then be attached to anti-CEA ds-scFv through disulfide bridging to yield the desired antibody-enzyme conjugate. Note: this is a simplified representation and some product heterogeneity will result due to lysine conjugation at the enzyme.

The first step in generating an anti-CEA to CPG2 conjugate requires the selective attachment of linker **19** to the lysine residues of CPG2. In order for this step to be successful, the linker must only react with lysine residues at the NHS ester end, leaving the substituted maleimide free for later disulfide conjugation. The results in *Section 2.1.3* and *2.1.4* confirm that linker **19** should be successful in this regard. Secondly, there should ideally be one linker attached to each CPG2 monomer. Therefore, the sites of attachment for scFv antibody fragments should aim to be limited to two per CPG2 molecule. This control of conjugation will also ensure that CPG2 activity is not significantly affected. Previous attempts at similar chemical conjugates have demonstrated that increasing substitution decreases CPG2 activity proportionally (74).

There is no evidence in the literature of attempts to strictly control and monitor the level of lysine modification when generating conjugates. Typically, protocols advise using between a 10- to 50-fold molar excess of cross-linking reagent to the amount of amine

---

containing protein (185). In fact, the equivalents of reagent used depends only on the concentration of the protein to be modified. For example, for a protein of 1 mg/ml a 20-fold excess is advised, whereas 50-fold would be recommended for 0.5 mg/ml (185). In order to monitor the number of linkers attached to CPG2, and more specifically to determine the amount of linker **19** required for attachment of one substituted maleimide per CPG2 monomer, the samples were analysed by LCMS. CPG2 in PBS (0.5 mg/ml) was incubated with 2, 5, and 8 equivalents of linker **19** in DMF at room temperature for 20, 40 and 60 minutes. At these time points the reaction was stopped by quenching with 150-fold excess of glycine in PBS.

The main peak in the spectrum shown in *Figure 2.7B* at 42,772 Da corresponds to one linker attached to CPG2 monomer (expected mass 42,785 Da). This was achieved with 2 equivalents of **19** for 1 h. The yield observed by mass spectrometry did not change when the reaction was left for over 1 h. Using 5 equivalents of linker, the main peak observed for all time points corresponded to two linkers per CPG2 monomer (observed 43,157, expected 43,167, *Figure 2.7C*). In addition, weaker mass peaks corresponding to three or four linkers attached could be seen on every attempt. The conjugation with 8 equivalents of **19** resulted in very poor ionisation of the sample, causing deconvolution to be unsuccessful. These chemical conjugation reactions are occurring on lysine and thus blocking basic residues of CPG2, resulting in a change in the ionisation properties of the enzyme. This has been reported to alter mass spectrometry results previously (186). Nevertheless, the results from 2 and 5 equivalents of linker suggest that at 8 equivalents many more lysine residues would be blocked which is undesirable for production of this antibody-enzyme conjugate.

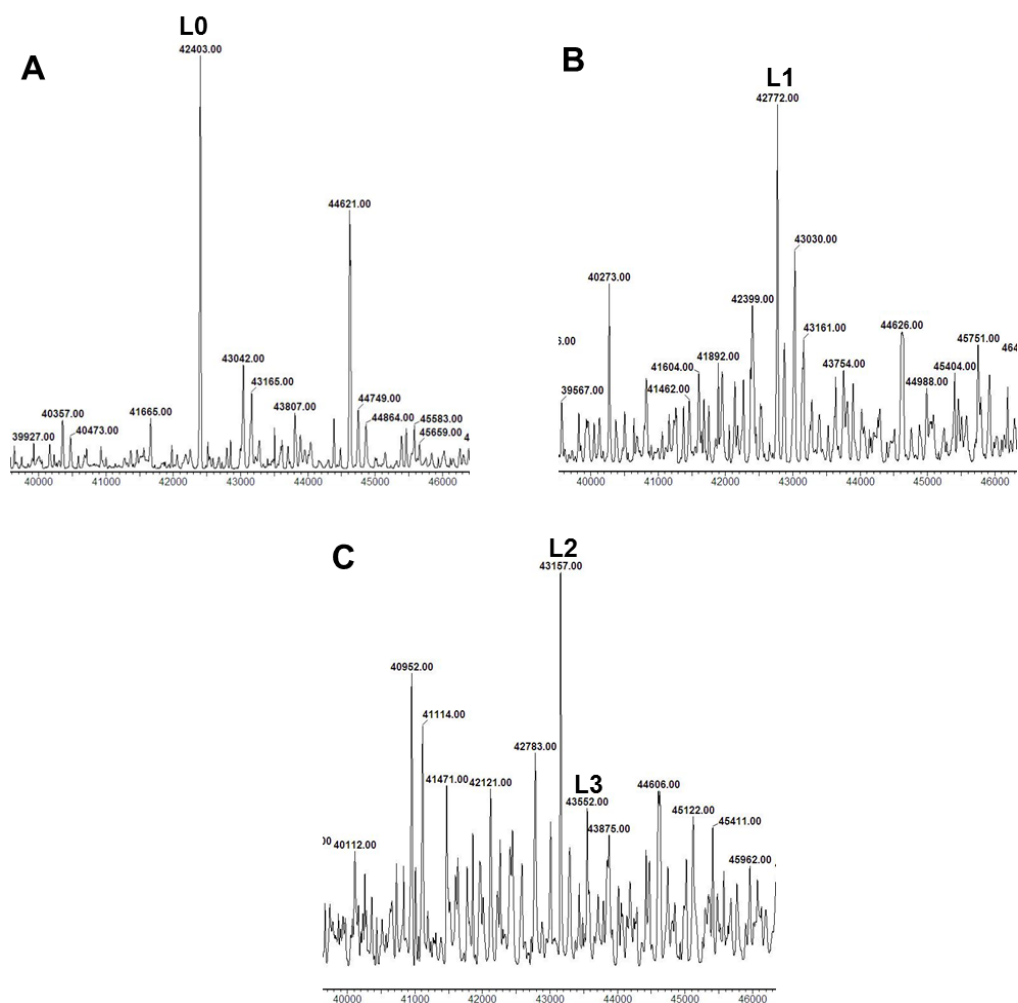


**Figure 2.7** LCMS results of CPG2 conjugation to disulfide to lysine linker **19**. **(A)** Unmodified CPG2; **(B)** 2 equivalents of linker for 1h; **(C)** 5 equivalents of linker for 1h. The labels L0, L1,...Ln correspond to CPG2 conjugated to n linker molecules.

These conjugation reactions were promising, as it appeared that limiting the number of equivalents of linker could be used to control the degree of modification. Furthermore, using just 2 equivalents of linker **19** for 1h gave a good yield of singly modified CPG2, as observed by LCMS. Using this result, the next step of the conjugation could be investigated.

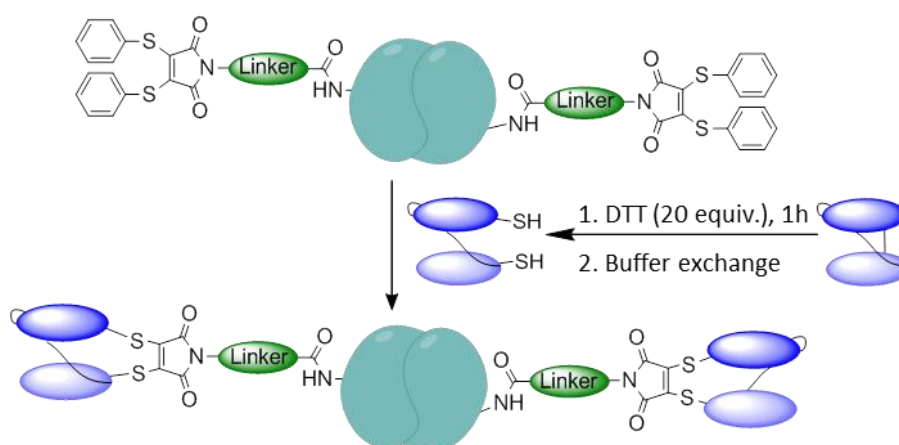
## 2.1.6 Conjugation of modified CPG2 to anti-CEA ds-scFv

### 2.1.6.1 Preliminary conjugation reactions

Conjugation of the ds-scFv fragments to modified CPG2 was initially attempted using two strategies. Firstly, a stepwise approach whereby the antibody is reduced with DTT (20 equivalents) for 1h, purified away from the reducing agent and subsequently

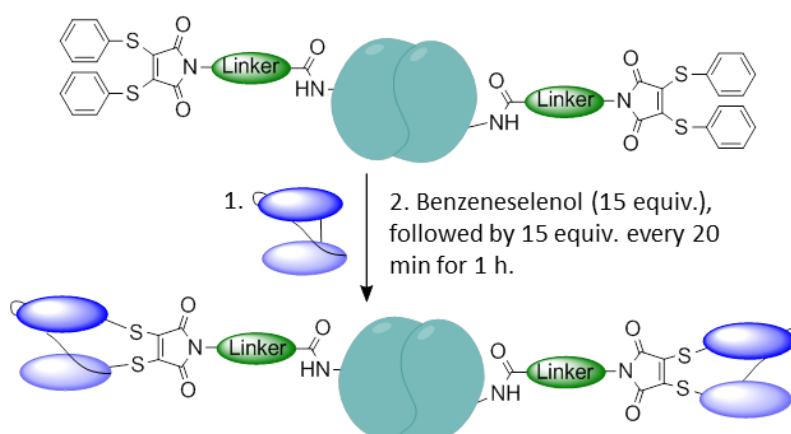
incubated with modified CPG2. The second approach used was the *in situ* procedure; scFv was added directly to modified CPG2 and the reducing agent benzeneselenol added. Conjugation attempts using both approaches resulted in a large amount of unreduced antibody remaining, even with low equivalents of ds-scFv. For the stepwise protocol, this was due to reoxidation of the scFv disulfide bond before successful maleimide bridging. In the case of the *in situ* conjugation ds-scFv reduction was not successful in the first instance, as little product or reduced antibody was present by SDS-PAGE. These issues therefore needed to be addressed to achieve the maximum yield of conjugate.

Using the stepwise method, reoxidation of the scFv fragment was beginning to occur during the purification and concentration stages. To overcome this issue, two changes were made to the stepwise approach to maintain the antibody fragment in its reduced form. First, the ds-scFv was buffer exchanged from PBS to a 50 mM phosphate buffer at pH 6.8 containing 1 mM EDTA. The EDTA suppresses re-oxidation of the cysteines through divalent metals such as  $\text{Cu}^{2+}$  and  $\text{Zn}^{2+}$  (121). Secondly, different purification approaches were investigated. Centrifugal ultrafiltration was found to most efficiently maintain the reduced antibody during purification and concentration. The improved stepwise approach is outlined in *Scheme 2.11*.



**Scheme 2.11** Modified CPG2 conjugation to anti-CEA ds-scFv via a stepwise reduction approach. The scFv fragment is first reduced with DTT and purified away from reducing agent via buffer exchange into 50 mM phosphate buffer containing 1 mM EDTA, pH 6.8. An excess of the reduced scFv is then added to the modified CPG2. Note: this is a simplified representation and some product heterogeneity will result due to lysine conjugation at the enzyme.

The *in situ* approach initially suffered low conjugation yields due to poor ds-scFv reduction. To combat this, a portionwise addition approach was developed (Scheme 2.12). Through addition of benzeneselenol at timed intervals, starting with an initial 15 equivalents and a subsequent 15 equivalents every 20 minutes for an hour, the scFv fragment was successfully reduced for the duration of the reaction. In comparison to other investigated strategies, this protocol allowed for greater amounts of the reducing agent to be used without rapid benzeneselenol oxidation or loss of solubility. Furthermore, the proteins were maintained well in solution under these conditions.



**Scheme 2.12** Modified CPG2 conjugation to anti-CEA ds-scFv via an *in situ* portionwise approach. The scFv fragment is added directly to the modified CPG2, after which an initial 15 equivalents of benzeneselenol is added, followed by 15 equivalents every 20 minutes for an hour. Note: this is a simplified representation and some product heterogeneity will result due to lysine conjugation at the enzyme.

Early conjugation reactions also revealed that the concentration of modified CPG2 could not be accurately determined by standard means, as the chemically conjugated thiophenol groups absorb UV light at 280 nm. To provide a more accurate measurement of modified CPG2 concentration, and so improve the conjugation protocol, a Bradford assay was developed. This assay is based on the absorbance of Coomassie Brilliant Blue G-250 dye; whilst the dye is normally red or green in its unbound form, when bound to protein it turns blue with an absorbance maximum of 595 nm. The extent of this absorbance is proportional to the amount of bound dye, and thus the concentration of protein in the sample. Thus, all subsequent conjugation attempts used modified CPG2 with a concentration based on that determined by Bradford assay.

---

During preliminary investigations, conjugation of scFv to CPG2 was also attempted using CPG2 modified according to current published protocols (185). Using these results for comparison, we could then determine if we had indeed succeeded in producing a more defined antibody-enzyme conjugate. As anticipated this conjugation resulted in a large yield of high molecular weight conjugates, facilitated by functionalising CPG2 with up to 50 substituted maleimides. In our efforts to produce a more defined antibody-enzyme conjugate, there are on average only two substituted maleimides per CPG2 molecule. Whilst our strategy successfully reduced the variety of conjugates produced, it also had a significant detrimental effect on conjugation yield. The very low yields achieved thus far highlighted a potential flaw; the likelihood of reduced antibody fragment conjugation via the two attached dithiomaleimides is low. Furthermore, the huge steric bulk of the attached CPG2 enzyme reduces the opportunity for conjugation at these two positions even further.

The results of conjugation using the literature protocol for modification also revealed that scFv bridging was less successful using the stepwise approach. Early signs of success were seen with the newly developed *in situ* portionwise method. This strategy has the greatest opportunity to maintain reduced antibody for conjugation, as well as having the many advantages of an *in situ* protocol, and so efforts were focused on conjugation using this technique.

### **2.1.6.2 Conjugation following protocol development**

To determine the validity of conjugation results, a series of key controls were carried out under the SDS-PAGE conditions used for analysis (*Figure 2.8*). These controls clearly demonstrate that no change in CPG2 is observed by SDS-PAGE in the presence of modification (*lane 6*), DMF (*lanes 5 and 7*) and reducing agent (*lane 9*). The antibody fragment also remains unchanged by DMF (*lane 4*), and shows the expected shift in molecular weight on reduction (*lane 10*). Furthermore, no higher molecular weight bands are observed on incubation of modified CPG2 with the ds-scFv in the absence of reducing agent (*lane 8*). These controls therefore confirm that the conjugation conditions do not have any effect on either protein by SDS-PAGE, and no cross-linking occurs in the absence of reducing agent.

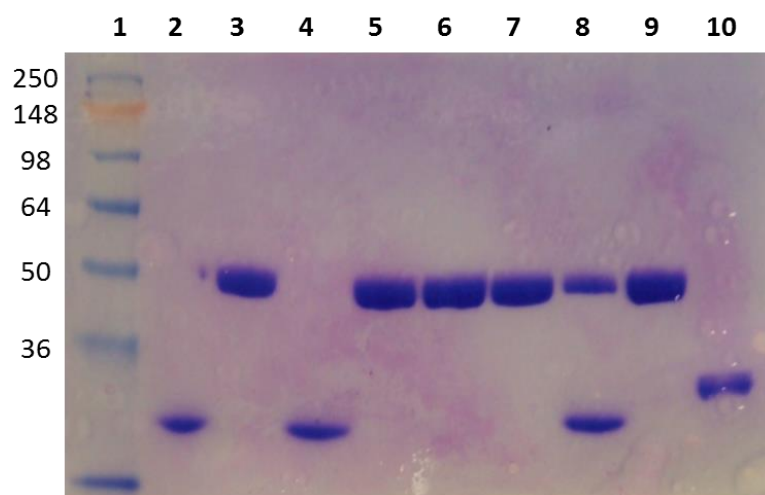


**Figure 2.8** SDS-PAGE analysis of controls. **Lane 1** contains protein ladder in kDa (SeeBlue® Plus2, Invitrogen). **Lane 2** contains ds-scFv. **Lane 3** contains CPG2. **Lane 4** contains ds-scFv with 10% DMF. **Lane 5** contains CPG2 with 10% DMF. **Lane 6** contains CPG2 modified with linker **11**. **Lane 7** contains CPG2 modified with linker **11** and with 10% DMF. **Lane 8** contains CPG2 modified with linker **11**, with 10% DMF and with ds-scFv. **Lane 9** contains CPG2 modified with linker **11**, with 10% DMF and benzeneselenol. **Lane 10** contains ds-scFv with 10% DMF and benzeneselenol.

Much effort was made to improve the success and therefore yield of conjugation by the portionwise *in situ* approach through investigation of a variety of modified CPG2 and scFv concentrations. In the example in *Figure 2.9*, CPG2 has been modified for 1 h using 2 equivalents of linker **11**. Following purification, modified CPG2 at concentrations of 3.5 mg/ml and 6 mg/ml were incubated with 3 and 5 equivalents of ds-scFv (previous work indicated higher equivalents gave no improvement) at 7 mg/ml and 10 mg/ml. 15 equivalents of benzeneselenol were added at the start of the reaction, then a further 15 equivalents every 20 min for 1 h. Early work on this approach revealed that both the reducing agent and the protein would begin to come out of solution if more was added after this point.

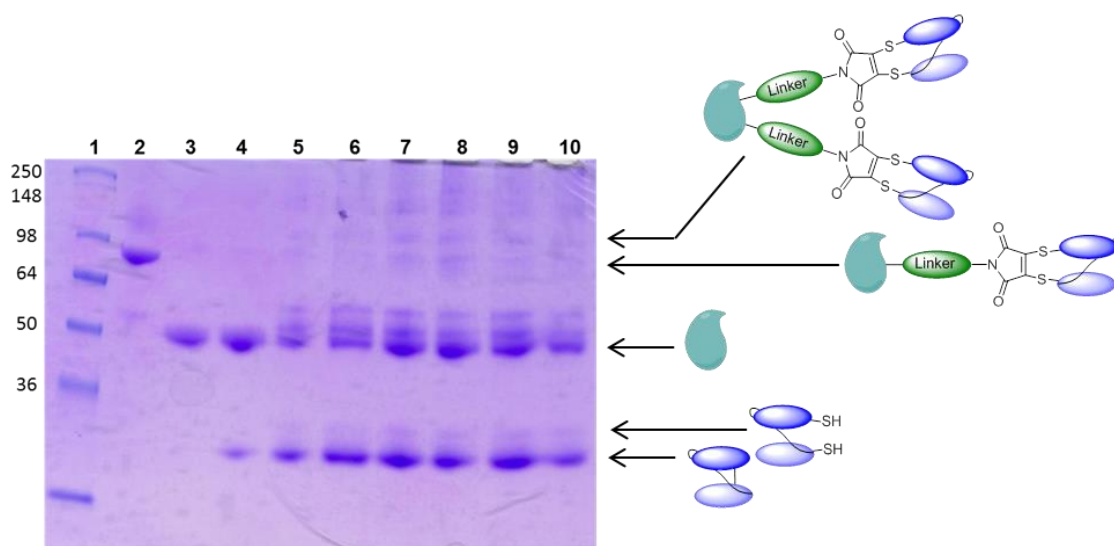


**Figure 2.9** SDS-PAGE analysis of an *in situ* portionwise conjugation. **Lane 1** contains protein ladder in kDa (SeeBlue® Plus2, Invitrogen). **Lane 2** is MFCEP fusion protein (~72 kDa - this serves as a molecular weight guide of the desired product). **Lane 3** is modified CPG2. **Lane 4** is modified CPG2 and ds-scFv. **Lanes 5 and 6** contain conjugations using modified CPG2 at 3.5 mg/ml with 3 and 5 equivalents of reduced scFv respectively, at 7 mg/ml. **Lane 7** contains a conjugation using modified CPG2 at 3.5 mg/ml with 3 equivalents of reduced scFv at 10 mg/ml. **Lanes 8 and 9** contain conjugations using modified CPG2 at 6 mg/ml with 3 and 5 equivalents of reduced scFv at 7 mg/ml. **Lane 10** contains a conjugation using modified CPG2 at 6 mg/ml with 3 equivalents of reduced scFv at 10 mg/ml. **Note:** mostly reoxidised scFv is observed as reaction samples have been taken after 2 h.

In all of the conjugation conditions in *Figure 2.9*, very faint bands can be seen at ~72 kDa, in line with MFCEP, and at ~100 kDa. Both of these suggest the conjugation product; CPG2 with one or two scFvs attached respectively (CPG2 monomer is ~45 kDa and scFv is ~27 kDa). However, stronger bands are also observed at ~60 kDa, just above the band for CPG2 monomer. This mass is unexpected, and given the results of the control experiments, must be generated only when scFv is reduced in the conjugation reaction. The band intensities observed in *Figure 2.9* are typical of all of the results obtained through the *in situ* portionwise approach. No significant change in yield for the supposed conjugation bands at ~72 kDa and 100 kDa was observed for different concentrations, equivalents of scFv fragment, or reaction times. In addition, substantial oxidised antibody was seen in all attempts. As earlier discussed, using current published modification protocols, CPG2 is generated with up to 50 substituted maleimides attached. Indeed, using this modified CPG2 for conjugation generated a

large yield of high molecular weight conjugates, with little to no free scFv remaining. Combined, these results suggest that in our efforts to produce a more defined antibody-enzyme conjugate, re-oxidation of the antibody disulfide is occurring before reaction with one of the few substituted maleimides on CPG2 can ensue. Hence, despite modified CPG2 and reduced antibody being present and in high concentration, the yield of the conjugate does not improve, as the ds-scFv simply reoxidises before meeting the desired reactive partner.

The results in *Figure 2.9* further indicate that modification with 2 equivalents of linker is limiting; the chance of reduced scFv reacting with a substituted maleimide is low and further restricted by reoxidation over time. Consequently, a series of conjugations were attempted using CPG2 functionalised with greater numbers of dithiophenolmaleimide. The aim was to establish if a balance could be achieved between increasing the yield of the desired conjugate without significantly increasing product heterogeneity.

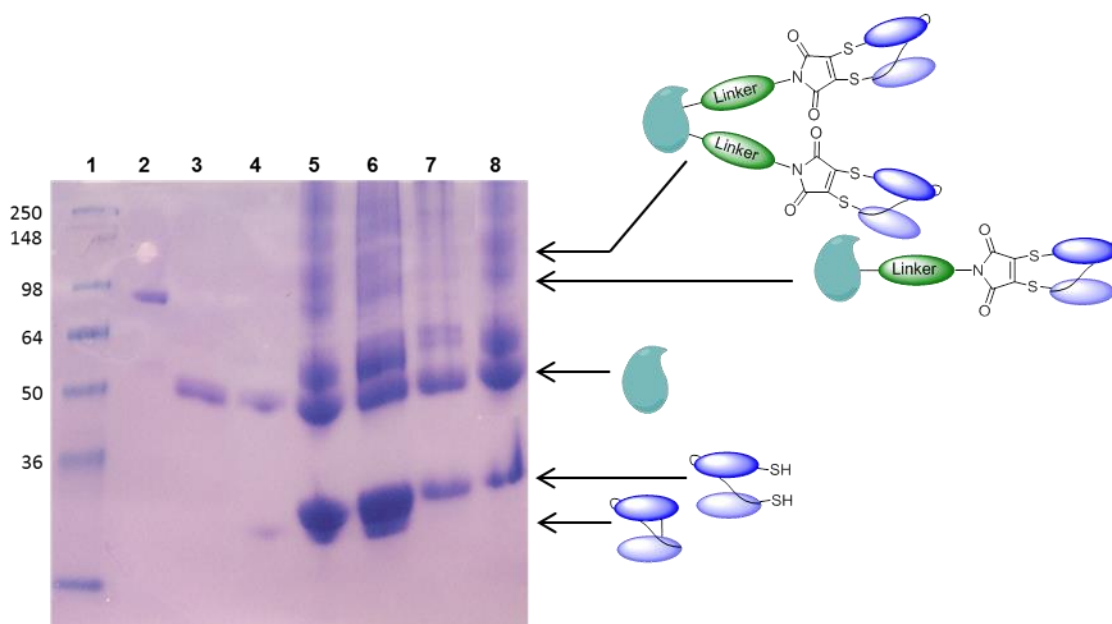


**Figure 2.10** SDS-PAGE analysis of *in situ* conjugations. **Lane 1** contains protein ladder in kDa (SeeBlue® Plus2, Invitrogen). **Lane 2** is MFCEP fusion protein (molecular weight of ~72 kDa). **Lane 3** contains modified CPG2. **Lane 4** contains modified CPG2 and ds-scFv. **Lanes 5 and 6** contain *in situ* portionwise conjugations where CPG2 was modified with 5 equivalents of linker **19** for 1 h, and incubated with 3 and 5 equivalents of ds-scFv respectively. **Lanes 7 and 8** contain *in situ* conjugations using selenocystamine dihydrochloride and TCEP, where CPG2 was modified with 5 equivalents of linker **19** for 1 h, and incubated with 3 and 5 equivalents of ds-scFv respectively.

---

In *Figure 2.10*, lanes 5 and 6 show the conjugation results of CPG2 modification with 5 equivalents of linker **19**, followed by incubation with 3 and 5 equivalents of ds-scFv using the *in situ* portionwise addition method. Consistent with earlier results, the same band pattern is observed. The bands proposed to be conjugate seen previously at ~72 kDa and ~100 kDa are present, as well as bands suggesting higher molecular weight conjugates. In addition, a strong band is once again seen just above CPG2 at ~60 kDa. In any conjugations attempted where over 5 equivalents of linker were used for CPG2 modification, the yield of these highly heterogeneous higher molecular weight conjugates increased. In addition, a significant amount of modified CPG2 remains indicating that these reactions are still far from high yielding. Currently practised cross-linking approaches for the production of antibody-enzyme conjugates, for example using the linker SMCC, typically produce a 30% crude yield of desirable conjugate, with 15% or less normally being recovered after purification (74). Indeed, using the designed disulfide to lysine linker these yields are not improving.

The results of an alternative *in situ* approach are also shown in *Figure 2.10*, where selenocystamine dihydrochloride **26** (*Figure 2.11*) and TCEP were used together as the reducing agent. In this case, the reducing ability of selenol is revealed through the *in situ* reduction of the diselenide bond of **26** with TCEP. Furthermore, a 4:1 ratio of TCEP to selenocystamine was used with the aim of preserving the reducing capacity of **26** for longer. Therefore, the reduced scFv could be maintained for a greater duration in the conjugation reaction, increasing the opportunity for reaction with substituted maleimide. These reagents also have the advantage of greater water solubility. *Figure 2.10* demonstrates that the reduced antibody was successfully maintained in the conjugation reaction mixture. Despite this, the same results are once again observed indicating that despite reduced scFv availability, the yield of conjugate does not increase. This observation raises the question once more of the identity of the band at ~60 kDa. This may either be a product of conjugation running unexpectedly low, or the result of a side reaction which competes with the bridging of the antibody fragment with a substituted maleimide. In order to establish the identity of each of the bands shown in SDS-PAGE, a number of conjugation reactions were repeated, and Western blot analysis of these samples carried out.

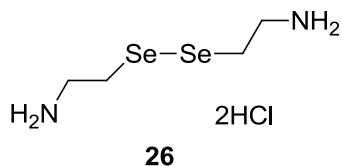


**Figure 2.11** Structure of selenocystamine dihydrochloride.

*Figure 2.12A* shows three controls and three sets of conjugation conditions using the *in situ* portionwise methodology. These results were then analysed by Western blot using antibodies to detect for the scFv fragment (*Figure 2.12B*) and for CPG2 (*Figure 2.12C*). This analysis therefore reveals the proteins contained within each band. In both Western blots the bands at ~72 kDa and ~100 kDa are seen, albeit very faintly, indicating that these are conjugates of CPG2 and scFv. The most intense stain however is observed in *Figure 2.12B* at ~60 kDa, and this is not observed in the Western blot for CPG2 (*Figure 2.12C*). This indicates that this strong band, observed in all of the conjugation reactions, is a product of ds-scFv alone. The molecular weight of the ds-scFv is ~27 kDa and so this band would correspond to two of these fragments. It is maintained despite prior heating of samples to 98°C in SDS, suggesting the fragments are covalently bonded. In the literature, the formation of ds-scFv dimers after reduction has been reported (187). The observation in the conjugation reactions that yield of conjugate did not improve despite the availability of reduced scFvs certainly points towards a competing side reaction. In these conjugation reactions there is a very high concentration of reduced scFv present and in comparison extremely few substituted maleimides, reaction to which is further hindered by the steric bulk of the attached CPG2. The formation of disulfides between reduced scFvs is therefore much more favourable, and this in turn decreases the amount of reduced antibody available for conjugation. This explains why an improvement in yield was not observed despite the high concentrations and equivalents of antibody fragment used. In fact, to turn the reaction in favour of conjugation would require greater levels of modification of CPG2. This inevitably results in highly heterogeneous antibody-enzyme conjugate.

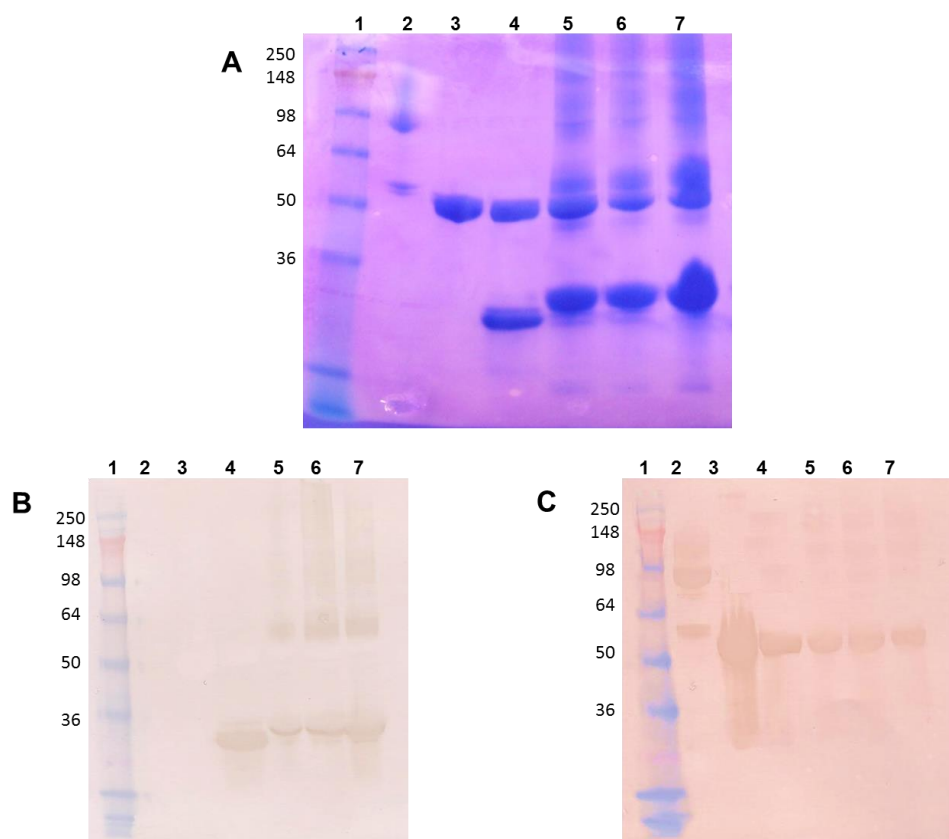


**Figure 2.12** (A) SDS-PAGE analysis of *in situ* conjugations. **Lane 1** contains protein ladder in kDa (SeeBlue® Plus2, Invitrogen). **Lane 2** contains MFECP fusion protein. **Lane 3** contains modified CPG2. **Lane 4** contains modified CPG2 and ds-scFv. **Lanes 5, 6 and 7** contain *in situ* portionwise conjugation attempts. (B) Western blot of SDS-PAGE shown in (A) for ds-scFv. (C) Western blot of SDS-PAGE shown in (A) for CPG2.

Given that conjugation to CPG2 lysine residues and subsequent disulfide bridging of the scFv fragment led to poor yields of conjugate and dimerisation of the reduced antibody, a final alternative approach was taken using these linkers. The disulfide to lysine linker **19** was reacted first with the ds-scFv under the *in situ* bridging conditions, with the aim of rapidly bridging the scFv leaving the NHS ester free for conjugation with CPG2. The ds-scFv was incubated with 2 and 5 equivalents of linker **19**, and 25 equivalents of benzeneselenol for 20 min. The results were then analysed by LCMS as shown in *Figure 2.13*.

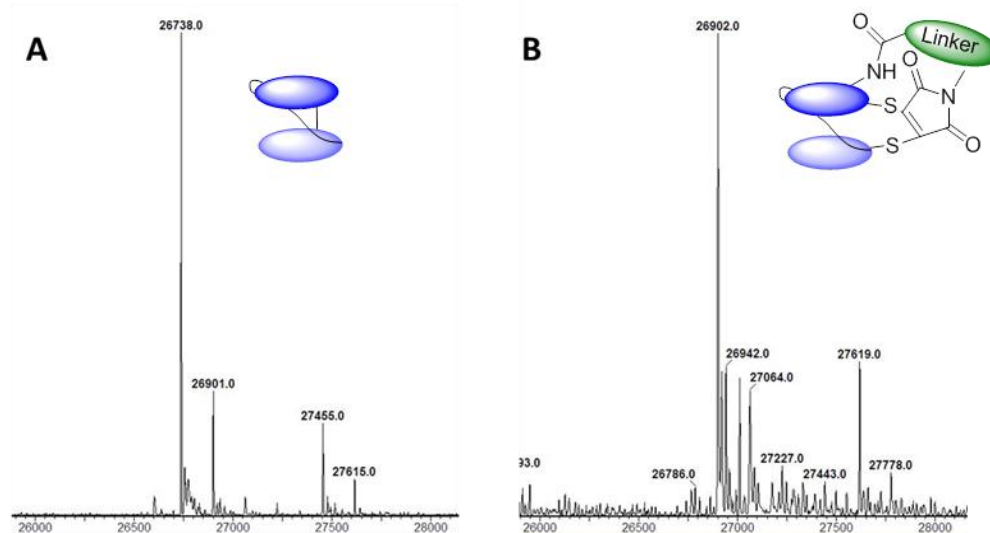


**Figure 2.13** LCMS results of ds-scFv conjugation to disulfide to lysine linker **19**. **(A)** Unmodified scFv (26,738 Da). **(B)** Result of scFv modification *in situ* with both 2 and 5 equivalents of linker **19** and 25 equivalents of benzeneselenol (26,902 Da).

In both cases, an increase in mass of 164 was observed for the scFv fragment. This corresponds to a single linker bridging the scFv via the substituted maleimide, in addition to reacting with a lysine residue. The disulfide bridging reaction is very fast, thus it is conceivable that once the maleimide has bridged the NHS ester end of the linker can react with a nearby lysine. These results indicate that, as expected, the linker cannot be used with the antibody fragment first. The presence of lysine residues in this protein prevents subsequent conjugation to CPG2 via the NHS ester.

In summary, employing a disulfide to lysine linker did not provide a route to better defined antibody-enzyme conjugates in reasonable yield. Remaining strategies to improve this yield would only result in increased product heterogeneity. In addition, several problems were encountered in this conjugation approach including difficulty in maintaining reduced scFv for the duration of the slow conjugation reaction, the incompatibility of high protein concentrations required for efficient conjugation with organic solvent and formation of scFv dimers. This investigation further highlights that the successful production of therapeutic antibody-enzyme conjugate would require site-specific conjugation at both the antibody and enzyme. For example, enzymes with a single incorporated cysteine or disulfide bond should be employed. The focus of this project thus moved on to generating homogeneous antibody-antibody conjugates, where site-specific modification could be achieved.

---

## 2.2 *Substituted maleimide reagents with a bioorthogonal handle*

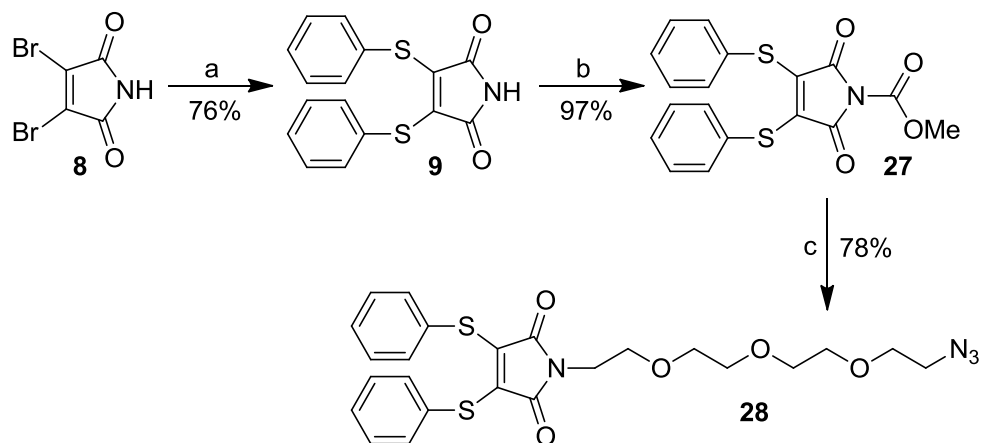
Recent literature has demonstrated the successful production of homogeneous antibody-protein conjugates through the site-specific introduction of bioorthogonal functionalities (90,91). This ‘indirect’ approach to conjugation, which requires modification of each protein, is demonstrated to be more successful than the traditional ‘direct’ approach, where a single protein undergoes chemical modification before direct attachment to another, unmodified protein (90). For example, Schultz *et al.* generated a homogeneous anti-HER2/anti-CD3 Fab bispecific (91). This homogeneity has been realised using the strain promoted azide-alkyne cycloaddition (SPAAC). Production of homogenous antibody conjugates using SPAAC first requires that the azide and strained alkyne are introduced to the proteins site-specifically. Presently this is achieved through introduction of an unnatural amino acid (UAA) to each of the proteins to be conjugated. These UAAs thus provide a means for site-specific chemical functionalisation. This technology, whilst elegant, is not readily transferred; each antibody to be conjugated must undergo prior investigation to determine appropriate mutation sites, substitution for the unnatural amino acid is often incomplete, and expression yields are generally low due to the cellular toxicity of artificial amino acids at the high concentrations necessary (151,152). To avoid these difficulties, an ideal site-directed conjugation technique would use residues natural to the protein that are revealed for modification only under defined conditions.

Our next generation maleimides can be used for the extremely efficient re-bridging of disulfide bonds in Fab and disulfide-stabilised scFv antibody fragments (170,171). Novel linkers were thus designed that incorporate the bioorthogonal handles necessary for the SPAAC reaction, an azide and strained alkyne, in addition to 3,4-substituted maleimides for selective disulfide bridging. Using these site-specific bioorthogonal handles, the project focused on generating homogeneous antibody-antibody conjugates with the ultimate aim of producing a homogeneous bispecific.

### 2.2.1 **Synthesis of an azide functionalised disulfide bridging linker**

A 3,4-substituted thiophenol maleimide linker containing an azide group **28** was the first bioorthogonal reagent to be synthesised (*Scheme 2.11*). From review of the literature, it is suggested that the ideal indirect cross-linking reagent should possess reasonable water

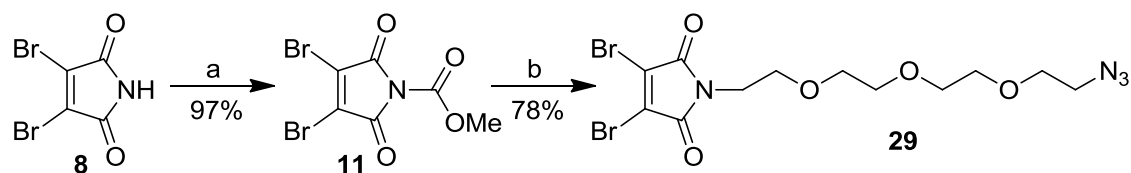
solubility, flexibility, and provide up to a 40 Å distance between the two proteins (90, 91). Thus, **28** was designed to contain a short PEG chain conferring reasonable aqueous solubility and flexibility to the linker, and this particular 3 unit PEG gives the desired ~20 Å length for combination with a similarly designed linker.



**Scheme 2.11** Reagents and conditions: (a) PhSH, NaHCO<sub>3</sub>, MeOH; (b) MeOCOCl, NMM, EtOAc; (c) NH<sub>2</sub>(CH<sub>2</sub>CH<sub>2</sub>O)<sub>3</sub>CH<sub>2</sub>CH<sub>2</sub>N<sub>3</sub>, DCM.

The azide linker **28** was simply obtained over just three steps. First, the commercially available dibromomaleimide **8** was converted to the thiophenol derivative **9** in 30 min at ambient temperature in 76% yield. The thiol maleimide **9** was subsequently functionalised with an *N*-(methoxycarbonyl) to produce **27** in excellent yield (97%). Reaction of activated dithiophenol maleimide **27** with the commercially available amine-PEG-azide under mild conditions furnished linker **28** in a good 78% yield.

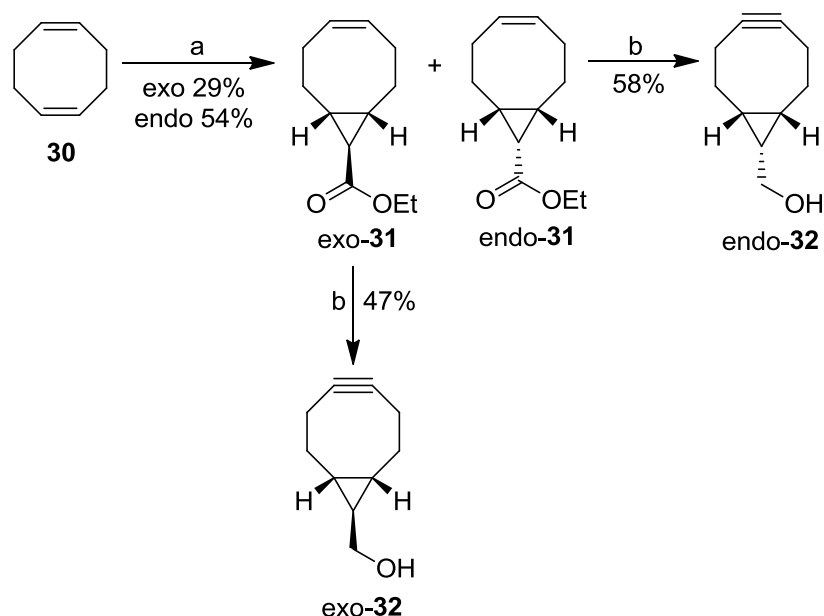
In an analogous approach, a dibromomaleimide version of the azide linker **29** was also synthesised (Scheme 2.12). Over just two steps, linker **29** was obtained in an overall 76% yield.



**Scheme 2.12** Reagents and conditions: (a) MeOCOCl, NMM, EtOAc; (b) NH<sub>2</sub>(CH<sub>2</sub>CH<sub>2</sub>O)<sub>3</sub>CH<sub>2</sub>CH<sub>2</sub>N<sub>3</sub>, DCM.

### 2.2.2 Synthesis of a strained alkyne functionalised disulfide bridging linker

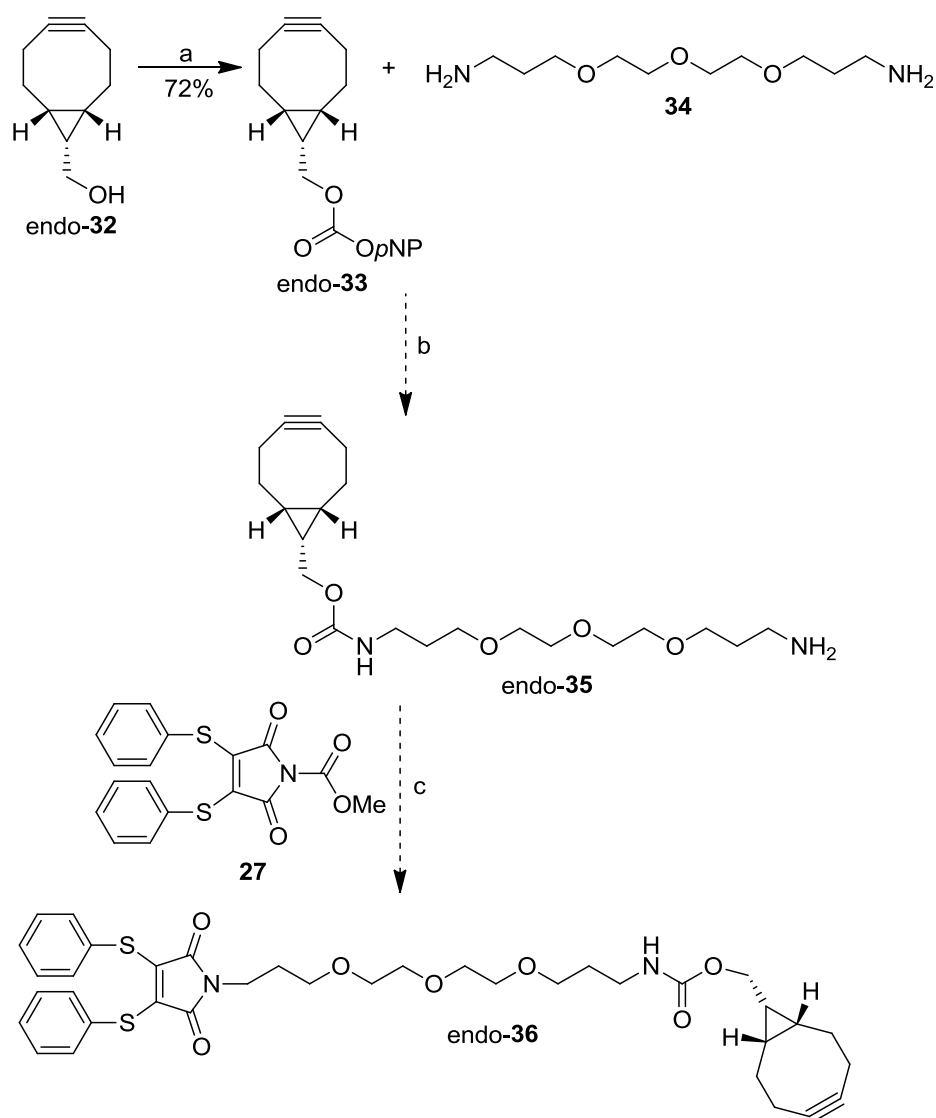
The first step towards synthesis of this linker required the selection of the appropriate strained alkyne. Dibenzocyclooctyne (DIBO) is a popular choice, owing to its relatively straightforward synthesis compared to alternatives (see *Section 1.8.2.4*). However, we felt the significant lipophilicity of this compound and others e.g. azadibenzocyclooctyne (DIBAC) and biarylazacyclooctynone (BARAC), to be a significant drawback as this can lead to non-specific binding to proteins (137). The bicyclo[6.1.0]nonyne (BCN) **32** was judged the most suitable as it displays excellent reaction kinetics ( $0.14 \text{ M}^{-1}\text{s}^{-1}$  for *endo*-**32** and  $0.11 \text{ M}^{-1}\text{s}^{-1}$  for *exo*-**32**) and it is  $C_s$  symmetrical (139) (*Scheme 2.13*). Furthermore, it is synthesised through the cyclopropanation of the cheaply available 1,5-cyclooctadiene **30**.



**Scheme 2.13** Reagents and conditions: (a) EtOCOCHN<sub>2</sub>, Rh(OAc)<sub>2</sub>, DCM, 0°C; (b) 1. LiAlH<sub>4</sub>, Et<sub>2</sub>O, 0°C; 2. Br<sub>2</sub>, DCM; 3. KO<sup>t</sup>Bu, THF, 0°C to reflux.

The synthetic route to BCN is outlined in *Scheme 2.13*. First, cyclopropanation of cyclooctadiene occurs readily over 40 h in an overall 83% yield. The diastereomers *exo*- and *endo*-**31** are obtained separately after difficult and lengthy purification by flash column chromatography. The individual stereoisomers are then subjected to reduction, bromination and elimination using only one final purification step to yield the corresponding hydroxyalkynes *exo*- and *endo*-**32** in 47% and 58% yield respectively. The difference in rate in the SPAAC reaction for these diastereomers is marginal, and so

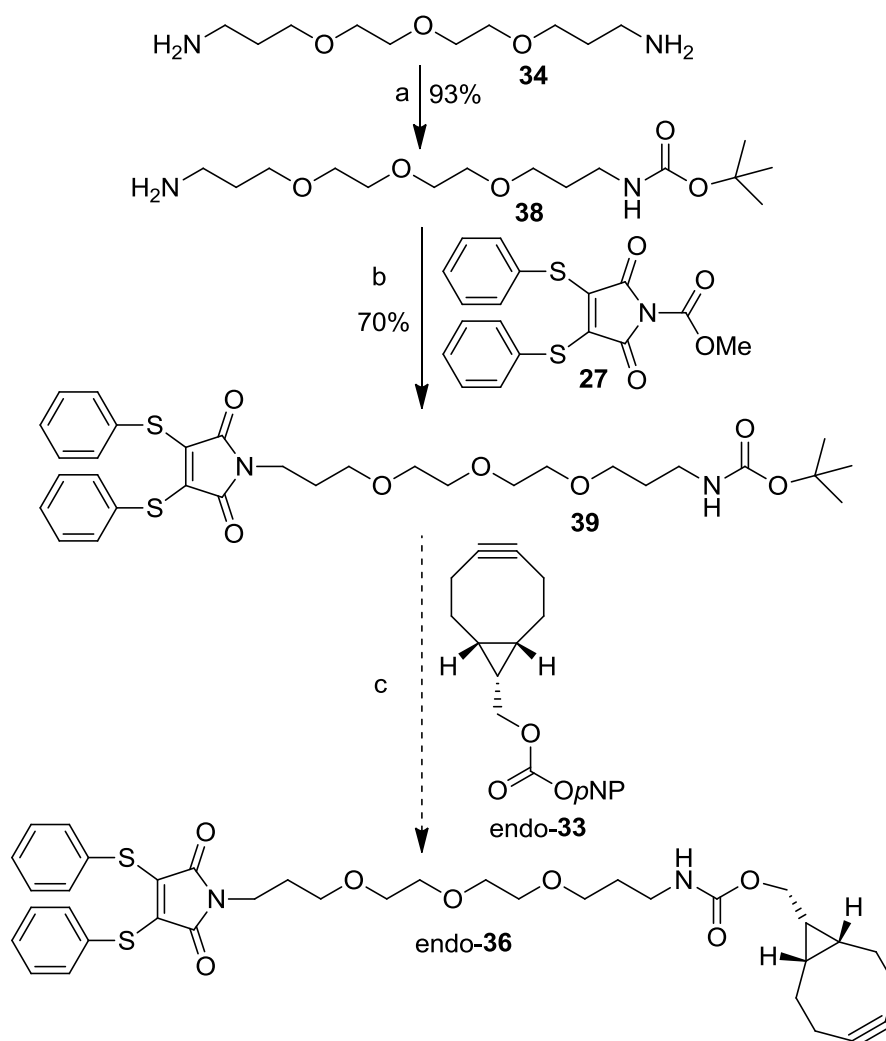
both isomers were used in linker synthesis. The devised synthetic route for the strained alkyne linker **36** is exemplified for *endo*-**32** in *Scheme 2.14*.



**Scheme 2.14** Reagents and conditions: (a) *p*-NO<sub>2</sub>PhOC(O)Cl, pyridine, DCM; (b) NEt<sub>3</sub>, DCM; (c) DCM.

In the first step towards linker **36**, the hydroxyalkyne **32** was functionalised with a *para*-nitrophenyl group to give **33** in 72% yield. The aim was to then couple **33** to 4,7,10-trioxa-1,13-tridecanediamine **34**, economically providing the desirable 3 PEG unit linker length. However, several attempts at this step using 5, 10 and 15 equivalents of the diamine-PEG simply resulted in addition of the alkyne at both amines. Higher equivalents successfully achieved monoaddition; however purification by flash column chromatography resulted in co-elution with the diamine PEG starting material (product **35** contained 10% diamine PEG by NMR). The next step **c** would have involved reaction of *N*-(methoxycarbonyl) thiophenol maleimide **27**, synthesised as shown in

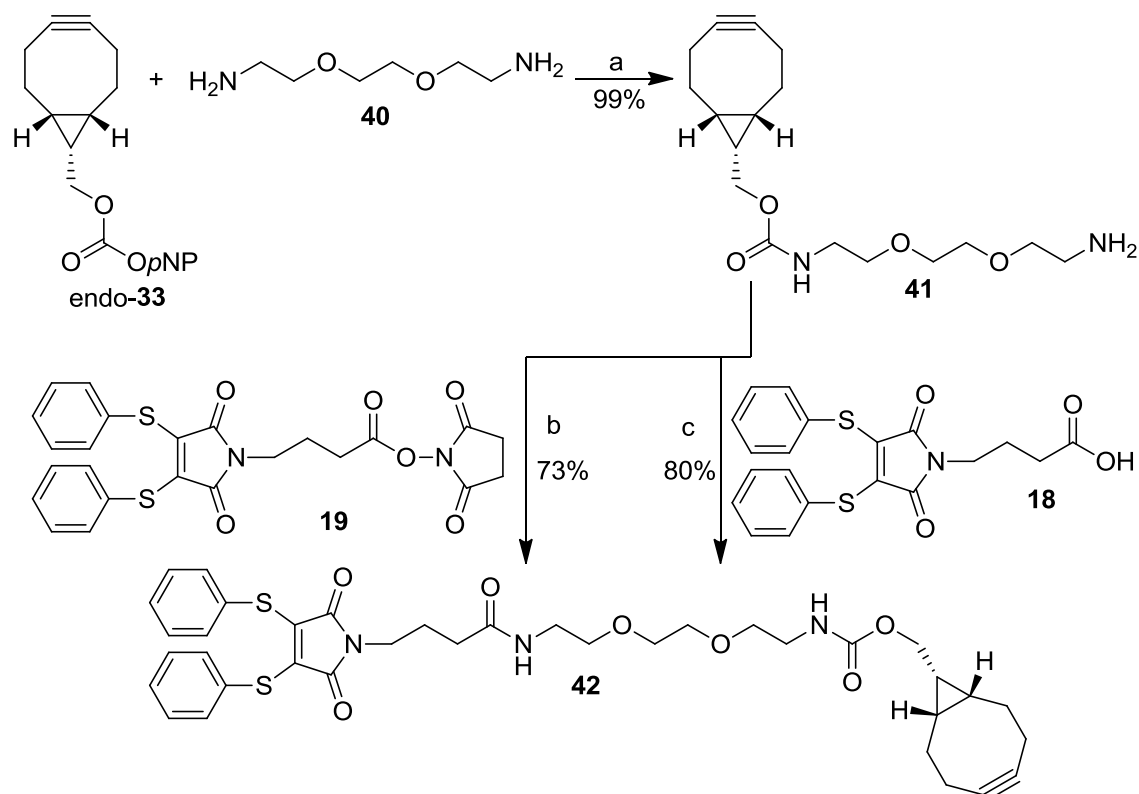




**Scheme 2.16** Reagents and conditions: (a) Boc<sub>2</sub>O, 1,4-dioxane; (b) NEt<sub>3</sub>, silica, DCM; (c) 1. TFA, DCM; 2. *Endo-33*, NEt<sub>3</sub>, DCM.

The diamine-PEG **34** was successfully monoprotected using Boc-anhydride to give **38** in 93% yield. The activated thiophenol maleimide **27** was subsequently able to react with the free amine generating **38** in 70% yield. It should be noted that triethylamine and silica are necessary in this step in order to produce the closed maleimide ring product (181). The next and final step in the synthesis of strained alkyne linker **36** is the removal of the Boc group and coupling to the *para*-nitrophenyl activated strained alkyne **33**. However, this route was terminated here as it was superseded by an alternative strategy that was being explored in parallel.

In tandem to the synthetic route towards the thiophenol maleimide strained alkyne linker shown in *Scheme 2.16*, an alternative approach was also pursued (*Scheme 2.17*).

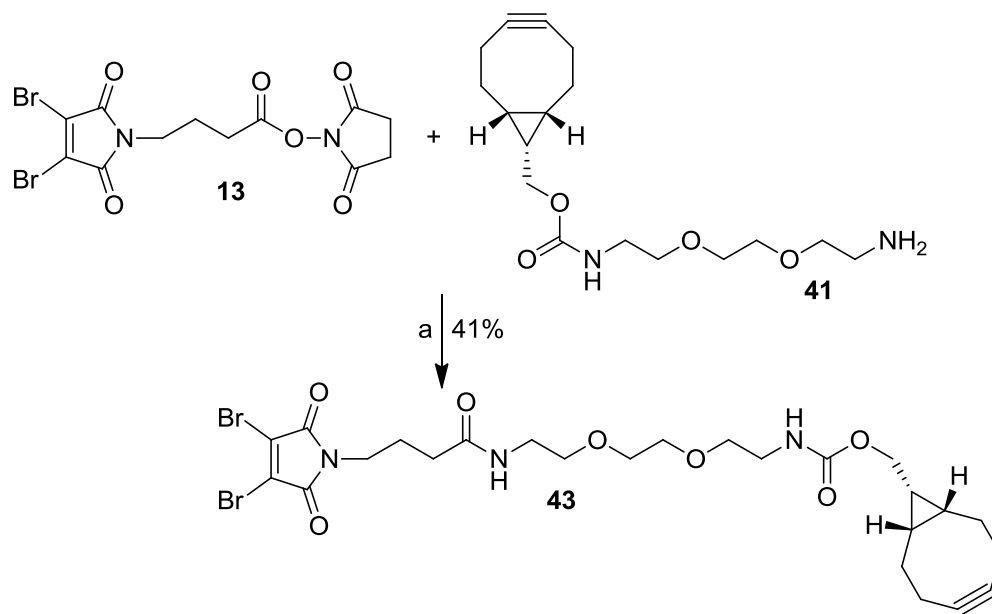


**Scheme 2.17** Reagents and conditions: (a)  $\text{NEt}_3$ , DMF; (b) DMF, overnight; (c) HBTU, HOBT, DIPEA, DMF, overnight.

The synthetic strategy outlined in *Scheme 2.17* first requires the successful monoaddition of commercially available 1,8-diamino-3,6-dioxaoctane **40**. This short diamine PEG is successfully used in the original BCN synthesis paper (139). Following literature procedure, the desired product **41** was readily formed in a pleasing 99% yield. It was then proposed that the previously synthesised dithiophenol maleimide linker **19** could be used for simple functionalisation of the strained alkyne. Indeed, addition of monoamine strained alkyne **41** to linker **19** in DMF generated the desired target **42** in a good 73% yield. Since this approach negates the requirement for protection and deprotection steps and proceeds with good yield, no further work towards the synthetic route using diamine **34** was carried out (*Scheme 2.16*). Later resynthesis of strained alkyne linker **42** also established that HBTU coupling could successfully be applied to directly link dithiophenolmaleimide carboxylic acid **18** to strained alkyne **41** in an excellent 80% yield (*Scheme 2.17*).

Following the success of the synthetic route outlined in *Scheme 2.17*, the same approach was used to produce dibromomaleimide strained alkyne linker **43** (*Scheme 2.18*). This instead used the previously synthesised linker **13**, and suffered a slightly lower yield

due to competing attack of monoamine **41** on the dibromomaleimide, as observed in *Section 2.1.3*.



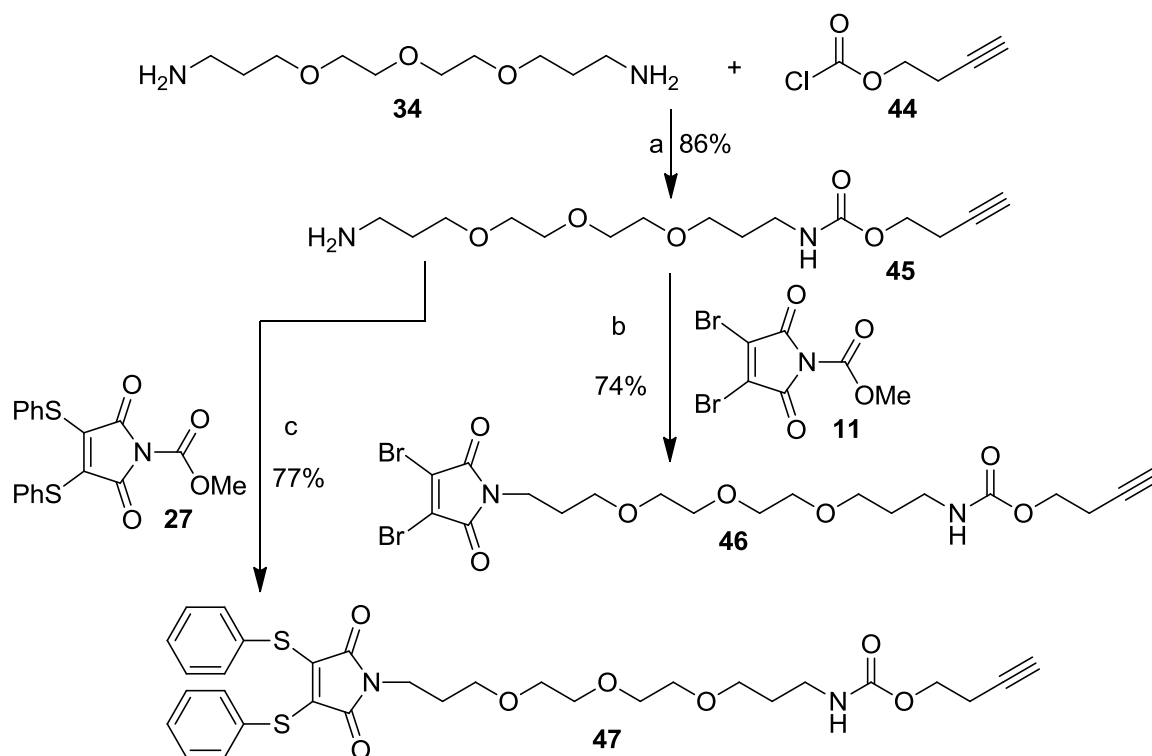
**Scheme 2.18** Reagents and conditions: (a) DMF, overnight.

### 2.2.3 Synthesis of a linear alkyne functionalised disulfide bridging linker

Despite the development of several strained alkyne structures, the rate of the strain-promoted azide-alkyne cycloaddition (SPAAC) still remains low by comparison to its copper-catalysed parent reaction (CuAAC) (188). In construction of antibody conjugates such as bispecifics, a chemical conjugation approach with a high rate of reaction has distinct advantages; large excesses of expensive reagents are not required to promote reaction and shorter reaction times reduce the opportunity for loss of protein activity through degradation or aggregation. Previously, concerns have been raised of protein damage in the CuAAC reaction through the copper mediated generation of reactive oxygen species. However, recent advances in CuAAC optimisation have now enabled the use an *in situ* reducing agent for fast and efficient bioconjugation without damage to the biological environment (189) (see *Section 2.2.7*). In order to explore the potential of copper-catalyzed bioconjugation, synthesis of a linear alkyne functionalised substituted maleimide was thus also pursued.

Using a simple synthetic route, both dibromo- and dithiophenolmaleimide versions of the desired linear alkyne could be generated from their corresponding *N*-(methoxycarbonyl) maleimides **11** and **27** respectively (*Scheme 2.19*). First, the commercially available alkyne chloroformate **44** underwent successful monoaddition to

diamine **34** (86%). After purification, the amino PEG alkyne **45** could then be added to the desired dibromo- or dithiophenolcarbamate to generate **46** and **47** respectively in good yield (74%, 77%).



**Scheme 2.19** Reagents and conditions: (a)  $\text{NEt}_3$ , DMF; (b) DCM; (c) DCM.

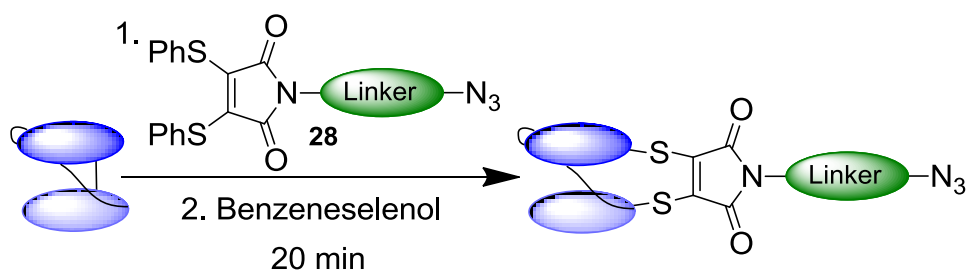
#### 2.2.4 Functionalisation of an anti-CEA ds-scFv fragment

As earlier discussed, the scFv is the smallest antibody fragment which retains full binding activity, and is a common component of many bispecific antibody formats e.g. BiTEs (Bispecific T-cell Engager) and DARTs (Dual-Affinity Re-Targeting), and antibody-enzyme conjugates. To examine the feasibility of our ‘click’ disulfide bridging approach to producing homogeneous protein-protein conjugate, we decided to first work with the anti-CEA disulfide-stabilised scFv fragment. Attempting to bring together two ds-scFv fragments homogeneously using this technology will give good precedent as to whether this approach could be used to readily generate homogeneous bispecifics in good yield.

The first step towards successful homogeneous bispecific production requires the efficient and site-specific introduction of the linker into the antibody fragment to be conjugated. Thus initial investigations focused on the development of suitable conjugation methods for each linker to the ds-scFv.

### 2.2.4.1 Disulfide bridging with an azide functionalised linker

As discussed previously, dithiomaleimide can be used with the reducing agent benzeneselenol for the *in situ* disulfide bridging of the ds-scFv fragment. Using this protocol, bridging of the scFv was first attempted using 2, 5 and 15 equivalents of the dithiophenolmaleimide azide linker **28** and between 15 and 25 equivalents of the reducing agent benzeneselenol (*Scheme 2.20*). The results were analysed by LCMS (*Figure 2.14*).



**Scheme 2.20** Bridging of anti-CEA ds-scFv with azide linker **28** via the *in situ* protocol.

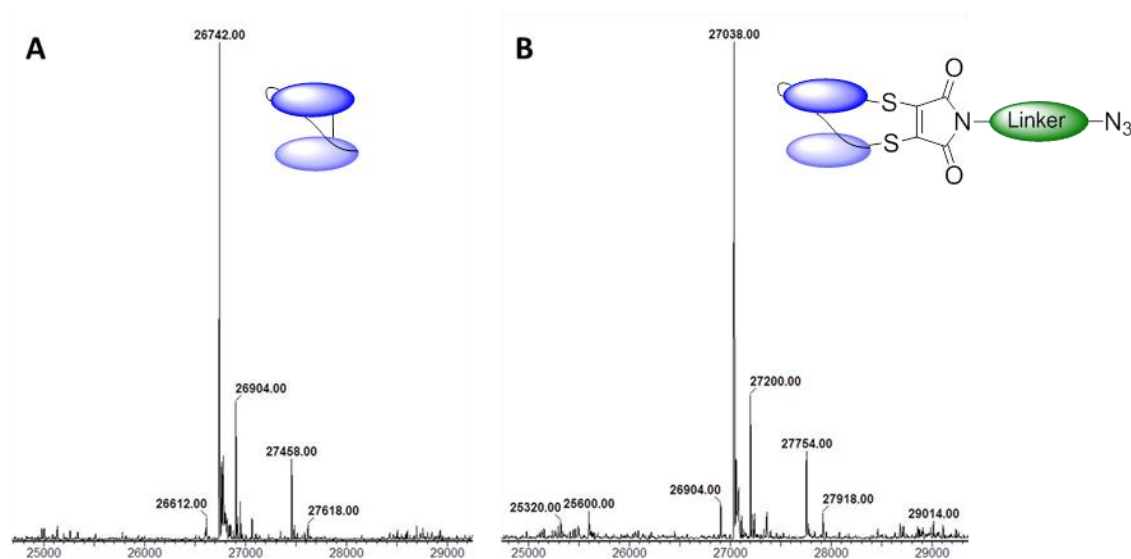
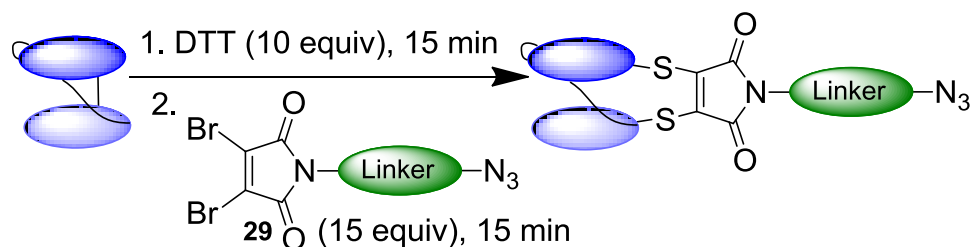


**Figure 2.14** LCMS analysis of bridging with linker **28**. **(A)** Unmodified anti-CEA ds-scFv (mass 26,742). **(B)** Modified with linker **28** (expected 27,038, observed 27,038).

The LCMS results of bridging with linker **28** are shown in *Figure 2.14*. The disulfide bond of the anti-CEA fragment was successfully bridged in all cases, using as little as 2 equivalents of linker **28** with 25 equivalents of reducing agent for full conversion. Achieving fully bridged material with low equivalents of linker is particularly desirable for future applications where these modifications may be carried out on a large scale.

For the dibromomaleimide azide linker **29** an *in situ* approach using benzeneselenol cannot be adopted, since this method relies on the release of the thiophenol groups from the maleimide by selenol for efficient reduction. Instead, sequential or stepwise disulfide bridging approaches can be used. In contrast to the *in situ* method, these protocols are based on reduction of the disulfide prior to bridging. In fact, the sequential and stepwise bridging strategies differ only in that there is an additional purification step in the latter; reducing agent is removed prior to bridging in the stepwise procedure.

Dithiothreitol (DTT) is established in the group as the choice reducing agent for the sequential or stepwise reduction of the ds-scFv. The developed sequential protocol employs 20 equivalents of DTT for 1 h, followed by 30 equivalents of dibromomaleimide. In order to use less reducing agent and so linker in this conjugation approach, a series of optimisation experiments were carried out using linker **29** with ds-scFv to determine if efficient bridging could be maintained with lower equivalents. Analysis by LCMS revealed that complete bridging of ds-scFv with **29** could be achieved using 10 equivalents of DTT for 15 min, followed by 15 equivalents of **29** (*Scheme 2.21*).



**Scheme 2.21** Bridging of anti-CEA ds-scFv with azide linker **29** via the sequential protocol.

At this point, it should be noted that optimisation of alternative bridging protocols to the *in situ* approach were sought due to reliance on benzeneselenol. Benzeneselenol is an intensely malodorous compound, does not dissolve in water and oxidises rapidly in air, becoming inactive as a reducing agent. For our protocols to be adopted generally for the production of homogeneous bispecifics, we endeavoured to develop methods using common, water soluble reagents such as DTT and TCEP. Unfortunately TCEP was found not to reduce the disulfide bond of the ds-scFv fragments used in this project, thus efforts focused on using DTT.

---

Disulfide bridging attempts using the sequential protocol with dithiophenolmaleimide azide linker **28** resulted in incomplete bridging. The large amount of free thiol generated through the combination of DTT and thiophenol leaving groups on the maleimide is the likely cause.

Stepwise bridging differs only from sequential in that a purification step is included after reduction. This should ensure that no free reducing agent is present prior to linker addition, and thus allows for significantly lower equivalents of valuable linker to be used for bridging. Furthermore, this protocol can be used in combination with dithiomaleimide based reagents. Following reduction with DTT (10 to 30 equivalents) for up to 1 h, scFv purification from free reducing agent was attempted using buffer exchange via desalting column or spin column, or a combination of the two. Using both linkers **28** and **29**, complete bridging was not observed via the stepwise approach. A small amount of unmodified scFv (up to ~10%) could always be seen by LCMS and analysis by SDS-PAGE revealed this to be re-oxidised ds-scFv. The re-oxidation of this disulfide occurs rapidly in the absence of reducing agent. This issue was overcome in later work (see *Section 2.3.2*).

#### **2.2.4.2 Disulfide bridging with a strained alkyne functionalised linker**

Pleasingly, the *in situ* and sequential conditions optimised for the azide linkers **28** and **29** were readily transferred to the dithiophenol- and dibromomaleimide analogues of the strained alkyne linkers **42** and **43**. The results were analysed by LCMS, and the desired mass increase of 487 can be observed (*Figure 2.15*).

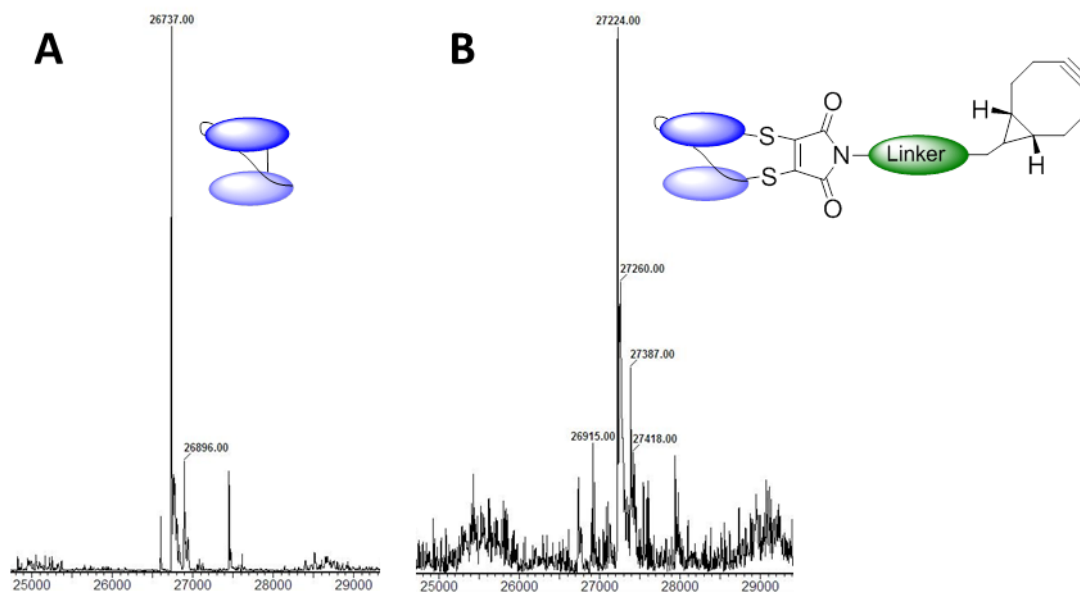


**Figure 2.15** LCMS analysis of bridging with linkers **42** and **43**. **(A)** Unmodified anti-CEA ds-scFv (mass 26,737). **(B)** Modified with linker **42** or **43** (expected 27,224, observed 27,224).

Although the correct mass was observed for disulfide bridging of the ds-scFv with the strained alkyne linker in the first instance, this did not remain the case when bridging was repeated.

#### 2.2.4.2.1 Stability of the strained alkyne

Upon repeating disulfide bridging of the scFv fragment with both strained alkyne linkers **42** and **43**, a different mass was observed by LCMS after modification. The expected mass is an increase of 487 Da on the unmodified ds-scFv; however an increase of 519 was observed (*Figure 2.16*). Linkers **42** and **43** were prepared as a concentrated stock in DMF and stored at -20 °C. The repeat modification used the same stock as the initial analysis, and had been stored in the freezer for one week.

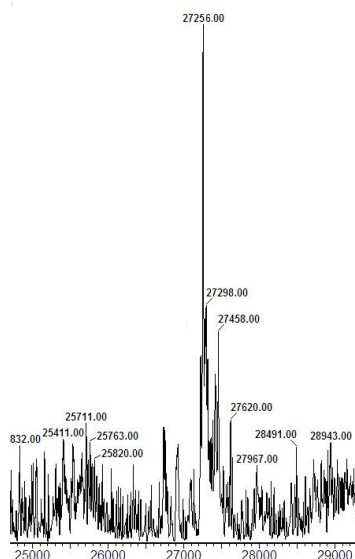


**Figure 2.16** Repeat LCMS analysis of ds-scFv bridging with linkers **42** and **43**. Expected 27,224, observed 27,256, a +32 increase.

To establish whether the strained alkyne linker is unstable in DMF, fresh stocks of both linkers **42** and **43** were prepared. Disulfide bridging with the newly prepared DMF stock was repeated, and the original expected mass of 27,224 was once again observed. However, on repeating this reaction a day later, the major peak observed was now 27,256. In fact, in the initial modification analysis using these linkers in *Figure 2.15B*, a minor peak can be seen at the very similar mass of 27,260. Thus it appears that this +32 species is rapidly generated in DMF.

The unexpected +32 species observed in DMF does not affect the efficiency of disulfide bridging, suggesting that no alterations have occurred to the substituted maleimide of molecules **42** and **43**. To investigate if the strained alkyne had been affected, an azide-fluorophore Chromeo 546, was added in large excess (100 equivalents) to a sample of the strained alkyne functionalised scFv that contained only the +32 species by mass spectrometry. After 1 h the reaction was analysed by LCMS to reveal no increase in mass for the attachment of the fluorophore. In fact, the lack of reaction could be observed by eye, since after purification by desalting column to remove free fluorophore, no pink/red colour could be seen in the protein fractions. This suggests therefore, that the +32 species of the strained alkyne linker is no longer active, and cannot be used to produce homogeneous antibody-antibody conjugate.

In the literature, the reactivity of cyclooctynes is described as “explosive” towards azides, but also “is air-sensitive and rearranges and polymerizes easily” (190). In regards to instability, many papers refer to early work describing the oxidation of the triple bond of cyclooctynes in air to form the corresponding cyclooctane-dione (191). It is plausible that through storage in DMF, over time any small amount of molecular oxygen present may react with the strained alkyne. This would account for the increase in 32 Da on the expected modified mass. Reaction at the strained alkyne triple bond would also explain the lack of reactivity on incubation with a large excess of azide. Unfortunately, re-isolation of the strained alkyne linkers from DMF was not achieved. In order to successfully use the strained alkyne linkers **42** and **43** in conjugation, alternative stock storage conditions were devised.

After screening a number of solvents for solubility to enable storage of linkers **42** and **43**, producing a DMSO stock was the most successful strategy. Storage of the strained alkyne linkers in DMSO at -20 °C resulted in the correct mass on disulfide bridging of the scFv fragment (*Figure 2.17*). LCMS analysis was repeated using the same linker stock in DMSO over a period of 6 months, and the correct expected mass was detected in each case. However, one drawback to using a DMSO stock was discovered; it is not compatible with the reducing agent benzeneselenol. Any trace of DMSO present in the reaction rapidly oxidises benzeneselenol, rendering it useless as a reducing agent. Consequently the *in situ* protocol cannot be adopted for ds-scFv modification with the strained alkyne linkers, and so sequential or stepwise protocols must be practiced.

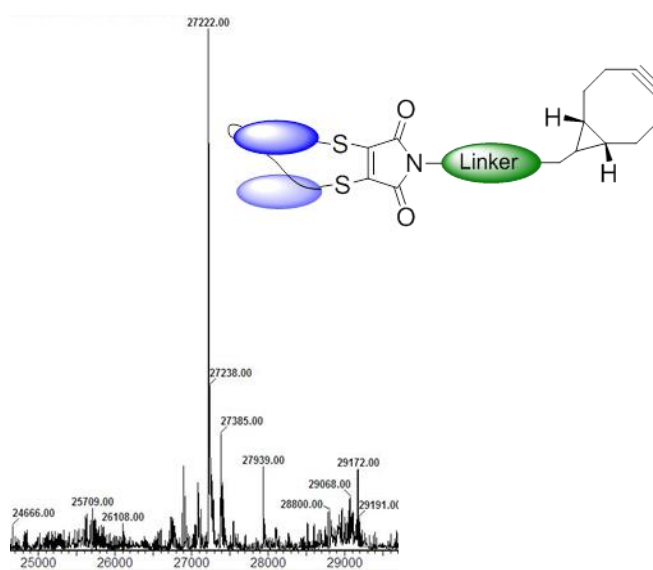


**Figure 2.17** LCMS analysis of ds-scFv bridging with linkers **42** and **43** prepared in a DMSO stock. Expected 27,224, observed 27,222.

The azide linkers **28** and **29**, and linear alkyne linkers **46** and **47**, did not show any change in mass by LCMS, and appear to be stable in DMF for over 12 months.

#### 2.2.4.3 Disulfide bridging with a linear alkyne functionalised linker

Disulfide bridging of the ds-scFv was also attempted using linear alkyne linkers **46** and **47**. The developed *in situ* procedure was followed using dithiophenolmaleimide linker **47**, and the sequential procedure using dibromomaleimide linker **46**. Both disulfide bridging protocols proceeded efficiently, yielding full conversion to the modified product as observed by LCMS (*Figure 2.18*).

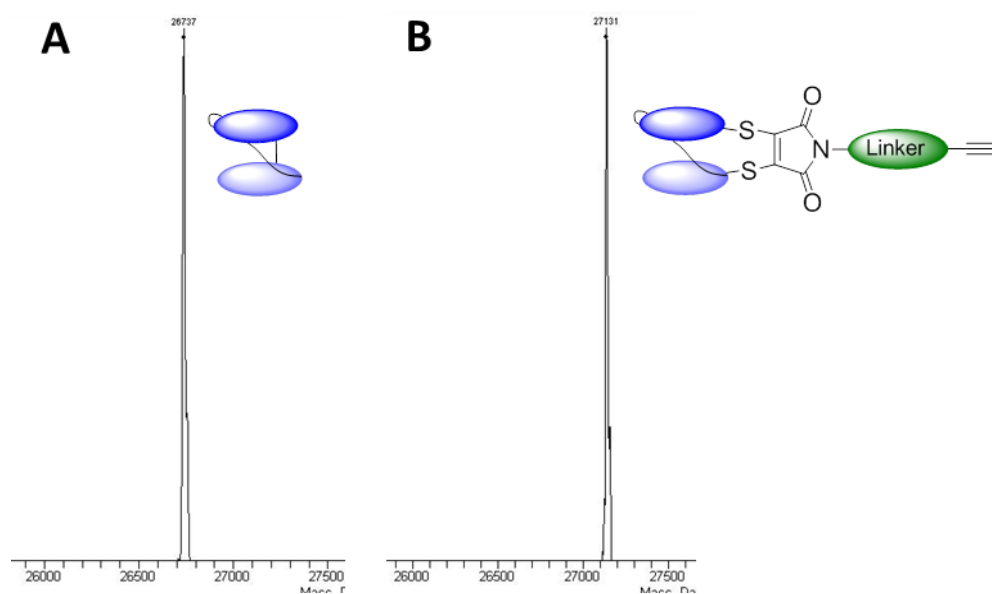


**Figure 2.18** LCMS analysis of bridging with linkers **46** and **47**. **(A)** Unmodified anti-CEA ds-scFv (mass 26,737). **(B)** Modified with linker **46** or **47** (expected 27,131, observed 27,131). **Note:** A different LCMS system is used here and in all proceeding mass spectrometry analysis.

Following the successful functionalisation of the ds-scFv antibody fragment with the azide, strained and linear alkyne linkers, bridging of a Herceptin Fab fragment was investigated. Both Fabs and scFvs are commonly used in a range of bispecific topologies.

## 2.2.5 Functionalisation of Herceptin Fab

The monoclonal IgG1 antibody Trastuzumab (Herceptin™) targets the HER2/neu receptor and has successfully been used to treat HER2+ breast cancer patients (192). The Fab fragment of this clinically relevant antibody can be readily obtained by enzymatic digest, and its incorporation into bispecific formats has therapeutic potential (91). Thus we decided to modify the single interchain disulfide bond of this fragment with our bioorthogonal linkers.

The Trastuzumab Fab was obtained using a sequential digest protocol with pepsin and papain. This is an established protocol in the group, and achieves yields of between 50-70%. Following digest, size exclusion chromatography purification was used to remove any undigested full antibody or F(ab')<sub>2</sub> fragment (*Figure 2.19*). This ensures that all results are due to reaction with the disulfide bond of the Fab fragment alone.

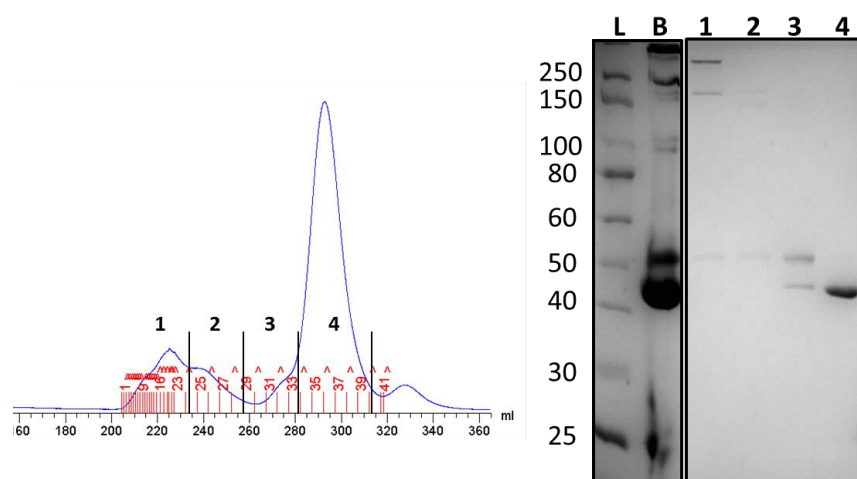
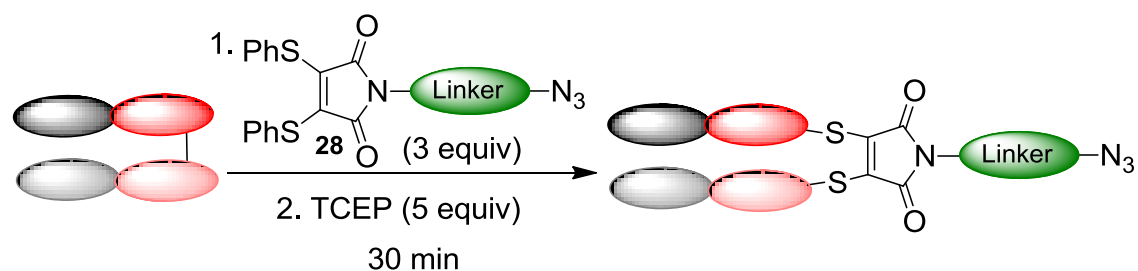


**Figure 2.19** Size exclusion chromatography purification of Fab digest. **Lane L** contains protein ladder in kDa (New England Biolabs). **Lane B** contains digest mixture before purification. **Lanes 1-4** correspond to isolated peaks 1-4, with **lane 4** containing pure Fab (~50 kDa).

### 2.2.5.1 Disulfide bridging with an azide functionalised linker

Unlike the ds-scFv, the single disulfide bond of the Fab fragment could be reduced with the water-soluble reducing agent TCEP, yielding the component heavy and light chains. Using either azide linker **28** or **29**, the Fab could be successfully fully modified using a sequential bridging protocol (*Scheme 2.22*). This was reliably achieved using 5 equivalents of TCEP for 1 h, followed by 8 equivalents of either linker **28** or **29** for 30 min. The reaction was monitored by LCMS and SDS-PAGE (*Figure 2.20*).





**Scheme 2.23** Bridging of Herceptin Fab with dithiophenolmaleimide azide linker **28** via the *in situ* protocol.

### 2.2.5.2 Disulfide bridging with a strained alkyne functionalised linker

Pleasingly, the sequential and *in situ* protocols developed using the azide linkers **28** and **29** could be applied to strained alkyne linkers **42** and **43** (Figure 2.21).

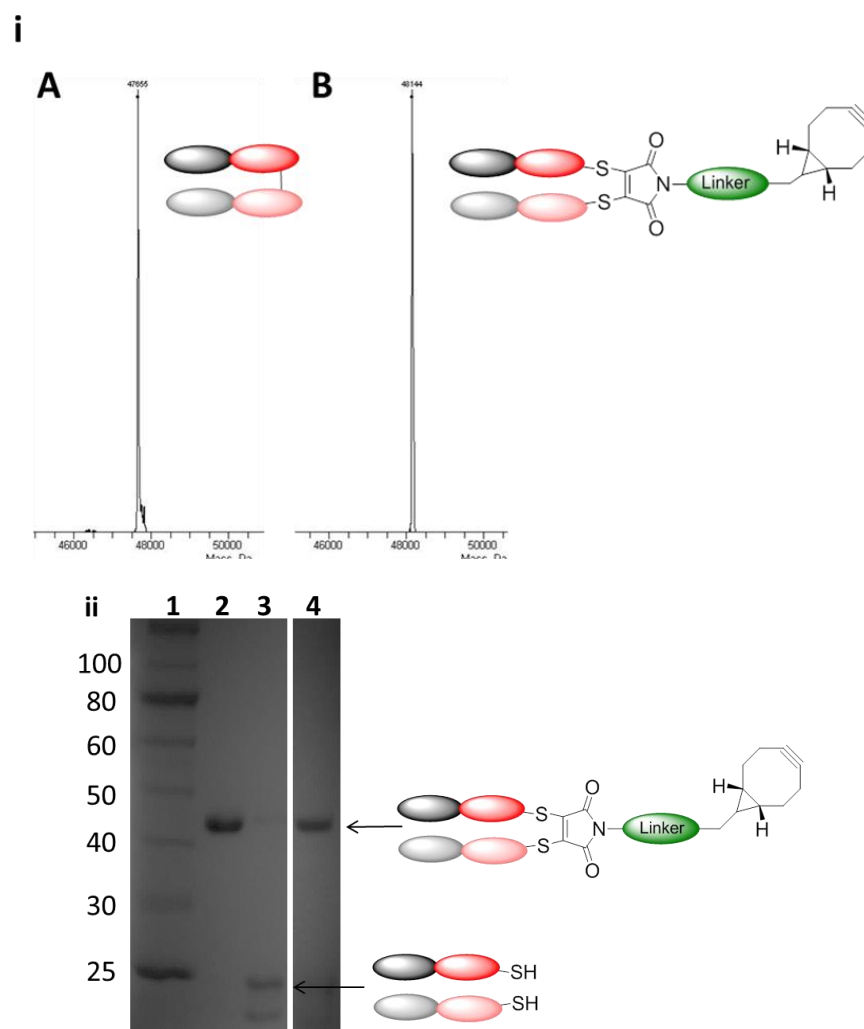


**Figure 2.21** [i] LCMS analysis of bridging with linkers **42** and **43**. **(A)** Unmodified Fab (mass 47,655). **(B)** Modified with linker **42** or **43** (expected 48,142, observed 48,144). [ii] SDS-PAGE analysis of Fab reduction and bridging. **Lane 1** contains protein ladder

in kDa (New England Biolabs). **Lane 2** contains unmodified Fab. **Lane 3** contains reduced Fab after treatment with TCEP. **Lane 4** contains Fab modified with linker **42**.

### 2.2.5.3 Disulfide bridging with a linear alkyne functionalised linker

Again, disulfide bridging could be achieved using the appropriate sequential or *in situ* protocol for linear alkyne linkers **46** and **47** (Figure 2.22).

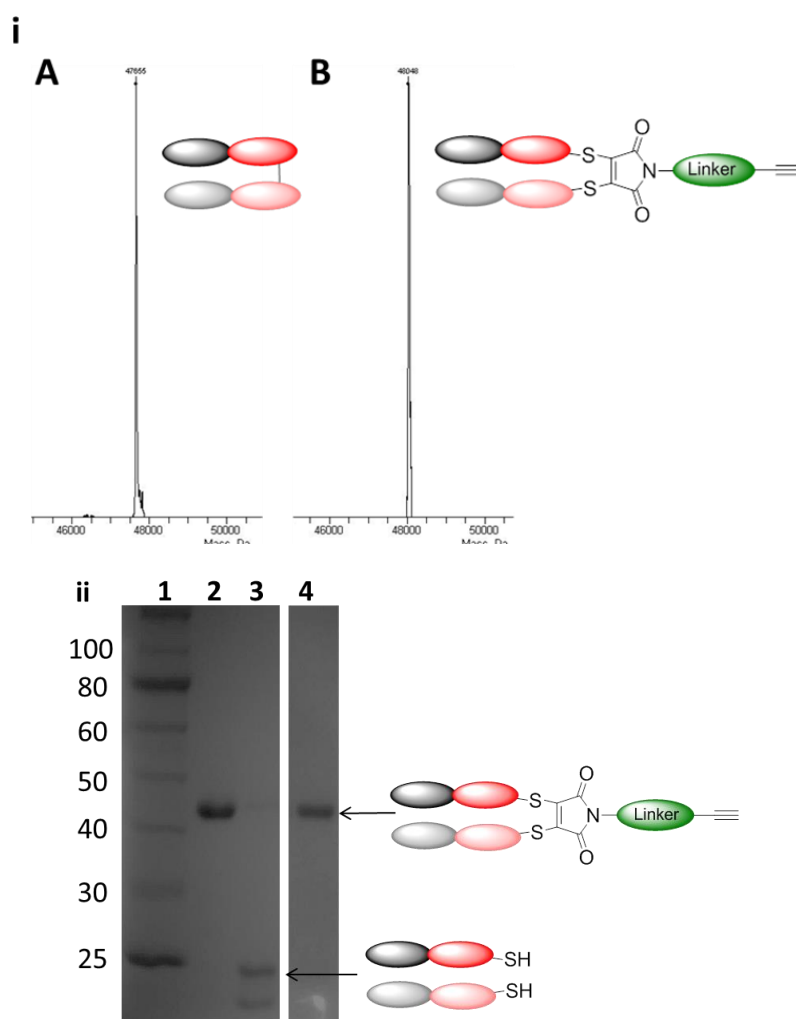
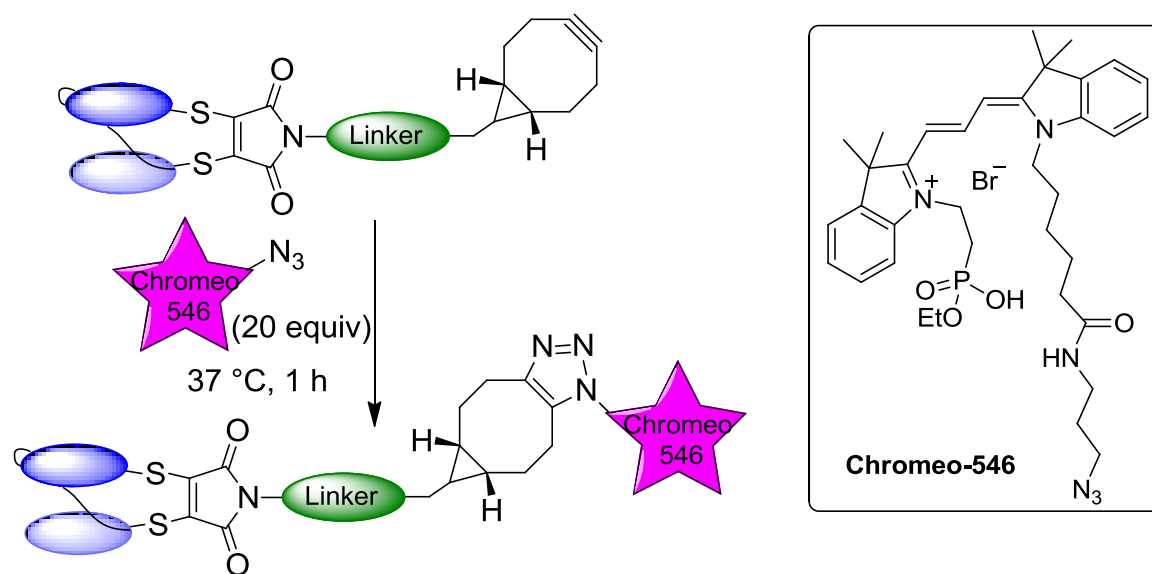


**Figure 2.22 [i]** LCMS analysis of bridging with linkers **46** and **47**. **(A)** Unmodified Fab (mass 47,655). **(B)** Modified with linker **46** or **47** (expected 48,049, observed 48,048). **[ii]** SDS-PAGE analysis of Fab reduction and bridging. **Lane 1** contains protein ladder in kDa (New England Biolabs). **Lane 2** contains unmodified Fab. **Lane 3** contains reduced Fab after treatment with TCEP. **Lane 4** contains Fab modified with linker **47**.

## 2.2.6 Copper-free conjugation towards homogeneous bispecifics

Before attempting to conjugate two antibody fragments, we decided to first investigate the scope of the SPAAC reaction. Initial tests focused on the attachment of small molecules to the azide or strained alkyne functionalised antibody fragments. First, the addition of an azide functionalised fluorophore, Chromeo 546, to strained alkyne functionalised ds-scFv or Fab was investigated.

In the literature, SPAAC reactions using the BCN strained alkyne synthesised in this project, as well as other popular alternatives such as DIBAC, typically use PBS buffer at pH 7.4 for conjugation (90,91,139). Accordingly, after disulfide bridging, the strained alkyne functionalised ds-scFv was buffer exchanged into PBS. This also served to remove any free linker present. After concentrating the antibody to 100  $\mu\text{M}$  (2.7 mg/ml), 20 equivalents of azide Chromeo 546 were added, and the reaction incubated at 37  $^{\circ}\text{C}$  (Scheme 2.24). The results of this early test SPAAC reaction between ds-scFv functionalised with strained alkyne linker **42** and azide Chromeo 546 are shown in Figure 2.23.



**Scheme 2.24** Cycloaddition of azide Chromeo 546 to strained alkyne functionalised scFv.

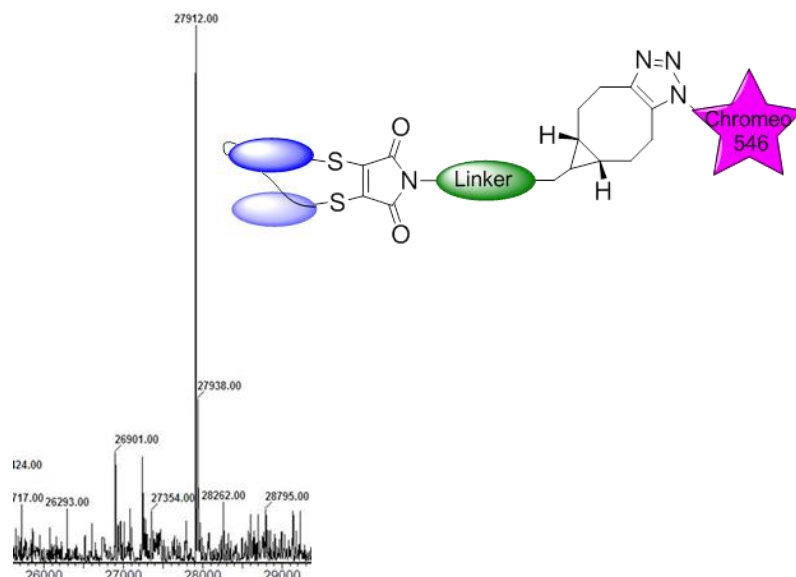
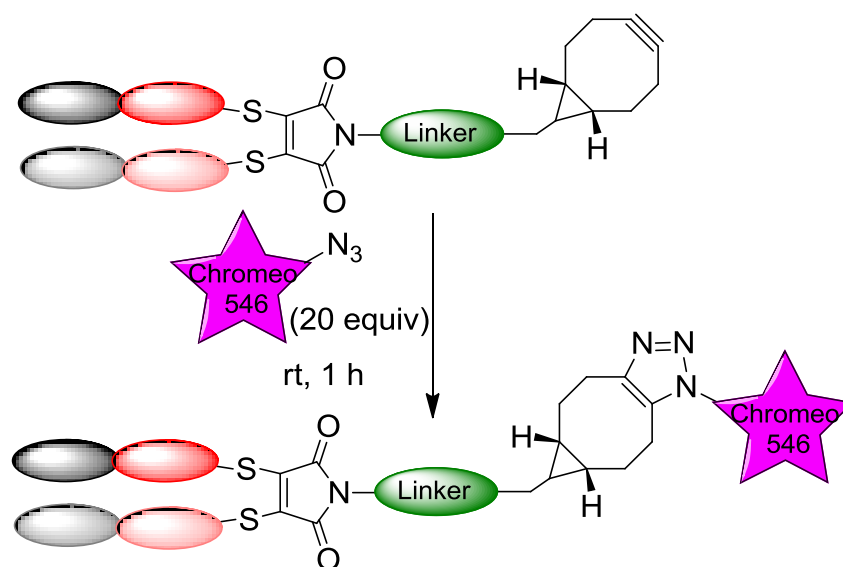


**Figure 2.23** LCMS analysis of reaction between strained alkyne functionalised ds-scFv and azide Chromeo 546. Expected 27,912, observed 27,912.

Pleasingly, the strained alkyne ds-scFv was functionalised with Chromeo 546 after only 1 h at 37 °C (*Figure 2.23*). No unmodified strained alkyne could be detected by LCMS.

The reaction of strained alkyne functionalised Fab with azide Chromeo 546 was also investigated. After disulfide bridging with either linker **42** or **43**, the modified Fab fragment was buffer exchanged into PBS. At concentrations around 100  $\mu\text{M}$  (4.8 mg/ml), the Fab fragment underwent complete modification with Chromeo 546 (20 equivalents) at room temperature after 1 h (*Scheme 2.25*). This reaction was monitored by LCMS (*Figure 2.24*).



**Scheme 2.25** Cycloaddition of azide Chromeo 546 to strained alkyne functionalised Fab.

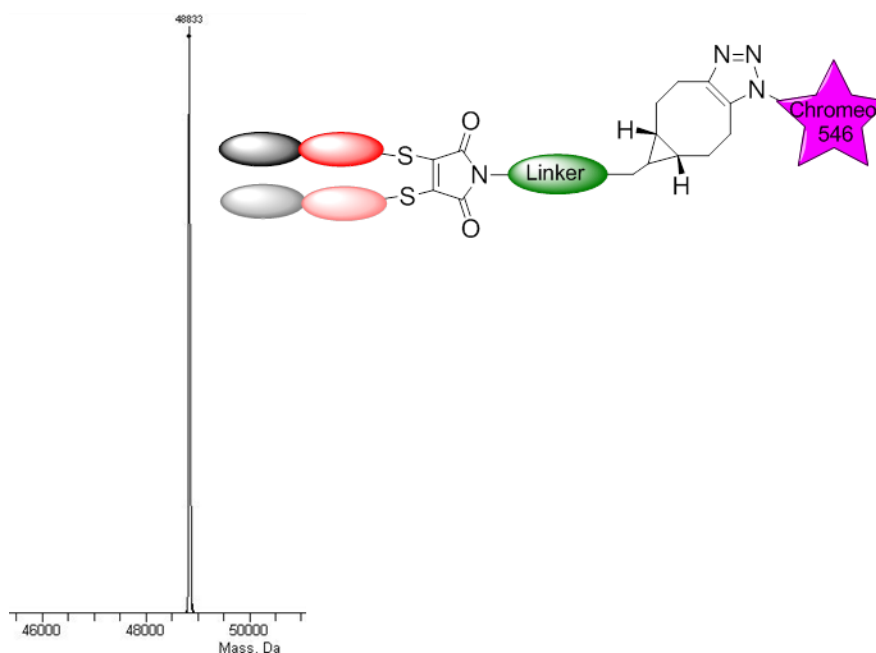
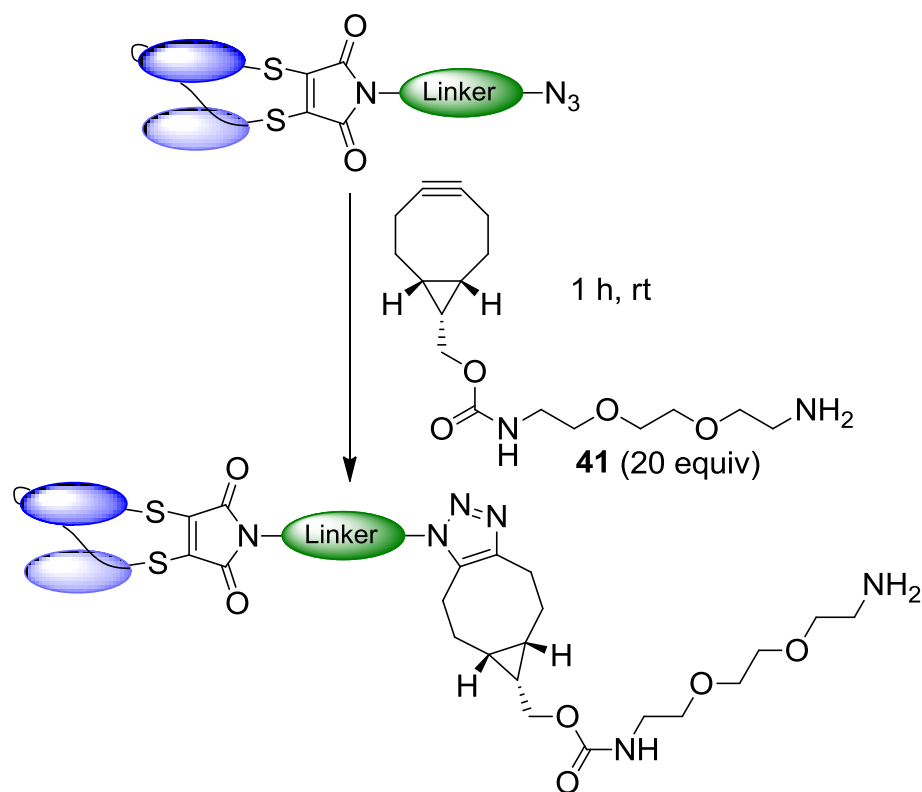


**Figure 2.24** LCMS analysis of reaction between strained alkyne functionalised Fab and azide Chromeo 546. Expected 48,830, observed 48,833.

Compared to its copper-catalysed relative, the slow rate of the SPAAC reaction is often stated as its foremost disadvantage. Our initial investigations certainly reveal this to be the case; a minimum of 20 equivalents of azide Chromeo 546 is required to achieve complete addition to strained alkyne functionalised ds-scFv or Fab at 100  $\mu$ M within 1 h at room temperature.

Reaction with azide Chromeo 546 confirmed that the strained alkyne was able to participate in the SPAAC reaction once conjugated to ds-scFv and Fab fragments. Construction of a homogeneous bispecific would require reaction between strained alkyne and azide functionalised antibody fragments. Thus the reactivity of azide linkers **28** and **29** was also verified. To this end, azide functionalised ds-scFv and Fab were reacted with monoamine PEG strained alkyne **41** (20 equivalents) for 1 h at room temperature. This is shown schematically for the scFv fragment in *Scheme 2.26*. The reaction was followed by LCMS (*Figure 2.25*).



**Scheme 2.26** Cycloaddition of strained alkyne **41** to azide functionalised scFv.

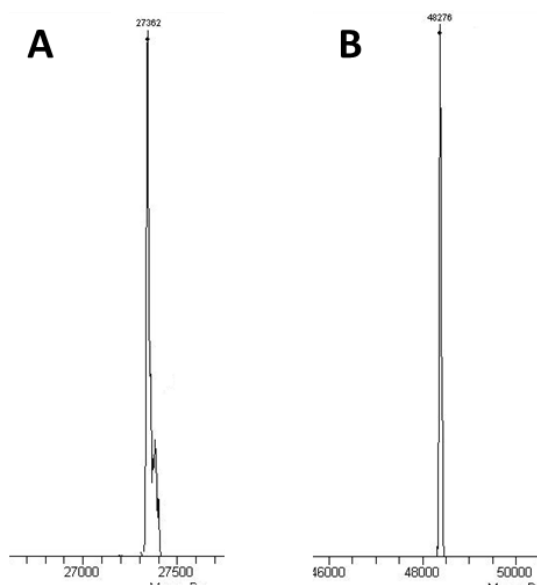
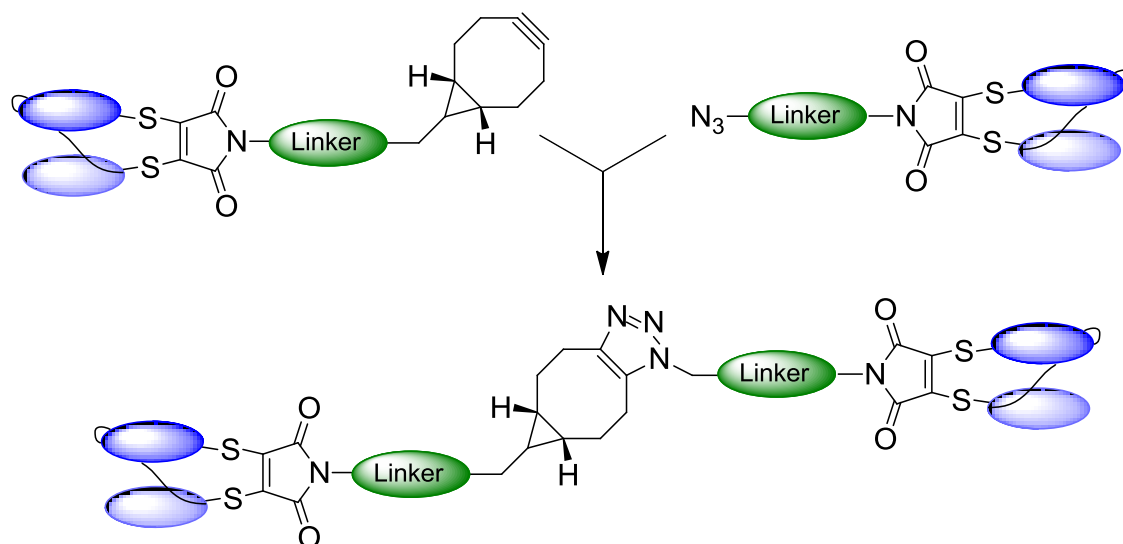


**Figure 2.25** LCMS analysis of reaction with strained alkyne **41** (324 Da). **(A)** Addition of **41** to azide functionalised ds-scFv. Expected 27,362, observed 27,362. **(B)** Addition of **41** to azide functionalised Fab. Expected 48,275, observed 48,276.

As shown in *Figure 2.25*, the azide group of linkers **28** and **29** remains active when conjugated to both of the model system antibody fragments, ds-scFv and Fab. Following this success, the ability of these linkers to produce homogeneous antibody fragment homodimer was investigated (*Scheme 2.27*).



**Scheme 2.27** Generation of scFv homodimer via SPAAC reaction.

First, the generation of scFv homodimer was pursued. In the literature, there are limited examples of site-specific protein-protein conjugation using the SPAAC reaction. The most relevant example was recently demonstrated by Schultz *et al.*, who successfully produced both a Fab homodimer and heterodimer using SPAAC chemistry (see *Section 1.8.2.4*) (91). To achieve this, strained alkyne and azide functionalised Fab fragments were concentrated to 10 mg/ml, and mixed in a 1:1 ratio in PBS at 37 °C for 72 h. Given the slow rate of reaction observed when using these linkers to attach small molecules, and such literature precedent, generation of scFv homodimer was first attempted at high concentration (*Figure 2.26*).

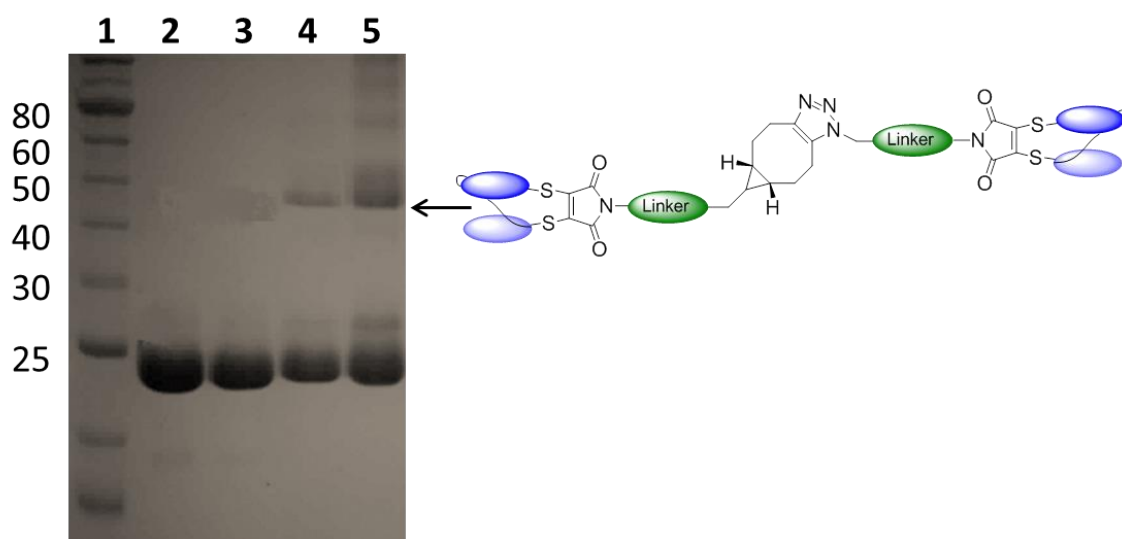


**Figure 2.26** SDS-PAGE analysis of generation of scFv homodimer. **Lane 1** contains protein ladder in kDa (New England Biolabs). **Lane 2** contains azide functionalised scFv. **Lane 3** contains strained alkyne functionalised scFv. **Lane 4** contains homodimer reaction sample after 1 h. **Lane 5** contains homodimer reaction sample after 24 h.

---

After disulfide bridging with the strained alkyne and azide linkers, the modified scFv fragments were purified by desalting column and subsequently concentrated to 10 mg/ml. The desalting column ensures no free linker remained after bridging. The functionalised fragments were then mixed in a 1:1 ratio. *Figure 2.26* shows the formation of a small amount of homodimer after 1 h (*lane 4*), and this yield increases slightly after 24 h (*lane 5*). However, these long reaction times also resulted in the appearance of higher molecular weight aggregates, as can be seen in *lane 5*. To investigate the source of these aggregates, the reaction was repeated with key controls (*Figure 2.27*).

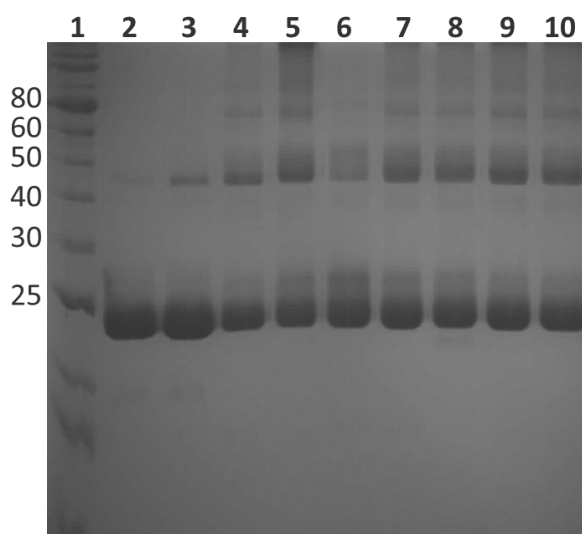


**Figure 2.27** SDS-PAGE analysis of generation of scFv homodimer with key controls at 37 °C. **Lane 1** contains protein ladder in kDa (New England Biolabs). **Lane 2** contains scFv control. **Lane 3** contains scFv incubated for 48 h. **Lane 4** contains azide functionalised scFv incubated for 48 h. **Lane 5** contains strained alkyne functionalised scFv incubated for 48 h. **Lanes 6 to 10** contain homodimer reaction sample after 1, 16, 24, 36 and 48 h respectively.

Samples of unmodified, azide functionalised and strained alkyne functionalised scFv were individually incubated at 37 °C at 10 mg/ml over 48 h (*Figure 2.27, lanes 3 to 5*). In all three controls there is a band at ~50 kDa, the same mass that would correspond to the formation of scFv dimer. Furthermore, strained alkyne functionalised scFv shows distinct formation of higher molecular weight aggregates (*Figure 2.27, lane 5*). These correspond to the aggregates observed in the homodimer reaction over time (*Figure 2.27, lanes 6 to 10*).

The results in *Figure 2.27* reveal a potential problem with the strained alkyne linker under the reaction conditions. In addition, the controls indicate the formation of non-specific scFv homodimer for all controls at this temperature and concentration, as a band at the expected mass of ~50 kDa is observed without incubation of the two SPAAC reaction partners. To determine if these issues are temperature dependent, the reaction was repeated at room temperature and 4 °C (*Figure 2.28*).

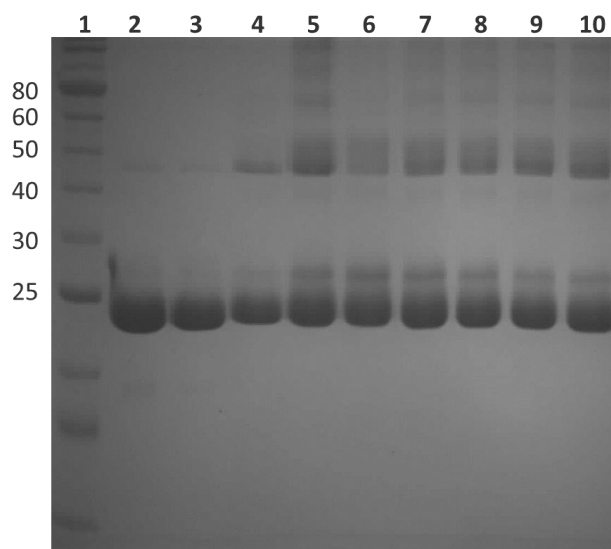


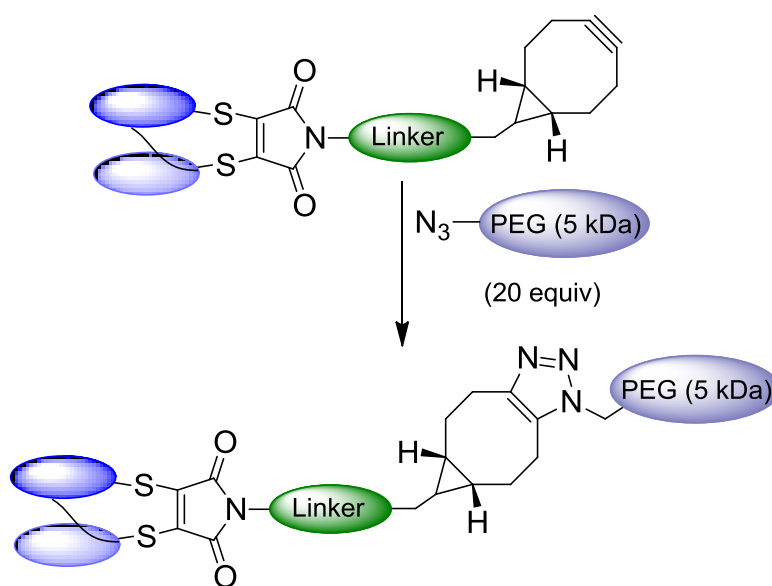
**Figure 2.28** SDS-PAGE analysis of generation of scFv homodimer with key controls at room temperature. **Lane 1** contains protein ladder in kDa (New England Biolabs). **Lane 2** contains scFv control. **Lane 3** contains scFv incubated for 48 h. **Lane 4** contains azide functionalised scFv incubated for 48 h. **Lane 5** contains strained alkyne functionalised scFv incubated for 48 h. **Lanes 6 to 10** contain homodimer reaction sample after 1, 16, 24, 36 and 48 h respectively.

*Figure 2.28* shows the SDS-PAGE analysis of the homodimer reaction and controls at room temperature. The unmodified scFv control and that incubated for 48 h are identical, suggesting the formation of non-specific homodimer for this sample was indeed temperature dependent (*lanes 2 and 3*). In the case of the azide functionalised scFv control the band at ~50 kDa is still present, though it is significantly less prominent than it was at 37 °C (*lane 4*). However, the strained alkyne functionalised scFv reveals an almost identical result to that at 37 °C (*lane 5*). Furthermore, the sample taken from the homodimer reaction after 48 h shows the same bands as observed in the strained alkyne control. Analogous results were observed when repeated at 4 °C.

*Figures 2.27* and *2.28* suggest the presence of the strained alkyne linker is causing non-specific binding between scFv molecules over time, resulting in high molecular weight

aggregates. This observation has previously been reported in the literature, and is thought to be due to the hydrophobic nature of strained alkynes (139,189). Furthermore, a significant proportion of the homodimer is formed non-specifically, as this band can be seen by SDS-PAGE when azide and strained alkyne modified scFv fragments are incubated alone. This is a likely side effect of the high protein concentration and long reaction time. Thus the actual yield of site-specific homodimer observed in these reactions is very poor. The yield did not improve when using an excess of either the azide or strained alkyne functionalised scFv reaction partners. Reactions using modified scFv at lower concentrations (1 mg/ml to 5 mg/ml) were also attempted. Although this significantly reduced the non-specific binding of both azide and strained alkyne functionalised scFv fragments, a negligible yield of homodimer was achieved.

The low homodimer yield achieved by the SPAAC reaction and the previous observation of strained alkyne instability, led us to question if the strained alkyne was still active over the time course of the reaction, and if so for how long. To test this, a 5 kDa azide PEG was used (*Scheme 2.28* and *Figure 2.29*).



**Scheme 2.28** Investigating strained alkyne stability under reaction conditions; a 5 kDa azide PEG was added to samples of strained alkyne functionalised scFv incubated at 37 °C for 0, 2, 16, 24 and 48 h.

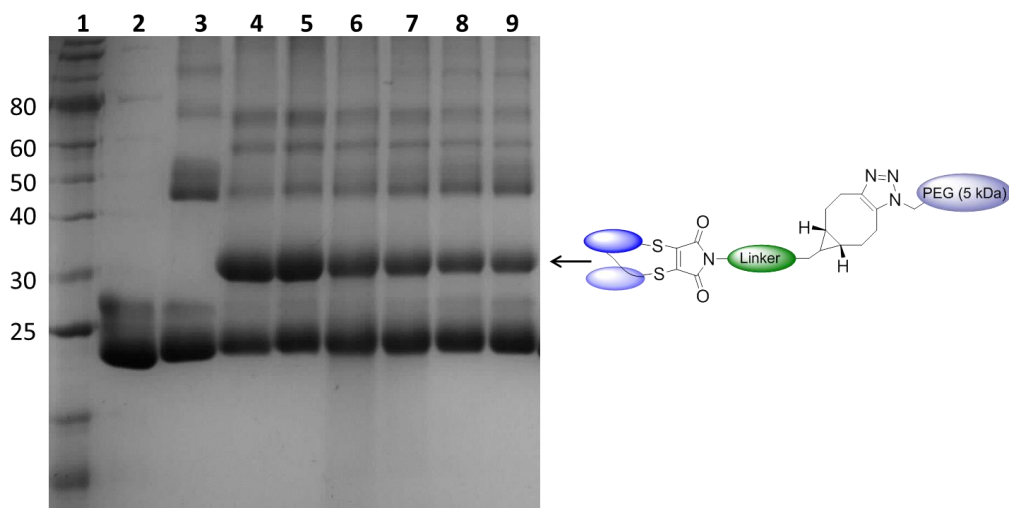
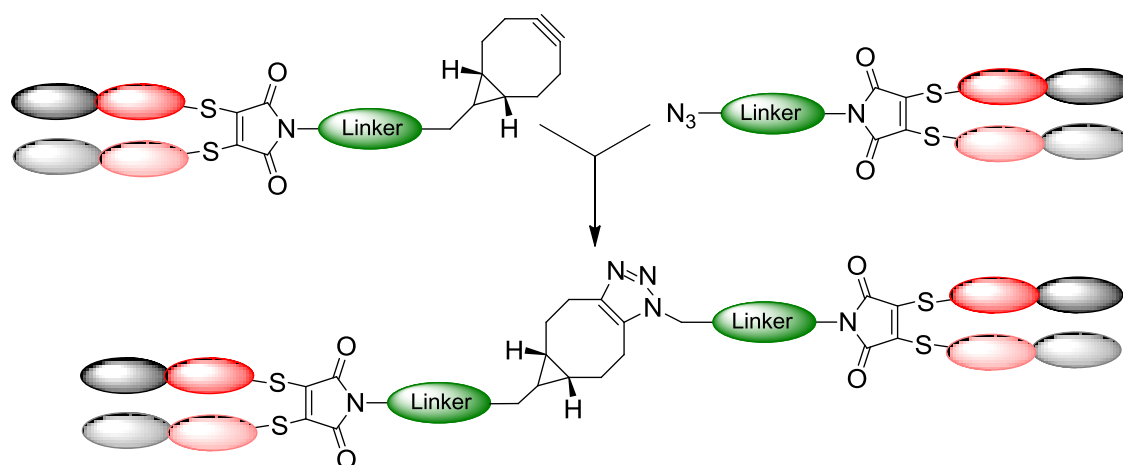


**Figure 2.29** SDS-PAGE analysis of reaction between strained alkyne scFv and 5 kDa azide PEG (20 equivalents) at 37 °C. **Lane 1** contains protein ladder in kDa (New England Biolabs). **Lane 2** contains unmodified scFv. **Lane 3** contains strained alkyne functionalised scFv incubated for 48 h. **Lane 4** is addition of azide at 0 h. **Lane 5** is addition of azide at 2 h. **Lane 6** is addition of azide at 16 h. **Lane 7** is addition of azide at 24 h. **Lane 8** is addition of azide at 36 h. **Lane 9** is addition of azide at 48 h.

Aliquots of strained alkyne functionalised scFv were incubated at 37 °C and 20 equivalents of azide PEG were added to samples at 0, 2, 16, 24 and 48 h. The band at ~30 kDa corresponds to the successful addition of the PEG azide to the strained alkyne scFv (*Figure 2.29*). The presence of this band at all time points reveals that there is active strained alkyne present over a 48 h time period. However, this yield does decrease over time, suggesting the strained alkyne is not stable. Moreover, addition of a large excess of azide PEG (20 equivalents) at 0 h still does not yield a single product; a significant amount of unreacted scFv remains.

Attempts at producing scFv homodimer using the SPAAC disulfide bridging linkers have revealed two key issues. Firstly, the high concentration and long reaction times required for conjugation of two antibody fragments results in significant aggregation due to non-specific protein binding. Second, the rate of reaction is very slow, particularly when linking two sterically hindered molecules via this approach. The reaction yield is further hampered by the instability of the strained alkyne. To determine if this is a scFv specific problem, the generation of a Fab homodimer was also attempted (*Scheme 2.29* and *Figure 2.30*).



**Scheme 2.29** Generation of Fab homodimer via SPAAC reaction.

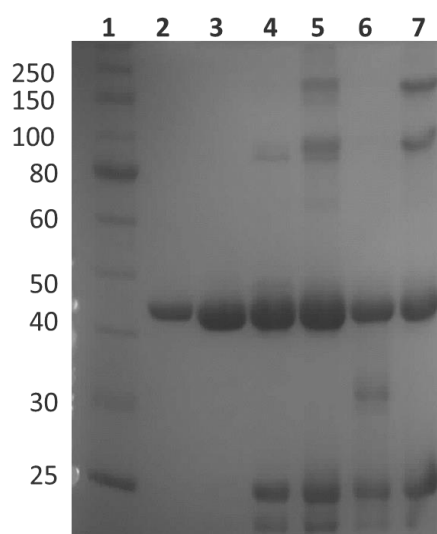


**Figure 2.30** SDS-PAGE analysis of generation of Fab homodimer at 37 °C. **Lane 1** contains protein ladder in kDa (New England Biolabs). **Lane 2** contains unmodified Fab. **Lane 3** contains unmodified Fab incubated for 48 h. **Lane 4** contains azide functionalised Fab incubated for 48 h. **Lane 5** contains strained alkyne functionalised Fab incubated for 48 h. **Lane 6** contains homodimer reaction sample at 0 h. **Lane 7** contains homodimer reaction sample at 48 h.

Attempts at generating Fab homodimer using the SPAAC linkers showed marked similarity to the result of the pursued scFv dimerisation. As can be seen in *Figure 2.30*, the azide functionalised Fab control *lane 4* contains a faint band at ~100 kDa. Furthermore, the strained alkyne control reveals two distinct bands running at ~100 and ~150 kDa (*lane 5*). The same two bands are apparent in the reaction mixture of 1:1 azide to strained alkyne functionalised Fab after 48 h, though in slightly higher yield (*lane 7*).

---

The results shown in *Figure 2.30* are representative of several attempts at Fab dimerisation. The appearance of multiple bands in *lane 5* indicates that non-specific protein binding is not limited to strained alkyne functionalisation of the scFv fragment. Furthermore, lowering concentration and temperature yielded the same effects; a reduction in non-specific aggregates at lower concentrations, however temperature did not reduce strained alkyne functionalised Fab non-specific binding. The two bands present in reaction *lane 7*, although the same weight as those in the strained alkyne control, are more pronounced. This suggests that these are also a result of incubating the two SPAAC Fab reaction partners. Nevertheless this result is unexpected, since dimerisation of Fab should in theory yield a single band at ~100 kDa.

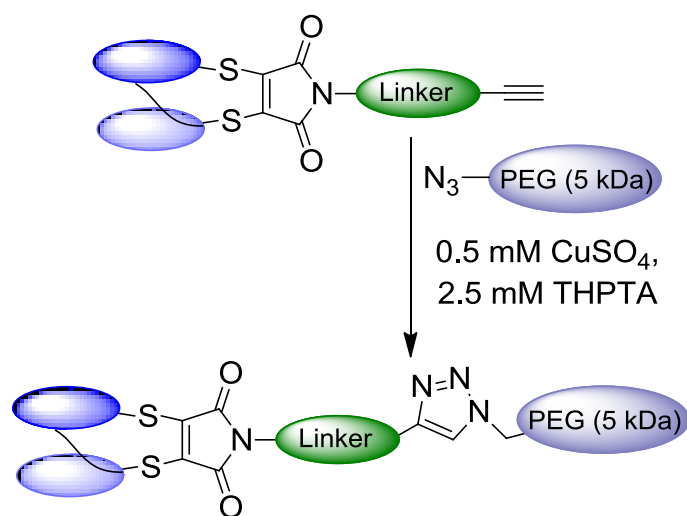
### **2.2.7 Copper-catalysed conjugation towards homogeneous bispecifics**

In organic and materials synthesis, the use of an *in situ* reducing agent provides a fast, efficient and convenient CuAAC procedure. Sodium ascorbate is the choice reducing agent for synthesis; however it has long been avoided for bioconjugation due to the copper mediated generation of reactive oxygen species. These species have been shown to cause oxidation, cleavage, cross-linking and even precipitation of biomolecules (194-196). However, recent advances in CuAAC optimisation have now enabled the use of sodium ascorbate for fast and efficient bioconjugation without damage to the biological environment (189).

The CuAAC protocol used in this project is based on that devised by Finn *et al.* (189). This procedure employs the water-soluble ligand THPTA (tris-(hydroxypropyltriazolylmethyl)amine). This ligand intercepts and reduces the reactive oxygen species generated by ascorbate reduction of dissolved oxygen, protecting the proteins from potential damage. Aminoguanidine is also added to the reaction to divert any by-products of ascorbate oxidation that have the capacity to covalently modify or cross-link proteins. Furthermore, due to the efficiency of sodium ascorbate as a reducing agent, copper need only be used in low concentrations. The source of copper in all of the CuAAC reactions in this project is CuSO<sub>4</sub>.

To develop the ideal conditions for the CuAAC using the ds-scFv and Fab antibody fragments, it was decided to first use azide PEG reagents. Successful addition of PEG to the linear alkyne functionalised antibody fragments is visible by SDS-PAGE. Thus this

avoids the requirement for mass spectrometry, which would necessitate prior thorough purification of CuAAC reactions to remove all of the small molecule components, resulting in loss of valuable antibody fragment. Initial attempts at the copper-catalysed click between linear alkyne functionalised scFv and azide PEG (2 or 5 kDa) resulted in little or no product for a variety of scFv concentrations (50 to 200  $\mu$ M) and excesses of PEG (10 to 100 equivalents). A review of the literature soon revealed the probable issue; protein hexahistidine-tags can strongly bind copper ions, leaving copper unavailable for catalysis and even inducing protein precipitation (189). To overcome this, it is suggested that the concentration of the metal-ligand complex may be increased to a maximum of 0.5 mM (*Scheme 2.30* and *Figure 2.31*).



**Scheme 2.30** CuAAC between a 5 kDa azide PEG and linear alkyne functionalised scFv.

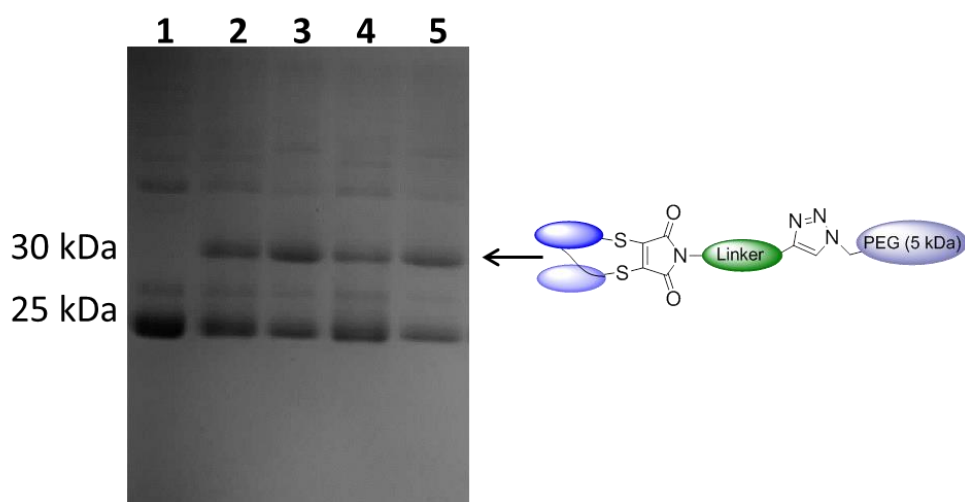


**Figure 2.31** SDS-PAGE analysis of reaction between linear alkyne functionalised scFv (100  $\mu$ M) and azide PEG (5 kDa), 0.5 mM CuSO<sub>4</sub>: 2.5 mM THPTA. **Lane 1** contains linear alkyne functionalised scFv left overnight under reaction conditions. **Lane 2**

contains linear alkyne scFv + 20 equivalents PEG azide, 1 h, rt. **Lane 3** contains linear alkyne scFv + 100 equivalents PEG azide, 1 h, rt. **Lane 4** contains linear alkyne scFv + 20 equivalents PEG azide, overnight, rt. **Lane 5** contains linear alkyne scFv + 100 equivalents PEG azide, overnight, rt.

The copper and ligand concentration were increased accordingly to promote the CuAAC between linear alkyne functionalised scFv and a 5 kDa azide PEG. As can be seen in *Figure 2.31*, site-specific PEGylated scFv was formed. However, these results represent the highest yielding CuAAC achieved using the linear alkyne functionalised scFv. Greater copper concentrations resulted in multiple higher molecular weight bands by SDS-PAGE, suggesting protein cross-linking or aggregation. In fact, the slight appearance of these bands can be seen in *Figure 2.31*. Furthermore, longer reaction times and reaction at 37 °C did not improve yield.

In tandem, the reaction of azide PEG with linear alkyne functionalised Fab was investigated. As the Fab is obtained by digest of a human IgG, it does not possess a hexahistidine-tag. The results of the reaction between linear alkyne Fab and azide PEG (2 and 5 kDa) are shown in *Figure 2.32*.

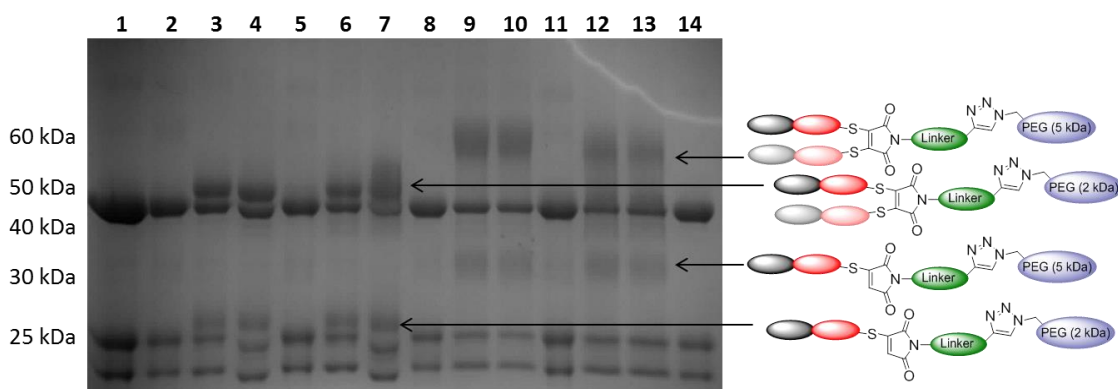


**Figure 2.32** SDS-PAGE analysis of reaction between linear alkyne functionalised Fab (100  $\mu$ M) and azide PEG (2 and 5 kDa), 0.2  $\mu$ M CuSO<sub>4</sub>: 1.0 mM THPTA. **Lane 1** contains linear alkyne functionalised Fab. **Lanes 2 to 4** contain linear alkyne Fab + 1, 20 and 100 equivalents PEG azide (2 kDa) respectively 1 h, rt. **Lanes 5 to 7** contain linear alkyne Fab + 1, 20 and 100 equivalents PEG azide (2 kDa) respectively left overnight, rt. **Lanes 8 to 10** contain linear alkyne Fab + 1, 20 and 100 equivalents PEG azide (5 kDa) 1 h, rt. **Lanes 11 to 13** contain linear alkyne Fab + 1, 20 and 100

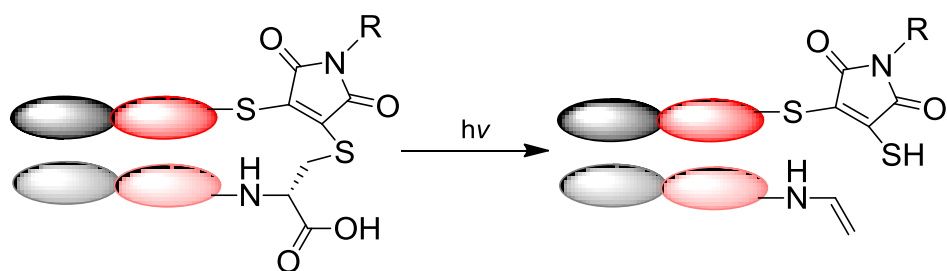
---

equivalents PEG azide (5 kDa) left overnight, rt. **Lane 14** contains linear alkyne functionalised Fab left overnight at rt.

The reaction of linear alkyne Fab with 1, 20 and 100 equivalents of azide PEG (2 and 5 kDa) was analysed after 1 h and overnight (*Figure 2.32*). CuAAC worked well using 200  $\mu\text{M}$   $\text{CuSO}_4$ , and higher concentrations did not improve reaction yield. Pleasingly, as can be seen in *lane 14*, no aggregation or cross-linking products can be seen for the linear alkyne Fab control incubated under the CuAAC conditions overnight. *Lane 12* clearly reveals that reaction with 20 equivalents of azide PEG overnight achieves almost complete site-specific PEGylation of the Fab fragment. Furthermore, *lane 13* indicates that increasing to 100 equivalents azide PEG does not improve the yield. This perhaps suggests that the remaining Fab is not able to participate in the CuAAC reaction, despite appearing to be fully functionalised with linear alkyne linker by mass spectrometry.

An unexpected result is observed in *Figure 2.32*; selective PEGylation of the Fab heavy chain. This can be clearly observed in *lanes 3, 4, 6 and 7* on reaction with the 2 kDa azide PEG, and *lanes 9, 10, 12 and 13* using the 5 kDa PEG. For heavy chain specific PEGylation to occur, this chain must also have been selectively modified with the linear alkyne Fab maleimide. Free heavy and light chain has been found to always be visible, to some degree, by SDS-PAGE after Fab disulfide bridging. However, LCMS analysis of the same samples would suggest that the Fab is fully re-bridged, and that there is no free heavy or light chain present.

There are several possible explanations for this unusual result. Firstly, this may simply be an effect of SDS-PAGE. Samples are prepared for analysis in SDS and heated to 98  $^{\circ}\text{C}$  for 2 min, thus these harsh conditions may have cleaved the maleimide bridge (this was found not to be the case, see *Section 2.3.4*). A second possible reasoning is slow reactivity of the light chain cysteine; research within the group has established that the heavy chain cysteine released by disulfide bond reduction reacts rapidly with modification reagents compared to the equivalent cysteine of the light chain. In fact, the light chain cysteine is C-terminal and hence this result is consistent with the expected higher  $\text{pK}_a$  of this residue. A final explanation is the possibility of decarboxylative enamide formation; the group is also investigating the observation of photochemical decarboxylation of C-terminal maleimide functionalised cysteine residues mediated by high intensity UV light (*Scheme 2.31*) (197).



**Scheme 2.31** The light chain cysteine residue of the Fab interchain disulfide is C-terminal. Under high intensity UV light, maleimide functionalised C-terminal cysteine residues can undergo a photo-electron transfer and subsequent decarboxylation to form the enamide (197).

One concern was the possibility of heavy chain selective modification via enamide formation promoted by solar UV. To determine if this is the case, disulfide bridging of the Herceptin Fab fragment was repeated using simple dithiophenol maleimide in the light and dark, and the two bridged samples left overnight (*Figure 2.33, lanes 1 and 2*). In addition, CuAAC of the linear alkyne functionalised Fab to 5 kDa azide PEG was repeated under these conditions (*Figure 2.33*).

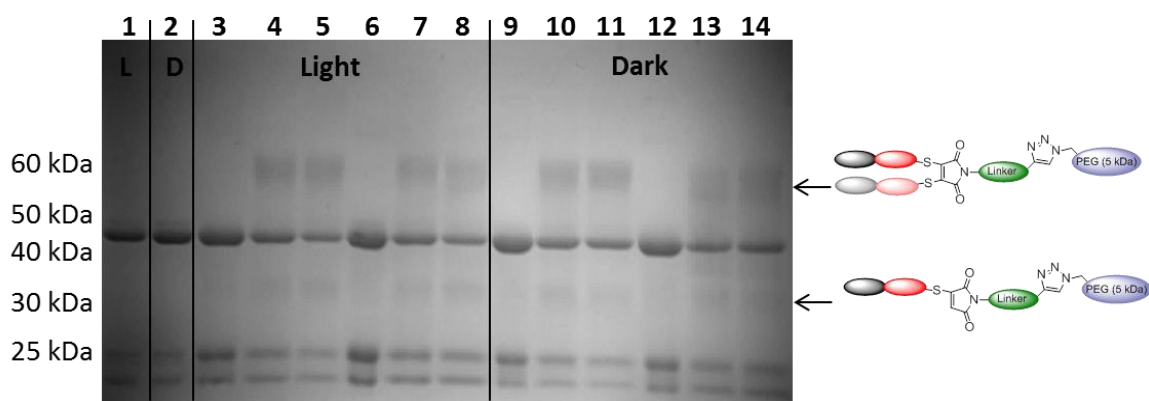


**Figure 2.33** SDS-PAGE analysis of disulfide bridged Fab fragment in the light and dark. **Lane 1** contains maleimide bridged Fab left overnight in the light. **Lane 2** contains maleimide bridged Fab left overnight in the dark. **Lanes 3 and 9** contain linear alkyne Fab under CuAAC conditions 1 h, rt. **Lanes 4 and 10** contain linear alkyne Fab + 20 equivalents azide PEG 1 h, rt. **Lanes 5 and 11** contain linear alkyne Fab + 100 equivalents azide PEG, 1 h, rt. **Lanes 6 and 12** contain linear alkyne Fab under CuAAC conditions overnight, rt. **Lanes 7 and 13** contain linear alkyne Fab + 20 equivalents azide PEG overnight, rt. **Lanes 8 and 14** contain linear alkyne Fab + 100 equivalents azide PEG overnight, rt.

Lanes 1 and 2 show the results of Fab fragment bridging with simple dithiophenol maleimide under light or dark conditions respectively, and left overnight (*Figure 2.33*). This reveals no significant difference in the amounts of heavy and light chain in either sample. Furthermore, the same is observed for the repeated CuAAC reactions in the light (*lanes 3 to 8*) and dark (*lanes 9 to 14*). Thus this suggests that enamide formation is not occurring as a result of UV exposure from light during the modification reaction.

It was decided to repeat PEGylation using the strained alkyne functionalised Fab. The purpose of this reaction was two-fold; to determine if this site-specific PEGylation of the heavy chain was CuAAC specific, and to directly compare the efficiency of the two ‘click’ reactions on the Fab fragment. The results are shown in *Figure 2.34*.

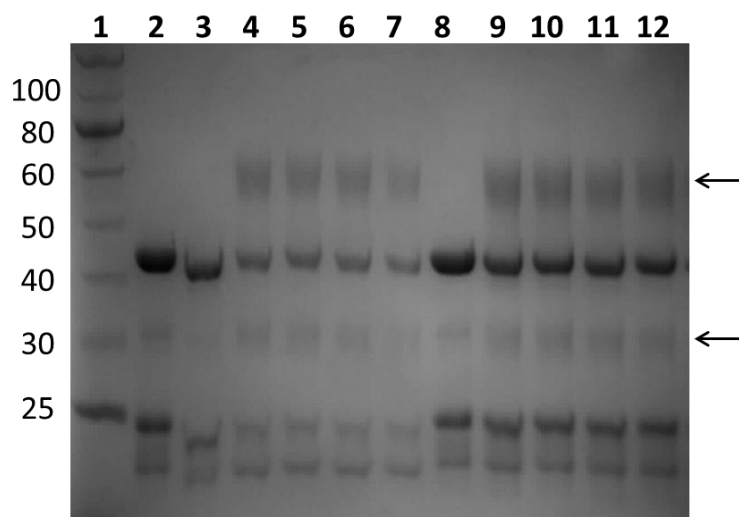


**Figure 2.34** SDS-PAGE analysis of CuAAC and SPAAC reaction between alkyne Fab and 5 kDa azide PEG. Arrows indicate PEGylated products. **Lane 1** contains protein ladder in kDa (New England Biolabs). **Lane 2** contains unmodified Fab control. **Lane 3** contains linear alkyne functionalised Fab. **Lane 4** contains linear alkyne bridged Fab + 20 equivalents azide PEG 1 h, rt. **Lanes 5 to 7** contain reaction sample after 2 h, 3 h and overnight respectively. **Lane 8** contains strained alkyne functionalised Fab. **Lane 9** contains strained alkyne functionalised Fab + 20 equivalents azide PEG 1 h, rt. **Lanes 10 to 12** contain reaction sample after 2 h, 3 h and overnight respectively.

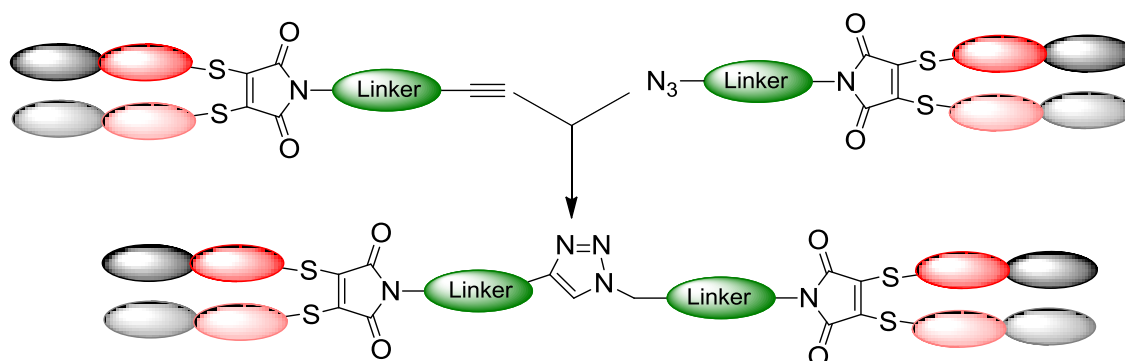
*Figure 2.34* clearly demonstrates that selective PEGylation of the heavy chain is not CuAAC specific. Furthermore, the difference in efficiency for the CuAAC and SPAAC reactions is very clear. For the same concentration, reaction time and temperature, little alkyne functionalised Fab remains in *lane 7* for the CuAAC reaction compared to that

---

remaining in *lane 12* for the SPAAC equivalent. As the linear alkyne Fab has shown no tendency for non-specific protein binding at high concentrations, and the CuAAC shows a greater efficiency and rate of reaction, it was anticipated that this approach would be more successful at generating homogeneous bispecific.

As attempted using the SPAAC disulfide bridging linkers, synthesis of scFv homodimer using the CuAAC alternative was sought. However, this was not successfully achieved. At a range of both scFv and Cu concentrations, either no homodimer product was obtained or at high Cu concentrations multiple bands appeared suggesting protein cross-linking or aggregation. As previously observed, the failing of this CuAAC coupling is likely to be due to the hexahistidine-tag of this antibody fragment.

The lack of a hexahistidine-tag on the Fab fragment, combined with the relative success of Fab via the CuAAC reaction, boded well for the construction a Fab homodimer (*Scheme 2.32*).



**Scheme 2.32** Generation of Fab homodimer via CuAAC reaction.

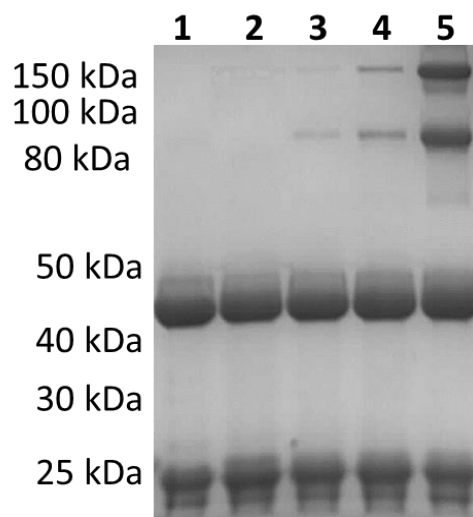


**Figure 2.35** SDS-PAGE analysis of generation of Fab homodimer at rt. **Lane 1** contains azide functionalised Fab left overnight at rt. **Lane 2** contains linear alkyne functionalised Fab left overnight at rt. **Lane 3** contains 2:1 mixture of azide functionalised Fab to linear alkyne functionalised Fab under CuAAC conditions 0 h, rt. **Lane 4** contains reaction sample after 1 h, rt. **Lane 5** contains reaction sample after leaving overnight at rt.

The results of the Fab-Fab conjugation via a CuAAC approach shown in *Figure 2.35* reveal the same two bands that were observed in *Figure 2.30* using the SPAAC method. However, in this case the same bands could not be seen for the alkyne functionalised Fab control. This suggests that the linear alkyne linkers **46** and **47** do not cause non-specific protein binding under the reaction conditions, unlike the strained alkyne linkers **42** and **43**. Furthermore, this indicates that the bands observed in *lanes 3* to *5* of *Figure 2.35* are a result of CuAAC between azide and linear alkyne functionalised Fab fragments.

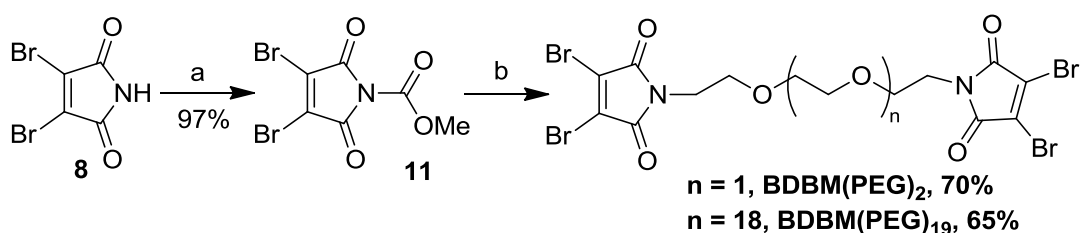
The results observed in *Figure 2.35* are representative of several attempts at Fab dimerisation using the copper-catalysed click disulfide bridging linkers. Using a 2:1 ratio of azide:alkyne (100  $\mu$ M) overnight at room temperature produced the greatest yield of the two observed product bands (*lane 5*). Again however, these two bands were not anticipated; dimerisation of Fab fragments would be expected to result in a band at  $\sim$ 100 kDa. The identity of the two bands is unclear, though perhaps related to the unusual result of selective heavy chain PEGylation observed in *Figures 2.32* and *2.34*. These results will be discussed further in *Section 2.3.4*.

## 2.3 Synthesis and application of a disulfide to disulfide linker

The conjugation of two antibody fragments site-specifically modified with a bioorthogonal handle was rapidly proving a problematic, low yielding approach to homogeneous antibody-antibody conjugate production. In tandem to this work, homobifunctional 3,4-substituted maleimide linkers for the direct conjugation of two antibody fragment disulfide bonds were also designed and developed. It was anticipated that the issues identified by conjugation attempts in the project thus far would aid the progress of this simple approach.

### 2.3.1 Synthesis of homobifunctional linkers

The linker design is simple; two disubstituted maleimides linked by a PEG chain to confer some flexibility and solubility to the molecule. The conjugation attempts thus far have indicated that it is difficult to obtain good yields using a site-specific approach, as the opportunity for reaction partners to meet is low. To determine if linker length can improve these yields, commercially available homogeneous PEG chains of distinct length were sought. Two diamine PEGs of distinct length were identified, and used to readily synthesise the *bis*-dibromomaleimide (BDBM) cross-linker molecules thus termed **BDBM(PEG)<sub>2</sub>** and **BDBM(PEG)<sub>19</sub>** (Scheme 2.33).

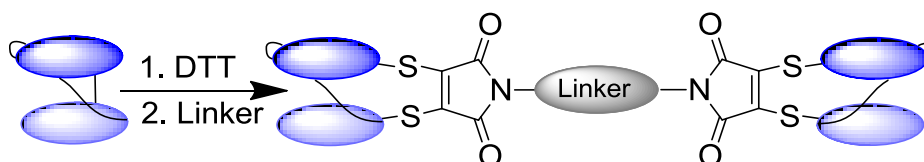


**Scheme 2.33** Reagents and conditions: (a) MeOCOC<sub>l</sub>, NMM, THF; (b) For **BDBM(PEG)<sub>2</sub>**: NH<sub>2</sub>CH<sub>2</sub>CH<sub>2</sub>(OCH<sub>2</sub>CH<sub>2</sub>)<sub>2</sub>NH<sub>2</sub>, DCM, 20 min. For **BDBM(PEG)<sub>19</sub>**: NH<sub>2</sub>CH<sub>2</sub>CH<sub>2</sub>(OCH<sub>2</sub>CH<sub>2</sub>)<sub>19</sub>NH<sub>2</sub>, overnight.

The synthesis used the *N*-(methoxycarbonyl)-3,4-dibromomaleimide **11** readily generated from commercially available dibromomaleimide **8** in 97% yield (Scheme 2.33). The carbamate **11** could then be taken on directly to react with either diamine PEG<sub>2</sub> or PEG<sub>19</sub> to obtain **BDBM(PEG)<sub>2</sub>** and **BDBM(PEG)<sub>19</sub>** in good yields, 70% and 65% respectively. This two-step reaction thus required only a single purification step.

### 2.3.2 Generation of scFv homodimer

To examine the feasibility of using *bis*-dibromomaleimide linkers to produce homogeneous antibody-antibody conjugate, we decided to first attempt to generate a homodimer of the ds-scFv fragment (*Scheme 2.34*).



**Scheme 2.34** Generation of scFv homodimer using linkers **BDBM(PEG)<sub>2</sub>** and **BDBM(PEG)<sub>19</sub>**.

For the production of homodimer, a stepwise protocol was adopted; the scFv was reduced with DTT (20 equivalents) and following buffer exchange, incubated with 0.5 equiv of linker **BDBM(PEG)<sub>2</sub>** or **BDBM(PEG)<sub>19</sub>**. The conjugation reaction was monitored by SDS-PAGE, and a distinct band at ~50 kDa was observed on incubation of **BDBM(PEG)<sub>19</sub>** with reduced scFv after only 1 h at room temperature (*Figure 2.36*). This corresponds to the molecular weight of scFv dimer. In contrast, the reduced scFv incubated with linker **BDBM(PEG)<sub>2</sub>**, although re-bridged, reveals only a faint band at ~50 kDa, suggesting poor dimer formation.

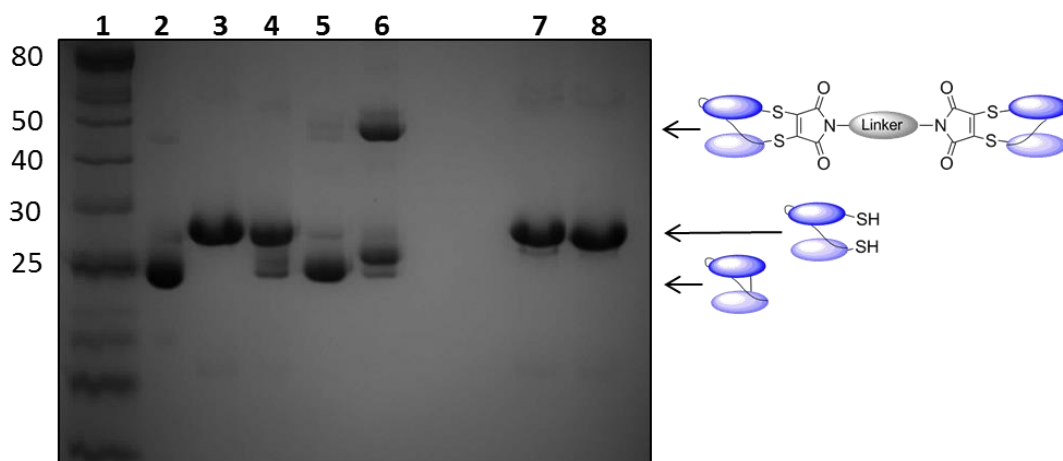


**Figure 2.36** SDS-PAGE analysis of initial investigation into the formation of scFv homodimer with linkers **BDBM(PEG)<sub>2</sub>** and **BDBM(PEG)<sub>19</sub>**. **Lane 1** contains protein ladder in kDa (New England Biolabs). **Lane 2** contains unmodified scFv. **Lane 3** contains scFv + DTT to afford reduced scFv. **Lane 4** contains reduced scFv (after buffer exchange) left for duration of experiment. **Lane 5** contains reduced scFv + **BDBM(PEG)<sub>2</sub>** to afford mainly disulfide bridged scFv (~25 kDa). **Lane 6** contains

---

reduced scFv + **BDBM(PEG)<sub>19</sub>** to afford scFv homodimer (~50 kDa) and disulfide bridged scFv monomer (~25 kDa). **Lane 7** contains a sample from lane 4 + reducing loading buffer. **Lane 8** contains a sample from lane 5 + reducing loading buffer.

The longer length of linker **BDBM(PEG)<sub>19</sub>** (19 PEG units, ~1 kDa), in combination with its flexibility, is likely to significantly reduce the steric hindrance which creates difficulty when attempting to link two large proteins. This is observed in the far greater conversion to homodimer obtained compared to linker **BDBM(PEG)<sub>2</sub>** (*Figure 2.36*). It was therefore decided that conditions for homogeneous protein-protein conjugation should be optimised using linker **BDBM(PEG)<sub>19</sub>**. Generation of homogeneous scFv dimer was further pursued in order to determine ideal conditions for maintaining antibody fragments in their reduced form whilst promoting bridging.

Following reduction, the scFv was eluted over a sephadex column to remove DTT and to buffer exchange the protein into conditions suitable for maintaining the reduced antibody. As discussed in *Section 2.1* and *2.2*, the disulfide bond of the scFv fragment rapidly re-forms in the absence of reducing agent. In the literature, reduced antibodies are often transferred into phosphate buffers containing up to 10 mM EDTA (121). To determine the ideal buffer conditions for maintaining the reduced scFv fragment a number of phosphate buffer concentrations (10-40 mM) with varying levels of EDTA (1-10 mM) were investigated. This study established that a 20 mM phosphate buffer containing 5 mM EDTA, pH 7.4 was sufficient for maintaining the reduced scFv for these conjugation reactions.

Following purification, the antibody fragment was concentrated to no greater than 1 mg/ml; higher concentrations promoted disulfide re-oxidation, as observed in *Section 2.1*. A series of optimisation experiments revealed incubation with 0.42 equiv of *bis*-dibromomaleimide cross-linker **BDBM(PEG)<sub>19</sub>** for 1 h at room temperature, or 4°C overnight, yielded the highest levels of homogeneous dimer (*Figure 2.37*).

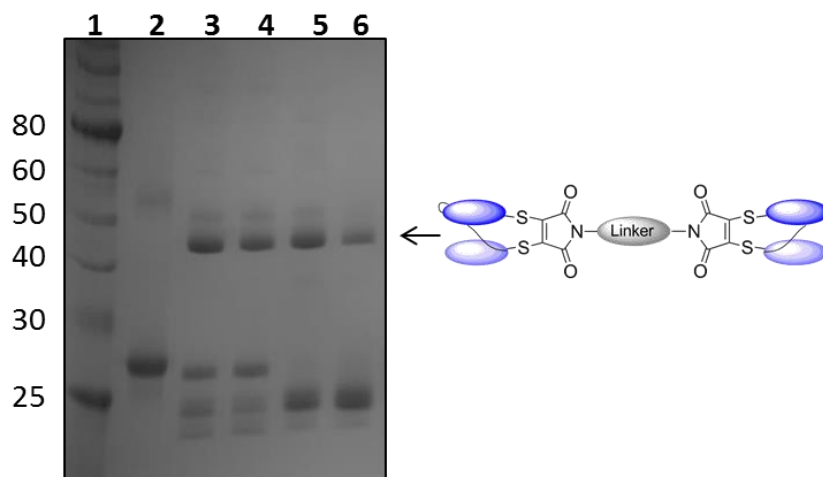


**Figure 2.37** SDS-PAGE analysis of scFv homodimer yield optimisation by varying equivalents of linker **BDBM(PEG)<sub>19</sub>**. **Lane 1** contains protein ladder in kDa (New England Biolabs). **Lane 2** contains reduced scFv. **Lane 3** contains scFv + 0.42 equiv. **BDBM(PEG)<sub>19</sub>**. **Lane 4** contains scFv + 0.5 equiv. **BDBM(PEG)<sub>19</sub>**. **Lane 5** contains scFv + 1.0 equiv. **BDBM(PEG)<sub>19</sub>**. **Lane 6** contains scFv + 2.0 equiv. **BDBM(PEG)<sub>19</sub>**.

After optimisation, the reaction was repeated using 1 mg of scFv and SDS-PAGE analysis revealed that after 1 h approximately 80% of starting material was consumed (*Figure 2.38[i]*, measured using ImageJ). After purification of the homodimer by size exclusion chromatography, an excellent 64% yield of pure, homogeneous scFv-scFv conjugate was obtained from 1 mg of scFv (*Figure 2.38[iii]*, 75% yield with respect to the limiting reagent **BDBM(PEG)<sub>19</sub>**). This yield represents a significant improvement on previous reports of direct chemical cross-linking of antibodies using natural amino acids, which have achieved yields in the 10-40% range (198-201). Notably the conjugate is homogeneous due to the site-selectivity of the methodology.

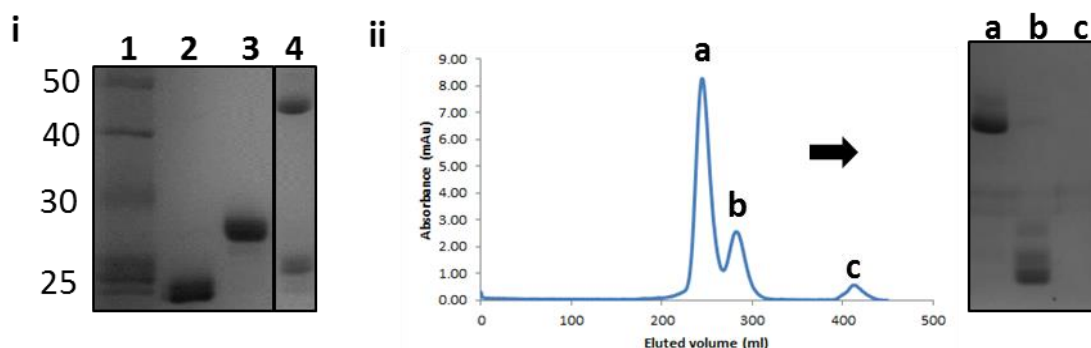
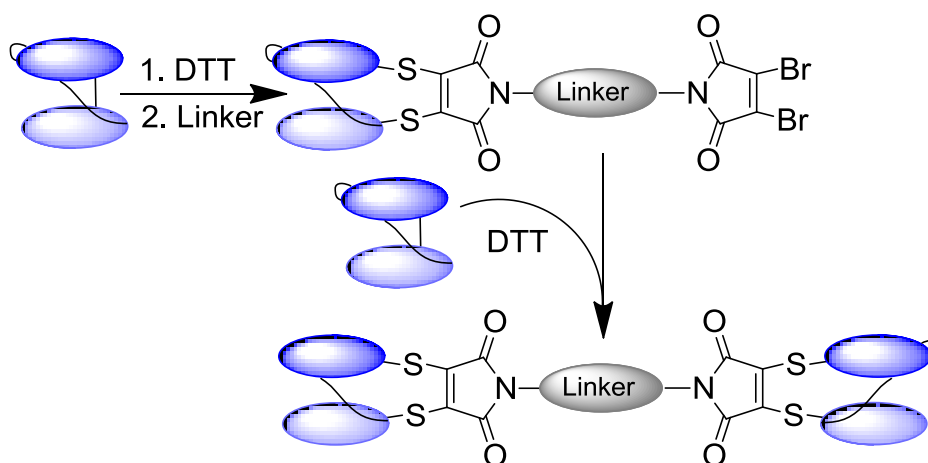


**Figure 2.38** Application of optimised conditions to large scale dimerisation of scFv: **[i]** SDS-PAGE analysis: **Lane 1** contains protein ladder in kDa (New England Biolabs). **Lane 2** contains unmodified scFv. **Lane 3** contains scFv + 20 equiv DTT to afford reduced scFv. **Lane 4** contains reduced scFv + 0.42 equiv **BDBM(PEG)<sub>19</sub>**, 1h rt to

afford scFv homodimer (~50 kDa) and disulfide bridged scFv monomer (~25 kDa). [ii] Size exclusion chromatography purification of pure scFv homodimer (**peak a**, ~50 kDa) from monomer starting materials (**peak b**) and unreacted linker (**peak c**) (Superdex 75, GE Healthcare).

Having successfully brought together two scFv fragments homogeneously in excellent yield using linker **BDBM(PEG)<sub>19</sub>**, a strategy was subsequently developed to bring together two scFv fragments with different target antigens. It was envisaged that this technology could be used to generate BiTEs (Bispecific T-cell Engager). The anti-CEA ds-scFv fragment was used to develop this method of producing scFv based bispecifics alone, as it is readily available from our collaborators (*Scheme 2.35*).



**Scheme 2.35** Developing a method suitable for bispecific production using the ds-scFv fragment.

Production of bispecific constructs using this technology first requires a single antibody fragment to be bridged with **BDBM(PEG)<sub>19</sub>** and thus functionalised with a dibromomaleimide (*Scheme 2.35*). A scouting reaction revealed single modification is easily achieved using 30 equivalents of linker to antibody (*Figure 2.39*). For the addition of the second antibody fragment to be successful, the dibromomaleimide functionalised fragment must first be purified away from any free linker. Desalting columns proved ineffective for purification from **BDBM(PEG)<sub>19</sub>**, perhaps due to the large size of the PEG molecule. The excess linker was however successfully removed via buffer exchange (repeated 3 times) using centrifugal ultrafiltration with a 10 kDa cut-off (Amicon Ultra-4 Centrifugal Filter Units).

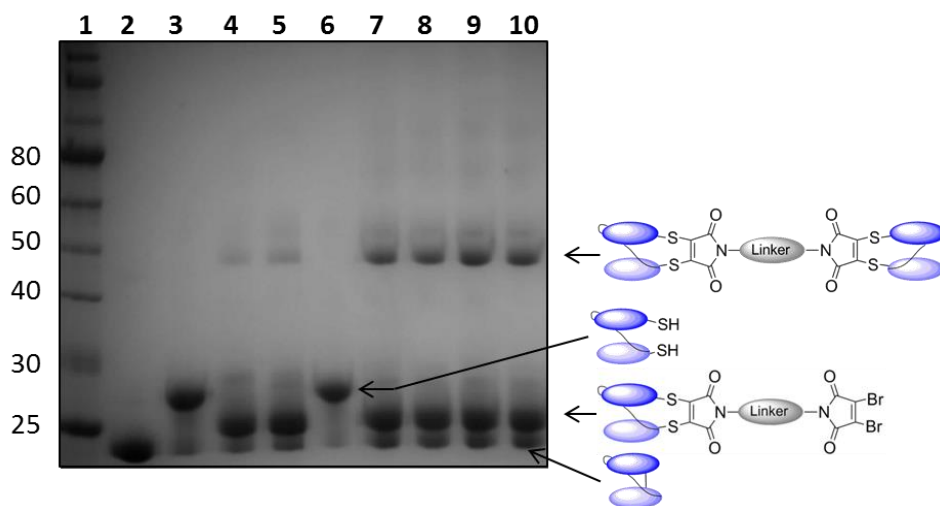
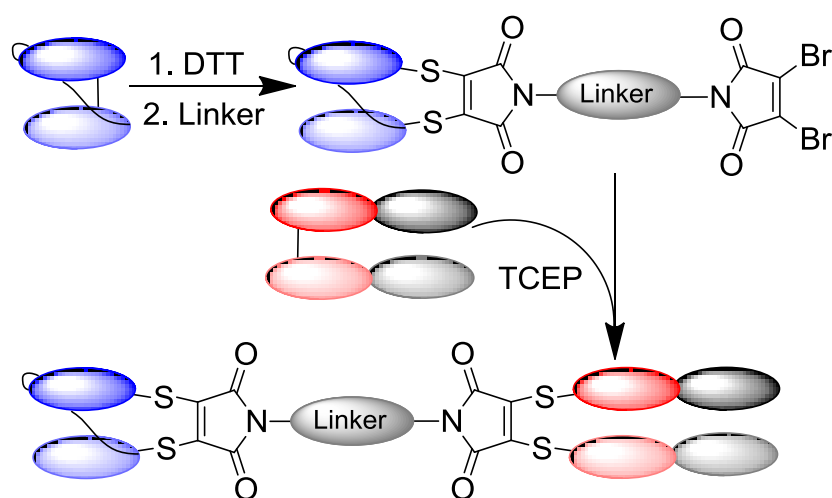


**Figure 2.39** SDS-PAGE analysis of generation of scFv-scFv conjugate via a route suitable for bispecific generation. **Lane 1** contains protein ladder in kDa (New England Biolabs). **Lane 2** contains unmodified scFv. **Lane 3** contains reduced scFv. **Lane 4** contains scFv bridged with **BDBM(PEG)<sub>19</sub>**. **Lane 5** contains scFv bridged with **BDBM(PEG)<sub>19</sub>** after purification. **Lane 6** contains second reduced scFv. **Lane 7** contains reduced scFv (1 mg/ml) + bridged scFv (1 mg/ml) left overnight at 4 °C. **Lane 8** contains reduced scFv (1 mg/ml) + bridged scFv (2 mg/ml) left overnight at 4 °C. **Lane 9** contains reduced scFv (1 mg/ml) + bridged scFv (3 mg/ml) left overnight at 4 °C. **Lane 10** contains reduced scFv (1 mg/ml) + bridged scFv (4 mg/ml) left overnight at 4 °C.

Following purification into conjugation buffer (20 mM phosphate buffer, 5 mM EDTA, pH 7.4) the dibromomaleimide functionalised scFv was incubated with purified, reduced scFv. Using reduced scFv at 1 mg/ml, a variety of bridged scFv concentrations and equivalents were trialed to determine the conditions required to obtain the greatest yield of homogeneous scFv-scFv conjugate. Some examples are included in *Figure 2.39*. The greatest yield was obtained using a 3:1 ratio of dibromomaleimide functionalised scFv to reduced scFv (*Figure 2.39, lane 9*). This yield could be achieved using a 3:1 ratio by either concentration or volume. Purification by size exclusion chromatography gave a 61% yield of pure, homogeneous scFv-scFv conjugate with respect to the limiting reagent, reduced scFv. Note, an excess of reduced scFv over bridged scFv was also attempted, however as expected this resulted in significant reoxidation and formation of reoxidised scFv dimers.

### 2.3.3 Generation of a homogeneous bispecific: scFv-Fab heterodimer

After the successful production of homogeneous scFv homodimer in high yield and the development of a strategy towards bispecific conjugates, it was next decided to target the generation of a true bispecific. For this it was decided to utilise the Herceptin Fab fragment investigated in *Section 2.2.5*, since it can be readily obtained by enzymatic digest and its incorporation into bispecific formats has therapeutic potential (91). Thus it was envisaged that the ds-scFv could be linked to the Fab fragment using **BDBM(PEG)<sub>19</sub>**, generating a conjugate that could simultaneously bind two different antigens (CEA and HER2) as a proof of concept (*Scheme 2.36*).



**Scheme 2.36** Generation of anti-CEA/anti-HER2 scFv-Fab bispecific.

To efficiently link these two different antibody fragments, it was decided to first functionalise the scFv with **BDBM(PEG)<sub>19</sub>**, as the Fab fragment was found to reoxidise less rapidly than the scFv disulfide. This was cleanly achieved by reducing the scFv as previously described, purifying by sephadex column and subsequently adding linker (30 equivalents). This reaction was complete in less than 5 min at room temperature, yielding dibromomaleimide functionalised scFv in quantitative yield. Excess linker was removed by buffer exchange. In tandem to this, the Fab fragment was reduced with TCEP (10 equivalents) and purified from reducing agent into the conjugation buffer. The concentrations of bridged scFv and reduced Fab were adjusted to 37.2  $\mu\text{M}$  (1 mg/ml for the scFv), and the antibodies mixed in a 2:1 ratio by volume (2.0 equivalents bridged scFv to 1.0 equivalent reduced Fab). This slight excess of functionalised scFv was found to be sufficient to promote bridging of the reduced Fab. The reaction was monitored by SDS-PAGE, and after 1 h at room temperature a strong band at  $\sim 80$  kDa

could be observed, corresponding to the scFv-Fab conjugate (*Figure 2.40[i]*). After purification by size exclusion chromatography, a pleasing 52% yield of homogeneous scFv-Fab bispecific was achieved (*Figure 2.40[ii]*).

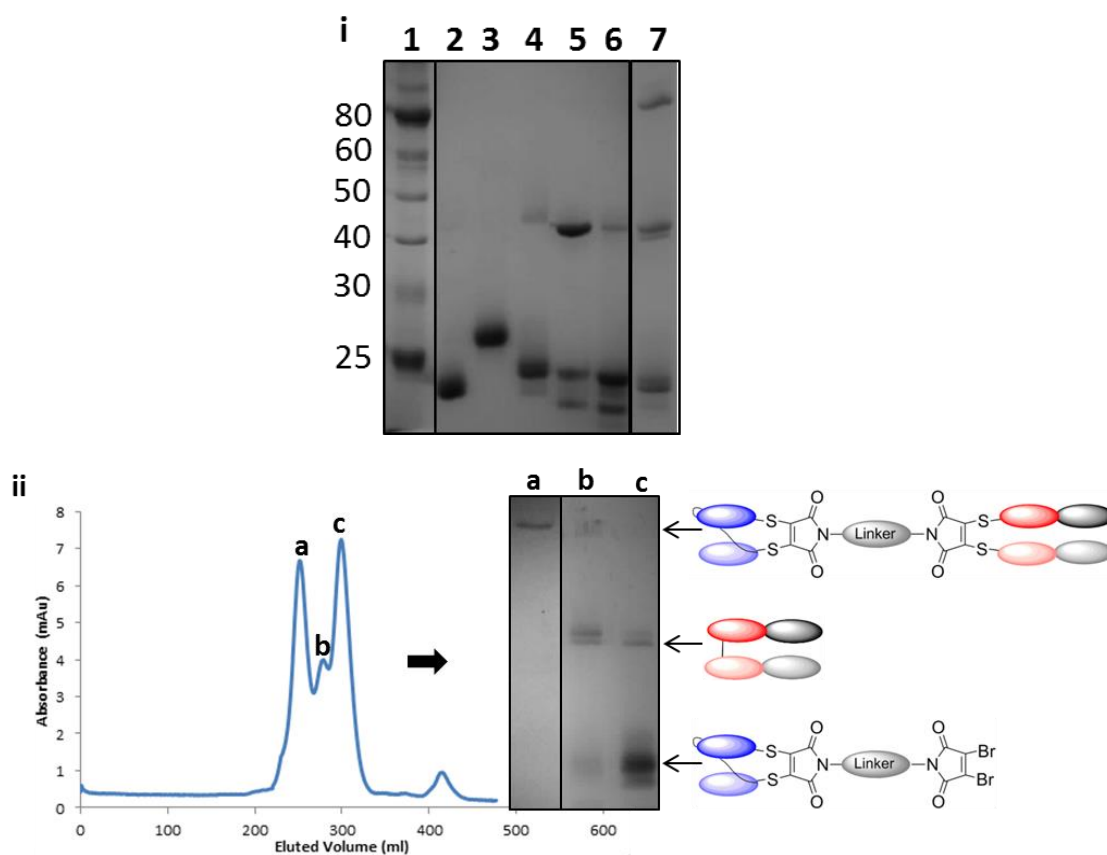
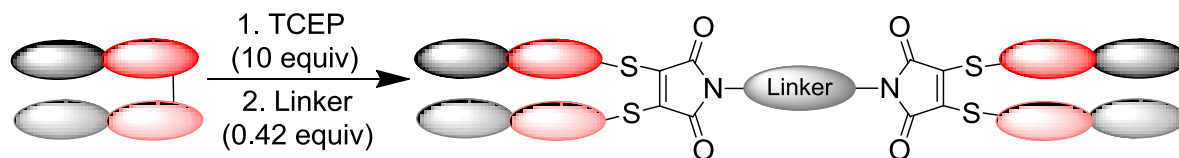


**Figure 2.40** Production of homogeneous scFv-Fab: **[i]** SDS-PAGE analysis: **Lane 1** contains protein ladder in kDa (New England Biolabs). **Lane 2** contains unmodified scFv. **Lane 3** contains scFv + 20 equiv DTT to afford reduced scFv. **Lane 4** contains reduced scFv + 30 equiv **BDBM(PEG)<sub>19</sub>** to afford disulfide bridged scFv monomer. **Lane 5** contains Fab. **Lane 6** contains Fab + 10 equiv TCEP to afford component heavy and light Fab chains. **Lane 7** contains bridged scFv + reduced Fab (2:1), 1 h rt to afford scFv-Fab conjugate (~80 kDa), re-oxidised Fab (~50 kDa) and scFv starting material (~25 kDa). **[ii]** Size exclusion chromatography purification of pure scFv-Fab heterodimer (**peak a**) from starting materials (**peak b** and **c**) (Superdex 75, GE Healthcare).

### 2.3.4 Generation of Fab homodimer

It was decided to next apply the optimised dimerisation protocol to generate Fab homodimer; many bispecific constructs are based on two Fab fragments and this would further demonstrate the scope of our conjugation technology. Using Herceptin Fab, the

fragment was reduced with TCEP (10 equivalents) and following purification incubated with **BDBM(PEG)<sub>19</sub>** (0.42 equivalents) for 1 h at room temperature (*Scheme 2.37*). The results of this conjugation are shown in *Figure 2.41*.



**Scheme 2.37** Generation of Fab homodimer using **BDBM(PEG)<sub>19</sub>**.

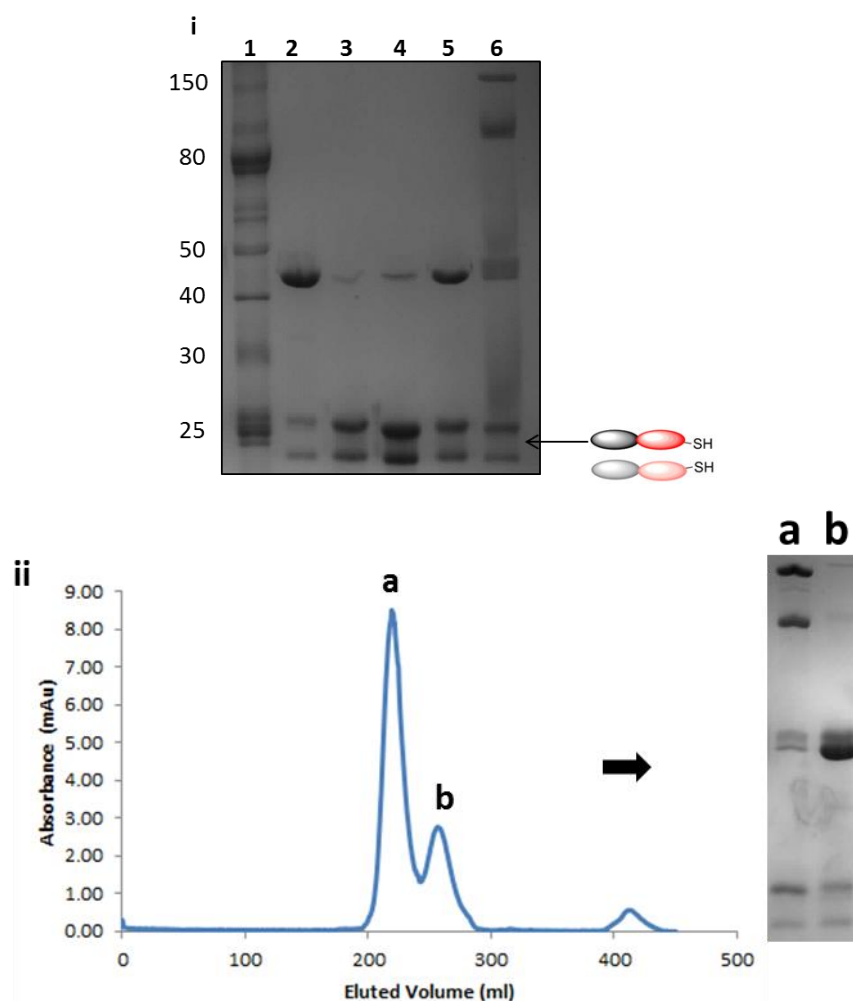


**Figure 2.41** Production of Fab homodimer: **[i]** SDS-PAGE analysis: **Lane 1** contains protein ladder in kDa (New England Biolabs). **Lane 2** contains unmodified Fab. **Lane 3** contains Fab + 10 equiv TCEP to afford component heavy and light Fab chains. **Lane 4** contains reduced Fab after purification from TCEP. **Lane 5** contains reduced Fab left for experiment duration. **Lane 6** contains Fab + 0.42 equiv **BDBM(PEG)<sub>19</sub>**, 1 h rt. **[ii]** Size exclusion chromatography purification of Fab-Fab reaction to separate product bands (**peak a**) from starting material (**peak b**) (Superdex 75, GE Healthcare).

---

The results of Fab homodimer generation with **BDBM(PEG)<sub>19</sub>** are consistent with those observed using the SPAAC and CuAAC linkers; two product bands, ~150 kDa and ~100 kDa using a 12% gel, are observed (*Figure 2.41[i], lane 6*). As can be seen in *Figure 2.41[ii]*, size exclusion chromatography (SEC) purification of the reaction mixture resulted in two peaks with the apparent two product bands being inseparable. This reaction was repeated with the Fab fragment of Rituximab, an anti-CD20 antibody regularly used to treat non-Hodgkin lymphomas. The same result was obtained, ruling out the possibility that this result is Herceptin Fab specific.

Given that these two bands are not separable by SEC, the possibility that this unusual result may be a result of preparation for SDS-PAGE analysis was tested. Generally samples are prepared in SDS and heated to 98 °C for two minutes. In the literature, the loss of maleimide-PEG as a result of this high temperature incubation in SDS has been described (202). This instability is reported to be avoided by heating samples below 60 °C. To test this theory, the Fab-Fab reaction samples were prepared in SDS and incubated at room temperature and between 40 to 100 °C for up to 30 min. However, no significant differences in these samples could be observed by SDS-PAGE, each contained the two product bands at ~150 kDa and ~100 kDa.

To investigate the formation of these two bands further, variations of the Fab dimerisation protocol were tested. For example, the Fab homodimer was generated via the two-step approach described in *Section 2.3.3*, as would be employed to produce a Fab-Fab bispecific. Furthermore, an *in situ* protocol was attempted. Both approaches again resulted in the appearance of two product bands by SDS-PAGE. Generation of Fab homodimer was also attempted using DTT as the reducing agent to determine if TCEP was the cause of this unusual result. However, the same results were observed. Fab homodimer reaction samples were left over 5 days to determine if the quantity of the two bands changed over this time; no change was observed.

The fractions collected from SEC purification of the Fab homodimer reaction were submitted for analysis by LCMS, the deconvoluted spectra of which are shown in *Figure 2.42*.

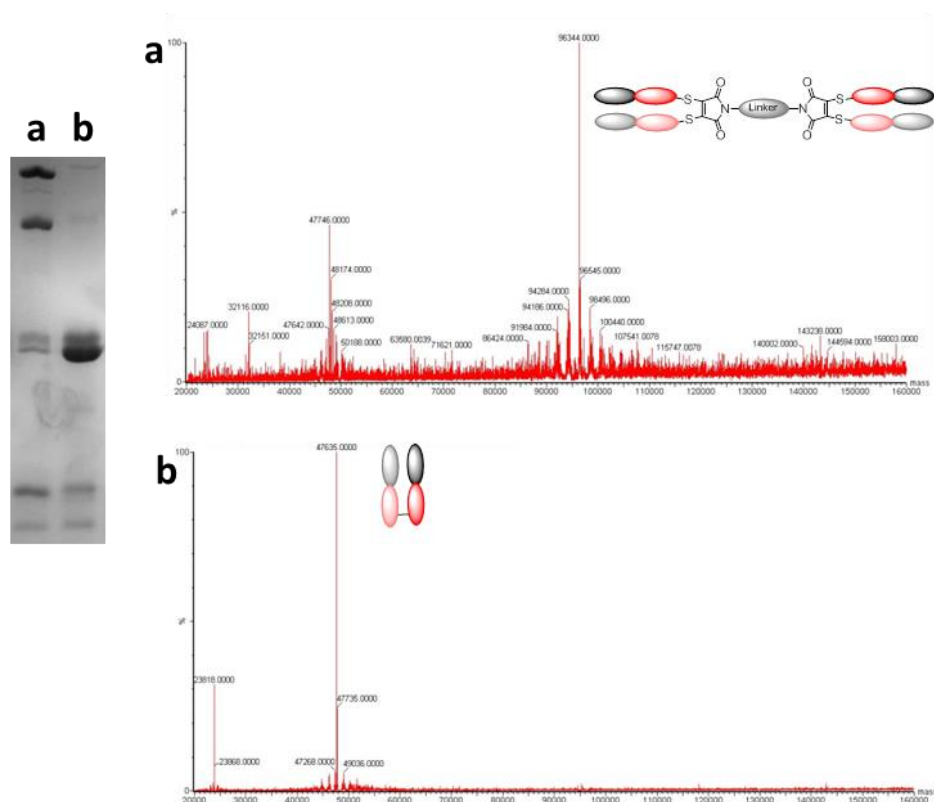
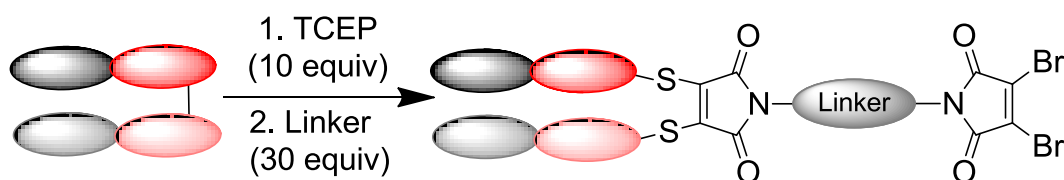


**Figure 2.42** Analysis of purified Fab homodimer reaction by LCMS. Spectra [a] and [b] correspond to SEC purified peaks **a** and **b** respectively. SDS-PAGE analysis is shown for comparison.

As can be seen in *Figure 2.42*, the predominant species observed by LCMS from analysis of SEC product peak **a** is the expected Fab homodimer at 96344 (calculated 96324). The +20 difference between the observed and calculated mass of the Fab homodimer is likely to be due to hydrolysis of one of the bridging maleimides. In addition to this peak, a mass of 47746 is observed. This corresponds to a 110 mass increase on unmodified Herceptin Fab (unmodified Fab mass is 47636). LCMS analysis of peak **b** reveals masses for the unmodified Fab observed at 47635 and a small amount of free Fab heavy and light chain. The presence of free heavy and light chain in peak **b** is not unexpected, as these chains are held together by strong non-covalent interactions which although not disturbed by SEC, would dissociate by mass spectrometry analysis. In addition to the purified SEC samples, Fab singly-bridged with **BDBM(PEG)<sub>19</sub>** was prepared (*Scheme 2.38*) and analysed by LCMS (*Figure 2.43*).



**Scheme 2.38** Generation of Fab singly-bridged with **BDBM(PEG)<sub>19</sub>**.

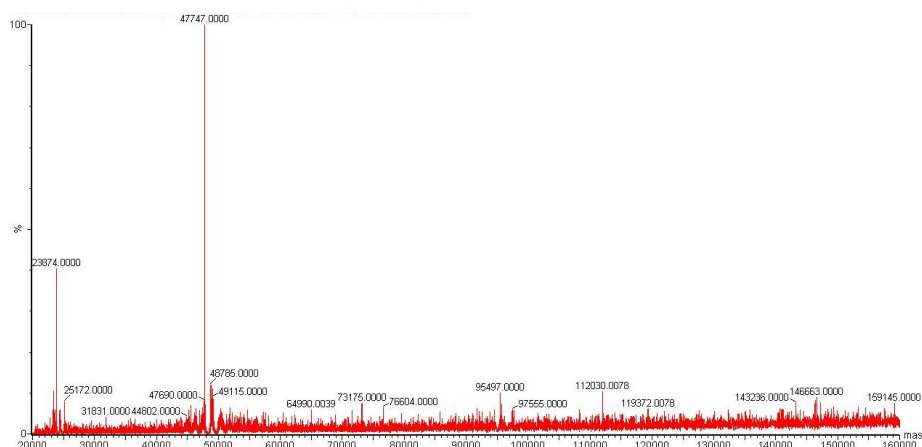


**Figure 2.43** Analysis of singly-bridged Fab by LCMS. Observed 47747, expected 48846.

As can be seen in *Figure 2.43*, LCMS analysis of singly-bridged Fab yielded a mass of 47747, rather than the expected 48846. Furthermore, this is the same mass additionally observed in analysis of SEC purification peak **a** (*Figure 2.42[a]*). Again this mass is approximately 110 units greater than unmodified Herceptin Fab. Review of the literature soon revealed that conventional electrospray ionisation mass spectrometry, as employed here, normally leads to the fragmentation of PEGs or complete ‘dePEGylation’ from proteins (203). Thus, this unexpected mass result seen for singly-bridged Fab and the Fab homodimer product is likely to be due to mass spectrometry promoted dePEGylation. Indeed the mass increase of 110 on unmodified Herceptin corresponds to a Fab fragment with dePEGylated maleimide attached.

Analysis of the Fab homodimer reaction by SEC and LCMS indicates that the reaction mixture contains the desired Fab homodimer product and unmodified Fab. The SEC purification generates two distinct peaks, which elute at the expected times for the approximately 100 kDa product and 50 kDa Fab starting material (*Figure 2.41*). The LCMS analysis of these two peaks reveals the mass of the desired Fab homodimer in SEC peak **a** and the unmodified Fab in peak **b** (*Figure 2.42*). This evidence strongly

suggests that the two product bands observed by SDS-PAGE are a result of the gel electrophoresis conditions.

Overall, an excellent 60% yield of pure Fab-Fab conjugate was obtained from 1 mg of Fab (71% yield with respect to the limiting reagent **BDBM(PEG)<sub>19</sub>**). The immunoreactivity of all three antibody conjugates, the scFv-scFv, Fab-Fab and scFv-Fab, was then analysed by ELISA.

### 2.3.5 Analysis of conjugates by ELISA

An enzyme-linked immunosorbent assay (ELISA) is a plate-based assay regularly employed for the detection and quantification of proteins. Typically an antigen is immobilised on the surface of a 96-well polystyrene plate, which passively binds to protein. The antigen can then be complexed with an antibody-enzyme conjugate. Detection is subsequently achieved through incubation of the conjugated enzyme with a substrate to produce a measurable product.

Having successfully generated scFv and Fab homodimer and an anti-CEA/anti-HER2 scFv-Fab bispecific, it was next decided to use an ELISA to assess the immunoreactivity of the purified conjugates in comparison to the unmodified scFv and Fab fragments that bound either CEA or HER2 respectively (*Figure 2.44[i] and [ii]*).

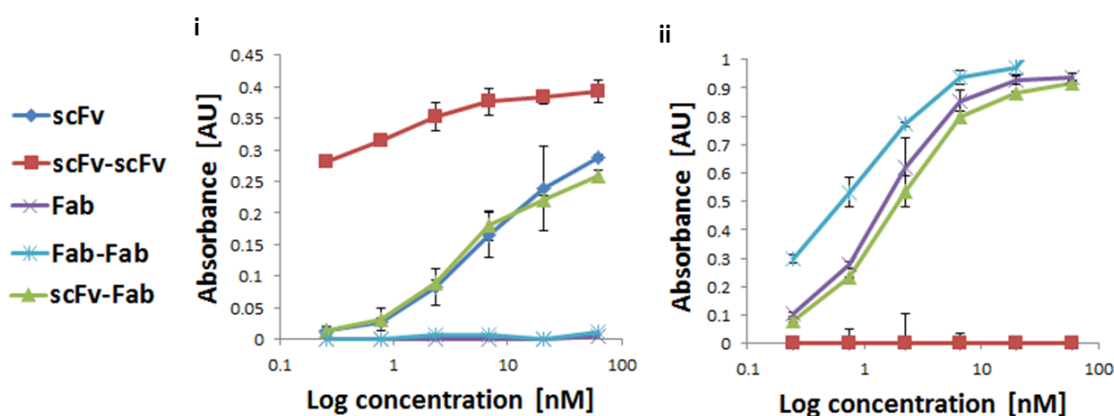


**Figure 2.44** ELISA analysis of conjugates and unmodified antibody fragments: [i] ELISA against full length CEA. [ii] ELISA against HER2.

Against CEA, the activity of the scFv homodimer was not only maintained, but remained high at low dilutions, suggesting dimerisation has successfully increased the

avidity of the antibody (*Figure 2.44[i]*). Pleasingly, the Fab homodimer also demonstrated an increase in avidity compared to unmodified Fab monomer (*Figure 2.44[ii]*). Most importantly, the scFv-Fab conjugate showed comparable antigen binding activity against both CEA and HER2 (*Figure 2.44[i]* and *[ii]*).

Given this success, the next target was to demonstrate that our heterodimeric conjugate could simultaneously bind its two target antigens. To achieve this, a sandwich ELISA was developed (*Figure 2.45[i]*). A 96-well plate was coated with CEA and the sample to be tested, e.g. scFv-Fab conjugate, was applied. Subsequent incubation with HER2-Biotin and Extravidin-Peroxidase would thus only lead to a signal if the sample successfully bound both CEA and HER2 antigens. Pleasingly, simultaneous binding activity was confirmed (*Figure 2.45[ii]*). Hence a homogeneous antibody conjugate with bispecific ability has successfully been produced using our disulfide-bridging technology.

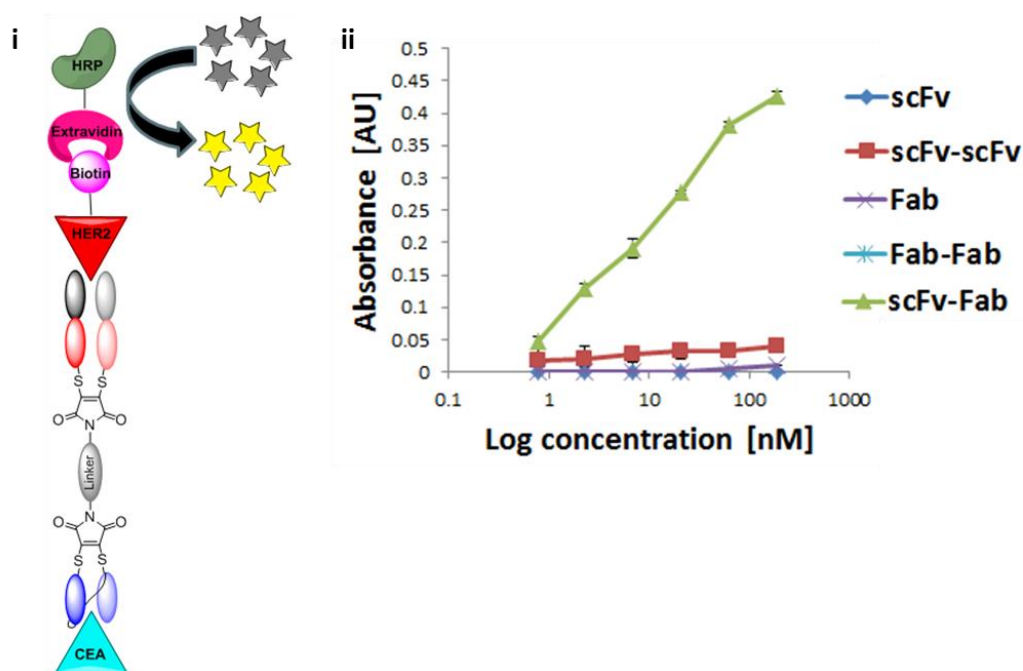


**Figure 2.45** Sandwich ELISA using **[i]** full length CEA coated plates and HER2 conjugated to Biotin, followed by Extravidin-Peroxidase. **[ii]** ELISA results.

### 2.3.6 Analysis of conjugates by FACS

Fluorescence activated cell-sorting (FACS) is a type of flow cytometry, described in *Section 1.7.3*. In a final investigation, FACS was used to assess the binding of our scFv homodimer and scFv-Fab bispecific to a CEA-positive cell line, A375 CEA, and a

HER2-positive cell line, BT-474. The monomer controls in *Figure 2.46* demonstrate that anti-CEA scFv binds only to A375CEA cells and anti-HER2 Fab only to BT474 cells (full set of controls in *Section 4.7.10*). Application of our scFv homodimer conjugate reveals that CEA binding activity and selectively is maintained after conjugation, with a shift in fluorescence being observed only on the A375CEA cell line (*Figure 2.46, homodimer*). Following this success, we tested our bispecific construct (*Figure 2.46, heterodimer*). In this case, scFv and Fab were detected both in the CEA-positive cell line A375CEA and the HER2-positive BT474. This demonstrates that the antibody fragments have maintained their distinct selectivity and binding activity *in vitro*, whilst being successfully chemically linked.

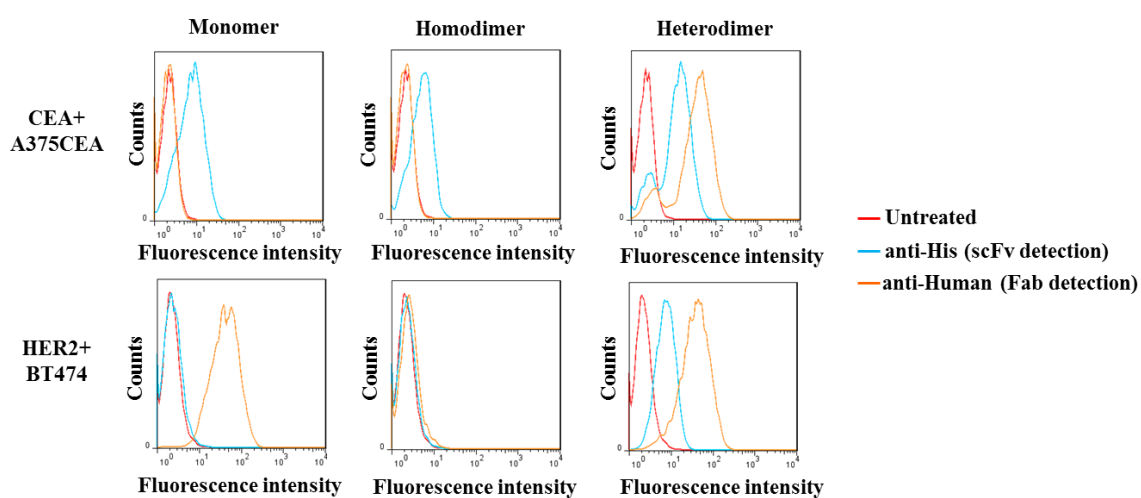


**Figure 2.46** Flow cytometry based binding assay of unmodified scFv and Fab (monomer), scFv dimer (homodimer) and scFv-Fab conjugate (heterodimer) to a CEA-positive cell line (A375CEA) and HER2-positive cell line (BT474).

To date, the generation of bispecifics for the clinic by chemical cross-linking has been unsuccessful, due to low yields and product heterogeneity. Here the rapid production of two homogeneous conjugates in high yield has been presented; an anti-CEA scFv homodimer and an anti-CEA/anti-HER2 scFv-Fab heterodimer. A third conjugate, anti-HER2 Fab homodimer has also been generated, which appears to be a single product by SEC and LCMS analysis, although the SDS-PAGE results remain unclear. These conjugates have been achieved using a *bis*-dibromomaleimide PEG linker, readily synthesised over two steps from the commercially available dibromomaleimide. Through targeting and bridging the disulfide bond of antibody fragments, the conjugates produced exhibit retention of activity by ELISA and cell binding assays. This platform has the potential to enable the facile generation of bispecifics from a range of antibody

---

fragment formats, and could be readily translated to other protein conjugates of choice, exploiting the versatility of the chemical conjugation approach.

---

## 2.4 Disulfide bridging for diagnostic applications

Several small side projects have been carried out to apply the disulfide bridging technology described herein to diagnostic applications, and efforts in these areas will now be covered.

### 2.4.1 Functionalisation of a scFv-Fc antibody construct

ScFv-Fc fusion proteins are widely used full antibody derivatives (*Figure 2.47*). The key advantage of these constructs over conventional monoclonal antibodies is their ease of production; they are generated by fusion of scFv fragments to the Fc region of different antibody isotypes (204). Hence only one polypeptide chain requires transfection and expression, simplifying production. Furthermore, they are readily purified by standard protein A chromatography, mediate the effector functions of the Fc fragment as would the whole antibody and have a lower molecular weight (~105 kDa) which can improve their tumour penetrating ability (204).

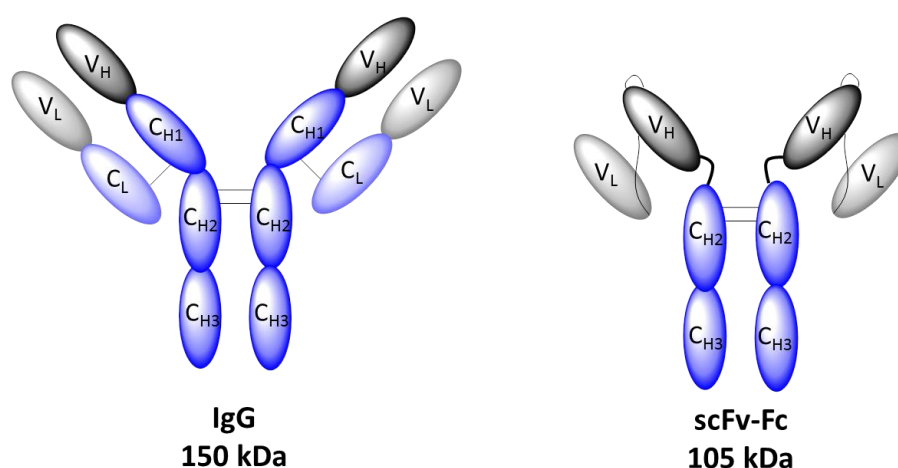


**Figure 2.47** Structure of a whole IgG (150 kDa) and a scFv-Fc construct (105 kDa).

Professor Tony Ng's group (King's College London) is investigating the use of labelled scFv-Fc constructs as tools for imaging protein-protein interactions in patient cell samples. This will be achieved by Fluorescence Resonance Energy Transfer (FRET) experiments. To obtain high-quality FRET data, the acceptor and donor chromophores must be installed site-specifically and in a defined number, and not affect the biophysical properties of the proteins under investigation (205). ScFv-Fc molecules contain only two disulfide bonds, located in the hinge region. Thus, modification of these disulfide bonds using our next generation maleimide disulfide bridging technology was investigated for FRET application.

First, a reduction study of a scFv-Fc construct was pursued using the water-soluble reducing agents, TCEP and DTT (*Figure 2.48*).

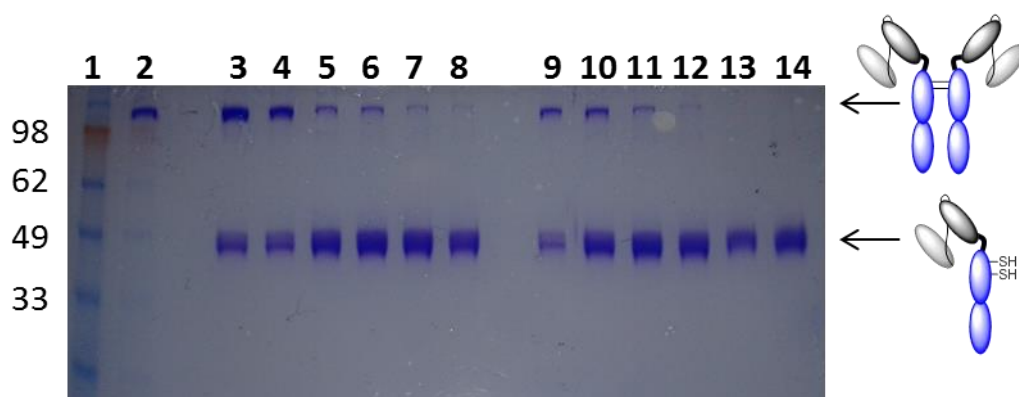


**Figure 2.48** SDS-PAGE analysis of scFv-Fc reduction study. **Lane 1** contains protein ladder in kDa (SeeBlue® Plus2, Invitrogen). **Lane 2** contains unmodified scFv-Fc. **Lanes 3 to 8** contain scFv-Fc + 3, 5, 8, 12, 20 and 50 equiv TCEP respectively. **Lanes 9 to 14** contain scFv-Fc + 3, 5, 8, 12, 20 and 50 equiv DTT respectively.

DTT was identified as a more effective reducing agent for the scFv-Fc construct (*Figure 2.48*). Following identification of the appropriate reduction conditions, disulfide bridging with dithiophenolmaleimide **9** was attempted. After reduction with DTT, the scFv-Fc was buffer exchanged into conjugation buffer (20 mM phosphate buffer, 5 mM EDTA, pH 7.4) and varying equivalents of dithiophenolmaleimide added (*Figure 2.49*).

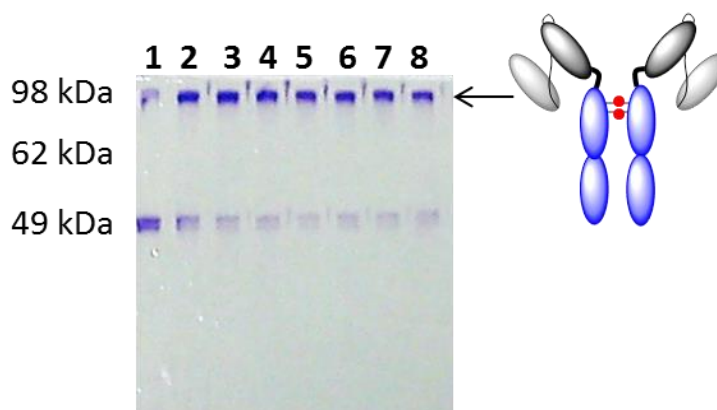
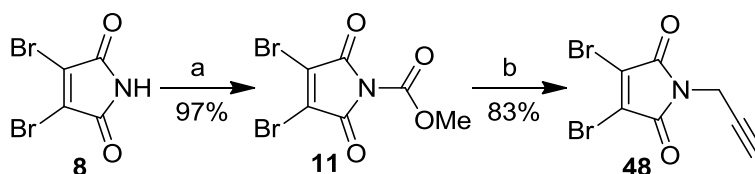


**Figure 2.49** SDS-PAGE analysis of scFv-Fc disulfide bridging with dithiophenolmaleimide **9** (represented as red circles). **Lane 1** contains reduced scFv-Fc left for experiment duration (1 h, over ice). **Lanes 2 to 8** contain reduced scFv-Fc with 2, 3, 4, 5, 8, 12 and 16 equivalents dithiophenolmaleimide respectively (1 h, over ice).

Disulfide bridging using dithiophenolmaleimide worked very effectively, as can be seen in *Figure 2.49*. Using up to 16 equivalents, almost complete bridging is achieved, with very little ‘half-antibody’ remaining. Significant yields of incorrectly bridged construct

as observed for the hinge region disulfides of full antibody molecules (described in *Section 1.8.3*), were not seen using this scFv-Fc construct. The same results were obtained using dibromomaleimide **8** for bridging. Knowing that the two disulfide bonds of the scFv-Fc construct could be successfully bridged using our next generation maleimides, a strategy for the introduction of fluorophores was devised.

Many fluorophores of interest are now commercially available as the azide derivative. This enables the synthesis of a single molecule for bioconjugation for which the desired fluorophore can be attached by click chemistry. In *Section 2.2*, the rate and efficiency of the CuAAC was found to be far beyond its copper-free SPAAC derivative. Thus it was decided to functionalise the scFv-Fc construct with a simple linear alkyne. To this end, a simple *N*-alkyne maleimide was generated (*Scheme 2.39*).



**Scheme 2.39** Reagents and conditions: (a) MeOCOCl, NMM, THF; (b) NH<sub>2</sub>CH<sub>2</sub>C≡CH, DCM.

The linear alkyne maleimide **48** was readily synthesised from the commercially available dibromomaleimide **8** via the established carbamate chemistry over two steps in an overall 81% yield. This simple *N*-alkyne dibromomaleimide was then used for disulfide bridging of the reduced scFv-Fc construct. Using DTT (20 equivalents) followed by purification into conjugation buffer, the scFv-Fc was incubated with alkyne dibromomaleimide **48** (20 equivalents). After 1 h over ice, almost complete rebridging to the original scFv-Fc was achieved (*Figure 2.50*). Only a small amount of half-antibody was observed. Note, at this stage it was not investigated if this small amount of half-antibody was the incorrectly bridged construct.

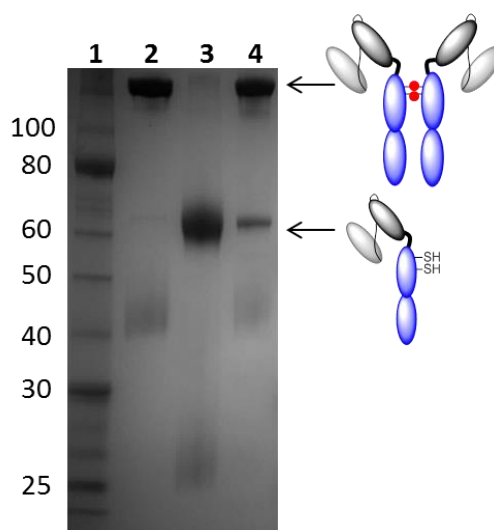


**Figure 2.50** SDS-PAGE analysis of scFv-Fc modification with *N*-alkyne dibromomaleimide **50**. **Lane 1** contains protein ladder in kDa (New England Biolabs). **Lane 2** contains unmodified scFv-Fc. **Lane 3** contains reduced scFv-Fc. **Lane 4** contains reduced scFv-Fc + **48** (20 equivalents).

Following successful installation of two alkyne molecules per scFv-Fc, CuAAC was attempted. For this, the azide derivative of the FRET suitable fluorophore Atto-565 (purchased from ATTO-TEC) was employed. Using the CuAAC conditions developed for the Fab fragment in *Section 2.2.7*, it was found that using 20 equivalents of the azide fluorophore for 1 h was sufficient to achieve a fluorophore to protein ratio (F/P) of 2.1 as measured by UV-Vis. This fluorescent scFv-Fc conjugate is due to be employed by Professor Ng's group.

This work demonstrates the facile transfer of the next generation maleimide disulfide bridging technology to other antibody constructs, successfully generating a homogeneously modified product. Modification of scFv-Fc constructs is of particular interest to the group as these would provide an excellent platform for the production of homogeneous ADCs with the increasingly desired DAR of 2 and significantly reduced production cost compared to full antibody constructs (103,149,206).

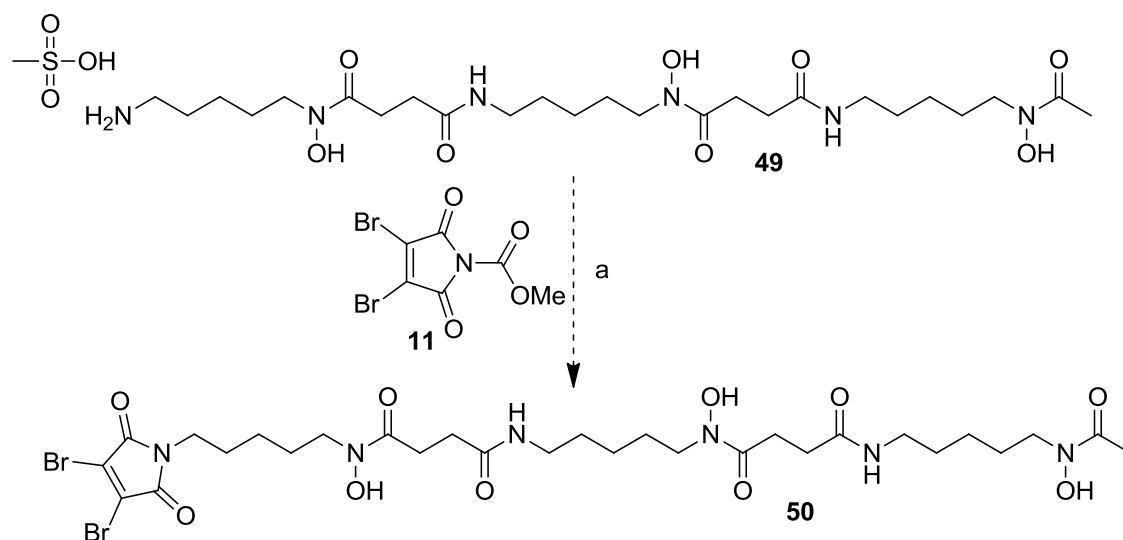
---

## 2.4.2 Disulfide bridging for Immuno-PET applications

As described in *Section 1.7.4*, immuno-positron emission tomography (PET) facilitates non-invasive tumour diagnosis. It is also a key technique in the growing field of theranostics and personalised medicine, effectively enabling “comprehensive immunohistochemical staining *in vivo*” (207). Antibody conjugates prepared for immuno-PET imaging currently rely on conventional modification methods which target lysine residues or cysteines, released through the reduction of interchain disulfide bonds. As discussed in *Section 1.8*, these approaches result in a heterogeneous mixture of conjugated antibody products, with variable numbers of chelators and different sites of attachment which can have a detrimental impact on the biophysical properties of the targeting antibody. In collaboration with Professor Philip Blower’s group at King’s College London, the application of the disulfide bridging technology described herein to full antibodies and antibody fragments for immuno-PET applications is being investigated.

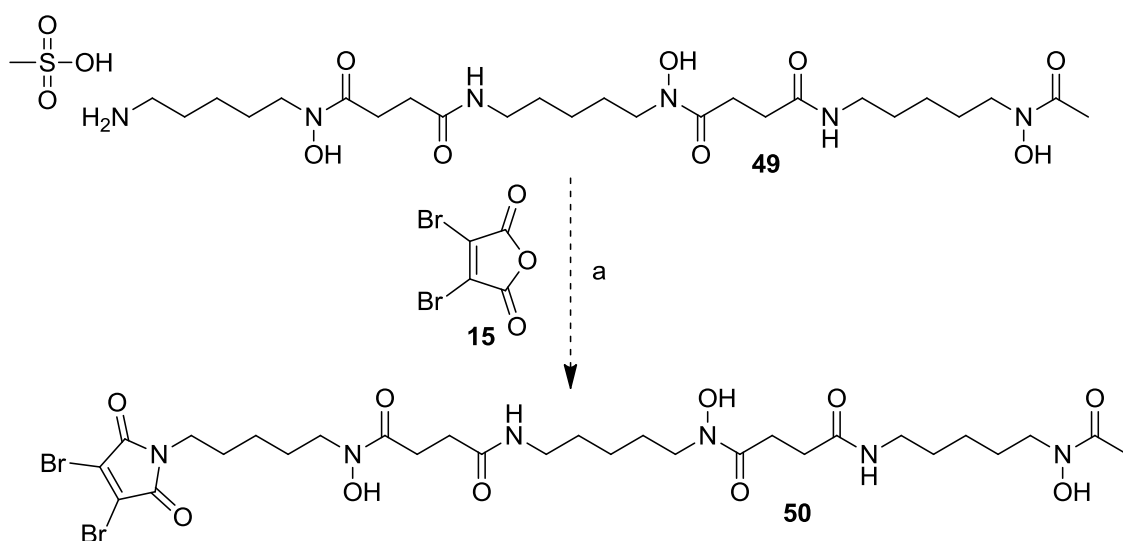
Antibody labelling with a suitable positron emitter such as zirconium-89 ( $^{89}\text{Zr}$ ) or gallium-67 ( $^{67}\text{Ga}$ ) is generally achieved by first labelling the antibody with a suitable chelator. Initial investigations thus focused on a general synthetic route to chelator functionalised next generation maleimides. Many chelators are incorporated into structures suitable for protein conjugation via a primary amine. Deferoxamine (DFO) is a commonly used chelator and is commercially available as the mesylate salt. Generation of a DFO functionalised disubstituted maleimide was therefore the first synthetic target.

Synthesis of a DFO functionalised disubstituted maleimide was first attempted as outlined in *Scheme 2.40*. Using the commercially available DFO mesylate salt **49**, reaction with the previously described dibromomaleimide carbamate **11** was attempted. DFO is a highly insoluble compound and so DMF was employed as the solvent. Nevertheless, after 24 h no reaction between DFO **49** and the carbamate **11** was observed. This synthetic route was also attempted using the dithiophenolmaleimide carbamate derivative **27** with up to 3 equivalents  $\text{NEt}_3$ ; however the desired product was not obtained.



**Scheme 2.40** Reagents and conditions: (a)  $\text{NEt}_3$ , DMF.

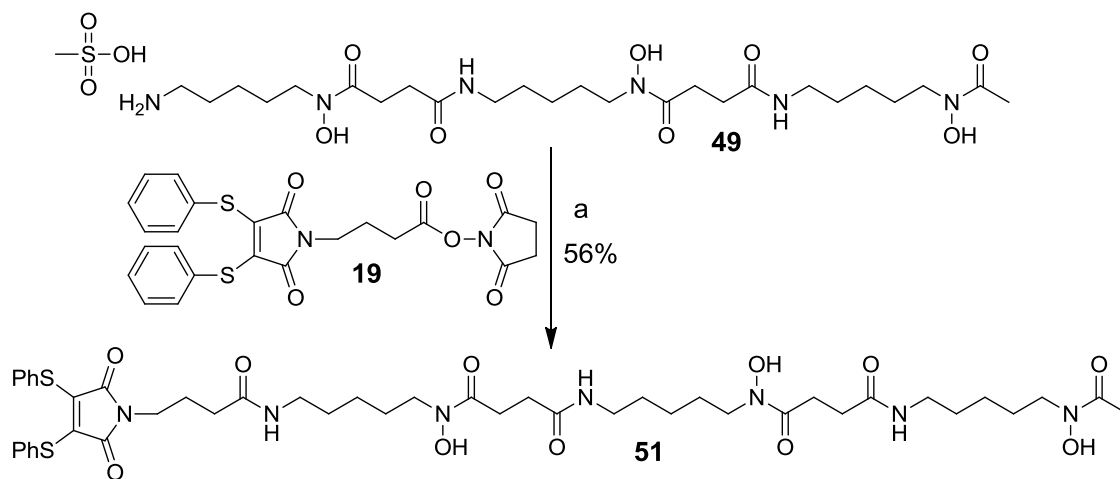
As an alternative simple synthetic route to chelator functionalised next generation maleimides, the synthesis in *Scheme 2.41* was attempted.



**Scheme 2.41** Reagents and conditions: (a) AcOH, reflux.

Given previous success on employing the dibromomaleic anhydride **15**, it was anticipated that the harsher conditions outlined in *Scheme 2.41* would readily yield dibromomaleimide-DFO **50**. This reaction routinely proceeds in acetic acid at reflux. On heating, the DFO mesylate **49** dissolved in acetic acid at approximately  $65\text{ }^\circ\text{C}$ . However, at reflux the reaction mixture rapidly changed to dark brown/black colour. TLC analysis of the solution revealed many spots, suggesting breakdown of the DFO compound. At temperatures slightly below reflux the same effect was observed.

In the literature, DFO conjugation to an antibody has been achieved using traditional maleimide chemistry (208). In this case, the DFO primary amine **49** was linked to the maleimide via NHS ester chemistry. Thus it was decided to take a similar route, and dithiophenolmaleimide-NHS ester linker **19** described in *Section 2.1* was employed. The synthetic route is shown in *Scheme 2.42*.



**Scheme 2.42** Reagents and conditions: (a) DIPEA, DMF, H<sub>2</sub>O.

Using a mixture of DMF and water, dithiophenolmaleimide-NHS ester linker **19**, DFO mesylate **49** and DIPEA were dissolved and stirred at room temperature for 1 h. After this time, water was added and the resulting solution left on ice for 1 h. This caused precipitation of the desired dithiophenolmaleimide-DFO product **51**, in a good 56% yield.

Following the successful synthesis of a DFO functionalised next generation maleimide, a suitable disulfide bridging protocol for combination with this modification reagent was investigated. Prostate-specific membrane antigen (PSMA) is a transmembrane protein expressed in all types of prostatic tissue, and is one of the best characterised oncogenic markers. Bridging of the single disulfide bond of an anti-PSMA ds-scFv provided by Dr Florian Kampmeier (Blower group, King's College London), was attempted. A DFO modified anti-PSMA ds-scFv is of interest to the group for immuno-PET imaging.

After establishing that the anti-PSMA ds-scFv had similar reducing properties to the anti-CEA ds-scFv employed in the project thus far, a stepwise bridging protocol was trialed. The results are shown in *Figure 2.51*.

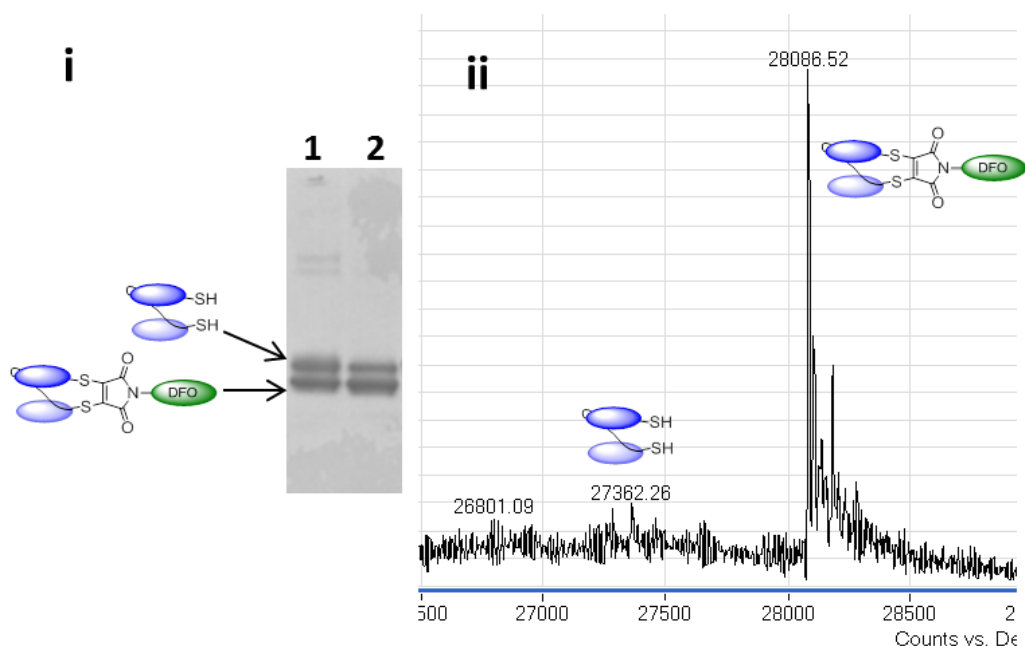


**Figure 2.51** First attempt at anti-PSMA ds-scFv modification using DFO functionalised dithiophenolmaleimide **53**. [i] SDS-PAGE analysis. **Lane 1** is reaction mixture before purification by SEC. **Lane 2** is post SEC. [ii] LCMS analysis of conjugation. Expected 28085, obtained 28086.

The results in *Figure 2.51* indicate that whilst bridging was achieved using dithiophenolmaleimide **51**, it was incomplete. This first attempt used **51** dissolved in DMF however, the DFO-dithiophenolmaleimide rapidly precipitated out of solution. Even using dilute stocks for modification and heating to 37 °C could not sufficiently maintain this reagent for efficient conjugation. Although dithiophenolmaleimide **51** does not dissolve well in water, its solubility was found to be slightly improved in DMSO. In fact, using a low stock concentration and 20% DMSO in buffer, complete modification of the ds-scFv was achieved after 2 h at 37 °C (*Figure 2.52*).

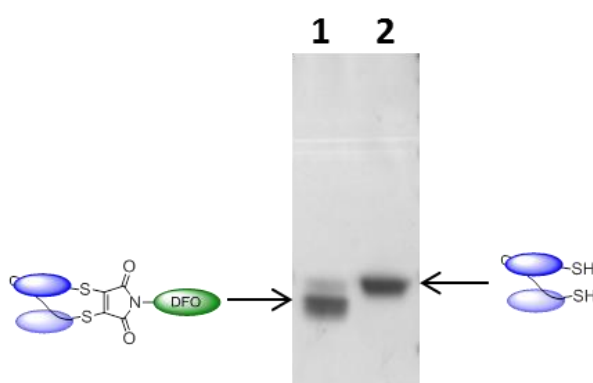


**Figure 2.52** SDS-PAGE analysis of improved conjugation between dithiophenolmaleimide-DFO **51** and anti-PSMA ds-scFv. **Lane 1** is reduced scFv (70

---

$\mu\text{M}$ ) + **51** (6 equivalents, 2 mM stock in DMSO) after 2 h at 37 °C to yield bridge scFv. **Lane 2** is a reduced scFv control.

The successfully DFO modified anti-PSMA scFv is currently undergoing investigation as an immuno-PET conjugate. The long-term aim of this collaboration is to synthesise a range of dithiophenolmaleimide based chelators as described in *Scheme 2.42* and employ these reagents for the preparation of full antibody immuno-PET conjugates. Successful combining of our disulfide bridging technology with radiometal chelators will facilitate the facile production of homogeneous radioimmunoconjugates.

---

### 3 Summary

In this thesis, a range of 3,4-substituted maleimide based linkers have been designed, synthesised and applied towards the development of homogeneous antibody conjugates for ADEPT and bispecific therapeutics. Initially, the generation of a disulfide to lysine linker for more defined antibody-enzyme conjugates was investigated (*Figure 3.1*). It was anticipated to provide a significant improvement on existing chemical conjugation techniques, as site-specific modification would be achieved at the antibody.

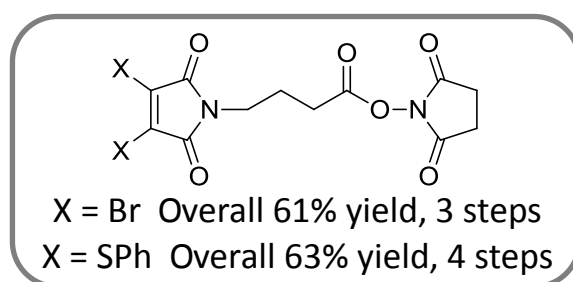


**Figure 3.1** Synthesised disulfide to lysine linkers.

Selectivity investigations revealed the dithiophenolmaleimide derivative of the disulfide to lysine linker to be a promising cross-linker design and so it was applied to the model system; an anti-CEA ds-scFv to CPG2 antibody-enzyme conjugate (*Figure 3.2*). Despite no evidence in the literature of attempting to strictly control and monitor the level of lysine modification when generating conjugates, a method for the relatively controlled conjugation of two linker molecules per CPG2 was achieved. For the conjugation of this modified CPG2 to the anti-CEA ds-scFv fragment, an *in situ* portionwise reduction approach was developed. This required the addition of the reducing agent benzeneselenol in 15 equivalent portions initially and every 20 minutes, for up to 1 h, successfully maintaining the antibody in its reduced form to promote conjugation. However, this approach generated only very low yields of the desired scFv-CPG2 conjugate.

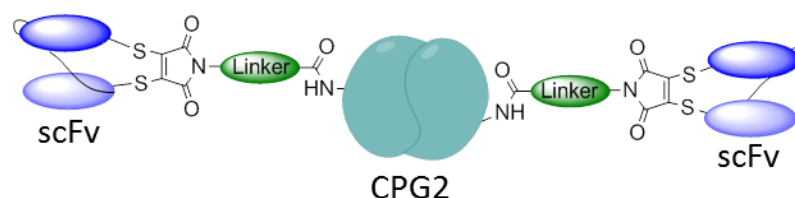


**Figure 3.2** Desired anti-CEA ds-scFv to CPG2 conjugate through employing a disulfide to lysine linker.

This strategy was largely impeded by a competing side reaction; the formation of scFv dimer. The dimer was generated as a result of the slow rate of conjugation due to the sterically encumbered macromolecules and the low number of 3,4-substituted maleimides with which the scFv cysteines must react. Remaining strategies to improve the yield of desired conjugate and decrease scFv dimerisation only served to increase product heterogeneity. This investigation demonstrated that the successful production of therapeutic antibody-enzyme conjugate would require site-specific conjugation at both the antibody and enzyme. For this to be achieved, mutagenesis of the CPG2 enzyme to incorporate a single cysteine or disulfide bond would be required. Whilst feasible, the focus of this research project shifted attention to consider the linking together of two antibody fragments already containing single disulfide bonds, to generate bispecifics.

Generation of homogeneous antibody-antibody conjugates via site-specific disulfide bridging was attempted via two main strategies; an indirect approach, where each antibody to be conjugated is first modified site-specifically with a chemoselective functional group, and a direct approach where one antibody fragment is modified site-specifically and then directly linked to a second, unmodified fragment.

For the indirect cross-linking strategy, disulfide bridging linkers for participation in strain-promoted and copper-catalysed azide-alkyne cycloadditions were synthesised (*Figure 3.3*). Both reactions held advantages; the SPAAC is simple, eliminating the requirement for copper, whereas the CuAAC alkyne linker is readily synthesised and has a considerably greater rate of reaction. All of the synthesised bioorthogonal linkers displayed efficient and quantitative bridging of scFv and Fab antibody fragments. In addition, the azide and alkyne functionalities were demonstrated to be excellent site-specific chemical handles for the installation of small molecules, for example fluorophores, on to the antibody.

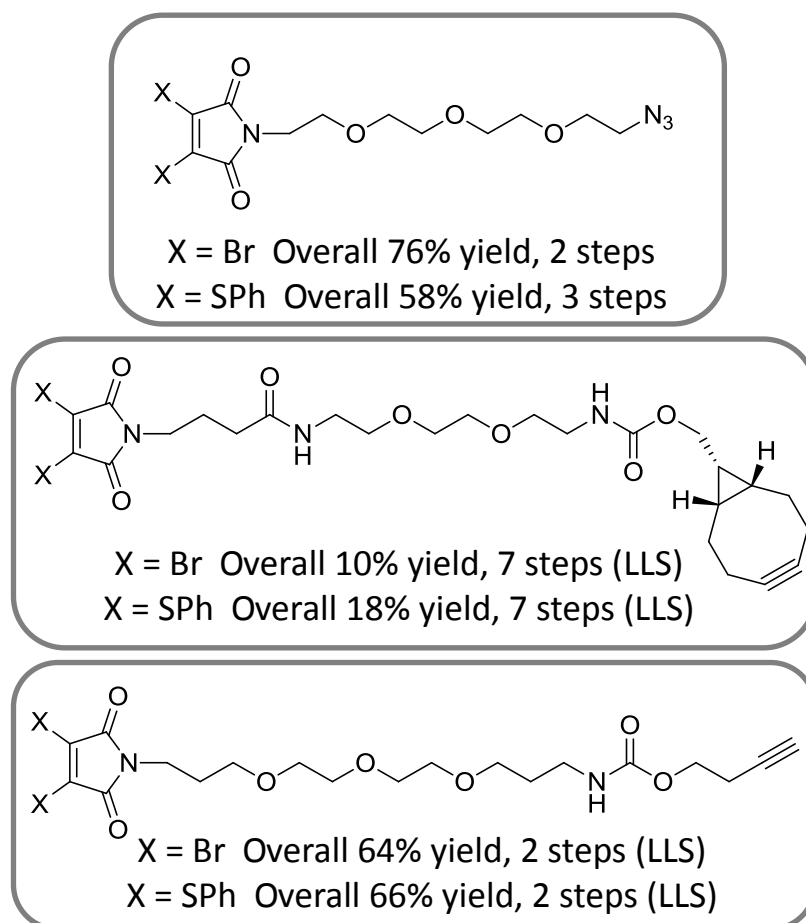


**Figure 3.3** 3,4-substituted maleimide linkers synthesised with azide, strained alkyne and linear alkyne functionalities suitable for SPAAC and CuAAC reactions.

Despite success site-specifically conjugating small molecules to antibody fragments using the SPAAC and CuAAC linkers, joining together two antibody fragments through this bioorthogonal approach proved troublesome. The high concentrations and long reaction times required to promote the SPAAC reaction between two antibody fragments resulted in significant protein aggregation. The strained alkyne component itself was found to be unstable under conditions suitable for antibody-antibody conjugation. The CuAAC reaction in comparison was found to be much more efficient; Herceptin Fab was readily modified with large PEG molecules within 1 h at room temperature. However, this reaction also required a large excess of either the azide or alkyne component to proceed to completion and was not readily compatible with the scFv fragment, the His tag of which immobilised the essential copper catalyst.

In tandem to the indirect cross-linking strategy, homobifunctional 3,4-substituted maleimide linkers for the direct conjugation of two antibody fragment disulfide bonds were also designed and developed. The conjugation attempts thus far have indicated that

it is difficult to obtain good yields using a site-specific approach, as the opportunity for reaction partners to meet is low. To determine if linker length can improve these yields, two *bis*-dibromomaleimide linkers of distinct length were synthesised (*Figure 3.4*).

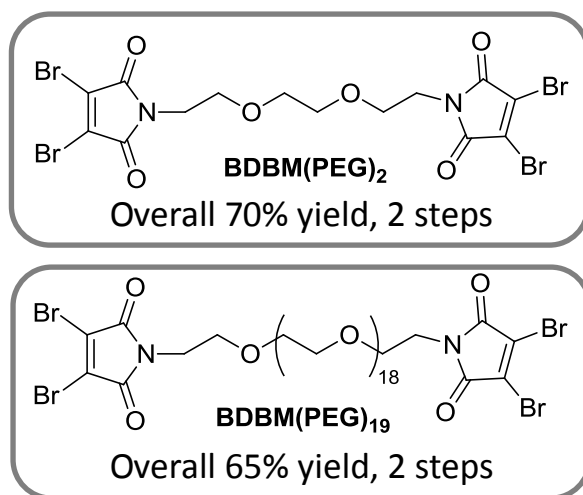
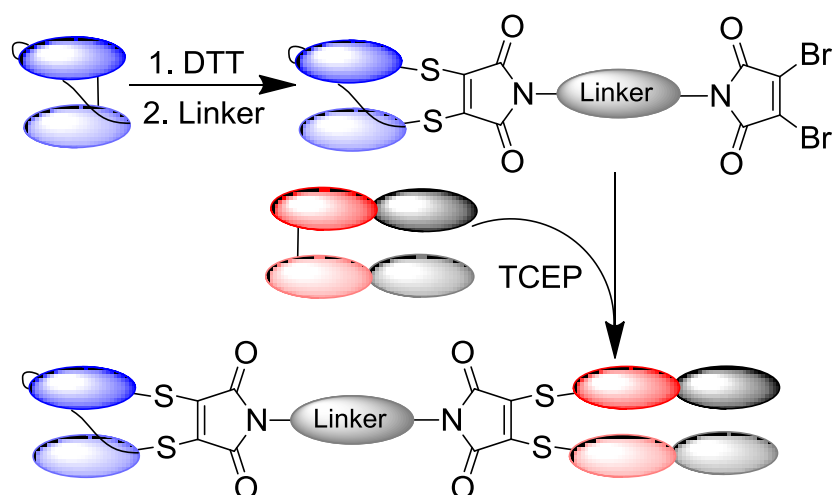


**Figure 3.4** Synthesised *bis*-dibromomaleimide cross-linkers.

The issues identified by conjugation attempts in the project thus far aided the rapid progress of this simple direct conjugation approach. Optimisation experiments yielded ideal buffer conditions to preserve antibody fragments in their reduced form, and maintaining reduced antibody concentrations below 1 mg/ml prevented unwanted side reactions. These improved conditions revealed not only that the disulfide to disulfide linkers are very effective in generating homogenous antibody-antibody conjugate, but also that linker length has a significant effect on conjugate yield. In fact, using linker **BDBM(PEG)<sub>19</sub>**, a 64% yield of pure, homogeneous scFv-scFv from 1 mg scFv was achieved (75% with respect to the limiting reagent **BDBM(PEG)<sub>19</sub>**). This yield represents a substantial improvement on previous reports of direct chemical cross-linking of antibodies using natural amino acids, which have achieved yields in the 10-40% range (193-196). Notably the conjugate is homogeneous due to the site-selectivity of the methodology.

Following the successful generation of homogeneous scFv homodimer, the **BDBM(PEG)<sub>19</sub>** linker technology was also applied to the generation of a true bispecific (*Scheme 3.1*). Through first site-selectively functionalising the anti-CEA scFv fragment with a single dibromomaleimide, anti-HER2 reduced Fab could be conjugated by

disulfide bridging to generate a site-specific, homogeneous anti-CEA/anti-HER2 bispecific in 52% yield after purification.



**Scheme 3.1** Generation of anti-CEA/anti-HER2 scFv-Fab bispecific using *bis*-dibromomaleimide cross-linker.

The direct conjugation approach using *bis*-dibromomaleimide linker **BDBM(PEG)<sub>19</sub>** represents the first example of homogeneous bispecific production through modification of naturally occurring amino acids. Through targeting and bridging the disulfide bond of antibody fragments, site-specificity was achieved whilst retaining antibody binding activity, as demonstrated by ELISA and cell binding assays. Furthermore, a sandwich ELISA was designed and developed which successfully demonstrated the ability of the anti-CEA/anti-HER2 construct to bind both of its antigen targets simultaneously. This direct conjugation approach by disulfide bridging thus delivers as an exciting chemical tool for the production of homogeneous bispecific therapeutics.

### 3.1 Future outlook

The research presented in this thesis demonstrates the facile transfer of our disulfide bridging technology to a variety of antibody fragments and constructs. The efficiency and site-selectivity of next generation maleimide bridging has facilitated the production of antibody-antibody conjugates homogeneously and in high yield. Having successfully created a bispecific with maintained antigen binding activity and demonstrated true bispecificity, application of the *bis*-dibromomaleimide cross-linker to the generation of a clinically relevant bispecific construct would be an exciting next step. Key to this would be the production of a bispecific T-cell engager (BiTE). Research into these

---

constructs has not yet established the ideal length of the cytolytic synapse generated by BiTEs (see *Section 1.6*). Using the *bis*-dibromomaleimide cross-linker design, a variety of different length PEG spacers could be readily incorporated between the two bridging maleimides. This would enable the rapid production of homogeneous BiTE constructs with an assortment of spacer lengths, enabling the cell-killing efficiency of the resulting cytolytic synapses to be readily compared. Indeed, the greater flexibility and rapid production of antibody conjugates offered by this chemical conjugation approach provides a distinct advantage over recombinant protein synthesis.

The attempted construction of an improved antibody-enzyme conjugate suitable for the therapeutic system ADEPT revealed that success of this approach would require site-specificity at both the antibody and enzyme. In the case of CPG2, which contains no disulfide bonds or free cysteine residues, the ideal solution would be to introduce a single cysteine residue at a defined site by mutagenesis. This would indeed be the simplest approach for many antibody-protein conjugates where a disulfide or cysteine residue is not naturally available in the protein. Therefore, as a necessary next step the applicability of the *bis*-dibromomaleimides to disulfide to cysteine conjugation should be investigated, as this would provide a valuable tool for homogeneous antibody-enzyme conjugate production and more generally for antibody-protein conjugates.

Having successfully linked two antibody fragments homogeneously using our next generation maleimides, an exciting further extension of this work would be the construction of triconjugates. Through installing a third point of attachment within the *bis*-dibromomaleimide linker design, this would open the door to a valuable and novel range of conjugates.

In conclusion, the versatility of the next generation maleimides in antibody bridging combined with the simplicity of the *bis*-dibromomaleimide linker approach yields a huge variety of options for development of this technology. It is hoped that the *bis*-dibromomaleimide cross-linkers will become an essential part of the protein chemists modification 'toolbox', realising the full potential of this efficient and simple approach.

---

## 4 Experimental

### 4.1 General Experimental Procedure

Solvents and reagents were purchased from suppliers and used without any further purification. All petroleum ether used had a boiling point range of 40 to 60 °C unless otherwise stated. All reactions were carried out at atmospheric pressure under argon with stirring unless otherwise stated. All buffer solutions were prepared with distilled water and filter-sterilised.

Normal phase silica gel (BDH) and sand (VWR) were used for flash chromatography. All reactions were monitored by thin layer chromatography (TLC) unless otherwise stated. TLC plates pre-coated with silica gel 60 F<sub>254</sub> on aluminium (Merck KGaA) were used. Visualisation was carried out by absorption of UV light (254 or 365 nm) or by dipping with potassium permanganate solution [KMnO<sub>4</sub> (1.25 g), Na<sub>2</sub>CO<sub>3</sub> (6.25 g), H<sub>2</sub>O (250 mL)].

Infra-red (IR) spectra were recorded on a Perkin Elmer Spectrum 100 FT-IT Shimadzu 8700 spectrophotometer. Wavelengths of maximum absorbance ( $V_{\max}$ ) are quoted in cm<sup>-1</sup>, and the abbreviations s, br, m, w indicate sharp, broad, medium and weak absorptions respectively.

<sup>1</sup>H Nuclear Magnetic Resonance (NMR) spectra were recorded at 400 MHz, 500 MHz and 600 MHz and <sup>13</sup>C NMR at 100 MHz, 125 MHz and 150 MHz on a Bruker AMX400, AMX500 and AMX600 at ambient temperature. Chemical shifts were measured in parts per million (ppm) and are quoted as  $\delta$ . Coupling constants,  $J$ , are quoted in Hertz (Hz) to 1 decimal place. Multiplicities for <sup>1</sup>H are shown as s (singlet), d (doublet), t (triplet), q (quartet), quin (quintet), m (multiplet), or a combination of these. All peaks should be taken as sharp unless otherwise described. Where necessary, assignments were made with the aid of DEPT, COSY, HMQC, HMBC or NOESY correlation experiments.

High and low resolution mass spectrometry were obtained by the EPSRC UK National Mass Spectrometry Facility (NMSF), Swansea or performed at UCL using a VG70 SE operating in modes ES, EI, FAB or CI (+ or -) depending on the sample. For the

---

majority of compounds, the purity was determined by accurate mass spectrometry and NMR spectroscopic analysis.

Melting points were measured on a Gallenkamp heating block and are not corrected.

Protein conjugation reactions were monitored by 16 or 12% glycine-SDS-PAGE with a 4% stacking gel under non-reducing conditions unless otherwise stated. A few examples employed pre-cast 4-12% Tris-Glycine gels (Novex®).

## **4.2 Proteins**

Anti-CEA ds-scFv was kindly provided by Maria Livanos and Dr Berend Tolner (UCL Cancer Institute) and expressed following literature procedure (170). CPG2 was kindly provided by Mologic Ltd and MFCEP fusion protein by the Chester and Sharma groups (UCL Cancer Institute) and expressed following literature procedure (78). Trastuzumab (Herceptin) was purchased from UCLH pharmacy. ScFv-Fc construct was kindly provided by Dr Gregory Weitsman, King's College London (unpublished work). Anti-PSMA ds-scFv was kindly provided by Dr Florian Kampmeier, King's College London (unpublished work).

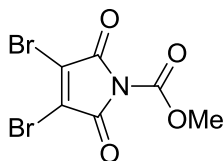
## **4.3 Abbreviations**

Within this text, room temperature is defined as between 19-22 °C. The term *in vacuo* refers to the removal of solvents by means of evaporation at a reduced pressure, provided by the in-house vacuum or an oil pump, using a Buchi® rotary evaporator. For NMR experiments, CDCl<sub>3</sub> is fully deuterated chloroform, DMSO is fully deuterated (D<sub>6</sub>) dimethyl sulfoxide, and MeOD is fully deuterated (D<sub>4</sub>) methanol. Solvents were chosen according to the position of solvent peak in spectra and solubility of substrate. THF is tetrahydrofuran, DCM is dichloromethane, EtOAc is ethyl acetate, MeOH is methanol, petrol is petroleum ether, Et<sub>2</sub>O is diethyl ether, MeCN is acetonitrile, DMF is dimethylformamide and AcOH is acetic acid.

---

## 4.4 Synthesis

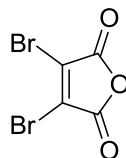
### *N*-(methoxycarbonyl)-3,4-dibromomaleimide (**11**)<sup>181</sup>



To a solution of 3,4-dibromomaleimide (1.00 g, 3.92 mmol) and *N*-methyl morpholine (0.43 ml, 3.92 mmol) in THF (35 ml), methyl chloroformate (0.30 ml, 3.92 mmol) was added and the reaction stirred for 20 min at room temperature. Then DCM (50 ml) was added to dissolve all solids. The organic phase was washed with H<sub>2</sub>O (3 x 40 ml), dried with MgSO<sub>4</sub>, filtered and concentrated *in vacuo* to yield **11** as a pale pink solid (1.18 g, 97%).

m.p. 116 – 118 °C (lit. m.p. 115 – 118 °C)<sup>181</sup>; <sup>1</sup>H NMR (500 MHz, CDCl<sub>3</sub>) δ 4.03 (s, 3H, CH<sub>3</sub>); <sup>13</sup>C NMR (125 MHz, CDCl<sub>3</sub>) δ 159.7 (C), 147.4 (C), 131.8 (C), 55.2 (CH<sub>3</sub>); IR (solid, cm<sup>-1</sup>) 2962 (s), 1765 (s), 1725 (s), 1600 (s); MS (EI) 315 (<sup>81,81</sup>M<sup>+</sup>, 35), 313 (<sup>81,79</sup>M<sup>+</sup>, 75), 310 (<sup>79,79</sup>M<sup>+</sup>, 35), 283 (45), 190 (75), 131 (100); Exact Mass calculated for C<sub>6</sub>H<sub>3</sub>NO<sub>4</sub><sup>79</sup>Br<sub>2</sub> 310.84233, observed 310.84297 (EI).

### 3,4-dibromofuran-2,5-dione (**15**)<sup>182</sup>

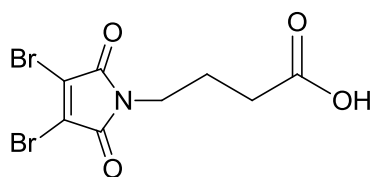


A solution of maleic anhydride (1.50 g, 15.3 mmol), aluminium trichloride (0.30 g, 0.21 mmol) and bromine (1.57 ml, 30.6 mmol) was heated to 160 °C with stirring in a sealed ampule, behind a blast shield, for 20 h. The reaction mixture was then cooled to room temperature and carefully opened to air through aqueous K<sub>2</sub>CO<sub>3</sub> solution. EtOAc was added and the solid filtered off and repeatedly washed with EtOAc. The filtrate was concentrated *in vacuo* to give **15** as a yellow solid (3.35 g, 86%).

m.p. 108-110°C, (lit. m.p. 113 – 114 °C)<sup>182</sup>; <sup>13</sup>C NMR (125 MHz, CDCl<sub>3</sub>) δ 164.4 (C), 125.9 (C); IR (solid, cm<sup>-1</sup>) 1767 (s), 1591 (m); MS (EI) 258 (<sup>81,81</sup>M<sup>+</sup>, 40), 255 (<sup>81,79</sup>M<sup>+</sup>, 20), 253 (<sup>79,79</sup>M<sup>+</sup>, 40), 169 (85), 167 (90), 133 (85), 131 (90); Exact Mass calculated for C<sub>4</sub>O<sub>3</sub><sup>79</sup>Br<sub>2</sub> 253.82087, observed 253.82040 (EI).

---

#### 4-(3,4-dibromo-2,5-dioxo-2,5-dihydro-1H-pyrrol-1-yl)-butanoic acid (**12**)

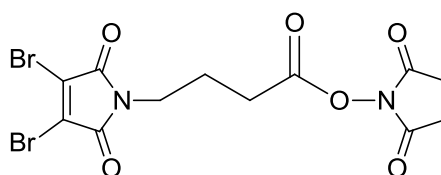


A mixture of  $\gamma$ -aminobutyric acid (340 mg, 3.29 mmol) and 2,3-dibromomaleic anhydride **15** (843 mg, 3.29 mmol) in AcOH (30 ml) was heated to reflux for 4 h. The AcOH was then removed *in vacuo* using repeated additions of toluene. EtOAc was added and the solid filtered and repeatedly washed with EtOAc. The filtrate was concentrated *in vacuo* to give **12** as a yellow powder (1.02 g, 91%).\*

m.p. 101-104°C;  $^1\text{H}$  NMR (500 MHz, MeOD)  $\delta$  3.65 (t, 2H,  $J = 6.8$ ,  $\text{NCH}_2\text{CH}_2$ ), 2.33 (t, 2H,  $J = 7.1$ ,  $\text{CH}_2\text{COOH}$ ), 1.87 (quin, 2H,  $J = 6.9$ ,  $\text{NCH}_2\text{CH}_2$ );  $^{13}\text{C}$  NMR (125 MHz, MeOD)  $\delta$  176.5 (C), 165.5 (C), 130.3 (C), 39.9 ( $\text{CH}_2$ ), 32.0 ( $\text{CH}_2$ ), 24.7 ( $\text{CH}_2$ ); IR (solid,  $\text{cm}^{-1}$ ) 3479 (w), 2930 (s), 1779 (s), 1704 (s), 1591 (m); MS (EI) 343 ( $^{81,81}\text{M}^+$ , 5), 341 ( $^{81,79}\text{M}^+$ , 10), 339 ( $^{79,79}\text{M}^+$ , 5), 297 (15), 295 (35), 293 (15), 282 (55), 270 (50), 268 (100), 266 (50), 133 (55), 131 (50); Exact Mass calculated for  $\text{C}_8\text{H}_7\text{O}_4\text{N}^{79}\text{Br}_2$  338.87363, observed 338.87323 (EI).

\*Note – for smaller scale reactions purification was achieved by column chromatography (1 : 1 EtOAc : Petrol).

#### 2,5-dioxopyrrolidin-1-yl 4-(3,4-dibromo-2,5-dioxo-2,5-dihydro-1H-pyrrol-1-yl)butanoate (**13**)



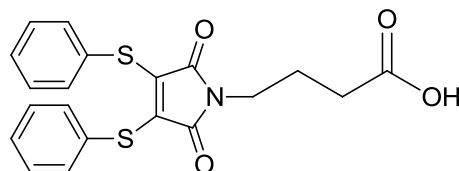
To a stirred solution of acid **12** (100 mg, 0.293 mmol) and *N*-hydroxysuccinimide (34 mg, 0.293 mmol) in EtOAc (3 ml) at 0 °C was added *N,N'*-dicyclohexylcarbodiimide (61 mg, 0.293 mmol). The reaction mixture was allowed to warm to room temperature and stirred overnight. The formed dicyclohexylurea was filtered off and the filtrate concentrated *in vacuo*. EtOAc (30 ml) was added and the solution washed with aqueous saturated  $\text{NaHCO}_3$  (20 ml),  $\text{H}_2\text{O}$  (10 ml) and brine (10 ml). The organic layer was



---

(50), 288 (40), 256 (30); Exact Mass calculated for  $C_{26}H_{20}N_2O_{10}S_2Na$  607.0457, observed 607.0485 (ES+).

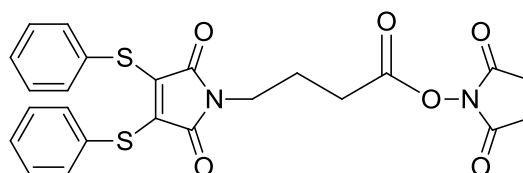
#### 4-(2,5-dioxo-3,4-bis-phenylsulfanyl-2,5-dihydro-pyrrol-1-yl)-butyric acid (**18**)



To acid **12** (72 mg, 0.211 mmol) in MeOH (4 ml) was added  $NaHCO_3$  (106 mg, 1.266 mmol). Thiophenol (50  $\mu$ l, 0.486 mmol) in MeOH (1 ml) was then added. After 1 h the solvent was removed *in vacuo*. Purification by column chromatography (gradient elution from DCM to 10% MeOH in DCM) yielded **18** as a sticky yellow foam (83 mg, 99%).

$^1H$  NMR (500 MHz, MeOD)  $\delta$  7.30-7.21 (m, 6H, Ar-H), 7.19-7.13 (m, 4H, Ar-H), 3.55 (t, 2H,  $J = 6.9$ ,  $NCH_2CH_2$ ), 2.31 (t, 2H,  $J = 7.1$ ,  $CH_2COOH$ ), 1.87 (quin, 2H,  $J = 7.0$ ,  $NCH_2CH_2$ );  $^{13}C$  NMR (125 MHz,  $CDCl_3$ )  $\delta$  176.5 (C), 168.3 (C), 137.2 (C), 132.2 (CH), 130.0 (CH), 129.2 (CH), 39.3 ( $CH_2$ ), 32.2 ( $CH_2$ ), 25.0 ( $CH_2$ ); IR (oil,  $cm^{-1}$ ) 3333 (s, br), 2946 (w), 2483 (br), 2072 (w), 1703 (m), 1449 (m); MS (EI) 399 ( $M^+$ , 15), 218 (25), 110 (100); Exact Mass calculated for  $C_{20}H_{17}NO_4S_2$  399.05935, observed 399.05964 (EI).

#### 2,5-dioxopyrrolidin-1-yl 4-(2,5-dioxo-3,4-bis(phenylthio)-2,5-dihydro-1H-pyrrol-1-yl)butanoate (**19**)

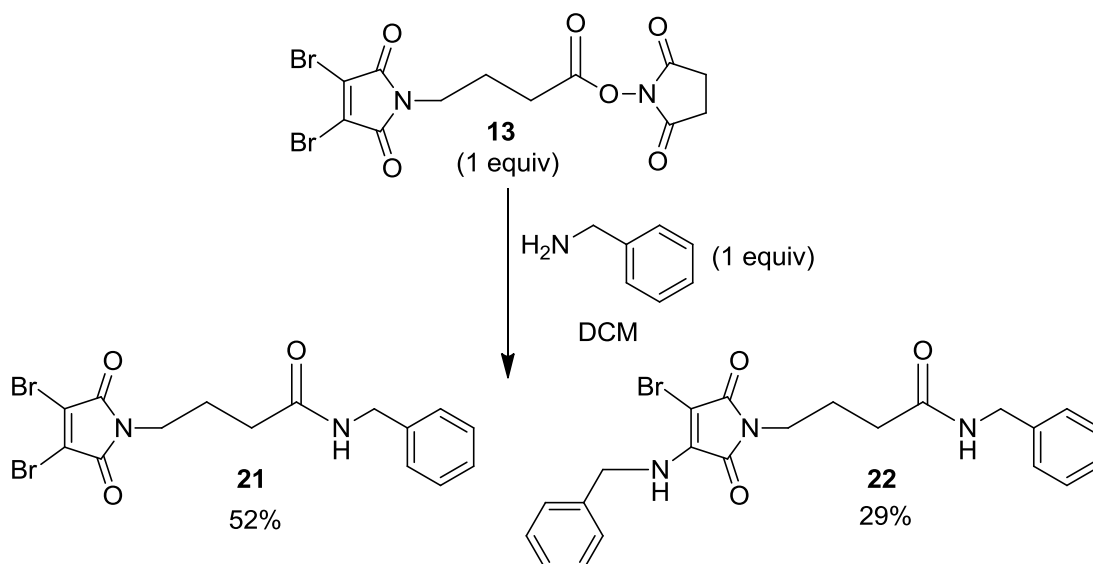


To a stirred solution of acid **18** (415 mg, 1.04 mmol) and *N*-hydroxysuccinimide (120 mg, 1.04 mmol) in EtOAc (15 ml) at 0 °C was added *N,N'*-dicyclohexylcarbodiimide (214 mg, 1.04 mmol). The reaction mixture was allowed to warm to room temperature and stirred overnight. The formed dicyclohexylurea was filtered off and the filtrate concentrated *in vacuo*. EtOAc (20 ml) was added and the solution washed with aqueous saturated  $NaHCO_3$  (20 ml),  $H_2O$  (30 ml) and brine (30 ml). The organic layer was

separated and dried over MgSO<sub>4</sub>. Purification by column chromatography (40% EtOAc in petrol) yielded **19** as a bright yellow powder (420 mg, 81%).

m.p. 41 – 43 °C; <sup>1</sup>H NMR (600 MHz, CDCl<sub>3</sub>) δ 7.28-7.24 (m, 6H, Ar-H), 7.19-7.08 (m, 4H, Ar-H), 3.61 (t, 2H, *J* = 7.2, NCH<sub>2</sub>), 2.82 (s, 4H, COCH<sub>2</sub>CH<sub>2</sub>CO), 2.63 (t, 2H, *J* = 7.2, CH<sub>2</sub>CO), 2.00 (quin, 2H, *J* = 7.2, NCH<sub>2</sub>CH<sub>2</sub>); <sup>13</sup>C NMR (125 MHz, CDCl<sub>3</sub>) δ 169.4 (C), 167.9 (C), 166.8 (C), 135.6 (C), 131.6 (CH), 129.4 (C), 129.3 (CH), 128.3 (CH), 37.7 (CH<sub>2</sub>), 28.5 (CH<sub>2</sub>), 25.4 (CH<sub>2</sub>), 23.6 (CH<sub>2</sub>); IR (solid, cm<sup>-1</sup>) 2937 (w), 1738 (s), 1705 (s); MS (EI): 496 (M<sup>+</sup>, 100), 382 (25), 269 (35), 218 (50); Exact Mass calculated for C<sub>24</sub>H<sub>20</sub>O<sub>6</sub>N<sub>2</sub>S<sub>2</sub> 496.07573, observed 496.07547 (EI).

#### 4.4.1 Selectivity investigation using 1:1 of Linker **13** : Amine



Benzylamine (3.76 μl, 0.034 mmol) was added to NHS ester **13** (15 mg, 0.034 mmol) stirring in DCM (3 ml). After 2 h the solvent was removed *in vacuo*. Purification by column chromatography (40% EtOAc in petrol) yielded amide **21** as a yellow solid (7.5 mg, 52%) and diaddition product **22** as a yellow oil (4.5 mg, 29%). Acid **12** was also recovered as a yellow powder (2.2 mg, 19%) and the data matched that previously obtained.

#### *N*-benzyl-4-(3,4-dibromo-2,5-dioxo-2,5-dihydro-1H-pyrrol-1-yl)butanamide (**21**)

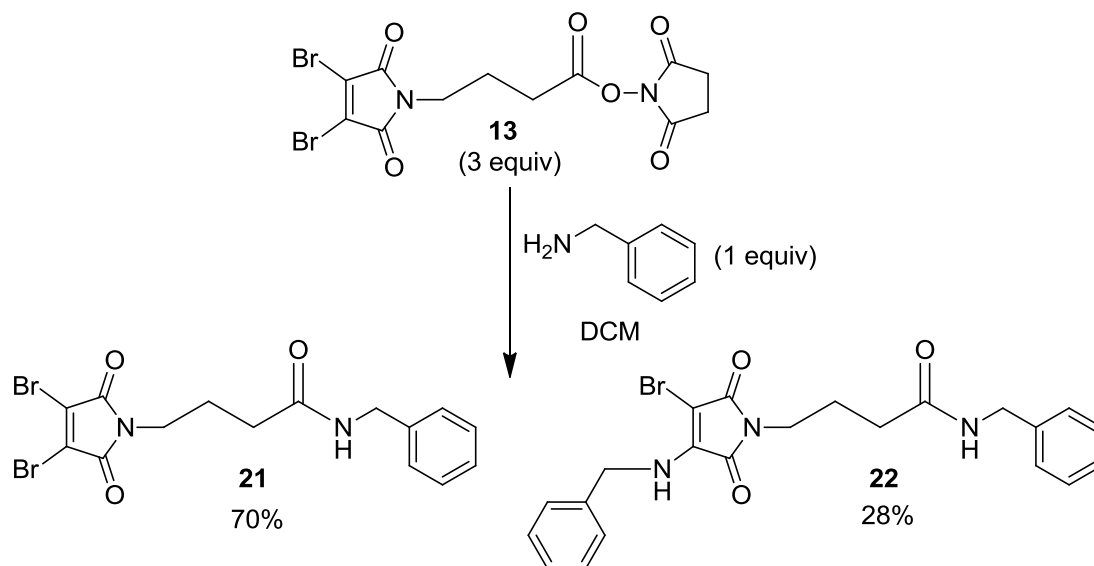
m.p. 104 – 105 °C; <sup>1</sup>H NMR (500 MHz, CDCl<sub>3</sub>) δ 7.38-7.27 (m, 5H, Ar-H), 5.86 (s, 1H, NHCH<sub>2</sub>), 4.42 (d, 2H, *J* = 5.7, NHCH<sub>2</sub>), 3.69 (t, 2H, *J* = 7.2, NCH<sub>2</sub>), 2.22 (t, 2H, *J* =

7.2,  $\text{CH}_2\text{CO}$ ), 2.00 (quin, 2H,  $J = 7.2$ ,  $\text{NCH}_2\text{CH}_2$ );  $^{13}\text{C}$  NMR (125 MHz,  $\text{CDCl}_3$ )  $\delta$  207.1 (C), 164.0 (C), 138.2 (C), 129.7 (C), 128.9 (CH), 128.0 (CH), 127.7 (CH), 43.9 ( $\text{CH}_2$ ), 39.2 ( $\text{CH}_2$ ), 31.0 ( $\text{CH}_2$ ), 25.7 ( $\text{CH}_2$ ); IR (solid,  $\text{cm}^{-1}$ ) 2929 (m), 1727 (m); MS (EI) 432 ( $^{81,81}\text{M}^+$ , 20), 430 ( $^{81,79}\text{M}^+$ , 40), 428 ( $^{79,79}\text{M}^+$ , 20), 324 (35), 268 (30), 149 (25), 106 (100); Exact Mass calculated for  $\text{C}_{15}\text{H}_{14}\text{N}_2\text{O}_3^{79}\text{Br}_2$  427.93656, observed 427.93672 (EI).

***N*-benzyl-4-(3-(benzylamino)-4-bromo-2,5-dioxo-2,5-dihydro-1H-pyrrol-1-yl)butanamide (22)**

$^1\text{H}$  NMR (500 MHz,  $\text{CDCl}_3$ )  $\delta$  7.40-7.25 (m, 10H, Ar-H), 6.16 (s, 1H,  $\text{NHCH}_2$ ), 5.63 (s, 1H,  $\text{NHCH}_2$ ), 4.84 (d, 2H,  $J = 6.4$ ,  $\text{NHCH}_2$ ), 4.43 (d, 2H,  $J = 5.7$ ,  $\text{NHCH}_2$ ), 3.57 (t, 2H,  $J = 7.2$ ,  $\text{NCH}_2$ ), 2.22 (t, 2H,  $J = 7.2$ ,  $\text{CH}_2\text{CO}$ ), 2.00 (quin, 2H,  $J = 7.2$ ,  $\text{NCH}_2\text{CH}_2$ );  $^{13}\text{C}$  NMR (125 MHz,  $\text{CDCl}_3$ )  $\delta$  207.2 (C), 164.0 (C), 138.2 (C), 136.9 (C), 131.0 (C), 129.2 (CH), 128.8 (CH), 128.4 (CH), 128.0 (CH), 127.8 (CH), 127.6 (CH), 118.4 (C), 47.1 ( $\text{CH}_2$ ), 43.7 ( $\text{CH}_2$ ), 38.0 ( $\text{CH}_2$ ), 29.8 ( $\text{CH}_2$ ), 25.2 ( $\text{CH}_2$ ); IR (solid,  $\text{cm}^{-1}$ ) 2928 (m), 1719 (m), 1657 (m); MS (ES+) 481 ( $[\text{M}+\text{Na}]^+$ , 20), 478 ( $[\text{M}+\text{Na}]^+$ , 100); Exact Mass calculated for  $\text{C}_{22}\text{H}_{22}\text{N}_3\text{O}_3^{79}\text{BrNa}$  478.0742, observed 478.0753 (ES+).

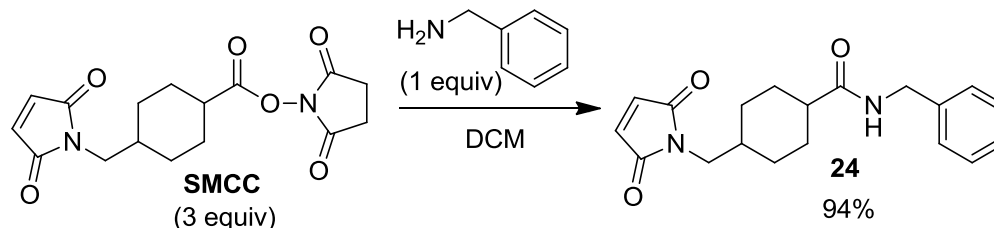
**4.4.2 Selectivity investigation using 3:1 of Linker 13 : Amine**



Benzylamine (1.67  $\mu\text{l}$ , 0.015 mmol) was added to NHS ester **13** (20 mg, 0.046 mmol) stirring in DCM (5 ml). After 3 h the solvent was removed *in vacuo*. Purification by column chromatography (40% EtOAc in petrol) yielded amide **21** as a yellow solid (4.5

mg, 70%) and diaddition product **22** as a yellow oil (1.9 mg, 28%). Data for compounds **21** and **22** match that given above.

#### 4.4.3 Selectivity investigation using 3:1 of SMCC : Amine

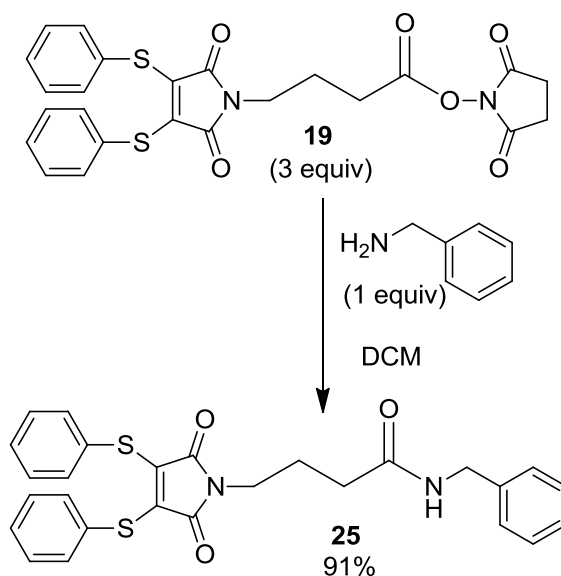


Benzylamine (1.63  $\mu$ l, 0.015 mmol) was added to succinimidyl-4-(N-maleimidomethyl)cyclohexane-1-carboxylate (SMCC) (15 mg, 0.045 mmol) stirring in DCM (5 ml). After 1 h the reaction was stopped and the solvent removed *in vacuo*. Purification by column chromatography (40% EtOAc in petrol) yielded a single product, amide **24** as a white solid (4.6 mg, 94%).

#### *N*-benzyl-3-((2,5-dioxo-2,5-dihydro-1H-pyrrol-1-yl)methyl)cyclohexanecarboxamide (**24**)

m.p. 187 – 188 °C; <sup>1</sup>H NMR (600 MHz, CDCl<sub>3</sub>)  $\delta$  7.33-7.23 (m, 5H, Ar-H), 6.68 (s, 2H, CH=CH), 5.77 (s, 1H, NHCH<sub>2</sub>), 4.41 (m, 2H, NHCH<sub>2</sub>), 3.36 (d, 2H, *J* = 7.2, NCH<sub>2</sub>), 2.01 (m, 1H, COCH), 1.91 (m, 2H, CHCH<sub>2</sub>), 1.70 (m, 2H, CHCH<sub>2</sub>), 1.47 (m, 2H, CHCH<sub>2</sub>), 1.25 (m, 1H, NCH<sub>2</sub>CH), 1.01 (m, 2H, CHCH<sub>2</sub>); <sup>13</sup>C NMR (125 MHz, CDCl<sub>3</sub>)  $\delta$  175.4 (C), 171.3 (C), 138.5 (C), 134.1 (CH), 129.0 (CH), 127.8 (CH), 127.6 (CH), 45.3 (CH<sub>2</sub>), 43.6 (CH<sub>2</sub>), 43.4 (CH), 36.5 (CH), 29.9 (CH<sub>2</sub>), 29.0 (CH<sub>2</sub>); IR (solid, cm<sup>-1</sup>) 3302 (s), 2929 (s), 1720 (s), 1621 (s), 1530 (m); MS (EI) 327 ([M+H]<sup>+</sup>, 35), 326 (M<sup>+</sup>, 100); Exact Mass calculated for C<sub>19</sub>H<sub>22</sub>N<sub>2</sub>O<sub>3</sub> 326.16249, observed 326.16212 (EI).

#### 4.4.4 Selectivity investigation using 3:1 of Linker **19** : Amine

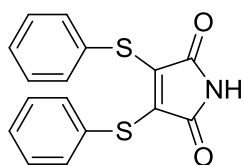


Benzylamine (1.47  $\mu\text{l}$ , 0.013 mmol) was added to NHS ester **19** (20 mg, 0.040 mmol) stirring in DCM (3 ml). After 3 h the solvent was removed *in vacuo*. Purification by column chromatography (gradient elution from  $\text{CHCl}_3$  to  $\text{CHCl}_3$  with 0.5% MeOH) yielded amide **25** exclusively, as a yellow solid (6 mg, 91%).

#### ***N*-benzyl-4-(2,5-dioxo-3,4-bis(phenylthio)-2,5-dihydro-1H-pyrrol-1-yl)butanamide (25)**

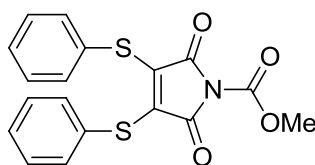
m.p. 102 – 104  $^{\circ}\text{C}$ ;  $^1\text{H}$  NMR (500 MHz,  $\text{CDCl}_3$ )  $\delta$  7.28-7.19 (m, 15H, Ar-H), 6.01 (bs, 1H,  $\text{NHCH}_2$ ), 4.42 (d, 2H,  $J = 5.7$ ,  $\text{NHCH}_2$ ), 3.57 (t, 2H,  $J = 6.8$ ,  $\text{NCH}_2$ ), 2.16 (t, 2H,  $J = 7.1$ ,  $\text{CH}_2\text{CO}$ ), 1.95 (quin, 2H,  $J = 6.8$ ,  $\text{NCH}_2\text{CH}_2$ );  $^{13}\text{C}$  NMR (125 MHz,  $\text{CDCl}_3$ )  $\delta$  171.1 (C), 167.3 (C), 138.3 (C), 136.7 (C), 132.0 (CH), 129.2 (CH), 129.1 (CH), 129.0 (C), 128.8 (CH), 128.6 (CH), 127.6 (CH), 43.8 ( $\text{CH}_2$ ), 38.2 ( $\text{CH}_2$ ), 29.8 ( $\text{CH}_2$ ), 25.0 ( $\text{CH}_2$ ); IR (solid,  $\text{cm}^{-1}$ ) 3291 (m), 2930 (m), 1703 (s), 1647 (m); MS (EI): 488 ( $\text{M}^+$ , 100), 250 (15); Exact Mass calculated for  $\text{C}_{27}\text{H}_{24}\text{O}_3\text{N}_3\text{S}_2$  488.12229, observed 488.12188 (EI).

---

**3,4-bis(phenylthio)-1H-pyrrole-2,5-dione (9)**<sup>168</sup>

To dibromomaleimide (300 mg, 1.18 mmol) and NaHCO<sub>3</sub> (595 mg, 7.08 mmol) in MeOH (20 ml), thiophenol (277  $\mu$ l, 2.71 mmol) in MeOH (2 ml) was slowly added. The reaction was stirred for 30 min at room temperature. The solvent was removed *in vacuo* and the residual material purified by column chromatography (gradient elution from 10% EtOAc in petrol to 30% EtOAc in petrol) to afford **9** as bright yellow crystals (281 mg, 76%).

m.p. 104 - 105 °C (lit. m.p. 102 – 104 °C)<sup>168</sup>; <sup>1</sup>H NMR (500 MHz, MeOD)  $\delta$  7.29-7.21 (m, 6H, Ar-H), 7.16-7.11 (m, 4H, Ar-H); <sup>13</sup>C NMR (125 MHz, MeOD)  $\delta$  169.3 (C), 137.6 (C), 132.4 (C), 130.7 (CH), 130.1 (CH), 129.1 (CH); IR (solid, cm<sup>-1</sup>) 3275 (m), 2924 (w), 1764 (m), 1715 (s); MS (EI): 315 ([M+2H]<sup>+</sup>, 10), 314 ([M+H]<sup>+</sup>, 20), 313 (M<sup>+</sup>, 100), 186 (15); Exact Mass calculated for C<sub>16</sub>H<sub>11</sub>NO<sub>2</sub>S<sub>2</sub> 313.02257, observed 313.02274 (EI).

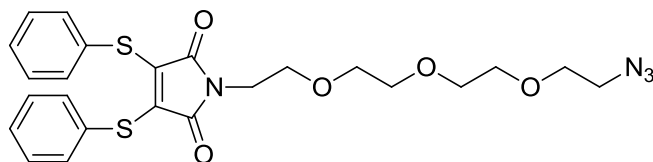
**Methyl 2,5-dioxo-3,4-bis(phenylthio)-2,5-dihydro-1H-pyrrole-1-carboxylate (27)**<sup>181</sup>

*N*-Methyl morpholine (183  $\mu$ l, 1.66 mmol) was added to a stirred solution of **9** (260 mg, 0.831 mmol) and methyl chloroformate (161  $\mu$ l, 2.08 mmol) in ethyl acetate (10 ml). The reaction mixture was left to stir for 30 min at room temperature. The mixture was then washed with water (2 x 20 ml), dried with MgSO<sub>4</sub>, filtered and concentrated *in vacuo* to yield **27** as a bright yellow powder (300 mg, 97%).

m.p. 111 – 113 °C (lit. m.p. 110 – 112 °C)<sup>181</sup>; <sup>1</sup>H NMR (500 MHz, CDCl<sub>3</sub>)  $\delta$  7.32-7.22 (m, 10H, Ar-H), 3.90 (s, 3H, NCH<sub>3</sub>); <sup>13</sup>C NMR (125 MHz, CDCl<sub>3</sub>)  $\delta$  161.8 (C), 147.8 (C), 137.2 (C), 132.4 (C), 129.5 (C), 129.3 (C), 129.1 (C), 54.4 (CH<sub>3</sub>); IR (solid, cm<sup>-1</sup>) 1805 (s), 1765 (s) 1720 (s), 1435 (m) 1322 (w); MS (ES<sup>+</sup>):372 (M<sup>+</sup>, 60), 329 (55), 271

(35), 270 (50), 269 (100); Exact Mass calculated for C<sub>18</sub>H<sub>13</sub>NO<sub>4</sub>S<sub>2</sub> 372.0364, observed 372.0377 (ES+).

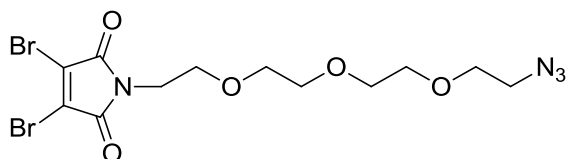
**1-(2-(2-(2-(2-azidoethoxy)ethoxy)ethoxy)ethyl)-3,4-bis(phenylthio)-1H-pyrrole-2,5-dione (28)**



11-Azido-3,6,9-trioxaundecan-1-amine (43  $\mu$ l, 0.22 mmol) was added to a stirred solution of **27** (80 mg, 0.22 mmol) in DCM (5 ml), and left to stir for 1 h at room temperature. The solvent was then removed *in vacuo* and the reaction mixture purified by column chromatography (gradient elution from 30% petrol in EtOAc to EtOAc) to yield **28** as a bright orange oil (45 mg, 78%).

<sup>1</sup>H NMR (600 MHz, CDCl<sub>3</sub>)  $\delta$  7.29-7.22 (m, 6H, Ar-H), 7.20-7.17 (m, 4H, Ar-H), 3.70 (t, 2H, *J* = 5.4, NCH<sub>2</sub>CH<sub>2</sub>O), 3.67-3.57 (m, 12H, OCH<sub>2</sub>), 3.37 (t, 2H, *J* = 5.4, CH<sub>2</sub>CH<sub>2</sub>N<sub>3</sub>); <sup>13</sup>C NMR (125 MHz, CDCl<sub>3</sub>)  $\delta$  166.9 (C), 138.6 (C), 131.6 (CH), 129.3 (CH), 128.9 (CH), 70.8 (CH<sub>2</sub>), 70.4 (CH<sub>2</sub>), 70.1 (CH<sub>2</sub>), 67.8 (CH<sub>2</sub>), 50.8 (CH<sub>2</sub>), 37.2 (CH<sub>2</sub>); IR (oil, cm<sup>-1</sup>) 2867 (w), 2098 (m), 1710 (s), 1580 (w), 1527 (w); MS (EI): 515 ([M+H]<sup>+</sup>, 20), 514 (M<sup>+</sup>, 65), 340 (100), 110 (80); Exact Mass calculated for C<sub>24</sub>H<sub>26</sub>N<sub>4</sub>O<sub>5</sub>S<sub>2</sub> 514.13391, observed 514.134269 (EI).

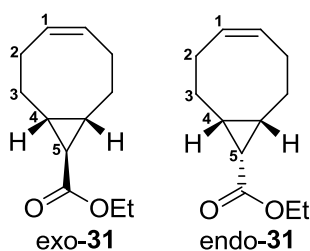
**1-(2-(2-(2-(2-azidoethoxy)ethoxy)ethoxy)ethyl)-3,4-dibromo-1H-pyrrole-2,5-dione (29)**



1-Azido-3,6,9-trioxaundecan-1-amine (63  $\mu$ l, 0.32 mmol) was added to a stirred solution of carbamate dibromomaleimide **11** (100 mg, 0.32 mmol) in DCM (5 ml). The mixture was stirred at room temperature for 3 h. After this time the solvent was removed *in vacuo* and the mixture purified by column chromatography (30% EtOAc in petrol) to yield **29** as a pale yellow oil (113 mg, 78%).

$^1\text{H}$  NMR (500 MHz,  $\text{CDCl}_3$ )  $\delta$  3.79 (t, 2H,  $J = 5.6$ ,  $\text{NCH}_2$ ), 3.65-3.58 (m, 12H, 6 x  $\text{OCH}_2$ ), 3.36 (t, 2H,  $J = 5.6$ ,  $\text{CH}_2\text{N}_3$ );  $^{13}\text{C}$  NMR (125 MHz,  $\text{CDCl}_3$ )  $\delta$  163.8 (C), 129.5 (C), 70.7 ( $\text{CH}_2$ ), 70.1 ( $\text{CH}_2$ ), 67.6 ( $\text{CH}_2$ ), 50.8 ( $\text{CH}_2$ ), 39.0 ( $\text{CH}_2$ ); IR (oil,  $\text{cm}^{-1}$ ) 3492 (br), 2867 (m), 2097 (s), 1786 (s), 1720 (s); MS (EI): 476 ( $[\text{Br}^{81,81}\text{M}+\text{NH}_4]^+$ , 50), 474 ( $[\text{Br}^{81,79}\text{M}+\text{NH}_4]^+$ , 100), 472 ( $[\text{Br}^{79,79}\text{M}+\text{NH}_4]^+$ , 50), 282 (10); Exact Mass calculated for  $[\text{C}_{12}\text{H}_{16}^{81,79}\text{Br}_2\text{N}_4\text{O}_5+\text{NH}_4]$  473.9806, observed 473.9799 (EI).

### Exo- and endo-ethyl bicyclo[6.1.0]non-4-ene-9-carboxylate (**31**)<sup>139</sup>



To a solution of 1,5-cyclooctadiene (19.6 ml, 160 mmol) and  $\text{Rh}_2(\text{OAc})_4$  (190 mg, 0.86 mmol) in DCM (10 ml) was added dropwise a solution of ethyl diazoacetate (2.10 ml, 20 mmol) in DCM (10 ml) over 3 h. The solution was stirred for 40 h at room temperature. The solvent was then removed *in vacuo* and the excess cyclooctadiene removed by a short plug of silica with petrol. Separation of the diastereomers was achieved by column chromatography (gradient elution from 1%  $\text{Et}_2\text{O}$  in petrol to 5%  $\text{Et}_2\text{O}$  in petrol) to yield **exo-31** (1.13 g, 29%) and **endo-31** (2.10 g, 54%) as colourless oils.

#### Exo-31

$^1\text{H}$  NMR (500 MHz,  $\text{CDCl}_3$ )  $\delta$  5.64 (m, 2H, H-1), 4.13 (q, 2H,  $J = 7.1$ ,  $\text{OCH}_2\text{CH}_3$ ), 2.28 (m, 2H,  $\text{HH-2}$ ), 2.18 (m, 2H,  $\text{HH-2}$ ), 2.10 (m, 2H,  $\text{HH-3}$ ), 1.56 (m, 2H,  $\text{HH-3}$ ), 1.48 (m, 2H, H-4), 1.25 (t, 3H,  $J = 7.1$ ,  $\text{CH}_2\text{CH}_3$ ), 1.19 (t, 1H,  $J = 4.7$ , H-5);  $^{13}\text{C}$  NMR (125 MHz,  $\text{CDCl}_3$ )  $\delta$  174.5 (C), 130.0 (C), 60.3 ( $\text{CH}_2$ ), 28.3 ( $\text{CH}_2$ ), 28.0 (CH), 27.8 (CH), 26.7 ( $\text{CH}_2$ ), 14.4 ( $\text{CH}_3$ ); IR (oil,  $\text{cm}^{-1}$ ) 2935 (w), 1719 (s); MS (EI): 194 ( $\text{M}^+$ , 15), 121 (95), 79 (90), 67 (100); Exact Mass calculated for  $\text{C}_{12}\text{H}_{18}\text{O}_2$  194.13013, observed 194.129448 (EI).

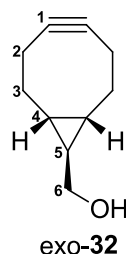
#### Endo-31

$^1\text{H}$  NMR (500 MHz,  $\text{CDCl}_3$ )  $\delta$  5.58 (m, 2H, H-1), 4.11 (q, 2H,  $J = 7.1$ ,  $\text{OCH}_2\text{CH}_3$ ), 2.46 (m, 2H,  $\text{HH-2}$ ), 2.16 (m, 2H,  $\text{HH-2}$ ), 2.05 (m, 2H,  $\text{HH-3}$ ), 1.79 (m, 2H,  $\text{HH-3}$ ), 1.68 (t,

---

1H,  $J = 8.7$ , H-5), 1.37 (m, 2H, H-4), 1.25 (t, 3H,  $J = 7.1$ ,  $\text{CH}_2\text{CH}_3$ );  $^{13}\text{C}$  NMR (125 MHz,  $\text{CDCl}_3$ )  $\delta$  172.3 (C), 130.0 (C), 60.3 ( $\text{CH}_2$ ), 27.0 ( $\text{CH}_2$ ), 24.2 (CH), 22.7 (CH), 21.2 ( $\text{CH}_2$ ), 14.4 ( $\text{CH}_3$ ).

**Exo-bicyclo[6.1.0]non-4-yn-9-ylmethanol (32)**<sup>139</sup>



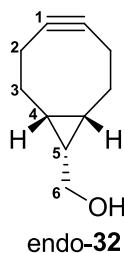
To a suspension of  $\text{LiAlH}_4$  (78 mg, 2.06 mmol) in  $\text{Et}_2\text{O}$  (8 ml) was added dropwise at 0 °C a solution of **exo-31** (400 mg, 2.06 mmol) in  $\text{Et}_2\text{O}$  (8 ml). The suspension was stirred at room temperature for 15 min, and then cooled down to 0 °C. Water was carefully added until the grey suspension turned white. The mixture was then washed with  $\text{Et}_2\text{O}$  (150 ml) and dried with  $\text{Na}_2\text{SO}_4$ . The filtrate was concentrated *in vacuo*.

Without further purification the alcohol was dissolved in DCM (15 ml). At 0 °C a solution of bromine (146  $\mu\text{l}$ , 2.83 mmol) in DCM (2 ml) was added dropwise. The reaction mixture was stirred for 15 min at room temperature and then quenched with 10%  $\text{Na}_2\text{S}_2\text{O}_3$  solution (5 ml), extracted with DCM (2 x 20 ml) and dried with  $\text{Na}_2\text{SO}_4$ . The organic layers were concentrated *in vacuo* to afford the dibromide (639 mg, quantitative).

Without further purification the dibromide (570 mg, 1.83 mmol) was dissolved in dry THF (20 ml). A solution of  $\text{KO}^t\text{Bu}$  (7.3 ml, 1M in THF) was added dropwise at 0°C. The solution was heated at reflux for 3 h. After cooling down to room temperature the mixture was quenched with saturated  $\text{NH}_4\text{Cl}$  solution (20 ml) and extracted with DCM (3 x 20 ml). The organic layers were combined, dried with  $\text{Na}_2\text{SO}_4$  and concentrated *in vacuo*. The residue was purified by column chromatography (gradient elution from 10%  $\text{EtOAc}$  in petrol to 80%  $\text{EtOAc}$  in petrol) to yield **exo-32** as a white solid (130 mg, 47%).

m.p. 63 – 65 °C;  $^1\text{H}$  NMR (500 MHz,  $\text{CDCl}_3$ )  $\delta$  3.50 (d, 2H,  $J = 6.4$ ,  $\text{H}_2$ -6), 2.36 (m, 2H,  $\text{HH}$ -2), 2.22 (m, 2H,  $\text{HH}$ -2), 2.11 (m, 2H,  $\text{HH}$ -3), 1.89 (s, 1H,  $\text{OH}$ ), 1.34 (m, 2H,  $\text{HH}$ -3), 0.66 (m, 3H, H-4, H-5);  $^{13}\text{C}$  NMR (125 MHz,  $\text{CDCl}_3$ )  $\delta$  98.9 (C), 66.4 ( $\text{CH}_2$ ), 29.7 ( $\text{CH}_2$ ), 27.1 (CH), 22.6 (CH), 21.8 ( $\text{CH}_2$ ); IR (solid,  $\text{cm}^{-1}$ ) 3323 (w, br), 2994 (m), 2915 (m); MS: Molecular ion not found.

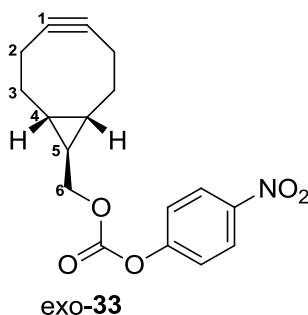
**Endo-bicyclo[6.1.0]non-4-yn-9-ylmethanol (32)**<sup>139</sup>



The same procedure used to generate **exo-32** was used for **endo-32**, yielding **endo-32** as a white solid (110 mg, 58%).

m.p. 63 – 65 °C;  $^1\text{H}$  NMR (500 MHz,  $\text{CDCl}_3$ )  $\delta$  3.69 (d, 2H,  $J = 7.8$ ,  $\text{H}_2$ -6), 2.21 (m, 6H,  $\text{HH}$ -2,  $\text{HH}$ -3), 1.56 (m, 3H,  $\text{HH}$ -3,  $\text{OH}$ ), 1.31 (m, 1H, H-5), 0.92 (m, 2H, H-4);  $^{13}\text{C}$  NMR (125 MHz,  $\text{CDCl}_3$ )  $\delta$  99.0 (C), 60.2 ( $\text{CH}_2$ ), 29.0 (CH), 21.6 ( $\text{CH}_2$ ), 21.4 (CH), 20.0 ( $\text{CH}_2$ ); IR (solid,  $\text{cm}^{-1}$ ) 3323 (w, br), 2994 (m), 2915 (m); MS: Molecular ion not found.

**Exo-bicyclo[6.1.0]non-4-yn-9-ylmethyl(4-nitrophenyl)carbonate (33)**<sup>139</sup>

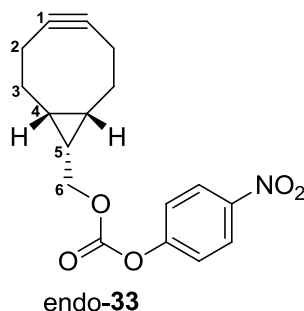


To a solution of **exo-32** (100 mg, 0.67 mmol) in DCM (15 ml) was added pyridine (135  $\mu\text{l}$ , 1.66 mmol) and 4-nitrophenyl chloroformate (168 mg, 0.83 mmol). The mixture was stirred for 30 min at room temperature and then quenched with saturated  $\text{NH}_4\text{Cl}$  solution (10 ml) and extracted with DCM (2 x 20 ml). The organic layers were combined, dried with  $\text{Na}_2\text{SO}_4$  and concentrated *in vacuo*. The residue was purified by

column chromatography (10% EtOAc in petrol) to afford **exo-33** as a white solid (140 mg, 67%).

m.p. 69 - 72 °C;  $^1\text{H}$  NMR (500 MHz,  $\text{CDCl}_3$ )  $\delta$  8.23 (d, 2H,  $J = 8.6$ , Ar-H), 7.37 (d, 2H,  $J = 8.6$ , Ar-H), 4.18 (d, 2H,  $J = 6.9$ ,  $\text{H}_2$ -6), 2.40 (m, 2H,  $\text{HH}$ -2), 2.24 (m, 2H,  $\text{HH}$ -2), 2.13 (m, 2H,  $\text{HH}$ -3), 1.22 (m, 2H,  $\text{HH}$ -3), 0.82 (m, 3H, H-4, H-5);  $^{13}\text{C}$  NMR (125 MHz,  $\text{CDCl}_3$ )  $\delta$  155.6 (C), 152.6 (C), 145.2 (C), 125.3 (CH), 122.0 (CH), 98.7 (C), 74.0 ( $\text{CH}_2$ ), 33.0 (CH), 23.6 ( $\text{CH}_2$ ), 22.8 (CH), 21.4 ( $\text{CH}_2$ ); IR (solid,  $\text{cm}^{-1}$ ) 2923 (w), 1747 (m), 1617 (w), 1595 (w), 1518 (m); MS (CI): 316 ( $[\text{M}+\text{H}]^+$ , 10), 272 (15), 214 (55), 140 (60), 133 (100), 91 (20), 85 (25); Exact Mass calculated for  $\text{C}_{17}\text{H}_{17}\text{NO}_5$  316.11849, observed 316.11855 (CI).

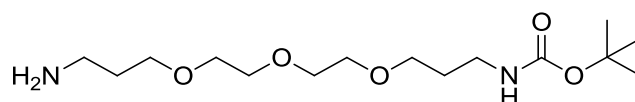
**Endo-bicyclo[6.1.0]non-4-yn-9-ylmethyl(4-nitrophenyl)carbonate (33)<sup>139</sup>**



The same procedure used to generate **exo-33** was used for **endo-33**, yielding **endo-33** as a white solid (100 mg, 72%).

$^1\text{H}$  NMR (500 MHz,  $\text{CDCl}_3$ )  $\delta$  8.26 (d, 2H,  $J = 8.2$ , Ar-H), 7.39 (d, 2H,  $J = 8.2$ , Ar-H), 4.39 (d, 2H,  $J = 8.3$ ,  $\text{H}_2$ -6), 2.23 (m, 6H,  $\text{HH}$ -2,  $\text{HH}$ -3), 1.58 (m, 2H,  $\text{HH}$ -3), 1.50 (m, 1H, H-5), 1.10 (m, 2H, H-4);  $^{13}\text{C}$  NMR (125 MHz,  $\text{CDCl}_3$ )  $\delta$  155.7 (C), 152.6 (C), 145.4 (C), 125.4 (CH), 121.8 (CH), 98.8 (C), 68.1 ( $\text{CH}_2$ ), 29.1 (CH), 21.4 ( $\text{CH}_2$ ), 20.6 ( $\text{CH}_2$ ), 17.3 (CH); IR (solid,  $\text{cm}^{-1}$ ) 2923 (w), 1747 (m), 1617 (w), 1595 (w), 1518 (m); MS (CI): 316 ( $[\text{M}+\text{H}]^+$ , 10), 272 (15), 214 (55), 140 (60), 133 (100), 91 (20), 85 (25); Exact Mass calculated for  $\text{C}_{17}\text{H}_{17}\text{NO}_5$  316.11849, observed 316.11855 (CI).

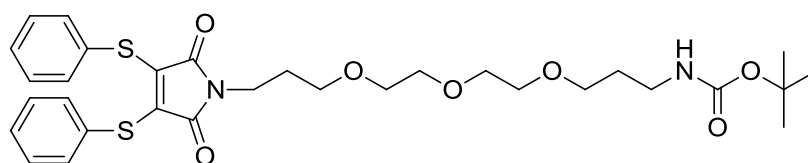
***tert*-butyl (3-(2-(2-(3-aminopropoxy)ethoxy)ethoxy)propyl)carbamate (38)**



4,7,10-trioxa-1,3-tridecanediamine (6.7 ml, 30.3 mmol) was dissolved in 1,4-dioxane (12 ml) and  $\text{Boc}_2\text{O}$  (1.10 g, 5.86 mmol) in 1,4-dioxane (7.5 ml) was added dropwise at room temperature over 90 min. The reaction mixture was then stirred for a further 90 min. The solvent was removed *in vacuo* and the resulting yellowish oil was dissolved in water, extracted with DCM (4 x 25 ml) and the combined organic phases dried with  $\text{MgSO}_4$ . The solvent was removed *in vacuo* to yield **38** as a yellow oil (1.65 g, 93%).

$^1\text{H}$  NMR (500 MHz,  $\text{CDCl}_3$ )  $\delta$  5.11 (s, 1H, NH), 3.64-3.53 (m, 12H,  $\text{OCH}_2$ ), 3.23 (m, 2H,  $\text{NHCH}_2$ ), 2.79 (t, 2H,  $J = 6.7$ ,  $\text{NH}_2\text{CH}_2$ ), 1.75 (m, 4H,  $\text{OCH}_2\text{CH}_2\text{CH}_2\text{O}$ ), 1.43 (s, 9H,  $\text{C}(\text{CH}_3)_3$ );  $^{13}\text{C}$  NMR (125 MHz,  $\text{CDCl}_3$ )  $\delta$  155.8 (C), 78.40 (C), 70.32 ( $\text{CH}_2$ ), 70.28 ( $\text{CH}_2$ ), 69.93 ( $\text{CH}_2$ ), 69.90 ( $\text{CH}_2$ ), 69.15 ( $\text{CH}_2$ ), 69.10 ( $\text{CH}_2$ ), 39.31 ( $\text{CH}_2$ ), 38.14 ( $\text{CH}_2$ ), 33.05 ( $\text{CH}_2$ ), 29.36 ( $\text{CH}_2$ ), 28.17 ( $\text{CH}_3$ ); IR (oil,  $\text{cm}^{-1}$ ) 3360 (w, br), 2930 (m), 2870 (m), 1704 (s); MS (EI): 320 ( $\text{M}^+$ , 100), 247 (80), 177 (60), 164 (40), 148 (50), 102 (40), 89 (50), 75 (35), 56 (30), 43 (50); Exact Mass calculated for  $\text{C}_{15}\text{H}_{32}\text{N}_2\text{O}_5$  320.23112, observed 320.24556 (EI).

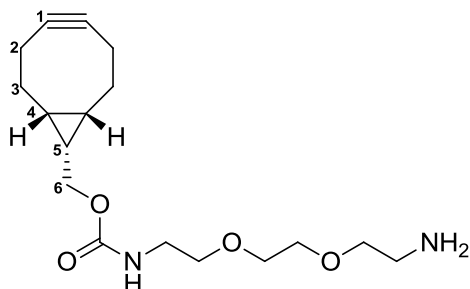
***tert*-butyl(3-(2-(2-(3-(2,5-dioxo-3,4-bis(phenylthio)-2,5-dihydro-1H-pyrrol-1-yl)propoxy)ethoxy)ethoxy)propyl)carbamate (39)**



Monoprotected diamine **38** (50 mg, 0.164 mmol) and triethylamine (23  $\mu\text{l}$ , 0.164 mmol) were added to a stirred solution of dithiophenol carbamate maleimide **27** (67 mg, 0.181 mmol) in chloroform (5 ml). After 30 min silica (100 mg) was added and the reaction mixture was stirred for a further 4 h. After filtration, the solvent was removed *in vacuo* and the resulting residue was purified by column chromatography (gradient elution from 30% EtOAc in petrol to 50% EtOAc in petrol) to yield **39** as an orange oil (71 mg, 70%).

$^1\text{H}$  NMR (500 MHz,  $\text{CDCl}_3$ )  $\delta$  7.29-7.23 (m, 6H, Ar-H), 7.21-7.19 (m, 4H, Ar-H), 3.63-3.56 (m, 8H,  $\text{OCH}_2$ ), 3.53 (m, 4H,  $\text{OCH}_2$ ), 3.45 (t, 2H,  $J = 6.0$ ,  $\text{NHCH}_2\text{CH}_2\text{CH}_2\text{O}$ ), 3.20 (m, 2H,  $\text{NH}_2\text{CH}_2$ ), 1.85 (pent., 2H,  $J = 6.2$ ,  $\text{OCH}_2\text{CH}_2\text{CH}_2\text{O}$ ), 1.75 (pent., 2H,  $J = 6.2$ ,  $\text{OCH}_2\text{CH}_2\text{CH}_2\text{O}$ ), 1.43 (s, 9H,  $\text{C}(\text{CH}_3)_3$ );  $^{13}\text{C}$  NMR (125 MHz,  $\text{CDCl}_3$ )  $\delta$  166.9 (C), 156.1 (C), 135.8 (C), 132.0 (C), 129.0 (C), 128.4 (C), 78.40 (C), 70.32 ( $\text{CH}_2$ ), 70.28 ( $\text{CH}_2$ ), 69.93 ( $\text{CH}_2$ ), 69.90 ( $\text{CH}_2$ ), 69.15 ( $\text{CH}_2$ ), 69.10 ( $\text{CH}_2$ ), 39.31 ( $\text{CH}_2$ ), 38.14 ( $\text{CH}_2$ ), 33.05 ( $\text{CH}_2$ ), 29.36 ( $\text{CH}_2$ ), 28.17 ( $\text{CH}_3$ ); IR (oil,  $\text{cm}^{-1}$ ) 3348 (w, br), 2927 (m), 2868 (m), 1704 (s), 1517 (w), 1476 (w), 1441 (w); MS (EI): 617 ( $[\text{M}+\text{H}]^+$ , 25), 616 ( $\text{M}^+$ , 80), 442 (60), 160 (40); Exact Mass calculated for  $\text{C}_{31}\text{H}_{40}\text{N}_2\text{O}_7\text{S}_2$  616.78850, observed 616.22809 (EI).

**Endo-bicyclo[6.1.0]non-4-yn-9-ylmethyl (2-(2-(2-aminoethoxy)ethoxy)ethyl)carbamate (**41**)<sup>139</sup>**

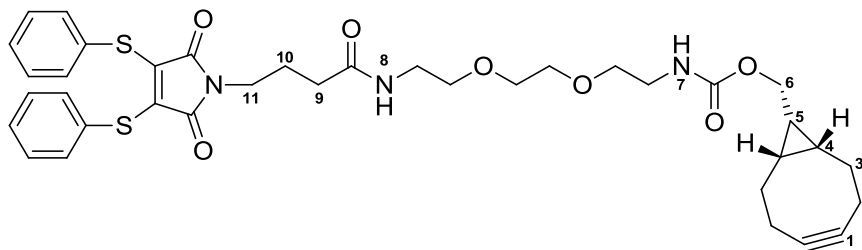


To a solution of activated *para*-nitrophenol alkyne **endo-33** (14 mg, 0.044 mmol) in DMF (1 ml) was added 1,8-diamino-3,6-dioxaoctane (38  $\mu\text{l}$ , 0.226 mmol) and triethylamine (19  $\mu\text{l}$ , 0.133 mmol). The reaction mixture was stirred at room temperature for 15 min. The mixture was concentrated *in vacuo*, taken up in DCM (20 ml) and extracted with 1 M NaOH (2 x 2 ml), followed by water (2 ml). The combined aqueous phases were extracted once more with DCM (10 ml) and the combined organic layers were dried with  $\text{MgSO}_4$ , filtered and concentrated *in vacuo*. The product **41** was isolated without further purification as a slightly yellow oil (14 mg, 99%).

$^1\text{H}$  NMR (600 MHz,  $\text{CDCl}_3$ )  $\delta$  5.37 (s, 1H, NH), 4.15 (m, 2H,  $\text{H}_2$ -6), 3.62-3.52 (m, 8H, 4 x  $\text{OCH}_2$ ), 3.37 (m, 2H,  $\text{NHCH}_2$ ), 2.89 (m, 2H,  $\text{CH}_2\text{NH}_2$ ), 2.30-2.19 (m, 6H, *HH*-2, *HH*-3), 1.98 (s, 2H,  $\text{NH}_2$ ), 1.58 (m, 2H, *HH*-3), 1.35 (m, 1H, H-5), 0.94 (m, 2H, H-4);  $^{13}\text{C}$  NMR (150 MHz,  $\text{CDCl}_3$ )  $\delta$  156.9 (C), 98.9 (C), 73.2 ( $\text{CH}_2$ ), 70.4 ( $\text{CH}_2$ ), 70.3 ( $\text{CH}_2$ ), 70.2 ( $\text{CH}_2$ ), 62.8 ( $\text{CH}_2$ ), 41.7 ( $\text{CH}_2$ ), 40.9 ( $\text{CH}_2$ ), 29.2 ( $\text{CH}_2$ ), 21.5 ( $\text{CH}_2$ ), 20.2 (CH), 17.9 (CH); IR (oil,  $\text{cm}^{-1}$ ) 2915 (m), 1707 (m); MS (EI): 325 ( $[\text{M}+\text{H}]^+$ , 70), 199 (30); Exact Mass calculated for  $\text{C}_{17}\text{H}_{29}\text{N}_2\text{O}_4$  325.2122 observed 325.2124 (EI).

---

**Endo-bicyclo[6.1.0]non-4-yn-9-ylmethyl (2-(2-(2-(4-(2,5-dioxo-3,4-bis(phenylthio)-2,5-dihydro-1H-pyrrol-1-yl)butanamido)ethoxy)ethoxy)ethyl)carbamate (42)**



**Synthesis of 42 via NHS ester linker**

To a solution of monoamine strained alkyne **41** (14 mg, 0.043 mmol) in DMF (0.5 ml) was added NHS ester **19** (21 mg, 0.043 mmol) in DMF (0.5 ml). The mixture was left to stir overnight at room temperature. The solvent was removed *in vacuo* and the residue purified by column chromatography (gradient elution DCM to DCM with 10% MeOH) to yield **42** as a dark yellow oil (22 mg, 73%).

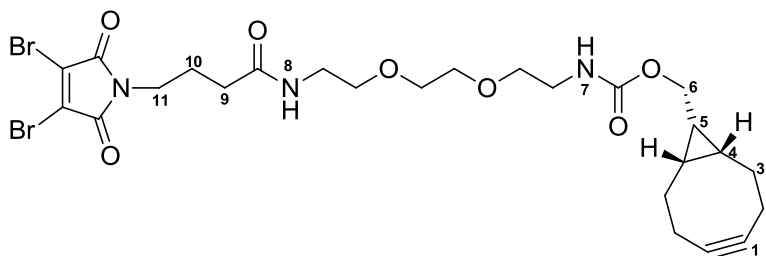
**Synthesis of 42 via HBTU coupling**

Dithiophenol maleimide carboxylic acid **18** (62 mg, 0.154 mmol), HOBt (10 mg, 0.077 mmol) and HBTU (58 mg, 0.154 mmol) were stirred in DMF (4 ml) under argon. DIPEA (40  $\mu$ l, 0.231 mmol) in DMF (1 ml) was then added, and the reaction stirred at room temperature for 15 min. Monoamine strained alkyne **41** (50 mg, 0.154 mmol) in DMF (1 ml) was then added. The reaction mixture was left to stir overnight and then DMF removed *in vacuo*. The mixture was redissolved in DCM and washed with saturated LiCl (10 ml), 15%  $K_2CO_3$  (10 ml), 15% citric acid (10 ml) and water (10 ml). The organic layer was then dried with  $MgSO_4$ . Purification by column chromatography (10% DCM in EtOAc to EtOAc) yielded **42** as a dark yellow oil (87 mg, 80%).

$^1H$  NMR (600 MHz,  $CDCl_3$ )  $\delta$  7.29-7.23 (m, 6H, Ar-H), 7.18 (m, 4H, Ar-H), 6.16 (s, 1H, NH-8), 5.21 (s, 1H, NH-7), 4.14 (m, 2H,  $H_2$ -6), 3.60-3.53 (m, 10H, 4 x  $OCH_2$ ,  $H_2$ -11), 3.45 (m, 2H,  $CH_2NH$ -7), 3.38 (m, 2H,  $CH_2NH$ -8), 2.30-2.15 (m, 8H,  $HH$ -2,  $HH$ -3,  $H_2$ -9), 1.92 (pent., 2H,  $J = 7.2$ ,  $H_2$ -10), 1.56 (m, 2H,  $HH$ -3), 1.33 (m, 1H, H-5), 0.95 (m, 2H, H-4);  $^{13}C$  NMR (150 MHz,  $CDCl_3$ )  $\delta$  172.1 (C), 167.3 (C), 156.9 (C), 135.6 (C), 132.4 (C), 131.9 (CH), 129.1 (CH), 128.9 (CH), 98.9 (C), 70.3 ( $CH_2$ ), 69.9 ( $CH_2$ ), 62.9 ( $CH_2$ ), 40.9 ( $CH_2$ ), 39.4 ( $CH_2$ ), 38.9 ( $CH_2$ ), 38.3 ( $CH_2$ ), 32.0 ( $CH_2$ ), 29.1 ( $CH_2$ ), 27.7 ( $CH_2$ ), 24.8 ( $CH_2$ ), 21.6 ( $CH_2$ ), 20.2 (CH), 17.9 (CH); IR (oil,  $cm^{-1}$ ) 2927 (s), 1701 (s),

1553 (m); MS (EI): 706 ( $[M+H]^+$ , 85), 616 (20), 556 (15), 530 (75); Exact Mass calculated for  $[C_{34}H_{43}N_3O_7S_2+H]$  706.2615 observed 706.2615 (EI).

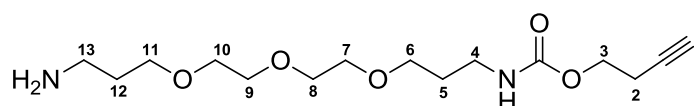
**Endo-bicyclo[6.1.0]non-4-yn-9-ylmethyl (2-(2-(2-(4-(3,4-dibromo-2,5-dioxo-2,5-dihydro-1H-pyrrol-1-yl)butanamido)ethoxy)ethoxy)ethyl)carbamate (43)**



To a solution of monoamine strained alkyne **41** (25 mg, 0.077 mmol) in DMF (1 ml) was added dibromomaleimide-NHS ester **13** (51 mg, 0.116 mmol) in DMF (1 ml). The mixture was left to stir overnight. The solvent was removed *in vacuo* and purified by column chromatography (gradient elution from DCM to DCM with 10% MeOH) to yield **43** as a yellow oil (20 mg, 41%).

$^1H$  NMR (600 MHz,  $CDCl_3$ )  $\delta$  6.13 (s, 1H, NH-8), 5.19 (s, 1H, NH-7), 4.14 (m, 2H,  $H_2$ -6), 3.67-3.55 (m, 10H, 4 x  $OCH_2$ ,  $H_2$ -11), 3.44 (m, 2H,  $CH_2NH$ -7), 3.39 (m, 2H,  $CH_2NH$ -8), 2.31-2.20 (m, 8H,  $HH$ -2,  $HH$ -3,  $H_2$ -9), 1.97 (pent., 2H,  $J = 7.2$ ,  $H_2$ -10), 1.58 (m, 2H,  $HH$ -3), 1.34 (m, 1H, H-5), 0.94 (m, 2H, H-4);  $^{13}C$  NMR (150 MHz,  $CDCl_3$ )  $\delta$  171.6 (C), 164.2 (C), 156.8 (C), 129.5 (C), 98.9 (C), 70.4 ( $CH_2$ ), 70.2 ( $CH_2$ ), 70.0 ( $CH_2$ ), 63.0 ( $CH_2$ ), 40.9 ( $CH_2$ ), 39.2 ( $CH_2$ ), 33.5 ( $CH_2$ ), 29.8 ( $CH_2$ ), 29.2 ( $CH_2$ ), 24.6 ( $CH_2$ ), 21.6 ( $CH_2$ ), 20.2 (CH), 17.9 (CH); IR (oil,  $cm^{-1}$ ) 3433 (w, br), 2955 (m), 2912 (m), 1721 (m), 1662 (m); MS (EI): 650 ( $[^{81,81}M+H]^+$ , 50), 648 ( $[^{81,79}M+H]^+$ , 100), 646 ( $[^{79,79}M+H]^+$ , 50), 493 (20), 472 (50), 304 (40), 234 (50), 199 (60); Exact Mass calculated for  $[C_{25}H_{33}^{81,79}Br_2N_3O_7+H]$  648.0740 observed 648.0738 (EI).

**But-3-yn-1-yl (3-(2-(2-(3-aminopropoxy)ethoxy)ethoxy)propyl)carbamate (45)**

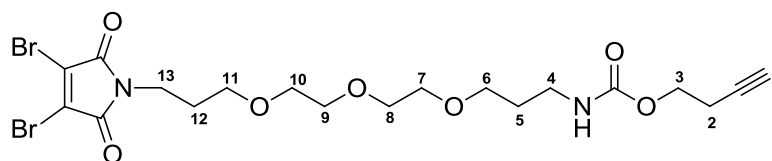


A mixture of 4,7,10-trioxa-1,3-tridecanediamine (946  $\mu$ l, 4.40 mmol) and triethylamine (135  $\mu$ l, 0.97 mmol) was cooled to  $-15$   $^{\circ}C$ . 3-Butynyl-1-yl chloroformate (50  $\mu$ l, 0.44 mmol) in DMF (5 ml) was then added dropwise over 1 h. The reaction was then stirred

at room temperature for 30 min. The solvent was removed *in vacuo* and the resulting oil purified by column chromatography (10% MeOH in DCM). The desired product **45** was obtained as a brown oil (120 mg, 86%).

$^1\text{H}$  NMR (600 MHz, MeOD)  $\delta$  4.10 (t, 2H,  $J = 6.0$ , H<sub>2</sub>-3), 3.64 (m, 8H, H<sub>2</sub>-7, H<sub>2</sub>-8, H<sub>2</sub>-9, H<sub>2</sub>-10), 3.60 (m, 2H, H<sub>2</sub>-4), 3.52 (t, 2H,  $J = 6.0$ , H<sub>2</sub>-11), 3.19 (t, 2H,  $J = 6.0$ , H<sub>2</sub>-6), 3.00 (t, 2H,  $J = 6.0$ , H<sub>2</sub>-13), 2.49 (td, 2H,  $J = 7.2$ ,  $J = 3.0$ , H<sub>2</sub>-2), 2.31 (m, 1H, H-1), 1.87 (pent., 2H,  $J = 6.0$ , H<sub>2</sub>-12), 1.75 (pent., 2H,  $J = 6.0$ , H<sub>2</sub>-5);  $^{13}\text{C}$  NMR (150 MHz, MeOD)  $\delta$  158.7 (C), 81.2 (C), 71.4 (CH<sub>2</sub>), 71.2 (CH<sub>2</sub>), 71.1 (CH<sub>2</sub>), 71.0 (CH), 63.8 (CH<sub>2</sub>), 40.2 (CH<sub>2</sub>), 39.0 (CH<sub>2</sub>), 30.9 (CH<sub>2</sub>), 29.5 (CH<sub>2</sub>), 20.0 (CH<sub>2</sub>); IR (oil, cm<sup>-1</sup>) 3331 (s, br), 1631 (m); MS (EI): 317 ([M+H]<sup>+</sup>, 100), 247 (10), 154 (5); Exact Mass calculated for [C<sub>15</sub>H<sub>28</sub>N<sub>2</sub>O<sub>5</sub>+H] 317.2071 observed 317.2073 (EI).

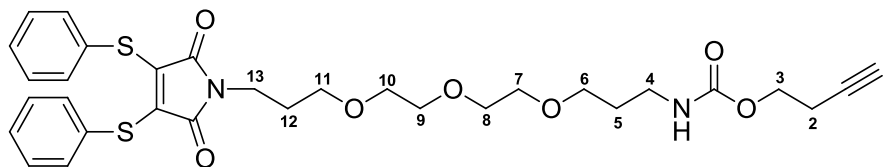
**But-3-yn-1-yl (3-(2-(2-(3-(3,4-dibromo-2,5-dioxo-2,5-dihydro-1H-pyrrol-1-yl)propoxy)ethoxy)ethoxy)propyl)carbamate (46)**



To a stirred solution of carbamate dibromomaleimide **11** (30 mg, 0.095 mmol) in DCM (3 ml) was added monoamine linear alkyne **45** (30 mg, 0.095 mmol). The reaction mixture was stirred at room temperature under argon for 3 h. The solvent was removed *in vacuo* and the mixture purified by column chromatography (DCM) to yield **46** as a yellow oil (39 mg, 74%).

$^1\text{H}$  NMR (600 MHz, CDCl<sub>3</sub>)  $\delta$  5.30 (s, 1H, NH), 4.13 (t, 2H,  $J = 6.0$ , H<sub>2</sub>-3), 3.66-3.52 (m, 12H, H<sub>2</sub>-6, H<sub>2</sub>-7, H<sub>2</sub>-8, H<sub>2</sub>-9, H<sub>2</sub>-10, H<sub>2</sub>-11), 3.47 (m, 2H, H<sub>2</sub>-13), 3.31 (m, 2H, H<sub>2</sub>-4), 2.47 (m, 2H, H<sub>2</sub>-2), 1.99 (m, 1H, H-1), 1.85 (pent., 2H,  $J = 6.0$ , H<sub>2</sub>-12), 1.77 (pent., 2H,  $J = 6.0$ , H<sub>2</sub>-5);  $^{13}\text{C}$  NMR (150 MHz, CDCl<sub>3</sub>)  $\delta$  166.3 (C), 157.2 (C), 129.7 (C), 81.0 (C), 70.5 (CH<sub>2</sub>), 70.4 (CH<sub>2</sub>), 70.3 (CH<sub>2</sub>), 70.0 (CH<sub>2</sub>), 67.9 (CH<sub>2</sub>), 62.6 (CH<sub>2</sub>), 60.4 (CH), 39.1 (CH<sub>2</sub>), 36.6 (CH<sub>2</sub>), 29.2 (CH<sub>2</sub>), 27.9 (CH<sub>2</sub>), 19.6 (CH<sub>2</sub>); IR (oil, cm<sup>-1</sup>) 3294 (s, br), 2948 (w), 1706 (m); MS (EI): 557 ([<sup>81,81</sup>M+H]<sup>+</sup>, 45), 555 ([<sup>81,79</sup>M+H]<sup>+</sup>, 100), 553 ([<sup>79,79</sup>M+H]<sup>+</sup>, 45), 477 (35), 324 (20); Exact Mass calculated for [C<sub>19</sub>H<sub>26</sub><sup>81,79</sup>Br<sub>2</sub>N<sub>2</sub>O<sub>7</sub>+H] 555.0106 observed 555.0152 (EI).

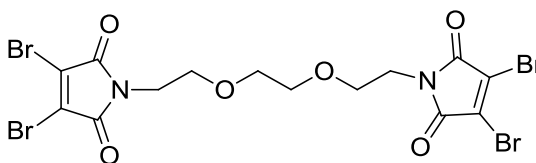
**But-3-yn-1-yl (3-(2-(2-(3-(2,5-dioxo-3,4-bis(phenylthio)-2,5-dihydro-1H-pyrrol-1-yl)propoxy)ethoxy)ethoxy)ethyl)carbamate (47)**



To a stirred solution of carbamate dithiophenol maleimide **27** (53 mg, 0.142 mmol) in DCM (5 ml) was added monoamine linear alkyne **45** (30 mg, 0.095 mmol). The reaction mixture was stirred at room temperature under argon for 45 min. The solvent was removed *in vacuo* and the mixture purified by column chromatography (DCM) to yield **47** as a yellow oil (45 mg, 77%).

$^1\text{H}$  NMR (600 MHz,  $\text{CDCl}_3$ )  $\delta$  7.30-7.18 (m, 10H, Ar-H), 5.35 (s, 1H, NH), 4.14 (t, 2H,  $J = 6.0$ , H<sub>2</sub>-3), 3.64-3.53 (m, 12H, H<sub>2</sub>-6, H<sub>2</sub>-7, H<sub>2</sub>-8, H<sub>2</sub>-9, H<sub>2</sub>-10, H<sub>2</sub>-11), 3.45 (m, 2H, H<sub>2</sub>-13), 3.29 (m, 2H, H<sub>2</sub>-4), 2.49 (m, 2H, H<sub>2</sub>-2), 1.99 (m, 1H, H-1), 1.86 (pent., 2H,  $J = 6.0$ , H<sub>2</sub>-12), 1.76 (pent., 2H,  $J = 6.0$ , H<sub>2</sub>-5);  $^{13}\text{C}$  NMR (150 MHz,  $\text{CDCl}_3$ )  $\delta$  167.0 (C), 156.3 (C), 135.7 (C), 131.9 (C), 129.5 (CH), 129.0 (CH), 128.5 (CH), 80.7 (C), 70.7 (CH<sub>2</sub>), 70.4 (CH<sub>2</sub>), 70.3 (CH<sub>2</sub>), 69.8 (CH<sub>2</sub>), 68.8 (CH<sub>2</sub>), 62.5 (CH<sub>2</sub>), 60.5 (CH), 39.3 (CH<sub>2</sub>), 36.6 (CH<sub>2</sub>), 29.4 (CH<sub>2</sub>), 28.6 (CH<sub>2</sub>), 19.6 (CH<sub>2</sub>); IR (oil,  $\text{cm}^{-1}$ ) 3293 (s, br), 2950 (w), 1708 (m), 1552 (m); MS (EI): 613 ( $[\text{M}+\text{H}]^+$ , 100), 536 (30), 354 (40), 154 (30); Exact Mass calculated for  $[\text{C}_{31}\text{H}_{36}\text{N}_2\text{O}_7\text{S}_2+\text{H}]$  613.2037 observed 613.2027 (EI).

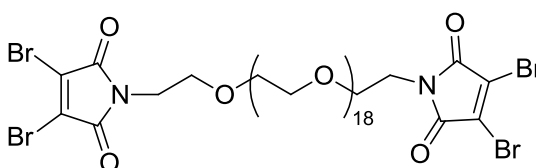
***N,N*-PEG2-bis-3,4-dibromomaleimide (BDBM(PEG)<sub>2</sub>)<sup>181</sup>**



2,2'-(Ethylenedioxy)bis(ethylamine) (0.2 ml, 1.38 mmol) was added to a stirred solution of *N*-(methoxycarbonyl)-3,4-dibromomaleimide (1.08 g, 3.45 mmol) in DCM (8 ml). After 20 min EtOAc (80 ml) was added and the organic layer extracted with saturated  $\text{NH}_4\text{Cl}$  solution (2 x 40 ml) and  $\text{H}_2\text{O}$  (3 x 40 ml). The organic layer was dried with  $\text{MgSO}_4$ , filtered and concentrated *in vacuo*. Purification by column chromatography (gradient elution from 10% EtOAc in petrol to 30% EtOAc in petrol) yielded **BDBM(PEG)<sub>2</sub>** as a pale yellow solid (600 mg, 70%).

m.p. 116 – 117 °C;  $^1\text{H}$  NMR (500 MHz,  $\text{CDCl}_3$ )  $\delta$  3.82 (t, 4H,  $J = 5.6$  Hz,  $\text{NCH}_2$ ), 3.65 (t, 4H,  $J = 5.6$  Hz,  $\text{NCH}_2\text{CH}_2\text{O}$ ), 3.58 (s, 4H,  $\text{OCH}_2\text{CH}_2\text{O}$ );  $^{13}\text{C}$  NMR (125 MHz,  $\text{CDCl}_3$ )  $\delta$  164.2 (C), 129.8 (C), 70.4 ( $\text{CH}_2$ ), 68.0 ( $\text{CH}_2$ ), 39.3 ( $\text{CH}_2$ ); IR (solid,  $\text{cm}^{-1}$ ) 2913 (s), 2882 (s), 1785 (s), 1720 (s), 1597 (s); MS (ES+) 651 ( $[\text{C}_{14}\text{H}_{12}\text{N}_2\text{O}_6\text{Na}^{79}\text{Br}_4\text{M}+\text{Na}]^+$ , 20), 649 ( $[\text{C}_{14}\text{H}_{12}\text{N}_2\text{O}_6\text{Na}^{81,81,79}\text{Br}_4\text{M}+\text{Na}]^+$ , 70), 647 ( $[\text{C}_{14}\text{H}_{12}\text{N}_2\text{O}_6\text{Na}^{81,81,79,79}\text{Br}_4\text{M}+\text{Na}]^+$ , 100), 645 ( $[\text{C}_{14}\text{H}_{12}\text{N}_2\text{O}_6\text{Na}^{81,79,79,79}\text{Br}_4\text{M}+\text{Na}]^+$ , 70), 643 ( $[\text{C}_{14}\text{H}_{12}\text{N}_2\text{O}_6\text{Na}^{79,79,79,79}\text{Br}_4\text{M}+\text{Na}]^+$ , 20); Exact Mass calculated for  $\text{C}_{14}\text{H}_{12}\text{N}_2\text{O}_6\text{Na}^{79}\text{Br}_4$  642.7327, observed 642.7355 (ES+).

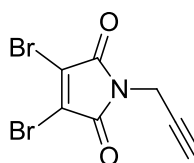
### ***N,N*-PEG19-bis-3,4-dibromomaleimide (BDBM(PEG)<sub>19</sub>)**



O,O'-Bis(2-aminoethyl)octadecaethylene glycol (50 mg, 0.06 mmol) was added to a stirred solution of N-(methoxycarbonyl)-3,4-dibromomaleimide (44 mg, 0.14 mmol) in DCM (2 ml). The reaction mixture was left at room temperature overnight, and then the solvent removed in vacuo. Purification by column chromatography (gradient elution from DCM to 5% MeOH in DCM) afforded **BDBM(PEG)<sub>19</sub>** as a pale yellow oil (53 mg, 65%).

$^1\text{H}$  NMR (600 MHz,  $\text{CDCl}_3$ )  $\delta$  3.81 (t, 4H,  $J = 6.0$ ,  $\text{NCH}_2$ ), 3.67-3.59 (m, 76H, 38 x  $\text{CH}_2$ );  $^{13}\text{C}$  NMR (150 MHz,  $\text{CDCl}_3$ )  $\delta$  164.0 (C), 129.6 (C), 70.7 ( $\text{CH}_2$ ), 70.2 ( $\text{CH}_2$ ), 67.7 ( $\text{CH}_2$ ), 39.0 ( $\text{CH}_2$ ); IR (oil,  $\text{cm}^{-1}$ ) 2865 (s), 1722 (s); MS (ES+) 1394 ( $[\text{C}_{48}\text{H}_{80}^{81,81,81}\text{M}+\text{NH}_4]^+$ , 20), 1392 ( $[\text{C}_{48}\text{H}_{80}^{81,81,81,79}\text{M}+\text{NH}_4]^+$ , 70), 1390 ( $[\text{C}_{48}\text{H}_{80}^{81,81,79,79}\text{M}+\text{NH}_4]^+$ , 100), 1388 ( $[\text{C}_{48}\text{H}_{80}^{81,79,79,79}\text{M}+\text{NH}_4]^+$ , 70), 1386 ( $[\text{C}_{48}\text{H}_{80}^{79,79,79,79}\text{M}+\text{NH}_4]^+$ , 20), 1346 (40), 1300 (10); Exact Mass calculated for  $\text{C}_{48}\text{H}_{80}^{81,81,79,79}\text{Br}_4\text{N}_2\text{O}_{23}\text{NH}_4$  1390.2192, observed 1390.2181 (ES+).

### **3,4-dibromo-1-(prop-2-yn-1-yl)-1H-pyrrole-2,5-dione (48)<sup>181</sup>**

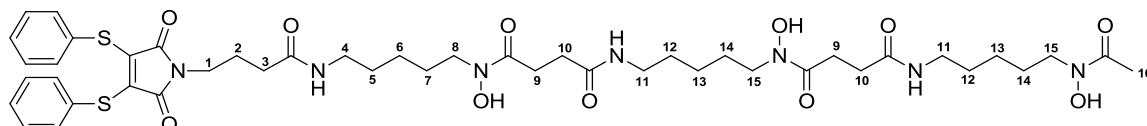


Propargylamine (13  $\mu\text{l}$ , 0.193 mmol) was added to a stirred solution of dibromomaleimide carbamate **11** (50 mg, 0.161 mmol) in DCM (2 ml). After 20 min,

EtOAc (10 ml) was added and the organic layer washed with saturated  $\text{NH}_4\text{Cl}$  (10 ml) and water (10 ml), dried with  $\text{MgSO}_4$ , filtered and concentrated *in vacuo* to yield **48** as a pale yellow solid (39 mg, 83%).

m.p. 118 - 120 °C;  $^1\text{H}$  NMR (500 MHz,  $\text{CDCl}_3$ )  $\delta$  4.38 (d, 2H,  $J = 2.5$ ,  $\text{CH}_2$ ), 2.27 (1H, t,  $J = 2.5$ ,  $\text{CH}$ );  $^{13}\text{C}$  NMR (125 MHz,  $\text{CDCl}_3$ )  $\delta$  162.7 (C), 129.9 (C), 76.1 (C), 72.6 (C), 28.7 ( $\text{CH}_2$ ); IR (solid,  $\text{cm}^{-1}$ ) 3020 (w), 2925 (m), 1735 (m); MS (EI): 296 ( $[\text{C}_7\text{H}_3^{81,81}\text{Br}_2\text{NO}_2+\text{H}]^+$ , 50), 294 ( $[\text{C}_7\text{H}_3^{81,79}\text{Br}_2\text{NO}_2+\text{H}]^+$ , 100), 292 ( $[\text{C}_7\text{H}_3^{79,79}\text{Br}_2\text{NO}_2+\text{H}]^+$ , 50); Exact Mass calculated for  $[\text{C}_7\text{H}_3^{79}\text{Br}_2\text{NO}_2+\text{H}]$  291.8603 observed 291.8606 (EI).

**$\text{N}^1$ -(5-(4-(2,5-dioxo-3,4-bis(phenylthio)-2,5-dihydro-1H-pyrrol-1-yl)butanamido)pentyl)- $\text{N}^1$ -hydroxy- $\text{N}^4$ -(5-(N-hydroxy-4-((5-(N-hydroxyacetamido)pentyl)amino)-4-oxobutanamido)pentyl)succinamide (51)**



Dithiophenolmaleimide-NHS ester **19** (42 mg, 0.085 mmol), deferoxamine mesylate salt (55 mg, 0.085 mmol) and DIPEA (17  $\mu\text{l}$ , 0.100 mmol) were dissolved in DMF (2.0 ml) and water (0.2 ml). The reaction mixture was stirred for 1 h at room temperature. The reaction was then quenched with water (8 ml), sealed and incubated in the freezer overnight. After this time, an orange/yellow solid had precipitated of solution. The solid was obtained by vacuum filtration and washed with water. The solid was the washed with DCM to remove dithiophenol carboxylic acid maleimide **18**, to yield **51** as a yellow solid (45 mg, 56%).

m.p. 156 - 160 °C; At 60 °C:  $^1\text{H}$  NMR (400 MHz, MeOD)  $\delta$  7.32-7.23 (m, 10H, Ar-H), 4.14 (s, 2H,  $\text{H}_2$ -1), 3.61 (t, 4H,  $J = 8.0$ ,  $\text{H}_2$ -15), 3.55 (t, 2H,  $J = 4.0$ ,  $\text{H}_2$ -8), 3.19 (m, 6H,  $\text{H}_2$ -4,  $\text{H}_2$ -11), 2.76 (m, 4H,  $\text{H}_2$ -9), 2.48 (t, 4H,  $J = 8.0$ ,  $\text{H}_2$ -10), 2.20 (t, 2H,  $J = 4.0$ ,  $\text{H}_2$ -3), 2.10 (s, 3H,  $\text{H}_3$ -16), 1.90 (pent., 2H,  $J = 8.0$ ,  $\text{H}_2$ -2), 1.66-1.35 (m, 18H,  $\text{H}_2$ -5,  $\text{H}_2$ -6,  $\text{H}_2$ -7,  $\text{H}_2$ -12,  $\text{H}_2$ -13,  $\text{H}_2$ -14);  $^{13}\text{C}$  NMR (125 MHz, MeOD)  $\delta$  174.8 (C), 168.4 (C), 137.4 (C), 132.7 (CH), 130.8 (C), 130.1 (CH), 129.3 (CH), 40.3 ( $\text{CH}_2$ ), 39.4 ( $\text{CH}_2$ ), 34.4 ( $\text{CH}_2$ ), 31.7 ( $\text{CH}_2$ ), 30.0 ( $\text{CH}_2$ ), 29.0 ( $\text{CH}_2$ ), 27.3 ( $\text{CH}_2$ ), 25.6 ( $\text{CH}_2$ ), 24.9 ( $\text{CH}_2$ ), 19.8 ( $\text{CH}_3$ ); IR (solid,  $\text{cm}^{-1}$ ) 3301 (w, br), 2928 (m), 1702 (m), 1617 (m), 1563 (m); MS (EI): 942 ( $[\text{M}+\text{H}]^+$ , (10)), 855 (20), 507 (35), 434 (100), 304 (90), 242 (50); Exact Mass calculated for  $[\text{C}_{45}\text{H}_{63}\text{N}_7\text{O}_{11}\text{S}_2+\text{H}]$  942.4100 observed 942.4107 (EI).

---

## **4.5 Application of disulfide to lysine linker**

### **4.5.1 *In situ* bridging of anti-CEA ds-scFv**

Anti-CEA ds-scFv was diluted in PBS with 10% DMF to a concentration of 70  $\mu\text{M}$  (1.87 mg/ml). Dithiophenolmaleimide **9** was added (5 equiv relative to scFv, 28 mM stock in DMF) followed by benzeneselenol (25 equiv relative to scFv, 70 mM stock in DMF) and the mixture incubated for 20 min at room temperature. The formation of bridged scFv was monitored by LCMS (expected 26,831, observed 26,831).

### **4.5.2 Incubation of CPG2 with dibromomaleimide or dithiophenolmaleimide**

CPG2 was diluted in PBS with 10% DMF to a concentration of 11.4  $\mu\text{M}$  (0.5 mg/ml). Dibromomaleimide **8** or dithiophenolmaleimide **9** (20 and 50 equiv relative to CPG2, 4.6 mM stock in DMF) were added to aliquots of CPG2 and the mixture left for 1 h at room temperature. The reaction was monitored by LCMS and no change in mass was observed (unmodified CPG2 42,403).

### **4.5.3 Conjugation of dithiophenolmaleimide-NHS ester linker to CPG2**

CPG2 was diluted in PBS with 10% DMF to a concentration of 11.4  $\mu\text{M}$  (0.5 mg/ml). Dithiophenolmaleimide-NHS ester linker **19** was added (2 equiv relative to CPG2, 4.6 mM stock in DMF) and the mixture incubated for 1 h at room temperature. Glycine (150 equiv relative to CPG2, 44 mM stock in PBS) was then added to quench the reaction. The formation of singly-modified CPG2 monomer was monitored by LCMS (expected 42,785, observed 42,772). Excess linker was removed using a desalting column (PD-10, GE Healthcare) and the modified CPG2 buffer exchanged into 50 mM phosphate, pH 6.8, 1 mM EDTA buffer for subsequent conjugation.

### **4.5.4 General method for the conjugation of modified CPG2 to anti-CEA ds-scFv via the stepwise protocol**

Anti-CEA ds-scFv in PBS (122  $\mu\text{M}$ , 3.26 mg/ml) was reduced with DTT (20 equiv relative to scFv, 122 mM stock in PBS) for 1 h at room temperature. DTT was then removed by centrifugal ultrafiltration (GE Healthcare, Vivaspin 500, 10 kDa cut-off) and buffer exchanged into 50 mM phosphate, pH 6.8, 1 mM EDTA buffer. After concentration, the reduced scFv was added to modified CPG2 at the desired molar ratio and the mixture incubated at room temperature. A variety of reaction time scales were investigated. For specific examples please see *Section 2.1.6*.

---

#### **4.5.5 General method for the conjugation of modified CPG2 to anti-CEA ds-scFv via the *in situ* portionwise protocol**

Anti-CEA ds-scFv in PBS with 10% DMF was prepared to the desired concentration. Modified CPG2 in PBS was also concentrated and prepared with 10% DMF. The ds-scFv was added to the modified CPG2 at the desired molar ratio. Benzeneselenol (15 equiv relative to scFv, 1000x stock in DMF) was immediately added. After this initial addition, benzeneselenol (15 equiv relative to scFv, 1000x stock in DMF) was then added every 20 min for 1 h. Reactions were carried out at room temperature and samples were taken after 90 min and analysed by SDS-PAGE. For specific examples of concentrations and molar ratios attempted please see *Section 2.1.6*.

#### **4.5.6 Bradford assay for determining concentration of modified CPG2**

The Coomassie (Bradford) protein assay kit from Thermo scientific was used. On every use a standard curve was determined using unmodified CPG2.

#### **4.5.7 General method for the conjugation of modified CPG2 to anti-CEA ds-scFv via the *in situ* protocol using selenocystamine dihydrochloride and TCEP**

Anti-CEA ds-scFv and modified CPG2 were prepared in PBS to the desired concentration. The ds-scFv was added to modified CPG2 at the desired molar ratio and Selenocystamine dihydrochloride (25 equiv relative to scFv, 1000x stock in PBS) immediately added, followed by TCEP (100 equiv relative to scFv, 1000x stock in PBS). The reaction mixture was left at room temperature and a variety of reaction time scales investigated. For specific examples please see *Section 2.1.6*.

#### **4.5.8 Western blot for ds-scFv and CPG2**

The membrane was blocked with a 5% solution of Marvel milk powder in PBS (Premier Foods) for 1 h at room temperature and subsequently washed three times with PBS-T and PBS. For ds-scFv detection the membrane was incubated with anti-tetra-His mouse IgG1-HRP (Quiagen, 1 : 1,000 in 1% Marvel solution) for 1 h. For CPG2 detection the membrane was incubated with the primary antibody (anti-CPG2, 1 : 1,000 in 1% Marvel solution) for 1 h. The membrane was washed three times with PBS-T and PBS and then incubated with the secondary antibody (anti-rabbit, 1 : 500 in 1% Marvel solution) for 1 h. Both membranes were then washed three times with PBS-T and PBS, and 3,3'-diamino-benzidine (DAB, 10 mg in 40 ml distilled water with 20  $\mu$ l H<sub>2</sub>O<sub>2</sub>)

---

added. Once bands were visible the membrane was washed with distilled water and air dried.

## ***4.6 Application of substituted maleimide reagents with a bioorthogonal handle***

### **4.6.1 General method for anti-CEA ds-scFv bridging with dithiophenolmaleimide linkers via the *in situ* protocol**

Anti-CEA ds-scFv was diluted in PBS with 10% DMF to a concentration of 70  $\mu$ M (1.87 mg/ml). The dithiophenolmaleimide linker was added (5 equiv relative to scFv, 28 mM stock in DMF) followed by benzeneselenol (25 equiv relative to scFv, 70 mM stock in DMF) and the mixture incubated for 20 min at room temperature. The formation of bridged scFv was monitored by LCMS. Note: DMSO is not compatible with benzeneselenol.

### **4.6.2 General method for anti-CEA ds-scFv bridging with dibromomaleimide linkers via the sequential protocol**

Anti-CEA ds-scFv was diluted in PBS to a concentration of 70  $\mu$ M (1.87 mg/ml) and reduced with DTT (10 equiv relative to scFv, 70 mM stock in PBS). After 15 min, the dibromomaleimide linker was added (15 equiv relative to scFv, 28 mM stock in DMF) and the mixture incubated for a further 15 min at room temperature. The formation of bridged scFv was monitored by LCMS.

### **4.6.3 Trastuzumab (Herceptin) Fab Fragment Preparation**

The pH of trastuzumab (0.5 ml, 6.41 mg/ml) and immobilised pepsin (0.15 ml) was lowered via washing with 20 mM sodium acetate buffer, pH 3.1 four times. Trastuzumab was then added to the pepsin and the mixture was incubated for 7 h at 37  $^{\circ}$ C whilst shaking (1100 rpm). The resin was then separated from the digest using a filter column and washed with digest buffer (50 mM phosphate, 150 mM NaCl, 1 mM EDTA, pH 6.8) three times. The digest was combined with the washes and the volume adjusted to 0.5 ml.

Next immobilised papain (0.5 ml, 0.25 mg/ml) was activated with 20 mM DTT (in digest buffer: 50 mM phosphate, 150 mM NaCl, 1 mM EDTA, pH 6.8) whilst shaking (1100 rpm) for 2 h at 37  $^{\circ}$ C. The resin was washed with digest buffer (without DTT) four times and the 0.5 mL of Herceptin-F(ab')<sub>2</sub> added. The mixture was incubated for

---

16 h at 37 °C whilst shaking (1100 rpm) in the dark. Then the resin was separated from the digest using a filter column, and washed with Borate buffer (25 mM sodium borate, 25 mM NaCl, 1 mM EDTA, pH 8.0) three times. The digest was combined with the washes and the buffer was exchanged completely for Borate buffer and the volume adjusted to 0.4 ml. The digest was analysed by SDS-PAGE and LCMS. Generally, the digest was purified by size exclusion (500 ml Superdex 75 column, GE Healthcare).

#### **4.6.4 General method for Herceptin Fab bridging with dibromo- and dithiophenol-maleimide linkers via the sequential protocol**

Herceptin Fab was diluted in Borate buffer (25 mM sodium borate, 25 mM NaCl, 1 mM EDTA, pH 8.0) to a concentration of 21  $\mu$ M (1.0 mg/ml) and reduced with TCEP (5 equiv relative to Fab, 10.5 mM stock in Borate buffer). After 1 h, the disubstituted maleimide linker was added (8 equiv relative to Fab, 10.5 mM stock in DMF) and the mixture incubated for a further 30 min at room temperature. The formation of bridged Fab was monitored by LCMS and SDS-PAGE.

#### **4.6.5 General method for Herceptin Fab bridging with dithiophenolmaleimide linkers via the *in situ* protocol**

Herceptin Fab was diluted in Borate buffer (25 mM sodium borate, 25 mM NaCl, 1 mM EDTA, pH 8.0) to a concentration of 21  $\mu$ M (1.0 mg/ml) and dithiophenolmaleimide linker added (3 equiv relative to Fab, 5.25 mM stock in DMF). TCEP (5 equiv relative to Fab, 10.5 mM stock in Borate buffer) was then added and the mixture incubated at room temperature for 30 min. The formation of bridged Fab was monitored by LCMS and SDS-PAGE.

#### **4.6.6 General method for SPAAC conjugation between azide or strained alkyne modified scFv or Fab and other functional molecule**

After purification from free linker using a desalting column (PD-10, GE Healthcare), the concentration of the azide or strained alkyne functionalised antibody fragment was adjusted to 100  $\mu$ M in PBS. The azide or strained alkyne other functional molecule e.g. azide-fluorophore, was then added (20 equiv relative to antibody fragment, 100 mM stock in DMF, DMSO or water as appropriate). The reaction mixture was incubated for 1 h at room temperature with moderate shaking (300 rpm). Results were analysed by LCMS and SDS-PAGE. Note for antibody fragment concentrations less than 100  $\mu$ M, the equivalents of other functional molecule should be increased accordingly.

---

#### 4.6.7 General method for generation of scFv or Fab homodimer via SPAAC

After purification from free linker using a desalting column (PD-10, GE Healthcare), the azide and strained alkyne functionalised antibody fragment were diluted in PBS to the desired concentration. The two functionalised antibody fragments were then mixed at the desired molar ratio and incubated with moderate shaking (300 rpm). 37 °C, room temperature and 4 °C were investigated, in addition to a variety of time scales. The results were analysed SDS-PAGE. For specific examples please see *Section 2.2.6*.

#### 4.6.8 Stock solutions for CuAAC conjugation<sup>188</sup>

- CuSO<sub>4</sub>, 20 mM stock in distilled water
- THPTA ligand\*, 50 mM stock in distilled water
- Sodium ascorbate, 50 mM stock in distilled water
- Aminoguanidine hydrochloride, 50 mM stock in distilled water

\*THPTA ligand was kindly provided by Antoine Maruani, UCL Chemistry and synthesised according to the published procedure (188).

#### 4.6.9 Final concentrations for CuAAC conjugation<sup>188</sup>

- CuSO<sub>4</sub>: 200 µM (was adjusted to 500 µM for ds-scFv due to His-tag)
- THPTA ligand: 1 mM (ligand to copper ratio is 5:1)
- Sodium ascorbate: 5 mM
- Aminoguanidine hydrochloride: 5 mM

#### 4.6.10 General procedure for 10 µl CuAAC conjugation between azide or linear alkyne functionalised antibody fragment and other functional molecule

The CuSO<sub>4</sub> and THPTA stocks were pre-mixed (5 µl CuSO<sub>4</sub>, 10 µl THPTA and 85 µl PBS) and a blue colour was observed. The azide or linear alkyne functionalised antibody fragment was concentrated to 167 µM in PBS (6 µl required for 10 µl reaction, therefore yielding final concentration of approximately 100 µM). The azide or linear alkyne other functional molecule was added (20 equiv relative to antibody fragment, 100 mM stock in DMF, DMSO or water as appropriate). The pre-mixed CuSO<sub>4</sub>:THPTA was added (2 µl) and the reaction mixed. Then, aminoguanidine hydrochloride (1 µl) and finally sodium ascorbate (1 µl) were added. The mixture was incubated at room temperature with mild shaking for 1 h. The results were analysed by LCMS or SDS-PAGE.

---

#### **4.6.11 General procedure to generate Fab homodimer via CuAAC**

The azide and linear alkyne functionalised Fab fragments were concentrated to the desired concentration in PBS, and mixed in the desired molar ratio. Following which the same stocks and final concentrations were used as described in *Section 4.6.8* and *4.6.9* to generate Fab homodimer. A variety of time scales were investigated and the results were analysed by SDS-PAGE. For specific examples please see *Section 2.2.7*.

#### **4.7 Application of disulfide to disulfide linkers**

##### **4.7.1 Disulfide bridging of scFv with linker BDBM(PEG)<sub>2</sub> to generate scFv-scFv homodimer**

Anti-CEA ds-scFv in PBS (1 mg/ml, 37.2  $\mu$ M) was reduced with DTT (20 equiv relative to scFv, 37.2 mM stock in PBS) for 1 h at room temperature. DTT was then removed using a desalting column (PD-10, GE Healthcare) and the reduced scFv buffer exchanged into conjugation buffer (20 mM phosphate buffer, 5 mM EDTA, pH 7.4). The scFv was concentrated to approximately 1 mg/ml and linker **BDBM(PEG)<sub>2</sub>** added (0.42 equiv relative to scFv, 3.72 mM stock in DMF). After 1 h at room temperature or overnight at 4 °C, the reaction was purified by size exclusion (500 ml Superdex 75 column, GE Healthcare).

##### **4.7.2 Disulfide bridging of scFv with linker BDBM(PEG)<sub>19</sub> to generate scFv-scFv homodimer**

Anti-CEA ds-scFv in PBS (1 mg/ml, 37.2  $\mu$ M) was reduced with DTT (20 equiv relative to scFv, 37.2 mM stock in PBS) for 1 h at room temperature. DTT was then removed using a desalting column (PD-10, GE Healthcare) and the reduced scFv buffer exchanged into conjugation buffer (20 mM phosphate buffer, 5 mM EDTA, pH 7.4). The scFv was concentrated to approximately 1 mg/ml and linker **BDBM(PEG)<sub>19</sub>** added (0.42 equiv relative to scFv, 3.72 mM stock in water). After 1 h at room temperature or overnight at 4 °C, the reaction was purified by size exclusion (500 ml Superdex 75 column, GE Healthcare).

##### **4.7.3 Disulfide bridging of scFv with linker BDBM(PEG)<sub>19</sub> to generate a scFv-scFv heterodimer**

Anti-CEA ds-scFv in PBS (1 mg/ml, 37.2  $\mu$ M) was reduced with DTT (20 equiv relative to scFv, 37.2 mM in PBS) for 1 h at room temperature. DTT was then removed using a desalting column (PD-10, GE Healthcare) and the reduced scFv buffer

---

exchanged into conjugation buffer (20 mM phosphate buffer, 5 mM EDTA, pH 7.4). The scFv was concentrated to approximately 1 mg/ml and linker **BDBM(PEG)<sub>19</sub>** added (30 equiv relative to scFv, 37.2 mM in water). After 10 mins excess linker was removed by buffer exchange (repeat 3 times, Amicon® Ultra-4 Centrifugal Filter Units, 10 kDa cut-off) into conjugation buffer, and the bridged scFv concentrated to approximately 1 mg/ml. Meanwhile, the second ds-scFv fragment was reduced and purified into conjugation buffer (20 mM phosphate buffer, 5 mM EDTA, pH 7.4) as described earlier. The reduced scFv concentration was adjusted to 37.2 μM, and bridged scFv (37.2 μM) mixed with the reduced scFv in a 3 : 1 ratio by volume respectively. After 1 h at room temperature or overnight at 4 °C, the reaction was purified by size exclusion (500 ml Superdex 75 column, GE Healthcare).

#### **4.7.4 Disulfide bridging of scFv and Fab with linker BDBM(PEG)<sub>19</sub> to generate scFv-Fab heterodimer**

Anti-CEA ds-scFv in PBS (1 mg/ml, 37.2 μM) was reduced with DTT (20 equiv relative to scFv, 37.2 mM in PBS) for 1 h at room temperature. DTT was then removed using a desalting column (PD-10, GE Healthcare) and the reduced scFv buffer exchanged into conjugation buffer (20 mM phosphate buffer, 5 mM EDTA, pH 7.4). The scFv was concentrated to approximately 1 mg/ml and linker **BDBM(PEG)<sub>19</sub>** added (30 equiv relative to scFv, 37.2 mM in water). After 10 mins excess linker was removed by buffer exchange (repeat 3 times, Amicon® Ultra-4 Centrifugal Filter Units, 10 kDa cut-off) into conjugation buffer, and the bridged scFv concentrated to approximately 1 mg/ml. Meanwhile, Herceptin Fab in Borate buffer (1 mg/ml, 25 mM sodium borate, 25 mM NaCl, 1 mM EDTA, pH 8.0) was reduced with TCEP (10 equiv relative to Fab, 37.2 mM in Borate buffer) for 1 h at room temperature. TCEP was then removed using a desalting column (PD-10, GE Healthcare) and the reduced Fab buffer exchanged into conjugation buffer (20 mM phosphate buffer, 5 mM EDTA, pH 7.4). The reduced Fab concentration was adjusted to 37.2 μM, and bridged scFv (37.2 μM) mixed with the reduced Fab in a 2 : 1 ratio by volume respectively. After 1 h at room temperature or overnight at 4 °C, the reaction was purified by size exclusion (500 ml Superdex 75 column, GE Healthcare).

---

#### **4.7.5 Disulfide bridging of Fab with linker BDBM(PEG)<sub>19</sub> to generate Fab-Fab homodimer**

Herceptin Fab in Borate buffer (1 mg/ml, 25 mM sodium borate, 25 mM NaCl, 1 mM EDTA, pH 8.0) was reduced with TCEP (10 equiv relative to Fab, 21 mM in Borate buffer) for 1 h at room temperature. TCEP was then removed using a desalting column (PD-10, GE Healthcare) and the reduced Fab buffer exchanged into conjugation buffer (20 mM phosphate buffer, 5 mM EDTA, pH 7.4). The Fab was concentrated to approximately 1 mg/ml and linker **BDBM(PEG)<sub>19</sub>** added (0.42 equiv relative to Fab, 2.10 mM stock in water). After 1 h at room temperature or overnight at 4 °C, the reaction was purified by size exclusion (500 ml Superdex 75 column, GE Healthcare).

#### **4.7.6 Protocol for CEA ELISA**

ELISA plates were coated with full length human CEA diluted to a final concentration of 1 µg/ml in PBS and incubated for 1 h at room temperature. After washing with PBS, the plates were blocked for 1 h at room temperature with a 5% solution of Marvel milk powder in PBS (Premier Foods). Plates were washed three times with PBS, and the serially diluted test samples (60 nM, 20 nM, 6.6 nM, 2.2 nM, 0.74 nM, 0.24 nM) of ds-scFv, Fab, scFv-scFv and scFv-Fab were added in PBS. The assay was incubated at room temperature for 1 h, washed three times with PBS-T and PBS, and the primary antibody (anti-tetra-His mouse IgG1, Quiagen, 1 : 1,000 in 1% Marvel solution) added. After 1 h the ELISA plates were washed again and the secondary antibody (ECL anti-mouse sheep IgG1 HRP linked, GE Healthcare, 1 : 1,000 in 1% Marvel solution) added and incubated for 1 h at room temperature. The plates were washed and 100 µL of 0.5 mg/mL *o*-phenylenediamine hydrochloride (Sigma-Aldrich) in a phosphate-citrate buffer with sodium perborate were added as substrate. Once colour was observed, the reaction was stopped by acidifying with 50 µL of 4 M HCl. Absorbance was immediately measured at 490 nm. Controls were included in every ELISA, in which PBS had been added to some of the wells instead of CEA or instead of antibody fragment. Each sample was tested in triplicate, and errors are shown as the standard deviation of the average.

#### **4.7.7 Protocol for HER2 ELISA**

ELISA plates were coated with HER2 diluted to a final concentration of 0.25 µg/mL in PBS and incubated for 1 h at room temperature. After washing with PBS, the plates

---

were blocked for 1 h at room temperature with a 5% solution of Marvel milk powder in PBS (Premier Foods). Plates were washed three times with PBS, and the serially diluted test samples (60 nM, 20 nM, 6.6 nM, 2.2 nM, 0.74 nM, 0.24 nM) of ds-scFv, Fab, scFv-scFv and scFv-Fab were added in PBS. The assay was incubated at room temperature for 1 h, washed three times with PBS-T and PBS, and anti-human IgG, Fab-specific-*HRP* antibody (Sigma-Aldrich, 1 : 5,000 in 1% Marvel solution) was added. After 1 h the plates were washed again and 100  $\mu$ L of 0.5 mg/mL *o*-phenylenediamine hydrochloride (Sigma-Aldrich) in a phosphate-citrate buffer with sodium perborate were added as substrate. Once colour was observed, the reaction was stopped by acidifying with 50  $\mu$ L of 4 M HCl. Absorbance was immediately measured at 490 nm. Controls were included in every ELISA, in which PBS had been added to some of the wells instead of HER2 or instead of antibody fragment. Each sample was tested in triplicate, and errors are shown as the standard deviation of the average.

#### **4.7.8 Protocol for Sandwich ELISA**

ELISA plates were coated with CEA diluted to a final concentration of 1  $\mu$ g/ml in PBS and incubated for 1 h at room temperature. After washing with PBS, the plates were blocked for 1 h at room temperature with a 5% solution of Marvel milk powder in PBS (Premier Foods). Plates were washed three times with PBS, and the serially diluted test samples (60 nM, 20 nM, 6.6 nM, 2.2 nM, 0.74 nM, 0.24 nM) of ds-scFv, Fab, scFv-scFv and scFv-Fab were added in PBS. The assay was incubated at room temperature for 1 h, washed three times with PBS-T and PBS, and HER2-Biotin (1 : 500 in 1% Marvel solution) was added. After 1 h the plates were washed again and Extravidin-Peroxidase (Sigma Aldrich, 1 : 2,000 in 1% Marvel solution) added. The plates were washed and 100  $\mu$ L of 0.5 mg/mL *o*-phenylenediamine hydrochloride (Sigma-Aldrich) in a phosphate-citrate buffer with sodium perborate were added as substrate. Once colour was observed, the reaction was stopped by acidifying with 50  $\mu$ L of 4 M HCl. Absorbance was immediately measured at 490 nm. Controls were included in every ELISA. Each sample was tested in triplicate, and errors are shown as the standard deviation of the average.

#### **4.7.9 Cell Lines**

The breast cancer cell lines BT474 and MDA-MB-468 were purchased from ATCC. The A375CEA was generated by stable transfection of the A375 melanoma cell line

---

(ATCC); in brief, A375 cells were transfected with pIRES-puro-CEA (kind gift of Dr. David Gilham) and stable clones selected using 1 µg/ml of puromycin (Sigma) over a period of two weeks. A375CEA and MDA-MB-468 cell lines were maintained at 37°C, 5% CO<sub>2</sub> in Dulbecco's Modified Eagle's Medium (DMEM, Gibco) containing 2mM L-glutamine and complemented with 10% foetal calf serum (Labtech International, UK). BT474 cells were maintained in HybriCare X-46 (ATCC), supplemented with 10% foetal calf serum.

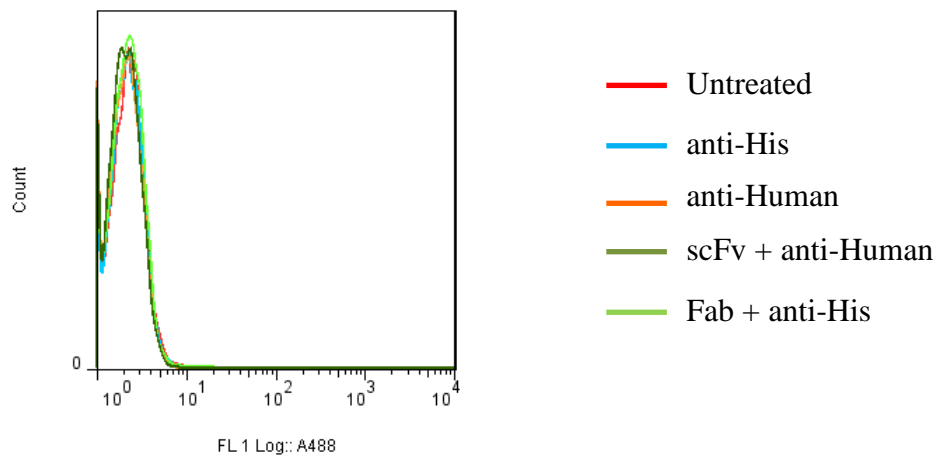
#### **4.7.10 Flow cytometry analysis**

Cell lines were prepared by removal of media and incubation with 10 ml of 0.2% EDTA for 10 min. The cells were then transferred to centrifuge tubes and pelleted (4 °C, 4 min, 1000 rpm). The EDTA solution was removed and 5 ml of fresh media added. Cells were counted and diluted to 1 million per ml, and 1 ml used for each condition to be tested. After washing with cold PBS, 200 µl of sample at 10 µg/ml was added and incubated for 1 h at 4 °C. Cells were washed with cold PBS twice, and incubated with 200 µl of detection antibody for 1 h at 4 °C. For scFv detection AlexaFluor488-conjugated Mouse anti-his tag (R&D Systems) was used and for Fab AlexaFluor488-conjugated Goat anti-human IgG (Molecular Probes). After further washing with cold PBS, the cells were suspended in 500 µl of cold PBS. Samples were analysed on a CyAn ADP High-Performance Flow Cytometer (Becton Dickinson); cells were gated according to size scattering, forward scattering and pulse width so only single cells were analysed. A total of 10,000 cell events were recorded per sample and data was analysed using FlowJo software (Tree Star Inc.).

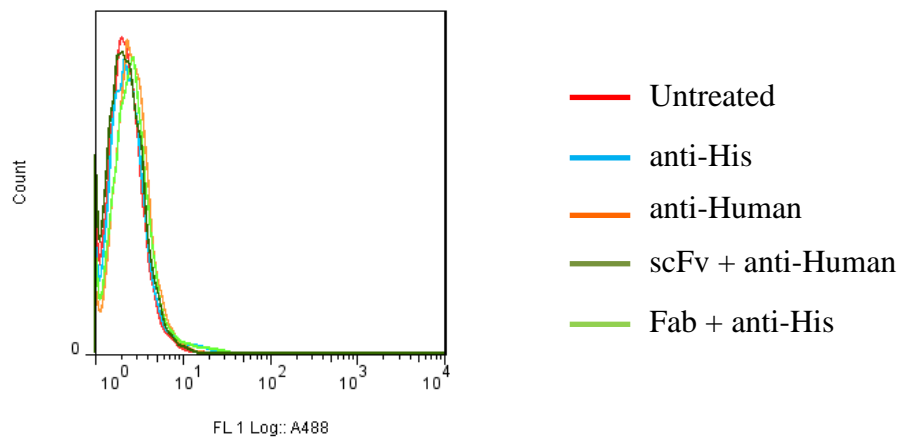
---

### 4.7.10.1 FACS controls

#### CEA-positive cell line A375CEA controls

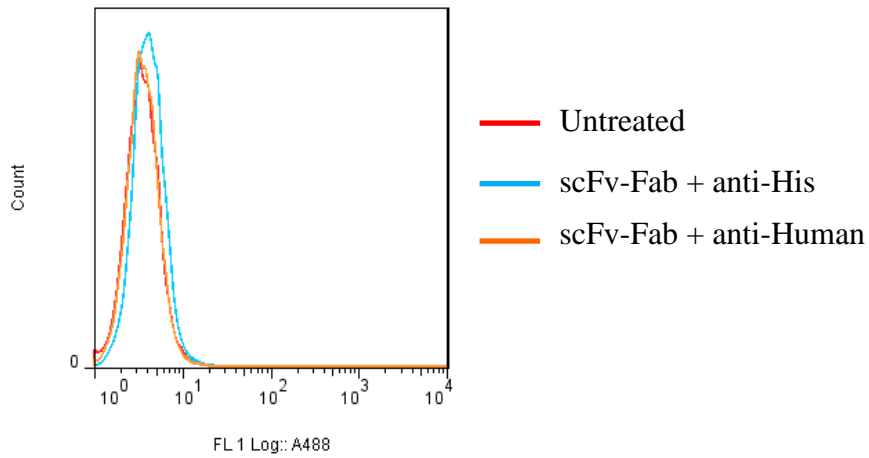
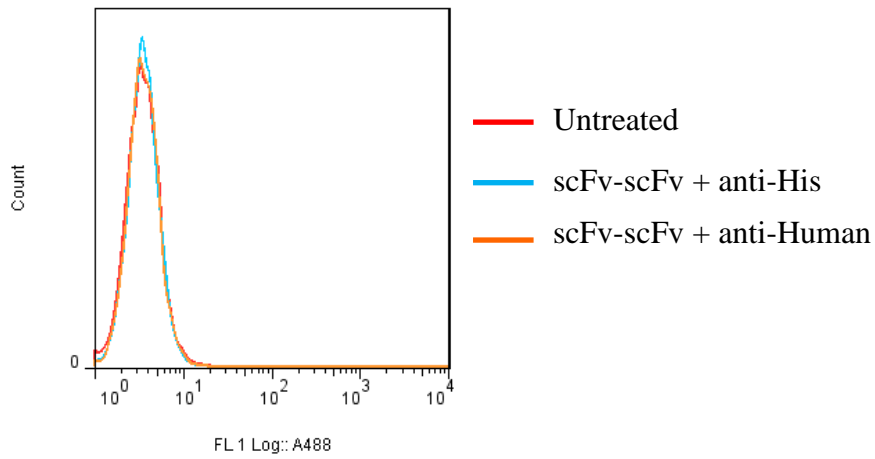
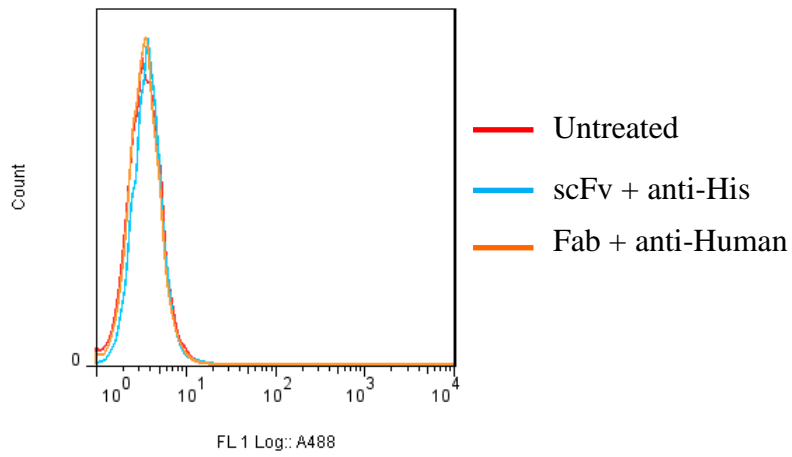


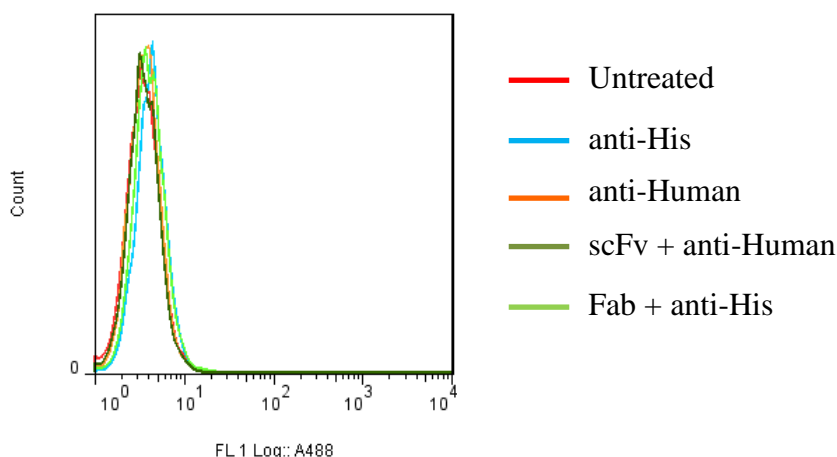
#### HER2-positive cell line BT474 controls



---

**CEA-negative and HER2-negative cell line MDA-MD-468**





## 4.8 Modification of scFv-Fc

### 4.8.1 scFv-Fc reduction study

Aliquots of scFv-Fc in Borate buffer (0.5 mg/ml, 25 mM sodium borate, 25 mM NaCl, 1 mM EDTA, pH 8.0) were reduced with TCEP (3, 5, 8, 12, 20 and 50 equiv relative to scFv-Fc, 0.5 mM in Borate buffer) and DTT (3, 5, 8, 12, 20 and 50 equiv relative to scFv-Fc, 0.5 mM stocks in Borate buffer) for 2 h at 37 °C. The samples were analysed by SDS-PAGE.

### 4.8.2 scFv-Fc bridging study

scFv-Fc in Borate buffer (0.5 mg/ml, 25 mM sodium borate, 25 mM NaCl, 1 mM EDTA, pH 8.0) was reduced with DTT (20 equiv relative to scFv-Fc, 0.5 mM in Borate buffer) for 2 h at 37 °C. DTT was then removed using a desalting column (PD-10, GE Healthcare) and the reduced scFv-Fc buffer exchanged into conjugation buffer (20 mM phosphate buffer, 5 mM EDTA, pH 7.4). The scFv-Fc was then prepared with 10% DMF to a concentration of 0.5 mg/ml and dithiophenolmaleimide **9** or dibromomaleimide **8** (2, 3, 4, 5, 8, 12 and 16 equiv relative to scFv-Fc, 0.5 mM in DMF) added. Samples were incubated for 1 h over ice and analysed by SDS-PAGE.

### 4.8.3 scFv-Fc modification with *N*-alkyne dibromomaleimide

scFv-Fc in Borate buffer (1.0 mg/ml, 25 mM sodium borate, 25 mM NaCl, 1 mM EDTA, pH 8.0) was reduced with DTT (20 equiv relative to scFv-Fc, 1 mM in Borate buffer) for 2 h at 37 °C. DTT was then removed using a desalting column (PD-10, GE Healthcare) and the reduced scFv-Fc buffer exchanged into conjugation buffer (20 mM

---

phosphate buffer, 5 mM EDTA, pH 7.4). The scFv-Fc was then prepared with 10% DMF to a concentration of 1.0 mg/ml and *N*-alkyne dibromomaleimide **48** (20 equiv relative to scFv-Fc, 1 mM in DMF) added. Samples were incubated for 1 h over ice and analysed by SDS-PAGE.

#### **4.8.4 CuAAC between alkyne functionalised scFv-Fc and azide Atto-565**

The CuSO<sub>4</sub> and THPTA stocks were pre-mixed (5 µl CuSO<sub>4</sub>, 10 µl THPTA and 85 µl PBS) and a blue colour was observed. Alkyne functionalised scFv-Fc was concentrated to 167 µM in PBS (30 µl). The azide Atto-565 (20 equiv relative to scFv-Fc, 50 mM stock in DMF). The pre-mixed CuSO<sub>4</sub>:THPTA was added (10 µl) and the reaction mixed. Then, aminoguanidine hydrochloride (5 µl) and finally sodium ascorbate (5 µl) were added. The mixture was incubated at room temperature with mild shaking for 1 h. The results were analysed by SDS-PAGE and UV-Vis.

#### **4.9 Modification of anti-PSMA ds-scFv with dithiophenolmaleimide-DFO**

Anti-PSMA ds-scFv in PBS (1 mg/ml, 37.2 µM) was reduced with DTT (20 equiv relative to scFv, 37.2 mM in PBS) for 1 h at room temperature. DTT was then removed using a desalting column (PD-10, GE Healthcare) and the reduced scFv buffer exchanged into conjugation buffer (20 mM phosphate buffer, 5 mM EDTA, pH 7.4). The scFv was concentrated to approximately 1 mg/ml and dithiophenolmaleimide-DFO **51** added (20% by volume relative to scFv in PBS, 2 mM stock in DMSO). After 2 h at 37 °C with moderate shaking (400 rpm), the reaction was purified by size exclusion (500 ml Superdex 75 column, GE Healthcare) and results analysed by LCMS and SDS-PAGE.

---

## 5 References

1. Carter, P. J. (2006) Potent antibody therapeutics by design. *Nat. Rev. Immunol.* 6, 343–57.
2. Beck, A., Wurch, T., Bailly, C., and Corvaia, N. (2010) Strategies and challenges for the next generation of therapeutic antibodies. *Nat. Rev. Immunol.* 10, 345–52.
3. Leavy, O. (2010) Therapeutic antibodies: past, present and future. *Nat. Rev. Immunol.* 10, 297.
4. Chames, P., Van Regenmortel, M., Weiss, E., and Baty, D. (2009) Therapeutic antibodies: successes, limitations and hopes for the future. *Br. J. Pharmacol.* 157, 220–33.
5. Köhler, G., and Milstein, C. (1975) Continuous cultures of fused cells secreting antibody of predefined specificity. *Nature* 256, 495–97.
6. Morrison, S. L. (1984) Chimeric Human Antibody Molecules: Mouse Antigen-Binding Domains with Human Constant Region Domains. *Proc. Natl. Acad. Sci.* 81, 6851–55.
7. Jones, P. T., Dear, P. H., Foote, J., Neuberger, M. S., and Winter, G. (1986) Replacing the complementarity-determining regions in a human antibody with those from a mouse. *Nature* 321, 522–5.
8. Gram, H., Strittmatter, U., Lorenz, M., Gluck, D., and Zenke, G. (1993) Phage display as a rapid gene expression system: production of bioactive cytokinephage and generation of neutralising monoclonal antibodies. *J. Immunol. Methods* 161, 169–176.
9. Zhao, X.L., Yin, J., Chen, W.Q., Jiang, M., Yang, G., and Yang, Z.H. (2008) Generation and characterisation of human monoclonal antibodies to G5, a linear neutralisation epitope on glycoprotein of rabies virus, by phage display technology. *Microbiol. Immunol.* 52, 89–93.
10. Jakobovits, A. (1995) Production of fully human antibodies by transgenic mice. *Curr. Opin. Biotechnol.* 6, 561–66.
11. Jakobovits, A., Green, L.L., Hardy, M.C., Maynard-Currie, C.E., Tsuda, H., Louie, D.M., Mendez, M.J., Abderrahim, H., Noguchi, M., Smith, D.H., Zeng, Y., David, N.E., Sasai, H., Garza, D., Brenner, D.G., Hales, J.F., McGuinness, R.P., Capon, D.J., and Klapholz, S. (1995) Production of antigen-specific human antibodies from mice engineered with human heavy and light chain YACs. *Ann. N. Y. Acad. Sci.* 764, 525–35.

- 
12. Osbourn, J., Jermutus, L., and Duncan, A. (2003) Current methods for the generation of human antibodies for the treatment of autoimmune diseases. *Drug Discov. Today* 8, 845–851.
  13. Leader, B., Baca, Q. J., and Golan, D. E. (2008) Protein therapeutics: a summary and pharmacological classification. *Nat. Rev. Drug Discov.* 7, 21–39.
  14. Jain, R. K. (1990) Physiological Barriers to Delivery of Monoclonal Antibodies and Other Macromolecules in Tumors. *Cancer Res.* 50, 814–19.
  15. Wu, A. M., and Senter, P. D. (2005) Arming antibodies: prospects and challenges for immunoconjugates. *Nat. Biotechnol.* 23, 1137–46.
  16. Rousseaux, J., Rousseaux-Prévost, R., and Bazin, H. (1983) Optimal conditions for the preparation of Fab and F(ab')<sub>2</sub> fragments from monoclonal IgG of different rat IgG subclasses. *J. Immunol. Methods* 64, 141–46.
  17. Coulter, A., and Harris, R. (1983) Simplified preparation of rabbit fab fragments. *J. Immunol. Methods* 59, 199–203.
  18. Filpula, D., and Mcguire, J. (1999) Single-chain Fv designs for protein, cell and gene therapeutics. *Exp. Opin. Ther. Patents* 9, 231–45.
  19. Holliger, P., and Hudson, P. J. (2005) Engineered antibody fragments and the rise of single domains. *Nat. Biotechnol.* 23, 1126–36.
  20. Weir, A. N. C., Nesbitt, A., Chapman, A.P., Antoniw, P., and Lawson, A.D.G. (2002) Formatting antibody fragments to mediate specific therapeutic functions. *Biochem. Soc. Trans.* 30, 512-16.
  21. Almog, O., Benhar, I., Vasmatzis, G., Tordova, M., Lee, B., Pastan, I., and Gilliland, G. L. (1998) Crystal structure of the disulfide-stabilised Fv fragment of anticancer antibody B1: conformational influence of an engineered disulfide bond. *Proteins* 31, 128–38.
  22. Huston, J. S., Levinson, D., Mudgett-Hunter, M., Tai, M. S., Novotný, J., Margolies, M. N., Ridge, R. J., Bruccoleri, R. E., Haber, E., and Crea, R. (1988) Protein engineering of antibody binding sites: recovery of specific activity in an anti-digoxin single-chain Fv analogue produced in *Escherichia coli*. *Proc. Natl. Acad. Sci. U.S.A.* 85, 5879–83.
  23. Bird, R.E., Hardman, K.D., Jacobson, J.W., Johnson, S., Kaufman, B.M., Lee, S.M., Lee, T., Pope, S.H., Riordan, G.S., and Whitlow, M. (1988) Single chain antigen binding proteins. *Science* 242, 423–26.

- 
24. Brinkmann, U., Reiter, Y., Jung, S. H., Lee, B., and Pastan, I. (1993) A recombinant immunotoxin containing a disulfide-stabilised Fv fragment. *Proc. Natl. Acad. Sci.* 90, 7538–42.
  25. Jung, S.-H., Pastan, I., and Lee, B. (1994) Design of interchain disulfide bonds in the framework region of the Fv of the monoclonal antibody B3. *Proteins* 19, 35–47.
  26. Reiter, Y., and Pastan, I. (1996) Antibody engineering of recombinant Fv immunotoxins for improved targeting of cancer. *Clin. Cancer Res.* 2, 245–252.
  27. Young, N.M., MacKenzie, C.R., Narang, S.A., Oomen, R.P., and Baenziger, J.E. (1995) Thermal stabilisation of a single-chain Fv antibody fragment by introduction of a disulphide bond. *FEBS Lett.* 377, 135-39.
  28. Schmidt, M.M., Thurber, G.M., and Wittrup, K.D. (2008) Kinetics of anti-carcinoembryonic antigen antibody internalisation: effects of affinity, bivalency, and stability. *Cancer Immunol. Immunother.* 57, 1879-90.
  29. Zhao, J.X., Yang, L., Gu, Z.N., Chen, H.Q., Tian, F.W., Chen, Y.Q., Zhang, H., and Chen, W. (2011) Stabilisation of the single-chain fragment variable by an interdomain disulfide bond and its effect on antibody affinity. *Int. J. Mol. Sci.* 12, 1-11.
  30. Yokota, T., Milenic, D. E., Whitlow, M., and Schlom, J. (1992) Rapid Tumor Penetration of a Single-Chain Fv and Comparison with Other Immunoglobulin Forms. *Cancer Res.* 52, 3402-8.
  31. Begent, R.H., Verhaar, M.J., Chester, K.A., Casey, J.L., Green, A.J., Napier, M.P., Hope-Stone, L.D., Cushen, N., Keep, P.A., Johnson, C.J., Hawkins, R.E., Hilson A.J., and Robson, L. (1996) Clinical evidence of efficient tumor targeting based on single-chain Fv antibody selected from a combinatorial library. *Nat. Med.* 2, 979-84.
  32. Adams, G.P., and Schier, R. (1999) Generating improved single-chain Fv molecules for tumor targeting. *J. Immunol. Methods* 231, 249-60.
  33. Adams, G.P., Schier, R., McCall, A.M., Simmons, H.H., Horak, E.M., Alpaugh, R.K., Marks, J.D., and Weiner, L.M. (2001) High affinity restricts the localisation and tumor penetration of single-chain Fv antibody molecules. *Cancer Res.* 61, 4750-55.
  34. Wochner, R.D., Strober, W., and Waldmann, T.A. (1967) The role of the kidney in the catabolism of Bence Jones proteins and immunoglobulin fragments. *J. Exp. Med.* 126, 207-21.
  35. Riechmann, L., Clark, M., Waldmann, H., and Winter, G. (1988) Reshaping human antibodies for therapy. *Nature* 332, 323-27.

- 
36. Ilinskaya, O.N., Koschinski, A., Repp, H., Mitkevich, V.A., Dreyer, F., Scholtz, J.M., Pace, C.N., and Markarov, A.A. (2008) RNase-induced apoptosis: Fate of calcium-activated potassium channels. *Biochimie* 90, 717-725.
37. Yazaki, P.J., Kassa, T., Cheung, C.W., Crow, D.M., Sherman, M.A., Bading, J.R., Anderson, A.L., Colcher, D., and Raubitschek, A. (2008) Biodistribution and tumor imaging of an anti-CEA single-chain antibody-albumin fusion protein. *Nucl. Med. Biol.* 35, 151-158.
38. Pastan, I., Hassan, R., FitzGerald, D.J., and Kreitman, R.J. (2006) Immunotoxin therapy of cancer. *Nat. Rev. Cancer* 6, 559-65.
39. Graff, C.P., Chester, K.A., Begent R.H., and Wittrup, K.D. (2004) Directed evolution of an anti-carcinoembryonic antigen scFv with a 4-day monovalent dissociation half-time at 37 °C. *Protein Eng. Des. Sel.* 17, 293-304.
40. Chapman, A.P., Antoniw, P., Spitali, M., West, S., Stephens, S., and King, D. (1999) Therapeutic antibody fragments with prolonged in vivo half-lives. *Nat. Biotechnol.* 17, 780-783.
41. Chapman, A.P. (2002) PEGylated antibodies and antibody fragments for improved therapy: a review. *Adv. Drug Delivery Rev.* 54, 531-45.
42. Crawford, J. (2002) Clinical benefits of pegylated proteins in oncology. *Cancer Treat. Rev.* 28 Suppl A, 1-2.
43. Harris, J.M., and Chess, R.B. (2003) Effect of pegylation on pharmaceuticals. *Nat. Rev. Drug Discovery* 2, 214-21.
44. Todorovska, A., Roovers, R.C., Dolezal, O., Kortt, A.A., Hoogenboom, H.R., and Hudson, P.J. (2001) Design and application of diabodies, triabodies and tetrabodies for cancer targeting. *J. Immunol. Methods* 248, 47-66.
45. Zhu, Z., Zapata, G., Shalaby, R., Snedecor, B., Chen, H., and Carter, P. (1996) High level secretion of a humanised bispecific diabody from *Escherichia coli*. *Biotechnology* 14, 192-196.
46. FitzGerald, K., Holliger, P., and Winter, G. (1997) Improved tumour targeting by disulphide stabilised diabodies expressed in *Pichia pastoris*. *Protein Eng.* 10, 1221-25.
47. Olafsen, T., Cheung, C.W., Yazaki, P.J., Li, L., Sundaresan, G., Gambhir, S.S., Sherman, M.A., Williams, L.E., Shively, J.E., Raubitschek, A.A., and Wu, A.M. (2004) Covalent disulfide-linked anti-CEA diabody allows site-specific conjugation and radiolabeling for tumor targeting applications. *Protein Eng. Des. Sel.* 17, 21-27.

- 
48. Huang, B.C., Davern, S., and Kennel, S.J. (2006) Mono and bivalent binding of a scFv and covalent diabody to murine laminin-1 using radioiodinated proteins and SPR measurements: effects on tissue retention in vivo. *J. Immunol. Methods* 313, 149-160.
49. Natarajan, A., Xiong, C.Y., Albrecht, H., DeNardo, G.L., and DeNardo, S.J. (2005) Characterisation of site-specific ScFv PEGylation for tumor-targeting pharmaceuticals. *Bioconjugate Chem.* 16, 113-21.
50. Ducry, L., and Stump, B. (2010) Antibody-drug conjugates: linking cytotoxic payloads to monoclonal antibodies. *Bioconjugate Chem.* 21, 5-13.
51. Zhao, R.Y., Wilhelm, S.D., Audette, C., Jones, G., Leece, B.A., Lazar, A.C., Goldmacher, V.S., Singh, R., Kovtun, Y., Widdison, W.C., Lambert, J.M., and Chari, R.V. (2011) Synthesis and evaluation of hydrophilic linkers for antibody-maytansinoid conjugates. *J. Med. Chem.* 54, 3606-23.
52. Sharkey, R.M., and Goldenberg, D.M. (2005) Perspectives on Cancer Therapy with Radiolabeled Monoclonal Antibodies. *J. Nucl. Med.* 46, 115-27.
53. Goldenberg, D.M., Sharkey, R.M., Paganelli, G., Barbet, J. and Chatal, J.-F. (2006) Antibody pretargeting advances cancer radioimmunodetection and radioimmunotherapy. *J. Clin. Oncol.* 24, 823-34.
54. Wakankar, A. A., Feeney, M. B., Rivera, J., Chen, Y., Kim, M., Sharma, V. K., and Wang, Y. J. (2010) Physicochemical stability of the antibody–drug conjugate Trastuzumab–DM1: Changes due to modification and conjugation processes. *Bioconjugate Chem.* 21, 1588–95.
55. Younes, A., Yasothan, U., and Kirkpatrick, P. (2012) Brentuximab vedotin. *Nat. Rev. Drug Discovery* 11, 19–20.
56. Oki, Y., and Younes, A. (2012) Brentuximab vedotin in systemic T-cell lymphoma. *Expert Opin. Biol. Ther.* 12, 623–32.
57. Vitetta, E.S., Thorpe, P.E. and Uhr, J.W. (1993) Immunotoxins: magic bullets or misguided missiles? *Immunol. Today* 14, 252-59.
58. Bernardes, G.J., Casi, G., Trussel, S., Hartmann, I., Schwager, K., Scheuermann, J., and Neri, D. (2011) A traceless vascular-targeting antibody-drug conjugate for cancer therapy. *Angew. Chem. Int. Ed.* 51, 941-944.
59. Choudhary, S., Mathew, M. & Verma, R.S. (2011) Therapeutic potential of anticancer immunotoxins. *Drug Discov. Today* 16, 495-503.
60. Green, D.J., Pagel, J.M., Pantelias, A., Hedin, N., Lin, Y., Wilbur, D.S., Gopal, A., Hamlin, D.K., and Press, O.W. (2007) Pretargeted radioimmunotherapy for B-cell lymphomas. *Clin. Cancer Res.* 13, 5598-603.

- 
61. Bagshawe, K.D. (1987) Antibody directed enzymes revive anti-cancer prodrugs concept. *Br. J. Cancer* 56, 531-2.
  62. Bagshawe, K.D., Springer, C.J., Searle, F., Antoniow, P., Sharma, S.K., Melton, R.G., and Sherwood, R.F. (1988) A cytotoxic agent can be generated selectively at cancer sites. *Br. J. Cancer* 58, 700-3.
  63. Senter, P.D. (1988) Anti-Tumor Effects of Antibody--Alkaline Phosphatase Conjugates in Combination with Etoposide Phosphate. *Proc. Natl. Acad. Sci.* 85, 4842-46.
  64. Springer, C.J., Poon, G.K., Sharma, S.K., and Bagshawe, K.D. (1994) Analysis of antibody-enzyme conjugate clearance by investigation of prodrug and active drug in an ADEPT clinical study. *Cell Biophys.* 24-25, 193-207.
  65. Springer, C.J., Dowell, R., Burke, P.J., Hadley, E., Davies, D.H., Blakey, D.C., Melton, R.G., and Niculescu-Duvaz, I. (1995) Optimisation of Alkylating Agent Prodrugs Derived from Phenol and Aniline Mustards: A New Clinical Candidate Prodrug (ZD2767) for Antibody-Directed Enzyme Prodrug Therapy. *J. Med. Chem.* 38, 5051-65.
  66. Springer, C.J., Antoniow, P., Bagshawe, K.D., Searle, F., Bisset, G.M., and Jarman, M. (1990) Novel prodrugs which are activated to cytotoxic alkylating agents by carboxypeptidase G2. *J. Med. Chem.* 33, 677-681.
  67. Springer, C.J., Bagshawe, K.D., Sharma, S.K., Searle, F., Boden, J.A., Antoniow, P., Burke, P.J., Rogers, G.T., Sherwood, R.F., and Melton, R.G., (1991) Ablation of human choriocarcinoma xenografts in nude mice by antibody-directed enzyme prodrug therapy (ADEPT) with three novel compounds. *Eur. J. Cancer* 27, 1361-1366.
  68. Bagshawe, K.D., Sharma, S.K., Springer, C.J., Antoniow, P., Boden, J.A., Rogers, G.T., Burke, P.J., Melton, R.G., and Sherwood, R.F. (1991) Antibody directed enzyme prodrug therapy (ADEPT): clinical report. *Dis. Markers* 9, 233-38.
  69. Bagshawe, K.D. (1995) Antibody-directed enzyme prodrug therapy for cancer: Its theoretical basis and application. *Mol. Med. Today* 1, 424-31.
  70. Bagshawe, K.D., and Begent, R.H. (1996) First clinical experience with ADEPT. *Adv. Drug Deliv. Rev.* 22, 365-67.
  71. Blakey, D.C., Burke, P.J., Davies, D.H., Dowell, R.I., East, S.J., Eckersley, K.P., Fitton, J.E., McDaid, J., Melton, R.G., Niculescu-Duvaz, I.A., Pinder, P.E., Sharma, S.K., Wright, A.F., and Springer, C.J. (1996) ZD2767, an improved system for antibody-directed enzyme prodrug therapy that results in tumor regressions in colorectal tumor xenografts. *Cancer Res.* 56, 3287-92.

- 
72. Napier, M.P., Sharma, S.K., Springer, C.J., Bagshawe, K.D., Green, A.J., Martin, J., Stribbling, S.M., Cushen, N., O'Malley, D., and Begent, R.H. (2000) Antibody-directed enzyme prodrug therapy: Efficacy and mechanism of action in colorectal carcinoma. *Clin. Cancer Res.* 6, 765-72.
73. Melton, R. G., Boyle, J. M., Rogers, G. T., Burke, P., Bagshawe, K. D., and Sherwood, R. F. (1993) Optimisation of small-scale coupling of A5B7 monoclonal antibody to carboxypeptidase G2. *J. Immunol. Methods* 158, 49-56.
74. Melton, R.G. (1996) Preparation and purification of antibody-enzyme conjugates for therapeutic applications. *Adv. Drug Delivery Rev.* 22, 289-301.
75. Bhatia, J., Sharma, S.K., Chester, K.A., Pedley, R.B., Boden, R.W., Read, D.A., Boxer, G.M., Michael, N.P., and Begent, R.H. (2000) Catalytic activity of an in vivo tumor targeted anti-CEA scFv-carboxypeptidase G2 fusion protein. *Int. J. Cancer* 85, 571-77.
76. Medzihradzky, K.F., Spencer, D.I., Sharma, S.K., Bhatia, J., Pedley, R.B., Read, D.A., Begent, R.H., and Chester, K.A. (2004) Glycoforms obtained by expression in *Pichia pastoris* improve cancer targeting potential of a recombinant antibody-enzyme fusion protein. *Glycobiology* 14, 27-37.
77. Sharma, S.K., Pedley, R.B., Bhatia, J., Boxer, G.M., El-Emir, E., Qureshi, U., Tolner, B., Lowe, K., Michael, N.P., Minton, N., Begent, R.H., and Chester, K.A. (2005) Sustained tumor regression of human colorectal cancer xenografts using a multifunctional mannosylated fusion protein in antibody-directed enzyme prodrug therapy. *Clin. Cancer Res.* 11, 814-25.
78. Mayer, A., Francis, R.J., Sharma, S.K., Tolner, B., Springer, C.J., Martin, J., Boxer, G.M., Bell, J., Green, A.J., Hartley, J.A., Cruickshank, C., Wren, J., Chester, K.A., and Begent, R.H. (2006) A phase I study of single administration of antibody-directed enzyme prodrug therapy with the recombinant anti-carcinoembryonic antigen antibody-enzyme fusion protein MFECP1 and a bis-iodo phenol mustard prodrug. *Clin. Cancer Res.* 12, 6509-16.
79. Michael, N.P., Chester, K.A., Melton, R.G., Robson, L., Nicholas, W., Boden, J.A., Pedley, R.B., Begent, R.H., Sherwood, R.F., and Minton, N.P. (1996) In vitro and in vivo characterisation of a recombinant carboxypeptidase G2-anti-CEA scFv fusion protein. *Immunotechnology* 2, 47-57.
80. Baggio, L.L., Huang, Q., Brown, T.J. and Drucker, D.J. (2004) A Recombinant Human Glucagon-Like Peptide (GLP)-1-Albumin Protein (Albugon) Mimics

---

Peptidergic Activation of GLP-1 Receptor-Dependent Pathways Coupled With Satiety, Gastrointestinal Motility, and Glucose Homeostasis. *Diabetes* 53, 2492-2500.

81. Schmidt, S.R. (2009) Fusion proteins as biopharmaceuticals – applications and challenges. *Curr. Opin. Drug Discovery Dev.* 12, 284-95.
82. Chames, P., and Baty, D. (2009) Bispecific antibodies for cancer therapy: the light at the end of the tunnel? *mAbs* 1, 539-47.
83. Chamow, S.M., and Ashkenazi, A. *Antibody Fusion Proteins*. 312 (Wiley-Blackwell: 1999).
84. Kogelberg, H., Tolner, B., Sharma, S.K., Lowdell, M.W., Qureshi, U., Robson, M., Hillyer, T., Pedley, R.B., Verwecken, W., Contreras, R., Begent, R.H., and Chester, K.A. (2007) Clearance mechanism of a mannosylated antibody-enzyme fusion protein used in experimental cancer therapy. *Glycobiology* 17, 36-45.
85. Heiss, M.M., Murawa, P., Koralewski, P., Kutarska, E., Kolesnik, O.O., Ivanchenko, V.V. Dudnichenko, Alexander S., Aleknaviciene, B., Razbadauskas, A., Gore, M., Ganea-Motan, E., Ciuleanu, T., Wimberger, P., Schmittel, A., Schmalfeldt, B., Burges, A., Bokemeyer, C., Lindhofer, H., Lahr, A., and Parsons, S.L. (2010) The trifunctional antibody catumaxomab for the treatment of malignant ascites due to epithelial cancer: Results of a prospective randomised phase II/III trial. *Int. J. Cancer* 127, 2209-21.
86. May, C., Sapra, P., and Gerber, H.-P. (2012) Advances in bispecific biotherapeutics for the treatment of cancer. *Biochem. Pharmacol.* 84, 1105-12.
87. Byrne, H., Conroy, P. J., Whisstock, J. C., and O’Kennedy, R. J. (2013) A tale of two specificities: bispecific antibodies for therapeutic and diagnostic applications. *Trends Biotechnol.* 31, 621–32.
88. Parashar, A., Sarkar, S., Ganguly, A., and Sharma, S. K. (2011) Bispecific Antibodies (Kontermann, R. E., Ed.) 349–367.
89. Kontermann, R. (2012) Dual targeting strategies with bispecific antibodies. *mAbs* 4, 182–197.
90. Hudak, J. E., Barfield, R. M., de Hart, G. W., Grob, P., Nogales, E., Bertozzi, C. R., and Rabuka, D. (2012) Synthesis of Heterobifunctional Protein Fusions Using Copper-Free Click Chemistry and the Aldehyde Tag. *Angew. Chem. Int. Ed.* 51, 4161-65.
91. Kim, C. H., Axup, J. Y., Dubrovskaya, A., Kazane, S. A., Hutchins, B. A., Wold, E. D., Smider, V. V., and Schultz, P. G. (2012) Synthesis of Bispecific Antibodies using Genetically Encoded Unnatural Amino Acids. *J. Am. Chem. Soc.* 134, 9918-21.

- 
92. Milstein, C., and Cuello, A.C. (1983) Hybrid hybridomas and their use in immunohistochemistry. *Nature* 305, 537–540.
93. Conroy, P.J., Hearty, S., Leonard, P., and O’Kennedy, R.J. (2009) Antibody production, design and use for biosensor-based applications. *Semin. Cell Dev. Biol.* 20, 10–26.
94. Baeuerle, P.A., Zugmaier, G., and Ruttinger, D. (2011) Bispecific T cell engager for cancer therapy. *Bispecific Antibodies* (Kontermann, R. E., Ed.) 273-287.
95. Frankel, S. R., and Baeuerle, P.A. (2013) Targeting T cells to tumor cells using bispecific antibodies. *Curr. Opin. Chem. Biol.* 17, 385–92.
96. Orfao, A., Schmitz, G., Brando, B., Ruiz-Arquelles, A., Basso, G., Braylan, R., Rothe, G., Lacombe, F., Lanza, F., Papa, S., Lucio, P., and San Miguel, J.F. (1999) Clinically useful information provided by the flow cytometric immunophenotyping of hematological malignancies: current status and future directions. *Clin. Chem.* 45, 1708–1717.
97. Jennings, C.D., and Foon, K.A. (1997) Recent advances in flow cytometry: application to the diagnosis of hematological malignancy. *Blood* 90, 2863–92.
98. Campana, D. (1994) Application of cytometry to study acute leukemia: *in vitro* determination of drug sensitivity and detection of minimal residual disease. *Cytometry* 18, 68–74.
99. Means, G.E., and Feeney, R.E. (1990) Chemical modifications of proteins: history and applications. *Bioconjugate Chem.* 1, 2-12.
100. Lundblad, R.L. (2005) *Chemical Reagents for protein modification* (CRC Press).
101. Sletten, E.M., and Bertozzi, C.R. (2009) Bioorthogonal chemistry: fishing for selectivity in a sea of functionality. *Angew. Chem. Int. Ed.* 48, 6974-98.
102. Wang, L., Amphlett, G., Blättler, W.A., Lambert, J.M., and Zhang, W. (2005) Structural characterisation of the maytansinoid-monoclonal antibody immunoconjugate, huN901-DM1, by mass spectrometry. *Protein Sci.* 14, 2436-46.
103. Junutula, J.R., Raab, H., Clark, S., Bhakta, S., Leipold, D.D., Weir, S., Chen, Y., Simpson, M., Tsai, S.P., Dennis, M.S., Lu, Y., Meng, Y.G., Ng, C., Yang, J., Lee, C.C., Duenas, E., Gorrell, J., Katta, V., Kim, A., McDorman, K., Flagella, K., Venook, R., Ross, S., Spencer, S.D., Lee Wong, W., Lowman, H.B., Vandlen, R., Sliwkowski, M.X., Scheller, R.H., Polakis, P., and Mallet, W. (2008) Site-specific conjugation of a cytotoxic drug to an antibody improves the therapeutic index. *Nature Biotechnol.* 26, 925-32.

- 
104. Pasut, G., Guiotto, A., and Veronese, F.M. (2004) Protein, peptide and non-peptide drug PEGylation for therapeutic application. *Exp. Opin. Ther. Patents* 14, 859-94.
105. Kubetzko, S., Sarkar, C.A., and Pluckthun, A. (2005) Protein PEGylation decreases observed target association rates via a dual blocking mechanism. *Mol. Pharmacol.* 68, 1439-54.
106. Junutula, J.R., Flagella, K.M., Graham, R.A., Parsons, K.L., Ha, E., Raab, H., Bhakta, S., Nguyen, T., Dugger, D.L., Li, G., Mai, E., Lewis, P., Gail, D., Hilaragi, H., Fuji, R.N., Tibbitts, J., Vandlen, R., Spencer, S.D., Scheller, R.H., Polakis, P., and Sliwkowski, M.X. (2010) Engineered thio-trastuzumab-DM1 conjugate with an improved therapeutic index to target human epidermal growth factor receptor 2-positive breast cancer. *Clin. Cancer Res.* 16, 4769-78.
107. Axup, J.Y., Bajjuri, K.M., Ritland, M., Hutchins, B.M., Kim, C.H., Kazane, S., Halder, R., Forsyth, J.S., Santidrian, A.F., Stafin, K., Lu, Y., Tran, H., Seller, A.J., Biroc, S.L., Szydlak, A., Pinkstaff, J.K., Tian, F., Sinha, S.C., Felding-Habermann, B., Smider, V.V., and Schultz, P.G. (2012) Synthesis of site-specific antibody-drug conjugates using unnatural amino acids. *Proc. Natl. Acad. Sci.* 109, 16101-6.
108. Jeger, S., Zimmermann, K., Blanc, A., Grunberg, J., Honer, M., Hunziker, P., Struthers, H., and Schibli, R. (2010) Site-specific and stoichiometric modification of antibodies by bacterial transglutaminase. *Angew. Chem. Int. Ed.* 49, 9995-7.
109. Willner, D., Trail, P.A., Hofstead, S.J., King, H.D., Lasch, S.J., Braslawsky, G.R., Greenfield, R.S., Kaneko, T., and Firestone, R.A. (1993) (6-Maleimidocaproyl)hydrazide of doxorubicin--a new derivative for the preparation of immunoconjugates of doxorubicin. *Bioconjugate Chem.* 4, 521-27.
110. Adair, J.R., Howard, P.W., Hartley, J.A., Williams, D.G., and Chester, K.A. (2012) Antibody-drug conjugates - a perfect synergy. *Expert Opin. Biol. Ther.* 12, 1191-1206.
111. Sun, M.M.C., Beam, K.S., Cervený, C.G., Hamblett, K.J., Blackmore, R.S., and Torgov, M.Y. (2005) Reduction-alkylation strategies for the modification of specific monoclonal antibody disulfides. *Bioconjugate Chem.* 16, 1282-90.
112. Younes, A., Bartlett, N.L., Leonard, J.P., Kennedy, D.A., Lynch, C.M., Sievers, E.L. and Forero-Torres, A. (2010) Brentuximab vedotin (SGN-35) for re-lapsed CD30-positive lymphomas. *N. Engl. J. Med.* 363, 1812-21.

- 
113. Liu, H., Chumsae, C., Gaza-Bulseco, G., Hurkmans, K., and Radziejewski, C.H. (2010) Ranking the susceptibility of disulfide bonds in human IgG1 antibodies by reduction, differential alkylation, and LC-MS analysis. *Anal. Chem.* 82, 5219-26
114. McAuley, A., Jacob, J., Kolvenbach, C.G., Westland, K., Lee, H.J., Brych, S.R., Rehder, D., Kleemann, G.R., Brems, D.N., and Matsumura, M. (2008) Contributions of a disulfide bond to the structure, stability, and dimerization of human IgG1 antibody CH3 domain. *Protein Sci.* 17, 95-106.
115. Adem, Y. T., Schwarz, K. A., Duenas, E., Patapoff, T. W., Galush, W. J., and Esue, O. (2014) Auristatin antibody drug conjugate physical instability and the role of drug payload. *Bioconjugate Chem.* 25, 656-64.
116. Isenman, D.E., Dorrington, K.J., and Painter, R.H. (1975) The structure and function of immunoglobulin domains. II. The importance of interchain disulfide bonds and the possible role of molecular flexibility in the interaction between immunoglobulin G and complement. *J. Immunol.* 114, 1726-29.
117. Press, E.M. (1975) Fixation of the first component of complement by immune complexes: effect of reduction and fragmentation of antibody. *Biochem. J.* 149, 285-88.
118. Chan, L.M., and Cathou, R.E. (1977) The role of the inter-heavy chain disulfide bond in modulating the flexibility of immunoglobulin G antibody. *J. Mol. Biol.* 112, 653-56.
119. Michaelsen, T.E., Brekke, O.H., Aase, A., Sandin, R.H., Bremnes, B., and Sandlie, I. (1994) One disulfide bond in front of the second heavy chain constant region is necessary and sufficient for effector functions of human IgG3 without a genetic hinge. *Proc. Natl. Acad. Sci.* 91, 9243-47.
120. Brekke, O.H., Michaelsen, T.E., and Sandlie, I. (1995) The structural requirements for complement activation by IgG: does it hinge on the hinge? *Immunol. Today* 16, 85-90.
121. Hermanson, G.T. (2008) *Bioconjugate Techniques*. (Academic Press).
122. Albrecht, H. A., Burke, P.A., Natarajan, A., Xiong, C., Kalicinsky, M., DeNardo, G.L., and DeNardo, S.J. (2004) Production of soluble ScFvs with C-terminal-free thiol for site-specific conjugation or stable dimeric ScFvs on demand. *Bioconjugate Chem.* 15, 16-26.
123. Jeger, S., Zimmermann, K., Blanc, A., Grünberg, J., Honer, M., Hunziker, P., Struthers, H., and Schibli, R. (2010) Site-specific and stoichiometric modification of antibodies by bacterial transglutaminase. *Angew. Chem. Int. Ed.* 49, 9995-7.

- 
124. Voynov, V.V., Chennamsetty, N., Kayser, V., Wallny, H., Helk, B., and Trout, B.L. Design and application of antibody cysteine variants. (2010) *Bioconjugate Chem.* 21, 385-92.
125. Volkin, D.B., Mach, H., and Middaugh, C.R. (1997) Degradative covalent reactions important to protein stability. *Mol. Biotechnol.* 8, 105-22.
126. Gomez, N., Vinson, A.R., Ouyang, J., Nguyen, M.D.H., Chen, X., Sharma, V.K., and Yuk, I.H. (2010) Triple light chain antibodies: factors that influence its formation in cell culture. *Biotechnol. Bioeng.* 105, 748-60.
127. Shen, B.Q., Xu, K., Liu, L., Raab, H., Bhakta, S., Kenrick, M., Parsons-Reponte, K.L., Tien, J., Yu, S.F., Mai, E., Li, D., Tibbitts, J., Baudys, J., Saad, O.M., Scales, S.J., McDonald, P.J., Hass, P.E., Eigenbrot, C., Nguyen, T., Solis, W.A., Fuji, R.N., Flagella, K.M., Patel, D., Spencer, S.D., Khawli, L.A., Ebens, A., Wong, W.L., Vandlen, R., Kaur, S., Sli-wkowski, M.X., Scheller, R.H., Polakis, P., and Junutula, J.R. (2012) Conjugation site modulates the in vivo stability and therapeutic activity of antibody-drug conjugates. *Nat. Biotechnol.* 30, 184-89.
128. Kolb, H.C., Finn, M.G., and Sharpless, K.B. (2001) Click Chemistry: Diverse Chemical Function from a Few Good Reactions. *Angew. Chem. Int. Ed.* 40, 2004-21.
129. Huisgen, R. (1963) Kinetics and Mechanism of 1,3-Dipolar Cycloadditions. *Angew. Chem. Int. Ed.* 2, 633-45.
130. Rostovtsev, V.V., Green, L.G., Fokin, V.V., and Sharpless, K.B. (2002) A stepwise huisgen cycloaddition process: copper(I)-catalyzed regioselective "ligation" of azides and terminal alkynes. *Angew. Chem. Int. Ed.* 41, 2596-9.
131. Tornøe, C.W., Christensen, C., and Meldal, M. (2002) Peptidotriazoles on Solid Phase: [1,2,3]-Triazoles by Regiospecific Copper(I)-Catalyzed 1,3-Dipolar Cycloadditions of Terminal Alkynes to Azides. *J. Org. Chem.* 67, 3057-64.
132. Wu, P., and Fokin, V.V. (2007) Catalytic Azide—Alkyne Cycloaddition: Reactivity and Applications. *Aldrichimica Acta* 40, 7-17.
133. Soares, E.V., Hebbelink, K., and Soares, H.M.V.M. (2003) Toxic effects caused by heavy metals in the yeast *Saccharomyces cerevisiae*: a comparative study. *Can. J. Microbiol.* 49, 336-43.
134. Agard, N.J., Prescher, J.A., and Bertozzi, C.R. (2004) A strain-promoted [3 + 2] azide-alkyne cycloaddition for covalent modification of biomolecules in living systems. *J. Am. Chem. Soc.* 126, 15046-7.

- 
135. Turner, R., Jarrett, A.D., Goebel, P., and Mallon, B.J. (1972) Heats of Hydrogenation. IX. Cyclic acetylenes and some miscellaneous olefins. *J. Am. Chem. Soc.* 95, 790-92.
136. Codelli, J.A., Baskin, J.M., Agard, N.J., and Bertozzi, C.R. (2008) Second-generation difluorinated cyclooctynes for copper-free click chemistry. *J. Am. Chem. Soc.* 130, 11486-93.
137. Jewett, J.C., Sletten, E.M., and Bertozzi, C.R. (2010) Rapid Cu-free click chemistry with readily synthesised biarylazacyclooctynones. *J. Am. Chem. Soc.* 132, 3688-90.
138. Debets, M.F., van Berkel, S.S., Schoffelen, S., Rutjes, F., van Hest, J., and van Delft, F.L. (2010) Aza-dibenzocyclooctynes for fast and efficient enzyme PEGylation via copper-free (3+2) cycloaddition. *Chem. Comm.* 46, 97-9.
139. Dommerholt, J., Schmidt, S., Temming, R., Hendriks, L.J.A., Rutjes, F.P.J.T., van Hest, J.C.M., Lefeber, D.J., Friedl, P., and van Delft, F.L. (2010) Readily accessible bicyclononynes for bioorthogonal labeling and three-dimensional imaging of living cells. *Angew. Chem. Int. Ed.* 49, 9422-5.
140. Borrmann, A., Milles, S., Plass, T., Dommerholt, J., Verkade, J.M.M., Wießler, M., Schultz, C., van Hest, J.C.M., van Delft, F.L., and Lemke, E. (2012) Genetic Encoding of a Bicyclo[6.1.0]nonyne-Charged Amino Acid Enables Fast Cellular Protein Imaging by Metal-Free Ligation. *Chembiochem* 13, 2094-9.
141. Beatty, K.E., Xie, F., Wang, Q., and Tirrell, D.A. (2005) Selective dye-labeling of newly synthesised proteins in bacterial cells. *J. Am. Chem. Soc.* 127, 14150-1.
142. Montclare, J.K., and Tirrell, D.A. (2006) Evolving Proteins of Novel Composition. *Angew. Chem. Int. Ed.* 118, 4630-33.
143. Deiters, A., and Schultz, P.G. (2005) In vivo incorporation of an alkyne into proteins in Escherichia coli. *Bioorg. Med. Chem. Lett.* 15, 1521-4.
144. Liu, C.C., and Schultz, P.G. (2010) Adding new chemistries to the genetic code. *Annu. Rev. Biochem.* 79, 413-44.
145. Rossin, R., Verkerk, P.R., van den Bosch, S.M., Vulderson, R.C.M., Verel, I., Lub, J., and Robillard, M.S. (2010) In vivo chemistry for pretargeted tumor imaging in live mice. *Angew. Chem. Int. Ed.* 49, 3375-8.
146. Rashidian, M., Dozier, J. K., and Distefano, M. D. (2013) Enzymatic Labeling of Proteins: Techniques and Approaches. *Bioconjugate Chem.* 24, 1277-94.

- 
147. Möhlmann, S., Mahlert, C., Greven, S., Scholz, P., and Harrenga, A. (2011) In vitro sortagging of an antibody Fab fragment: overcoming unproductive reactions of sortase with water and lysine side chains. *ChemBioChem* 12, 1774–80.
148. Williamson, D. J., Fascione, M. A., Webb, M. E., and Turnbull, W. B. (2012) Efficient N-terminal labeling of proteins by use of sortase. *Angew. Chem. Int. Ed.* 51, 9377–80.
149. Dennler, P., Chiotellis, A., Fischer, E., Brégeon, D., Belmant, C., Gauthier, L., Lhospice, F., Romagne, F., and Schibli, R. (2014) Transglutaminase-Based Chemo-Enzymatic Conjugation Approach Yields Homogeneous Antibody – Drug Conjugates. *Bioconjugate Chem.* 25, 569-78.
150. Jeger, S., Zimmermann, K., Blanc, A., Gruenberg, J., Honer, M., Hunziker, P., Struthers, H., and Schibli, R. (2010) Site-specific and stoichiometric modification of antibodies by bacterial transglutaminase. *Angew. Chem. Int. Ed.* 49, 9995–97.
151. Ren, H., Xiao, F., Zhan, K., Kim, Y.P., Xie, H., Xia, Z., and Rao, J. (2009) A bio-compatible condensation reaction for the labeling of terminal cysteine residues on proteins. *Angew. Chem. Int. Ed.* 48, 9658-62.
152. Besanceney-Webler, C., Jiang, H., Zheng, T., Feng, L., Soriano Del Amo, D., Wang, W., Klivansky, L.M., Marlow, F.L., Liu, Y., and Wu, P. (2011) Increasing the Efficacy of Bioorthogonal Click Reactions for Bioconjugation: A Comparative Study. *Angew. Chem. Int. Ed.* 50, 8051-56.
153. Menard, A., Huang, Y., Karam, P., Cosa, G., and Auclair, K. (2012) Site-specific fluorescent labeling and oriented immobilisation of a triple mutant of CYP3A4 via C64. *Bioconjugate Chem.* 23, 826-36.
154. Simon, M., Zangemeister-Wittke, U., and Pluckthun, A. (2011) Facile Double-Functionalisation of Designed Ankyrin Repeat Proteins using Click and Thiol Chemistries. *Bioconjugate Chem.* 23, 279-86.
155. Casi, G., Huguenin-Dezot, N., Zuberbuhler, K., Scheuermann, J., and Neri, D. (2012) Site-specific traceless coupling of potent cytotoxic drugs to recombinant antibodies for pharmacodelivery. *J. Am. Chem. Soc.* 134, 5887-92.
156. Loscha, K. V., Herlt, A. J., Qi, R., Huber, T., Ozawa, K., and Otting, G. (2012) Multiple-site labeling of proteins with unnatural amino acids. *Angew. Chem. Int. Ed.* 51, 2243-6.
157. Liebscher, S., Schöpfel, M., Aumüller, T., Sharkhuukhen, A., Pech, A., Höss, E., Parthier, C., Jahreis, G., Stubbs, M. T., and Bordusa, F. (2014) N-terminal protein

---

modification by substrate-activated reverse proteolysis. *Angew. Chem. Int. Ed.* **53**, 3024-8.

158. Petersen, M.T., Jonson, P.H., and Petersen, S.B. (1999) Amino acid neighbours and detailed conformational analysis of cysteines in proteins. *Protein Eng.* **12**, 535-48.

159. Fodje, M.N., and Al-Karadaghi, S. (2002) Occurrence, conformational features and amino acid propensities for the  $\alpha$ -helix. *Protein Eng. Des. Selec.* **15**, 353-58.

160. Bernardes, G.J., Chalker, J.M., Errey, J.C., and Davis, B.G. (2008) Facile conversion of cysteine and alkyl cysteines to dehydroalanine on protein surfaces: versatile and switchable access to functionalised proteins. *J. Am. Chem. Soc.* **130**, 5052-53.

161. Griffith, H., and McConnell, M.H. (1966) A Nitroxide-Maleimide Spin Label. *Proc. Natl. Acad. Sci.* **55**, 8-11.

162. May, J.M. (1989) Interaction of a permeant maleimide derivative of cysteine with the erythrocyte glucose carrier. Differential labelling of an exofacial carrier thiol group and its role in the transport mechanism. *Biochem. J.* **263**, 875-81.

163. Singh, R. (1994) A sensitive assay for maleimide groups. *Bioconjugate Chem.* **5**, 348-51.

164. Rogers, L.K., Leinweber, B.L., and Smith, C.V. (2006) Detection of reversible protein thiol modifications in tissues. *Anal. Biochem.* **358**, 171-184.

165. Baldwin, A. D., and Kiick, K. L. (2011) Tunable Degradation of Maleimide-Thiol Adducts in Reducing Environments. *Bioconjugate Chem.* **22**, 1946-53.

166. Tedaldi, L. M., Smith, M. E. B., Nathani, R., and Baker, J. R. (2009) Bromomaleimides; new reagents for the selective and reversible modification of cysteine. *Chem. Commun.* **43**, 6583-85.

167. Smith, M. E. B., Schumacher, F. F., Ryan, C. P., Tedaldi, L. M., Papaioannou, D., Waksman, G., Caddick, S., and Baker, J. R. (2010) Protein modification, bioconjugation, and disulfide bridging using bromomaleimides. *J. Am. Chem. Soc.* **132**, 1960-5.

168. Schumacher, F. F., Nobles, M., Ryan, C. P., Smith, M. E. B., Tinker, A., Caddick, S., and Baker, J. R. (2011) In situ maleimide bridging of disulfides and a new approach to protein PEGylation. *Bioconjugate Chem.* **22**, 132-6.

169. Ryan, C. P., Smith, M. E. B., Schumacher, F. F., Grohmann, D., Papaioannou, D., Waksman, G., Werner, F., Baker, J. R., and Caddick, S. (2011) Tunable reagents for multi-functional bioconjugation: reversible or permanent chemical modification of proteins and peptides by control of maleimide hydrolysis. *Chem. Commun.* **47**, 5452-4.

- 
170. Schumacher, F. F., Sanchania, V. A., Tolner, B., Wright, Z. V. F., Ryan, C. P., Smith, M. E. B., Ward, J. M., Caddick, S., Kay, C. W. M., Aeppli, G., Chester, K. A., and Baker, J. R. (2013) Homogeneous antibody fragment conjugation by disulfide bridging introduces “spinostics”. *Sci. Rep.* 3, 1525.
171. Castañeda, L., Maruani, A., Schumacher, F. F., Miranda, E., Chudasama, V., Chester, K. A., Baker, J. R., Smith, M. E. B., and Caddick, S. (2013) Acid-cleavable thiomaleamic acid linker for homogeneous antibody-drug conjugation. *Chem. Commun.* 49, 8187-9.
172. Brocchini, S., Balan, S., Godwin, A., Choi, J., Zloh, M., and Shaunak, S. (2006) PEGylation of native disulfide bonds in proteins. *Nat. Protoc.* 1, 2241-52.
173. Shaunak, S. S., Godwin, A., Choi, J., Balan, S., Pedone, E., Vijayarangam, D., Heidelberger, S., Teo, I., Zloh, M., and Brocchini, S. (2006) Site-specific PEGylation of native disulfide bonds in therapeutic proteins. *Nat. Chem. Bio.* 2, 312-3.
174. Balan, S. B., Choi, J., Godwin, A., Teo, I., Laborde, C.M., Heidelberger, S., Zloh, M., Shaunak, S., and Brocchini, S. (2007) Site-specific PEGylation of protein disulfide bonds using a three-carbon bridge. *Bioconjugate Chem.* 18, 61-76.
175. Brocchini, S., Godwin, A., Balan, S., Choi, J., Zloh, M., and Shaunak, S. (2008) Disulfide bridge based PEGylation of proteins. *Adv. Drug Deliv. Rev.* 60, 3-12.
176. Volkin, D.B., Mach, H., and Middaugh, C.R. (1997) Degradative covalent reactions important to protein stability. *Mol. Biotechnol.* 8, 105-22.
177. Hibino, H. H., Inanobe, A., Furutani, K., Murakami, S., Findlay, I., and Kurachi, Y. (2010) Inwardly rectifying potassium channels: their structure, function, and physiological roles. *Physiol. Rev.* 90, 291-366.
178. Patel, Y.C. (1999) Somatostatin and its receptor family. *Front. Neuroendocrinol.* 20, 157-98.
179. Dubowchik, G. M., Firestone, R. A., Padilla, L., Willner, D., Hofstead, S. J., Mosure, K., Knipe, J. O., Lasch, S. J., and Trail, P. A. (2002) Cathepsin B-labile dipeptide linkers for lysosomal release of doxorubicin from internalising immunoconjugates: model studies of enzymatic drug release and antigen-specific in vitro anticancer activity. *Bioconjugate Chem.* 13, 855-69.
180. Schumacher, F. F., Nunes, J. P. M., Maruani, A., Chudasama, V., Smith, M. E. B., Chester, K. A., Baker, J. R., and Caddick, S. (2014) Next generation maleimides enable the controlled assembly of antibody-drug conjugates via native disulfide bond bridging. *Org. Biomol. Chem.* 12, 7261-69.

- 
181. Castañeda, L., Wright, Z. V. F., Marculescu, C., Tran, T. M., Chudasama, V., Maruani, A., Hull, E. A., Nunes, J. P. M., Fitzmaurice, R. J., Smith, M. E. B., Jones, L. H., Caddick, S., and Baker, J. R. (2013) A mild synthesis of N-functionalised bromomaleimides, thiomaleimides and bromopyridazinediones. *Tetrahedron Lett.* *54*, 3493–95.
182. Dubernet, M., Caubert, V., Guillard, J., and Viaud-Massuard, M.-C. (2005) Synthesis of substituted bis(heteroaryl)maleimides. *Tetrahedron* *61*, 4585-93.
183. Song, H. Y., Ngai, M. H., Song, Z. Y., MacAry, P. A., Hobley, J., and Lear, M. J. (2009) Practical synthesis of maleimides and coumarin-linked probes for protein and antibody labelling via reduction of native disulfides. *Org. Biomol. Chem.* *7*, 3400–6.
184. Fletcher, S. A. *Unpublished work* (2014) UCL PhD.
185. Protocols available online for SMCC and sulfo-SMCC heterobifunctional cross-linkers from Thermo Scientific.
186. Lazar, A. C., Wang, L., Blättler, W. A., Amphlett, G., Lambert, J. M., and Zhang, W. (2005) Analysis of the composition of immunoconjugates using size-exclusion chromatography coupled to mass spectrometry. *Rapid Commun. Mass Spectrom.* *19*, 1806–14.
187. Schouten, A., Roosien, J., Bakker, J., and Schots, A. (2002) Formation of disulfide bridges by a single-chain Fv antibody in the reducing ectopic environment of the plant cytosol. *J. Biol. Chem.* *277*, 19339–45.
188. Zhang, X., and Zhang, Y. (2013) Applications of azide-based bioorthogonal click chemistry in glycobiology. *Molecules* *18*, 7145–59.
189. Hong, V., Presolski, S. I., Ma, C., and Finn, M. G. (2009) Analysis and optimisation of copper-catalysed azide-alkyne cycloaddition for bioconjugation. *Angew. Chem. Int. Ed.* *48*, 9879-83.
190. Tummatorn, J., Batsomboon, P., Clark, R. J., Alabugin, I. V., and Dudley, G. B. (2012) Strain-promoted azide-alkyne cycloadditions of benzocyclononynes. *J. Org. Chem.* *77*, 2093–7.
191. Krebs, A., and Kimling, H. (1970) 3.3.6.6-tetramethyl-1-thiacycloheptin ein isolierbares siebenring-acetylen. *Tetrahedron Lett.* *10*, 761–64.
192. Hudis, C. A. (2007) Trastuzumab – mechanism of action and use in clinical practice. *N. Eng. J. Med.* *357*, 39-51.
193. Sletten, E. M., and Bertozzi, C. R. (2008) A hydrophilic azacyclooctyne for Cu-free click chemistry. *Org. Lett.* *10*, 3097–9.

- 
194. Levensgood, M.R., Kerwood, C. C., Chatterjee, C., and van der Donk, W. A. (2009) Investigation of the substrate specificity of lactacin 481 synthetase by using nonproteinogenic amino acids. *Chembiochem* 10, 911-9.
195. Wang, Q., Chan, T. R., Hilgraf, R., Fokin, V. V., Sharpless, K. B., and Finn, M. G. (2003) Bioconjugation by copper(I)-catalyzed azide-alkyne [3 + 2] cycloaddition. *J. Am. Chem. Soc.* 125, 3192-3.
196. Liu, P.Y., Jiang, N., Zhang, J., Wei, X., Lin, H. H., and Yu, X. Q. (2006) The oxidative damage of plasmid DNA by ascorbic acid derivatives in vitro: the first research on the relationship between the structure of ascorbic acid and the oxidative damage of plasmid DNA. *Chem. Biodivers.* 3, 958-66.
197. Richards, D. A. *Unpublished work* (2014) UCL PhD.
198. Karpovsky, B. Y. B., Titus, J. A., Stephany, D. A., and Segal, D. M. (1984) Production of target-specific effector cells using hetero-cross-linked aggregates containing anti-target cell and anti-Fc gamma receptor antibodies. *J. Exp. Med.* 160, 1686-1701.
199. Reusch, U., Sundaram, M., Davol, P. A., Olson, S. D., Davis, J. B., Demel, K., Nissim, J., Rathore, R., Liu, P. Y., and Lum, L. G. (2006) Anti-CD3 x anti-epidermal growth factor receptor (EGFR) bispecific antibody redirects T-cell cytolytic activity to EGFR-positive cancers in vitro and in an animal model. *Clin. Cancer Res.* 12, 183-90.
200. Lee, R. J., Fang, Q., Davol, P. a, Gu, Y., Sievers, R. E., Grabert, R. C., Gall, J. M., Tsang, E., Yee, M. S., Fok, H., Huang, N. F., Padbury, J. F., Larrick, J. W., and Lum, L. G. (2007) Antibody targeting of stem cells to infarcted myocardium. *Stem cells* 25, 712-7.
201. Khalili, H., Godwin, A., Choi, J., Lever, R., Khaw, S. P., and Brocchini, S. (2013) Fab-PEG-Fab as a potential antibody mimetic Fab-PEG-Fab as a potential antibody mimetic. *Bioconjugate Chem.* 24, 1870-1882.
202. Zhang, C., Liu, Y., Feng, C., Wang, Q., Shi, H., Zhao, D., Yu, R., and Su, Z. (2014) Loss of PEG chain in routine SDS-PAGE analysis of PEG-maleimide modified protein. *Electrophoresis* 00, 1-4.
203. Lu, X., Gough, P. C., DeFelippis, M. R., and Huang, L. (2010) Elucidation of PEGylation site with a combined approach of in-source fragmentation and CID MS/MS. *J. Am. Soc. Mass Spectrom.* 21, 810-8.
204. Repp, R., Kellner, C., Muskulus, A., Staudinger, M., Nodehi, S. M., Glorius, P., Akramiene, D., Dechant, M., Fey, G. H., van Berkel, P. H. C., van de Winkel, J. G. J., Parren, P. W. H. I., Valerius, T., Gramatzki, M., and Peipp, M. (2011) Combined Fc-
-

---

protein- and Fc-glyco-engineering of scFv-Fc fusion proteins synergistically enhances CD16a binding but does not further enhance NK-cell mediated ADCC. *J. Immunol. Methods* 373, 67–78.

205. Snapp, E. L., and Hegde, R. S. (2006) Rational Design and Evaluation of FRET Experiments to Measure Protein Proximities in Cells. *Curr. Protoc. Cell Biol.* Unit-17.9.

206. Drake, P. M., Albers, A. E., Baker, J., Banas, S., Bar, R. M., Bhat, A. S., Hart, G. W. De, Garofalo, A. W., Holder, P., Jones, L. C., Kudirka, R., Mcfarland, J., Zmolek, W., and Rabuka, D. (2014) Aldehyde Tag Coupled with HIPS Chemistry Enables the Production of ADCs Conjugated Site-Specifically to Different Antibody Regions with Distinct in Vivo Efficacy and PK Outcomes. *Bioconjugate Chem.* 25, 1331-41.

207. van Dongen, G. A. M. S., Visser, G. W. M., Lub-de Hooge, M. N., de Vries, E. G., and Perk, L. R. (2007) Immuno-PET: a navigator in monoclonal antibody development and applications. *Oncologist* 12, 1379–89.

208. Zeglis, B. M., and Lewis, J. S. (2011) A practical guide to the construction of radiometallated bioconjugates for positron emission tomography. *Dalton Trans.* 40, 6168-95.

---

## 6 Appendix

The following articles have been published as a result of the work reported in this thesis:

**Hull, E. A.**, Livanos, M., Miranda, E., Smith, M. E. B., Chester, K. A., and Baker, J. R. (2014) Homogeneous Bispecifics by Disulfide Bridging. *Bioconjug. Chem.* *25*, 1395-1401.

Castañeda, L., Wright, Z. V. F., Marculescu, C., Tran, T. M., Chudasama, V., Maruani, A., **Hull, E. A.**, Nunes, J. P. M., Fitzmaurice, R. J., Smith, M. E. B., Jones, L. H., Caddick, S., and Baker, J. R. (2013) A mild synthesis of N-functionalised bromomaleimides, thiomaleimides and bromopyridazinediones. *Tetrahedron Lett.* *54*, 3493–95.